Do bacteria implicated in Ventilator-Associated Pneumonia adapt to antibiotic exposure?

Jacob Isaac Parkes

MRes Biological Sciences

University of Salford

School of Science, Engineering & Environment

October 2020

CONTENTS

CONTENTS 1

ACKNOWLEDGEMENTS 4

ABSTRACT 5

1. INTRODUCTION 6

1.1 Bacteria: so small… yet have a huge impact… 6

1.2 Dybioses – the shift in balance… 6

1.3 Antibiotics 8

1.4 Antimicrobial Resistance – the current scale of an ever-growing crisis 11

1.5 Ventilator-Associated Pneumonia 15

1.5.1 Ventilator Associated Pneumonia – Diagnosis 15

1.5.2 Ventilator Associated Pneumonia – Epidemiology & Aetiology 20

1.6 - Pathogenesis & Microbiology of Ventilator-Associated Pneumonia 24

1.7 *Pseudomonas aeruginosa* 25

1.7.1 Genetics of *Pseudomonas aeruginosa* 29

1.7.2 *Pseudomonas aeruginosa* and virulence factors 31

1.8 - Research Aims and Potential Outcomes 39

2 - METHODS & MATERIALS 41

2.1.1 - Media Preparation 41

2.1.2 - Source of Parent Strain 41

2.2 - *Pseudomonas aeruginosa* adaptation to antibiotics 41

2.3 Measurement of Growth and Biofilm Production 44

2.4 - Measurement of Growth under Co-infection conditions 47

2.5 - Measurement of Growth under restricted carbon resources – 20% Glucose and 20% Alanine 49

2.6 - Analysis of expression of antimicrobial and virulence factor associated genotypes via Whole-Genome Sequencing 51

3 - RESULTS 55

3.1 *Pseudomonas aeruginosa* adapts to antibiotic prophylaxis over continuous application 55

3.2 Overall growth and biofilm formation were affected as a result of adaptation towards antibiotics 60

3.2.1 Biofilm Formation 67

3.2.2 CFU analysis and calculated Growth Rate 74

3.3 Co-infection with *Staphylococcus aureus* has an effect on the overall population growth and biofilm formation 76

3.3.1 Interaction of *P. aeruginosa* strains with of *S. aureus* 76

3.3.2 Biofilm Formation under *S. aureus* co-infection conditions 85

3.4 Growth within restricted carbon media has a drastic effect on the *P. aeruginosa* growth and biofilm formation universally 94

3.4.1 Growth of *P. aeruginosa* strains 94

3.4.2 Biofilm Formation under Minimal Medium conditions 106

3.5 Changes in SNP frequency and layout was detected between each adapted strain of *P. aeruginosa* in response of antibiotic exposure 119

4 - DISCUSSION 126

4.1 *Pseudomonas aeruginosa* adapts to a wide range of currently prescribed antibiotics 126

4.2 *Pseudomonas aeruginosa* AMR adaptations create differences in growth patterns 131

4.3 Biofilm formation is affected as a result of adaptation to antibiotics 133

4.4 *Pseudomonas aeruginosa* adaptation to antibiotics affects growth within S. aureus co-culture 138

4.5 Under limited carbon sources, *P. aeruginosa* displays a variation in both growth and biofilm formation against nutrient rich conditions 143

4.6 Whole genome sequencing detected variations in SNPs as P. aeruginosa developed resistance to antibiotics 145

5 CONCLUSION 149

6 REFERENCES 150

7 APPENDICES 173

ACKNOWLEDGEMENTS

I wish to express thanks to my Supervisor, Dr. Joe Latimer, and Co-Supervisors, Dr. Ian Goodhead, Dr. Sarah Withers, and, Dr. Chloe James, and to all of the technical staff, for their support over the period of time that I have been able to conduct research for this thesis. I hope that the knowledge I have gained from this, and over the years at Salford under their tutelage, will guide me to further understand the world in which we live.

I also wish to acknowledge the team I have worked with, specifically my colleagues Alex Thompsett, Lizzie Barber and, Holly McGlinn, for their support in the lab. I wish them the best with their pursuits.

Finally, to my family and friends, all of whom have given a great amount of patience whilst I have dedicated time to research. Your support has been greatly appreciated over the course of my Masters. I wish to dedicate this work specifically to my nan, whom over the years has dealt with her fair share of bacterial infections. Without you, perhaps there may never have been an inspiration to study infectious disease.

ABSTRACT

Antibiotics have been key to the treatment of bacterial infections since their introduction, but the increasing levels of antimicrobial resistance is a concern. Patients with serious respiratory conditions, such as those often encountered within critical care units like ventilator-associated pneumonia (VAP), are most under threat as a result of increasing resistance, especially due to the patients' critical condition. Despite a better understanding of increasing resistance, other effects of treatment with antibiotics on bacterial phenotypes remain poorly understood, and it is therefore important and timely to identify and study key traits that bacteria present because of adaptation to antimicrobial treatment. In this study, a clinical strain of *Pseudomonas aeruginosa* was exposed to antibiotics that are commonly prescribed to treat VAP patients, and tested its ability to grow and form biofilms through *in vitro* testing under a number of experimental conditions, including co-infection and limited growth media. Whole genome sequencing data was collected to identify genetic mutations correlated to such growth. The findings included in this thesis indicates that the *P. aeruginosa* clinical strain was able to adapt to all antibiotics prescribed, including the Ceftazidime/Avibactam combination. Further analysis of growth and biofilm formation patterns included as part of study indicate that the adapted bacteria differ in growth patterns and biofilm formation in contrast to the un-adapted Parent. Further evidence is needed, however, to clarify whether these differences are indeed as a result of adaptation to antibiotics. Subsequent whole genome sequencing detected SNPs in several genes of interest, including the OprD domain. Future studies should continue to analyse the genetic expression of adapted strains through transcriptomics, and incorporate methods that are more applicable to patient lung environments.

1. INTRODUCTION

1.1 Bacteria: so small… yet have a huge impact…

Interactions between microorganisms and their host environment has played a crucial role in how life has developed. Although academic and medical studies tend to focus on those microorganisms – principally bacteria, viruses and others, that lead to infections, these pathogenic microbes are largely outnumbered by numerous other species that have either more beneficial or neutral effects on the host. Recent advances in microbiological research has pointed to the existence of the microbiome, a large microcosm that exists within both humans and other members of both animal and plant kingdoms composed of microorganisms, that influence us in multiple ways (Dang & Marsland, 2019; Wilson & Nicholson, 2017). Largely, these effects are beneficial, such as allowing the host to process certain foods that otherwise would be difficult to digest, such as lactose (Forsgård, 2019). Further theories have led to conclusions that the composition of the microbiome may have an effect on mental health, such as the proposed gut-brain axis (Montiel-Castro *et al.*, 2013). What has also been highlighted is that the crosstalk between both the host and bacteria is crucial to ensure the survival of this delicate balance between microorganisms and the internal environment (Lin *et al.*, 2019; Mulcahy & Mcloughlin, 2016). The key assumption towards anything relating to the health of a microbiome has been that the more diverse the microflora is within the microbiome, the more healthy it, and the host, are (Mosca *et al.*, 2016). Previous research has highlighted key groups of bacteria that are associated with a healthy microbiome, most notably those belonging to the Firmicutes and Bacteroidetes phyla (Johnson *et. al.*, 2017). It is important to note, however, that the composition of bacteria that make up a microbiome vary, based on their location within the host. Whilst most research has been conducted on the gut microbiome, largely due to its diversity, what is typically noted to be a healthy lung microbiome may differ. Studies that have examined the composition of the lung microflora have indicated that Firmicute and Bacteroidetes phyla do exist, though not to the same levels as that within other sites such as the gut (Dang & Marsland, 2019; Dickson *et al.*, 2013). Other, specific groups have been identified and attribute to what is classified as part of a healthy lung microbiome, such as *Prevotella, Veillonella, Streptococcus* and *Pseudomonas* (Dickson *et al.*, 2013).

1.2 Dybioses – the shift in balance…

It is largely suspected that a change in the structure of the endemic microbiome leads to disease. Dysbiosis is the term used to describe these changes, which indicates that there has been a change in the balance of microorganisms that exist within the internal host environment (Brusselaers *et. al.*, 2019; L. Wang *et al.*, 2019; Zakharkina *et al.*, 2017). The causes behind these circumstances can vary, but dysbiosis can often lead to one such species of bacteria to outcompete others, and ultimately trigger a cascade of events leading to pathogenesis. Dysbiosis can result in the establishment of chronic disease alongside a pre-existing co-morbidity. Examples of these chronic disorders include inflammatory-bowel disease (IBD) and diabetes (Wilkins *et al.*, 2019). In relation to the human lung, several different forms of dysbiosis can be related different respiratory conditions. One such example includes an investigation into individuals with asthma, which found that there was an increased proportion of bacteria belonging to the *Proteobacteriae*, a phylum of bacteria that includes pathogenic genera such as *Salmonella, Escherichia, Vibrio and Helicobacter* (Dickson *et al.*, 2013; Hilty *et al.*, 2010). The increase was found to have been driven by species belonging to the *Haemophilus, Moraxella,* and *Neisseria* genera, all of which contain members associated with respiratory illness (Hilty *et al.*, 2010). This has been associated with prior colonisation by such microflora, with individuals having been exposed to these species at a young age, and thus the bacteria have colonised their microbiomes, specifically the laryngeal microbiome (Bisgaard *et al.*, 2007). This pre-disposition to what is normally expected from a healthy colonisation can lead to individuals being at risk of developing conditions such as asthma, or worse, for example Chronic Obstructive Pulmonary Disease (COPD). How these individuals are exposed to potential pathogenic organisms are likely based on environmental changes.

In the same way as the microbiome, much of the research on dysbiosis has been focused on the gut microbiome. This has also been the case with regards to the likely factors that predispose individuals to risks of developing dysbiosis. In most cases, it has been deduced that the changes that lead to dysbiosis are linked to prior exposure to antibiotics (DeGruttola *et. al.*, 2016; Rosa *et. al.*, 2018), which result in populations of microorganisms associated with a balanced gut microbiome being destroyed and recolonised by either harmful or opportunistic species.

Antibiotics can potentially play a role in how the immune system interacts with key microorganisms that occupy a microbiome, which may have a much larger impact on the host. In most cases, antibiotics act in a broad-range manner, wiping out an array of species as a means of control, the end result impacting what key cytokines are present in the environment. It is thought that the increase in allergic disorders over the last few decades has been due to cleaner lifestyles that individuals in higher income countries live in, as proposed by the "hygiene hypothesis" (Ubeda & Pamer, 2012). Research into *Helicobacter pylori,* a commonly occurring bacterial species found in the stomach, has found that colonisation with such is inversely proportional to the development of asthma in childhood (Chen & Blaser, 2008; Ubeda & Pamer, 2012). The presence of *H. pylori* within the stomach can induce an accumulation of white blood cells, including both T-helper and T-regulatory cells, and has been suggested that due to such can activate the immune system in a way that reduces the effects of asthma (Chen & Blaser, 2008; Ubeda & Palmer, 2012). Experiments using mice models have found that the application of antibiotics such as vancomycin and kanamycin exacerbated symptoms of allergy and made individual mice more prone to anaphylactic shock 8 weeks after the application of antibiotic regimen (Bashir *et. al.*, 2004; Ubeda & Pamer, 2012; Watanabe *et. al.*, 2010). It is likely that the absence of key microbes at an early age due to antibiotic application which are introduced at a later stage can lead to such reactions taking place, as the immune system fails to recognise these organisms as beneficial or commensal to the host. This dysbiosis, due to the lack of species needed for balance, can lead to pathology.

1.3 Antibiotics

Various moulds and plant extracts containing antibacterial properties have been used since ancient times to treat bacterial infections, with the earliest evidence of such practice being documented from the ancient Sudan civilisation (Nelson *et. al.*, 2010). Further accounts indicate that other civilisations have used agents derived from natural sources to treat infection: Documents from Ancient China describe the use of fermented soybean to cure skin infections such as furuncles (pimples) and carbuncles (Kourkouta *et al.*, 2018). Antibiotics that are attributed to modern day practice did not enter mainstream production until the mid-20th Century after Penicillin was extracted and refined from the fungal species *Penicillium*

chrysogenum (Aminov, 2010; Fleming, 1929). At this point, the so-called "antibiotic era" gave rise to multiple different types of agents (Table 1.1).

Chemically, antibiotics that are used for human medication can be separated into five different groups based off the molecules that make up key parts of their composition. The first, non-ribosomal peptides (NRP), are a group of antibiotics derived from amino acids that are synthesised outside of the ribosome (Durand *et al.*, 2019). Polyketides (PKs), are another group, which originate from acetyl coenzyme A or malonyl coenzyme A, both of which are involved in fatty acid biosynthesis (Durand *et al.*, 2019). Both of these groups make up 50% of all current antibiotics in use. The last three groups are made up of hybrids between NRPs and PKs; composed of several carbohydrate units with amine groups (aminoglycosides); and others made up of various other molecules (Durand *et al.*, 2019). Examples of antibiotics belonging to the last group include fusidic acid and metronidazole, both of which are often prescribed as cream-based treatments for skin infections (Gillet *et al.*, 2017; Haas *et al.*, 2017). All of these functional groups have specific means of action upon bacteria when applied, specifically targeting different organelles or functions within the microorganisms. The effects of antibiotics on bacterial populations can vary between bacteriostatic; inhibiting cellular growth and thus limiting the expansion of population, to bactericidal, killing the cells outright (Kohanski *et al.*, 2010).

Modes of antibiotic action can be defined based upon the group of each antibiotic agent belongs to. For example, penicillins are a group of antibiotics that act upon the formation of the peptidoglycan cell wall of bacteria (Table 1.1) (Lederberg, 1955), thus leaving the cell open to destruction or lysis. Others, such as quinolones, a class of drugs derived from nalidixic acid, attack bacteria by targeting them at a DNA-level, specifically DNA-isotopoisomerase enzymes which are response for the breakage and re-joining reactions in DNA synthesis (Kohanski *et al.*, 2010). Others act at a deeper genetic level, focusing on RNA synthesis. Rifamycin is a drug that focuses on this by binding and inhibiting the action of RNA polymerase enzyme 41–43, which subsequently prevents stable binding of DNA-dependent transcription (Kohanski *et al.*, 2010).

Table 1.1: Modes of action and resistance mechanisms of commonly prescribed antibiotics (Davies & Davies, 2010)

Antibiotic class	Example(s)	Target	Mode(s) of resistance
β-lactams	Penicillins (ampicillin), cephalosporins (cephamycin), penems (meropenem), monobactams (aztreonam)	Peptidoglycan synthesis	Hydrolysis, efflux, altered target
Aminoglycosides	Gentamicin, streptomycin, spectinomycin	Translation	Phosphorylation, acetylation, nucleotidylation, efflux, altered target
Glycopeptides	Vancomycin, teicoplanin	Peptidoglycan synthesis	Reprogramming peptidoglycan synthesis
Tetracyclines	Minocycline, tigecycline	Translation	Monooxygenation, efflux, altered target
Macrolides	Erythrsomycin, azithrsomycin	Translation	Hydrolysis, glycosylation, phosphorylation, efflux, altered target
Lincosamides	Clindamycin	Translation	Nucleotidylation, efflux, altered target
Streptogramins	Synercid	Translation	C-O lyase (type B streptogramins), acetylation (type A streptogramins), efflux, altered target
Oxazolidianones	Linezolid	Translation	Efflux, altered target
Phenicols	Chloramphenicol	Translation	Acetylation, efflux, altered target
Quinolones	Ciprofloxacin	DNA replication	Acetylation, efflux, altered target
Pyramidines	Trimethoprim	C_1 metabolism	Efflux, altered target
Sulfonamides	Sulfamethoxazole	C_1 metabolism	Efflux, altered target
Rifamycins	Rifampin	Transcription	ADP-ribosylation, efflux, altered target
Lipopeptides	Daptomycin	Cell membrane	Altered target
Cationic peptides	Colistin	Cell membrane	Altered target, efflux

Whilst the invention of new antibiotics allowed scientists to focus on understanding and developing new chemical agents based on their interaction with target molecules, it also gave birth to new generations within the different classes of drugs. Whilst benzylpenicillin (or Penicillin-G), belongs to the first generation of beta-lactam class antibiotics (as reviewed by Aminov, 2017), the likes of Piperacillin are part of the fourth generation, having been developed in the 1970's and introduced as a prescription in 1981 (Coussens *et al.*, 2018). Modifications to core functional groups of each class of antibiotic led to these subsequent

generations. Further development of penicillin-based antibiotics included modifications to the central 6-aminopenicillinic acid, thus leading to subsequent generations of penicillins (Aminov, 2017). The existence of multiple derivatives of antibiotics has been crucial to overcome pre-existing resistance that bacteria have built up when treatment with the prior generation was excessive (Aminov, 2017). As time has passed, more classes of antibiotics, which have different effects upon the target bacteria have been developed. Of note are carbapenems, which are antibiotics considered as last resort by healthcare professionals due to the current levels of antibiotic resistance, and thus preserving their effectiveness is of great importance (Hawkey & Livermore, 2012).

1.4 Antimicrobial Resistance – the current scale of an ever-growing crisis

Antimicrobial resistance (AMR), as reported by the World Health Organisation (WHO) has been recognised as a major global health threat (WHO, 2017). AMR refers to how bacteria have developed mutations that lead to prescriptions used to tackle these organisms becoming less effective, or in some cases useless (Woodford & Ellington, 2007). Short generation times lead to more rapidly evolving populations and the introduction of new genotypes which subsequently give rise to newly resistant strains. The way in which bacteria mutate, or gain the ability to mutate can largely be grouped based on the method of transmission. Both horizontal and vertical methods of transmission are key ways that bacteria exchange genetic material between either the same or subsequent generations. One of the most widely documented with regards to AMR is conjugation, which where one bacterial cell which contains a genetic element conferring resistance, such as a plasmid, transfers such across to another individual bacterial cell through the means of pili attachment (Davies & Davies, 2010; Li *et al.*, 2019). The two cells that are involved in the conjugation process may be of the same species, or potentially different species, phyla or another major domain. The microbiome provides the ideal environment for the spread of these genes, largely due to the number and diversity of bacteria, and the continuing presence of both factors alongside changes in the environment provides a means to mutate in order to adapt and survive (Baron *et al.*, 2018). In essence, the microbiome has been seen as the ideal environment for a microbial "evolutionary arms race" (Baron *et al.*, 2018). A government report from 2014 details that at least 50,000 deaths were attributed to antimicrobial resistant infections in both Europe and North America alone (O'Neill, 2014). However, data regarding the true value of AMR related

deaths to date is largely scarce due to fluctuations in global data (Naylor *et al.*, 2018). The economical impact of AMR, however, is estimated to range between $21,832 per case, to over $3 trillion in GDP loss (Naylor *et al.*, 2018). If left at the current state, it is estimated that these costs could rise to $210 trillion globally by 2050 (Dodds, 2017), with 10 million deaths annually related to infection with AMR pathogens, approximately half of the entire death toll recorded from the Spanish Flu pandemic of 1918-19 (Naylor *et al.*, 2018; O'Neill, 2014).

The WHO recently published a list of "priority pathogens" that action is to be taken against considering their AMR status, with the highest priority assigned to three types of bacteria: *Acinetobacter baumanii; Pseudomonas aeruginosa;* and *Enterobacteriaceae* (WHO, 2017). The sources of resistance are varied, through environmental contamination, however, overprescribing is the largest contributing factor (Llor & Bjerrum, 2014). A recent study into area differentials in England found hot-and-coldspots of antibiotic prescribing, with areas of high levels of prescriptions found in the North (Mölter *et al.*, 2018). Factors that increase prescribing include high unemployment and lower socioeconomic status (Beuscart *et al.*, 2017). It is important, however, to consider that other variables, such as population density or doctor-patient relationships, may well shape the overall antibiotic prescribing rate in those areas. The theory of lower socioeconomic status affecting prescription rates can also be argued thrsough global antibiotic consumption rates, where from 2000-2015, Lower or Middle Income Countries (LMICs) increased their levels by 114%, from 11.4 to 24.5 billion Defined Daily Doses (DDDs) (Klein, Van Boeckel, *et al.*, 2018). In comparison to High Income Countries (HICs), this is considerably higher (increased 6% between 2000-2015; 9.7 to 10.3 billion DDDs) (Klein, Van Boeckel, *et al.*, 2018).

At the turn of the 21st Century, however, it was found that the biggest consumer of antibiotics were HICs, specifically Spain, Greece, Belgium, France, New Zealand and Ireland (Figure 1.1) (Klein, Van Boeckel, *et al.*, 2018). The same conclusion as before can potentially be one possible explanation for this increase (increased/high population density in countries), Other factors, such as lack of effective healthcare controls or education tools, could also play a role in the increased levels of antibiotic consumption, and thus potential resistance towards such agents.

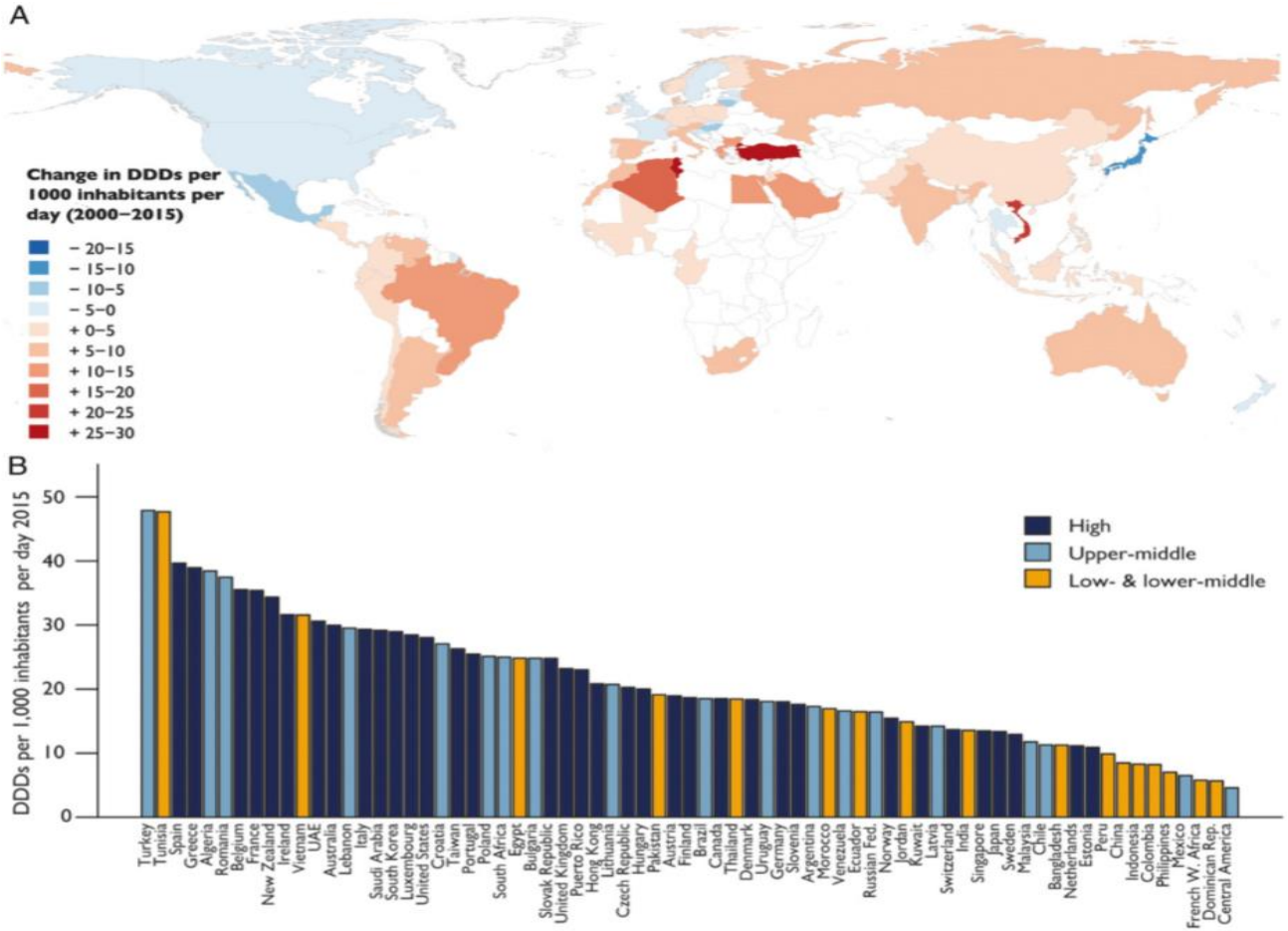

Figure 1.1: Global antibiotic consumption by country (2000-2015). The global map (top) displays the change in the national antibiotic consumption rate between 2000 and 2015 in Defined Daily Doses (DDDs) per 1,000 individuals. Histogram (bottom) indicates the antibiotic consumption rate by country for 2015 in DDDs per 1,000 inhabitants per day (Klein *et al.*, 2018).

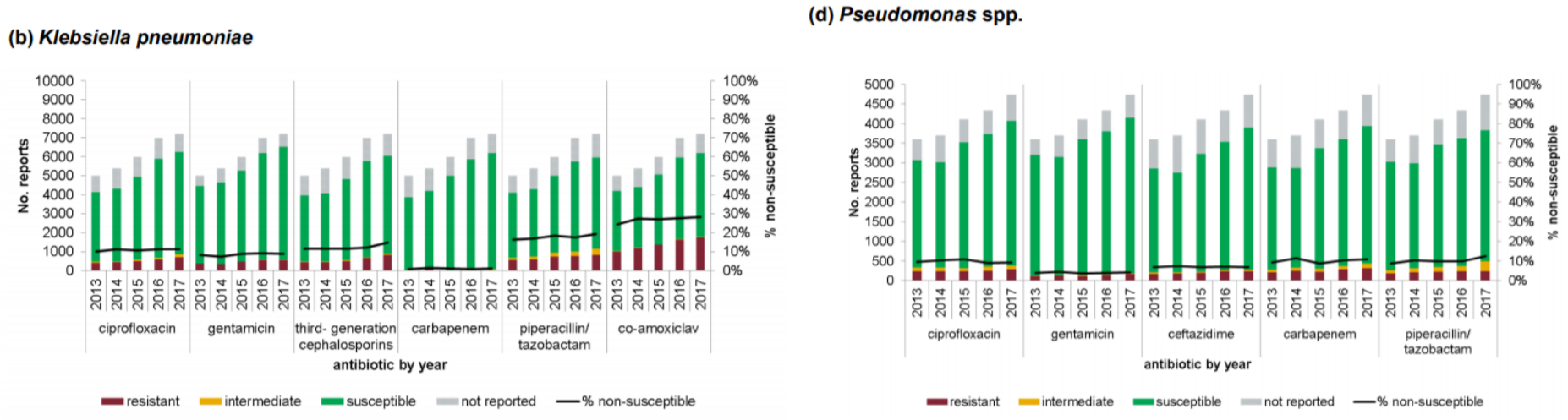

Figure 1.2: *Klebsiella pneumoniae* (left) and *Pseudomonas aeruginosa* (right) bloodstream isolates from healthcare centres in England, proportions of which are non-susceptible to antibiotics indicated (grey = unknown, green = susceptible, yellow = intermediate, red = resistant) (Public Health England, 2017).

In the UK, antimicrobial resistance trends were broadly stable, but Public Health England (PHE) found a small but increasing pattern of resistance towards certain antibiotics (Figure 1.2; Public Health England, 2017). One example was *Klebsiella pneumoniae*, where the numbers of isolates becoming clinically resistant to a number of antibiotics; including third-generation cephalosporins, such as ceftazidime, and carbapenems, grew between 2013 and 2017 (Figure 1.2; Public Health England, 2017).

An important area of medicine that continues to be greatly affected relates specifically to the respiratory system. Of particular focus to this study is the condition Ventilator-Associated Pneumonia (VAP). Within this area, evidence of increased resistance towards antibiotics is proving highly problematic in overall treatment (Bonten *et al.*, 2004; Denis *et al.*, 2019; Tedja *et al.*, 2014). The manner in which bacteria evolve mechanisms to counter such treatment is of considerable significance to research.

1.5 Ventilator-Associated Pneumonia

VAP is a commonly diagnosed condition within ICUs that affects between 8-28% of patients who are mechanically ventilated (Hunter, 2006). As a result of various complications regarding treatment of such patients, and the ever-increasing scale of antibiotic resistance, physicians are finding it difficult to manage VAP with little-to-no assistance of new antimicrobial agents being available for treatment. The attributable costs of VAP can range drastically, with figures from cases in the United States ranging between $1728 to $10,000 per event (Sosa-Hernandez *et al.*, 2019). Moreover, a review of treatment in Canada calculated the annual total cost of treating VAP to CAN$46 million (£26,960,600) (Muscedere *et al.*, 2008; Sosa-Hernandez *et al.*, 2019). Thus, it is essential to review our current knowledge on both antimicrobial resistance and lower-respiratory tract infections, as well as current practice attitudes when it comes to treatment, in order to reduce the risk of further mortalities within ICU settings and further economic costs as a result.

1.5.1 Ventilator Associated Pneumonia – Diagnosis

VAP is a condition that affects patients who have been severely compromised by a previous injury or severe infection within the respiratory system; such as cystic fibrosis, emphysema, or acute-respiratory distress syndrome (ARDS), and thereby require mechanical ventilation

(Hunter, 2006). Whilst undergoing ventilation, due to the use of the endotracheal tube, patients can contract VAP, due to opportunistic infection by microbes that bypass the host's natural defences (Park, 2005; Patil & Patil, 2017). The risk of infection can be increased thrsough the length of mechanical ventilation, prolonged stay within the ICU, and any previous antimicrobial treatment the patient may have had prior to ICU (Bonten *et al.*, 2004; Tuon *et al.*, 2017). It is important to clinicians to diagnose symptoms early in order to reduce the potential mortality and morbidity risk. Unfortunately, many cases often go undiagnosed until late-stage infection. One such issue is patient sedation as a result of ventilation, which means that the patient is unable to convey any issues they may have (Abdelrazik Othman & Salah Abdelazim, 2017). Diagnosis using clinical parameters has been found to either over-diagnose, or under-diagnose VAP, as evidence from necropsy studies have suggested (Fàbregas *et al.*, 1999). Thus, diagnosis relies on other methods.

Clinical signs of VAP include presentation of fever (>39°C), tachycardia, leucocytosis, purulent sputum, and a new or persistent infiltrate upon consultation via radiograph (Koenig & Truwit, 2006). However, these have limited diagnostic value, as most of these can be interpreted subjectively without any standardised system in place as when to commence treatment (Kalil *et al.*, 2016; Koenig & Truwit, 2006). Thus, it is often left to the presence of microbes within sputum samples to interpret whether antibiotic treatment should begin. The choice of microbiological sample, however, is another consideration that is often confounded by the sensitivity and specificity of the result, as well as the issue of whether such techniques would affect the patient (Koenig & Truwit, 2006; Micek *et al.*, 2015; Rello & Bunsow, 2016). At present, however, there is no 'gold standard' in terms of diagnosing VAP. Whilst it tends to rely heavily on the identification of the microbiological specimen, the time it takes to identify the microbe, and the method in which samples are taken can be a big issue. Examples of issues range from contamination of samples from the oropharyngeal tract (Goel *et al.*, 2016), where sample techniques such as bronchoalveolar lavages (BALs) can pick bacteria from the oropharyngeal microbiome alongside that consisting within the lung, leading to inaccurate microbial diagnosis. Another issue is potential harm to the patient leading to further potential complications, such as use of a lung biopsy, an invasive technique which can lead to internal bleeding and subsequent inflammation as a result of tissue damage. Microbiological samples also lack a reference standard in order to clearly diagnose VAP due to the complications and

debate surrounding safer, yet less accurate non-invasive techniques, and the more accurate invasive methods (Estella & Álvarez-Lerma, 2011). One accurate method would be to implement a lung biopsy, in order to collect lung tissue for histopathological examination to understand whether VAP or another respiratory condition is present based on cell structure and function (Fàbregas *et al.*, 1999). The use of biopsy methods, such as bronchoscopy and Protected Specimen Brush (PSB), has been used to collect samples that can be quantitatively cultured, and used then to differentiate between bacterial colonisation and infection (Ioanas *et al.*, 2001). The samples collected can be subsequently be stained with Gram-stain and Giemsa stain to assess the quality of the sample in terms of both bacterial (Gram-stain) and to compare the ratio of these bacterial cells to human cells (Giemsa) (Ioanas *et al.*, 2001; Marquette *et al.*, 1994). However, this is a highly invasive method. The invasive nature of biopsies can be a dangerous choice, as variables such as the condition of the patient, the potential physical stress to them, and the sensitive nature of operating with a ventilator present, could cause further harm (Rello & Bunsow, 2016). Questioning the method further, a previous study that conducted lung biopsies on post-mortem patients for the presence of VAP frequently reported false positives for the presence of VAP (Fabregas *et al.*, 1996), in absence of histopathology for pneumonia.

In most cases, sputum and bronchoalveolar lavage (BAL) samples are used, but these samples lack specificity and sensitivity due to the timing of infection, not collecting the bacterial sample at the apex of infection, and depend on experience of the operator at hand (Koenig & Truwit, 2006). The sample may also be contaminated by the presence of human squamous epithelial cells of the upper respiratory tract, or oropharyngeal secretions (Katayama *et al.*, 2010), which, due to the presence of two different microbiomes, both lung and pharyngeal, may not represent a definitive result for VAP microbiology. An interesting study by Fabregas *et. al.* (1999) highlighted the importance of early diagnosis when comparing radiological findings from recently deceased patients for common factors that may be present for VAP. They found that radiological infiltrates, alongside two of the three factors of leucocytosis, fever and purulent secretions provided an overall case sensitivity of 69% and specificity of 75% (Fàbregas *et al.*, 1999; Gunasekera & Gratrix, 2016). Other circulating biomarkers have been proposed to identify the presence of bacterial VAP within patients, for example procalcitonin (PCT) (Zilahi *et al.*, 2016). The presence of increased levels of PCT within a

patient has been associated with the increased prevalence of bacterial infection (Zilahi *et al.*, 2016), thus it seen as a promising marker to commence antimicrobial therapy. However the cost per patient, and potential inaccuracies in diagnostics due to rises in PCT as a result of patient stress and other non-bacterial causes may limit its application as a method (Lee, 2013). Thus, part of the problem when it comes to dealing with antibiotic resistance in this scenario is the subjective manner of medical staff interpretation as to when to commence treatment. This in turn leads to the issue of premature treatment; where if therapy is commenced too early or without confirmation of bacterial infection, can lead to the selection for resistance factors in residual microbial populations, or the potential for opportunistic infection from invading pathobionts. A survey conducted in 2014 indicated that doctors' perception of treatment timing is largely based on a variety of sources, largely due to the difficulty of diagnosis based on clinical evidence alone (Browne *et al.*, 2014). The reliability of such decisions, however, are to be debated. Responses from UK based healthcare agencies indicated a mix of diagnostic criteria for VAP have been used by physicians, including guidelines from the Canadian Thoracic Society, American Thoracic Society, Hospitals in Europe for Infection Control through Surveillance (HELICS), and the British Society of Antimicrobial Therapy (Table 1.2) (Browne *et al.*, 2014)

Table 1.2: Recognised criteria for the diagnosis of Ventilator-associated Pneumonia (VAP) (Browne *et al.*, 2014).

Guideline	Radiological Criteria	Clinical Criteria	Clinical Criteria
American Thoracic Society and Infectious Diseases Society of America	Presence of new or progressive radiographic infiltrates	**AND** at least two of: 1. Fever > 38°C 2. White cell count >12,000/mm^3 or <4,000/mm^3 3. Purulent secretions	
British Society of Antimicrobial Chemotherapy	New or persistent infiltrate on CXR	**AND/OR** Purulent tracheal secretions	**AND** Increased O_2 requirement **AND** Core temperature >38.3°C **AND** Blood leucocytosis (> 10,000/$mm^{3)}$ or leukopenia (<4,000/mm^3)
Association of Medical Microbiology and Infectious Disease Canada and Canadian Thoracic Society	One of the following abnormalities on CXR: 1. Evidence of alveolar infiltrates OR 2. Evidence of air bronchograms OR 3. New or worsening infiltrates	AND 2 or more of: 1. Temperature >38°C or <36°C 2. Leukopenia or leucocytosis 3. Purulent tracheal secretions 4. Decreased PaO_2	
Hospitals in Europe Linked for Infection Control thrsough Surveillance project (HELICS)	Two or more serial chest X-rays or CT-scans with a suggestive image of pneumonia for patients with underlying cardiac or pulmonary disease. In patients without underlying cardiac of pulmonary disease **one** CXR or CT scan is different	**AND** at least one of the following: 1. Fever 38°C with no other cause 2. Leukopenia (<4,000 WCC/mm^3) or leucocytosis (>12,000 WCC/mm^3)	**AND** at least one of the following: 1. New onset of purulent sputum, or change in character of sputum (colour, odour, quantity, consistency) 2. Cough or dyspnoea or tachypnoea 3. Suggested auscultation (rales or bronchial breath sounds), rhonchi, wheezing 4. Worsening gas exchange (e.g. O_2 desaturation/increased O_2 requirements/ventilation demand

The fact that there is a potential conflict in diagnostic and treatment guidelines is concerning, as each of these protocols may have different timelines or screening indications that may be outdated or insufficient in evidence, or may have different approaches based upon legal systems within their country of origin. Certain ethical considerations may be in place in certain countries that prevents certain interventions, which may cause potential issues such as prolonging treatment, or reduction in antibiotic dosage, that in effect can enhance potential for microbial resistance and morbidity/mortality.

1.5.2 Ventilator Associated Pneumonia – Epidemiology & Aetiology

VAP is a common infection within hospital environments, having a specific prevalence of between 13-16% (Trubiano & Padiglione, 2015). Whilst it has been reported that mortalities as a direct result of VAP are between 20-40% (Chastre & Fagon, 2002; Craven & Hjalmarson, 2010), these numbers tend to be overinflated as most occurrences of patient death is largely due to the underlying condition or comorbidity as a result of infection (Trubiano & Padiglione, 2015). The more accurate figure associated with direct VAP mortality is approximately 10%, although this value may drop as low as 1% if considerable precaution is taken to reduce factors that may prolong time spent in the ICU or increase risk of further infection (Bekaert *et al.*, 2011). It is important to note though that such figures may have increased since publication, so it is likely as a result of an increase in antibiotic resistance in specific species, or as a result in changes in medical practice that this may have changed. In some publications, they mention a similarly diagnosed condition; Ventilator-Associated Tracheobronchitis (VAT), which can be easily confused with VAP due to their overlap of similar microbiological criteria based on either qualitative and quantitative findings from endotracheal aspirate specimens (Craven & Hjalmarson, 2010). Thus, it is important that physicians are certain to report either a new or persistent infiltrate, though this may be difficult under critical circumstances (Craven & Hjalmarson, 2010).

There has been an increasing trend of multi-drug resistant (MDR) pathogens becoming more common in VAP-related cases. Pathogens include *Klebsiella pneumoniae*, *Escherichia coli*, *Pseudomonas aeruginosa*, and *Acinetobacter baumannii* (Craven & Hjalmarson, 2010; Hunter, 2006; Lorente *et al.*, 2007). The presence of these, and other microorganisms that are associated with VAP, differ depending on the stage recognised and diagnosed by the practitioner. Early-onset VAP, which is defined as an infection that has developed within the

first four days of ventilation, are typically colonised by "community" microorganisms; those of which are associated with Community-Acquired Pneumonia (Cilloniz *et al.*, 2016). The causative bacterial species are typically gram-positive, and include *Staphylococcus aureus*, *Streptococcus pneumoniae, Haemophilus influenzae* and anaerobes, and together make up between 20-30% of cases of VAP overall (Cilloniz *et al.*, 2016; Golia *et al.*, 2013). Early-onset VAP has been reported with an association of better clinical prognosis (Cilloniz *et al.*, 2016), however, further studies have noticed a increasing trend of MDR-pathogens being the causative agents of early-onset VAP, one such being Methicillin-resistant *S. aureus* (MRSA) (Khan *et al.*, 2016; Nair & Niederman, 2015), adding further complications to treatment and increasing the length of time spent in the ICU. The presence of MDR microorganisms in these circumstances also causes debate as to whether the classification of early-onset should be revised regarding the exact time of differentiation between early-onset to late-onset, and whether the inception point should be based on date of admission as opposed to intubation (Nair & Niederman, 2015; Restrepo *et al.*, 2013). Late-onset VAP is defined as VAP that has developed beyond the first four days of ventilation (Giard *et al.*, 2008), and the infection is typically characterised by gram-negative bacterial pathogens. These include enteric gram-negative bacilli (rod-shaped) bacteria, *P. aeruginosa*, and non-fermentative bacteria (which include *A. baumannii and Stenotrophomonas maltophilia*) (Ali *et al.*, 2016; Cilloniz *et al.*, 2016; R. Khan *et al.*, 2016; Nair & Niederman, 2015). Within this group of pathogens, MRSA can also be implicated as a causative agent of late-onset cases of VAP (Cilloniz *et al.*, 2016). Polymicrobial infections are also very common with regards to VAP, and are typically characterised by interactions between both *P. aeruginosa* and *Candida albicans*; a commonly isolated species of fungi within immunocompromised patients (Ferrer *et al.*, 2015; Rodrigues *et al.*, 2017).

The epidemiological profile of VAP is complex, firstly due to conflicts regarding distinction between early- and late-onset data. It can be further complicated due to the subjective nature of diagnosis. Information regarding VAP tends to be derived from two sources; reports specifically focusing on the microbiology or pure epidemiology of VAP as a result of surveillance programmes, and the second set is as an ongoing effort to contain the infection (Shorr *et al.*, 2011). The latter set provides information regarding the initial rate of VAP within a particular setting (Shorr *et al.*, 2011). Most surveillance studies have been conducted by

either national or international groups, of which tend to include large sample sizes and a number of varying academic and medical institutions being involved in providing data, each using their own methods. One such study includes the International Nosocomial Infection Control Consortium (INICC). A surveillance of 173 ICUs from 25 countries spanning 4 continents indicated that there was a lower rate of ventilator use in ICUs as opposed to surveillance data published in U.S. journals (Rosenthal *et al.*, 2010). However, device-associated infections (DAIs) were reported in higher numbers than the U.S. studies within the INICC report. It is possible that the study has included several institutions from areas that have poor hygiene controls. The INICC report included hospitals from Pakistan, Vietnam, Thailand and India, alongside others, as part of their study sample, all of whom are well known to be areas of low healthcare controls, and in recent research, areas of high MDR bacteria prevalence (Fletcher, 2015; Levy & Bonnie, 2004; Rosenthal *et al.*, 2010). Several species of bacteria were found in some of these institutions aswell, including MRSA, *Enterobacteria* resistant to ceftazidime (extended spectrum β-lactam producers) and *P. aeruginosa* resistant to fluoroquinolones, and prevalence of such were much higher within these compared to the survey conducted by the North American equivalent (Rosenthal *et al.*, 2010). Interesting to note however, enterococcal isolates were much lower, thus, it is likely that the three mentioned are far more commonly isolated species from sputum and ETT samples. Upon further examination into the background as to how much is spent per capita on healthcare, there are major socioeconomic factors that can affect infection rate within ICUs. In most INICC hospitals, it was reported that there is a lack of official regulations regarding hand hygiene, alongside insufficient funding into infection control programmes (Rosenthal *et al.*, 2010). In further detail, one study investigating the implementation of infection control within ICUs in low- and middle-income countries found that six middle-income countries out of a total of 16 overall had no surveillance care programme for VAP (Alp *et al.*, 2019). No evidence of surveillance within low-income countries was reported (Alp *et al.*, 2019). Because of the lack of sufficient GDP, low-income countries often find themselves overcrowded in ICU settings, along with the lack of sufficient numbers of medical supplies, and insufficiently trained medical staff to use specialist equipment properly (Rosenthal *et al.*, 2010; Rosenthal, 2016). When comparing the types of ICU and the infection rates within each one, the highest number tends to predominate from both trauma and neurosurgical ICUs (Shorr *et al.*, 2011), where

the number of cases are measured at 51.7 cases per 1000 days (trauma) and 25.3 cases per 1000 days (neurosurgical) (Rosenthal *et al.*, 2010; Shorr *et al.*, 2011). This is possibly due to the critical situation patients are in within both ICUs, with patients often being in the most severe circumstances when it comes to their personal health. Studies within US hospitals, which have a number of health regulations implemented and a much larger budget when it comes to healthcare, a similar trend was noted that VAP and hospital-acquired infections (HAIs) in general were highest in trauma ICUs (Shorr *et al.*, 2011). Interestingly, the National Healthcare Surveillance Network (NHSN) mentions that mixed medical ICU wards at non-teaching hospitals were the least prone to infection (2 cases per 1000 ventilator days; Edwards *et. al.*, 2009), most likely due to less mistakes being made by staff-in-training, and the fact that there are a high number of competing factors between bacteria at both species and environmental levels.

From all populations, it has been found that those in Western Europe undergoing heart surgery are the most prone to VAP, with episodes being reported at a rate of 13.9 per 1000 ventilator days, in comparison to INICC cardiothoracic ICUs, the rate is less than 10 cases per 1000 ventilator days (Shorr *et al.*, 2011).

Individuals who have undergone cardiothoracic surgery are often one of the key groups that are ignored with regards to VAP (Hortal, Muñoz, *et al.*, 2009; Shorr *et al.*, 2011), largely due to the fact that most studies focussing on the incidence of VAP after heart surgery are assessed from the perspective of single institutions with case-mix bias. It may be possible that a nosocomial infection may have been contracted through complications in surgery. Upon further examination into potential risk factors that may affect such patients, and VAP patients in general, advanced age and underlying conditions are the most prominent, whilst the type of surgery that can greatly increase such risk tends to be valvular replacement (Hortal, Giannella, *et al.*, 2009). From examining the risk of VAP development in heart trauma patients, specifically those who have experienced cardiac arrest; Hortal *et. al.* (2009) found that certain invasive measures during the course of surgery, including the need of inotropic support, intra-aortic balloon, or ascending aorta surgery. There is no evidence to suggest that the pathogens that cause VAP after major heart surgery are similar to those in other patients within ICUs (Hortal, Muñoz, *et al.*, 2009).

1.6 - Pathogenesis & Microbiology of Ventilator-Associated Pneumonia

Infection tends to progress based on the presence of biofilms within the EET and micro-aspiration of secretions as a result of ventilation (Gunasekera & Gratrix, 2016). The ETT provides a way in which microorganisms can bypass the natural barriers and immune defences the host body poses, such as the secretion of mucus from goblet cells and subsequent removal from the trachea by cilia cells (Koerner, 1997). However, the tube also provides a vessel for pathogenic bacteria to enter the lung as a result of exposure to the oral microbiome, and potential influx of gastric acid as a response to ventilation (Abdel-Gawad *et al.*, 2009). The endotracheal tube cuff can also act as a barrier to the exit of bacteria from the lower respiratory tract, thus perpetuating the issue due to the continuous entry of biofilms from the tube surrounding into the bronchi. This can extend the need for thoracic suctioning, which can cause further physiological stress to the patient, and increase the level of inflammation within the lung from trauma (Craven & Hjalmarson, 2010).

Both VAP and the closely related VAT tend to occur 48 hrs after intubation (Niederman *et al.*, 2005). The types of bacterial species that enter the trachea and lungs can contribute to disease progression. This is dependent on virulence within those species, and between that of others (Solh, Akinnusi, Wiener-Kronish, Lynch, & Pineda, 2008). Whilst it is the case that certain species are more commonly implicated than others, most cases of VAP tend to occur as a polymicrobial infection (Walkey *et. al.*, 2009). Previous reports have indicated that between 30-70% of diagnosed cases consist of more than one bacterial species (Bouza *et al.*, 2001; Joseph *et. al.*, 2010). These pathogens tend to infiltrate from either external sources, or from other microbiomes such as the oropharyngeal and gut and coalesce within the endotracheal tube. They are then able to disperse within the patient as mechanical ventilation takes place. Studies have frequently identified interactions between bacteria and the fungal species *Candida albicans* as a major source of infection (Fourie & Pohl, 2019; Fourie *et al.*, 2016; Harriott & Noverr, 2011; He *et al.*, 2014). Whilst fungal infections are common within ICU environments due to the critical nature of the patient, such pathogens are rarely the cause of VAP (Fourie & Pohl, 2019). The competitive nature of both fungi and bacteria at an inter-species level causes initial antagonism that can lead to further complications as the organisms produce factors to counter one another (Trejo-Hernández *et al.*, 2014). Thus, it is often the case that bacteria tend to be the major pathogens that are isolated from patients.

1.7 *Pseudomonas aeruginosa*

A commonly isolated bacterial pathogen from VAP patients is *Pseudomonas aeruginosa*, responsible for approximately 11-13.8% of all nosocomial infections (Driscoll *et al.*, 2007).

P. aeruginosa is a gram-negative bacillus that is often a prominent member of nosocomial infections. *P. aeruginosa* is widespread in nature, being found in waterborne and soil-based environments (Djordjevic *et al.*, 2017), and is recognised as a commensal within the human lung microbiome. However, under particular circumstances, the bacteria can be a causal agent within respiratory infections, such as VAP. According to a surveillance study conducted by the International Nosocomial Control Consortium, *P. aeruginosa* has been identified as a major pathogen due to its ability to resist several antibiotics (Rosenthal, 2016). This is based upon a longitudinal study comprised of 703 ICUs located worldwide between 2010-2015 (Rosenthal, 2016). Additionally, the European Centre for Disease Prevention and Control (ECDC) conducted a similar study by analysing data on nosocomial infections within ICUs across 15 European countries (plus Iceland, Liechtenstein and Norway) in 2014. The data they collected found that *P. aeruginosa* was the most frequently isolated microorganism in ICU-acquired pneumonia episodes and one of the most prevalent in ICU-acquired urinary tract and bloodstream infections (ECDC, 2017). As it is also classified as one of the ESKAPE pathogens identified by the WHO (Jagadevi *et. al.*, 2018; Santajit & Indrawattana, 2016), the level of clinical importance this species has makes it the subject of ongoing study and surveillance globally (Figure 1.3).

Regarding *P. aeruginosa* infections within ICUs, this prevalence increases, with a range between 13.2-22.8% when the pathogen has been identified (Driscoll *et al.*, 2007; Weinstein *et al.*, 2005). However, the data published may not be relevant to the current situation. More recent data reported that the global percentage of VAP cases caused by *P. aeruginosa* was 15.6% as of 2016 (Ramírez-Estrada *et al.*, 2016). The value of reported *P. aeruginosa* VAP cases in 2016 was also reported not to change even with the implementation of appropriate care bundles (Ramírez-Estrada *et al.*, 2016). Mortality associated with *P. aeruginosa* VAP is as high as 13.5%, even with appropriate antibiotic treatment (Ramírez-Estrada *et al.*, 2016). The mortality rate, however, increases if multi-drug resistant (MDR) strains are involved in the disease, to as high as 35.8%. Alarmingly, there has been a recent increase in the number of reports of carbapenem resistant bacterial strains of *P. aeruginosa*. This group of antibiotics

are widely-used within ICU cases, including VAP, due to their broad-range activity against multiple phyla of bacteria (Crandon *et al.*, 2016). Recent efforts to try and conserve use of carbapenems, such as Meropenem and Doripenem, have been proposed, such as the implementation of stewardship programmes (Gupta *et al.*, 2011).

A recent study conducted an analysis within healthcare centres in Thailand, and had found that there has been 15% increase of carbapenem-resistant *Pseudomonas aeruginosa* infections, to an overall percentage value of 30% between 2009-2013 (Palavutitotai *et al.*, 2018). A similar percentage was reported within 27 hospital in 14 European and Mediterranean states. Upon genomic analysis of strains collected from multiple infection types, including respiratory, bloodstream and skin infections, 30.6% of *Pseudomonas* strains isolated and sequenced during the trial in 2011 were found to express the metallo-β-lactamase group of genes (Castanheira *et al.*, 2014). Because of this, it is important that current healthcare systems take into consideration the prevalence of such resistance, particularly within an intrinsic setting, as areas such as ICUs can be seen as a reservoir for mutation and spread of infection due to a combination of both high-levels of antibiotic prescription, and potential misuse of these agents due to inappropriate antibiotic treatment (Luyt *et al.*, 2014; Mölter *et al.*, 2018; Zhang, 2015). Therefore, it is important to emphasise appropriate antibiotic use and to implement strategies, such as care bundles, to minimise potential spread of antibiotically resistant infection.

Due to extensive antibiotic resistance profile, its implication within VAP as a source of chronic infection, and its versatile genomic expression, *P. aeruginosa* is a bacterial species that is of particular importance in research and healthcare in general. Further emphasis of this comes from the O'Neill report, which estimates that infections from AMR pathogens, such as *P. aeruginosa*, will lead to 10 million deaths annually by 2050 (O'Neill, 2014). While this estimate could be inaccurate, it is undoubtedly an issue for which the global community must be prepared. Examining pathogens such as *P. aeruginosa* is essential in order to understand how the bacteria adapts to medical prophylaxis. Though there are issues in terms of understanding the full impact the bacteria may have at a host level due to ethical and physical constraints, the use of *in vitro* designs are nonetheless still effective. Through these means, we can create systems that allow us to examine the effects of antibiotics on bacteria within a controlled manner, and examine their DNA in order to understand changes in genetic structure which

may have led to adaptation. The endpoint of these experiments can help us define how *P. aeruginosa* functions to survive, and thus could provide crucial information on new potential targets for new approaches in antibiotic therapy.

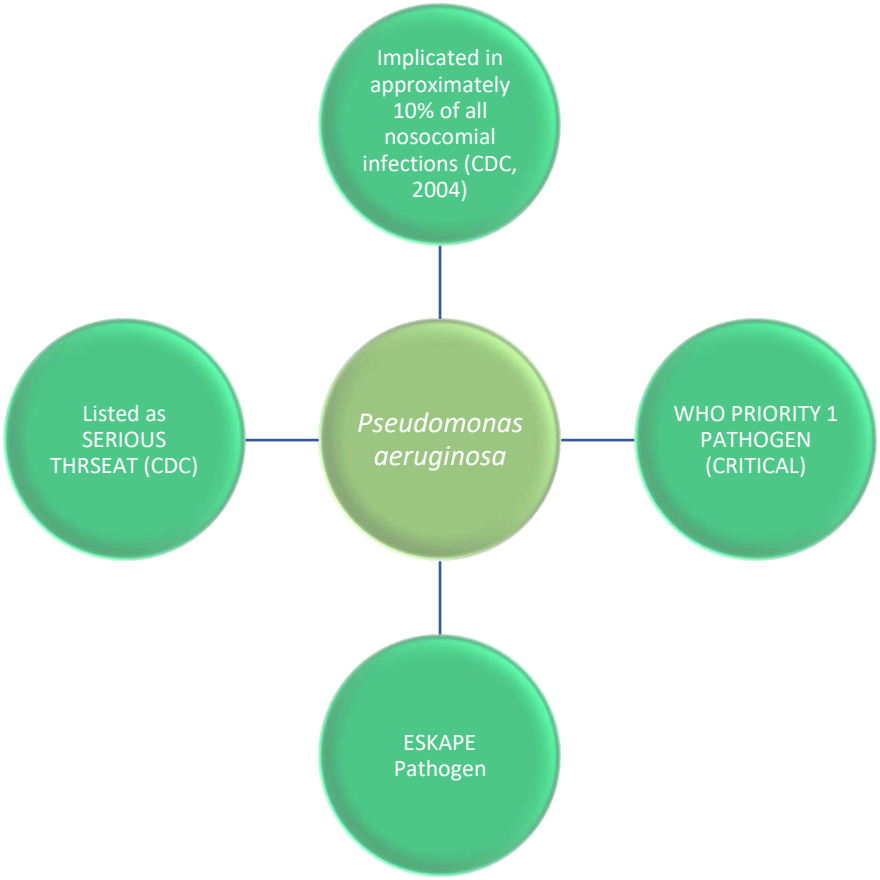

Figure 1.3: The clinical importance of *Pseudomonas aeruginosa*. The species has been classified as a Type 1 (Critical) pathogen by the World Health Organisation

1.7.1 Genetics of *Pseudomonas aeruginosa*

P. aeruginosa has been identified as a pathogen exhibiting extensive levels of antibiotic resistance, with its genetic makeup being composed of high levels of intrinsic and acquired resistance mechanisms. The first strain of *P. aeruginosa* to be sequenced was PAO1. This was first identified from a patient wound in Australia following a community-based study into genetic recombination (Holloway, 1955; Stover *et al.*, 2000). The strain, known to be the largest sequenced at the time, consists of a 6.3 mega base pair (6,300,000 base pairs) genome with 5570 predicted open reading frames (Botelho *et al.*, 2019; Stover *et al.*, 2000). No recent gene duplication was found within PAO1, indicating that the large genome resulted from genetic and functional diversity. This may explain why *P. aeruginosa* has such an extensive resistance profile, as the number of genes contained within its core genome may allow for it to adapt to treatment, as a result mutation under selective pressure. Indeed, it has been reported that genome size, alongside subsequent predicted regulatory genes, and complexity reflects the evolutionary adaptation of *P. aeruginosa* to various environments (Klockgether *et. al.*, 2011; Stover *et al.*, 2000), and in the presence of antibiotics (Long *et al.*, 2016; Wistrand-Yuen *et al.*, 2018). Alongside this, PAO1 strain *P. aeruginosa* has been found to contain approximately 150 genes that can encode proteins related to the outer membrane, all of which are involved in adhesion, motility, antibiotic resistance, and, virulence factor export (Botelho *et al.*, 2019; Chevalier *et al.*, 2017). This adds potential further issues to healthcare professionals, as key genes that may be involved in antibiotic resistance may well be intrinsic factors within the core genome.

P. aeruginosa appears to be, over time, expanding its genetic repertoire through the acquisition of new metabolic functions (Schick & Kassen, 2018). From further examination into *P. aeruginosa* colonisation in cystic fibrosis patients, it has been found that the bacterium adapts upon initial infection into various forms that are associated with chronic infection. A total of 18 distinct morphologies were identified across 120 populations of *P. aeruginosa*, all of which were of various strains (Schick & Kassen, 2018). These populations contained significantly more colony morphotypes within medium sufficiently rich with nutrient as opposed to minimal medium, thus displaying the ability of the species extent to adapt to stimuli within a particular environment.

Standard PAO1 laboratory isolates have also indicated that individual strains have an ability to adapt independently to metabolic changes, as they can produce a variety of molecular products, suggesting that alterations at a transcriptional and translational level and further evolution during culture and storage in lab environments (Botelho *et al.*, 2019). This has a potential, however, that when it comes to experimentation with *P. aeruginosa* that, even when using a reference strain, the reliability of results could be affected.

The structure of the *P. aeruginosa* genome is composed of a large number of core genes, in which strain specific genes are interspersed within (Dettman *et. al.*, 2013; Jeukens *et al.*, 2014; Klockgether *et al.*, 2011; Mulcahy, Isabella, & Lewis, 2013). These strain specific regions are also known to provide elements of variation within the genome, and mainly comprise the accessory genome. In total, the pan-genome is described as: 1) the core genome, which contains all of the genetic features that are identified in *P. aeruginosa* universally, and 2) the accessory genome, containing strain specific genes. The accessory genome genes tend to be inserted *en bloc* and encoded in specific loci, allowing the bacteria to express adaptive phenotypes (Botelho *et al.*, 2019; Valot *et al.*, 2015). The accessory genome of *P. aeruginosa* is extensive, and provides the means of genetic diversity within this species (Klockgether *et al.*, 2011). In comparison to other species, such as *Staphylococcus aureus*, *P. aeruginosa* displays a larger than average size (Boissy *et al.*, 2011; Botelho *et al.*, 2019).

The accessory genome presents various forms of genetic elements which modulates expression levels of elements within the bacteria. These genetic factors include integrons, transposons, genomic islands (GIs), prophages, plasmids and integrative and conjunctive elements (ICEs) (Klockgether *et al.*, 2011; Kung *et al.*, 2010). In general, microorganisms with larger genomes tend to be subject to horizontal gene transfer from different species (Baltrus, 2013). As *P. aeruginosa*, as aforementioned, has one of the largest bacterial genomes known as of present, it is not surprising to note that the majority of these genes have been acquired thrsough HGT. Most elements transfer and insert themselves within other areas of the genome, and are composed of a mosaic structure that is different to other mobile genetic elements (MGEs) (Botelho *et al.*, 2019). Once DNA from a foreign source is integrated into the genome of *P. aeruginosa*, it undergoes the same selective pressure as the core genome, and as a result, it may lose part of its original composition (Kung *et al.*, 2010). The MGEs target specific areas of the core genome that have plasticity, thus these regions are hotspots for

such (Kung *et al.*, 2010; Oliveira *et. al.*, 2017). The role of MGEs within bacteria can provide multiple benefits to the host, such as allowing them to persist for longer within a hostile environment, and changing genetic expression levels of certain molecules the cell may produce that aids it in quorum sensing and virulence (Kung *et al.*, 2010). However, these elements insert themselves into the genome of hosts as a means of self-preservation, and can at times cause mutations within the host that may be costly (Botelho *et al.*, 2019; Rankin *et al.*, 2011).

1.7.2 *Pseudomonas aeruginosa* and virulence factors

Different strains of *P. aeruginosa* have different long-term effects on the progression of VAP. Strains O6 and O11, which are the most common, are associated with a clinical resolution of 60%, whereas the more pathogenic O1 and O2 serotypes have often been implicated in cases resulting in a higher chance of mortality (Lu *et al.*, 2014). The differences between these strains have been thought to be due to individual expression of certain virulence factors, which in turn, provoke immunological and microbiological responses. Virulence factors are proteins or carbohydrates that are expressed by bacteria in order to increase their chances of survival, often through the production of molecules that allow growth and reproduction (Niu *et al.*, 2013) (Figure 1.4). These factors contribute to the pathogenicity of a bacterial species. The result of virulence factor production often leads to an immune response and subsequent host damage (Niu *et al.*, 2013).

One of the major virulence factors however that is often expressed during *Pseudomonas* infections is the Type III Secretion System (T3SS). It is often expressed during an acute infection, which more often or not causes significant mortality in trauma patients (Gellatly & Hancock, 2013; A. Hauser, Cobb, & Bodí, 2002; A. R. Hauser, 2009). The T3SS of P. aeruginosa is encoded by 36 genes on a series of 5 operons, with an additional 6 genes coding for effector proteins that are assorted randomly within the bacterial chromosome (A. R. Hauser, 2009). 4 of these effector proteins are expressed differently between different strains and isolates of *P. aeruginosa* (Yahrs & Wolfgang, 2006). Two of the effector proteins are the exotoxins; exoS and exoU, though it is rare that both of these are expressed together (Shaver & Hauser, 2004). These toxins, alongside others, can be injected directly into the cytoplasm of host cells (Hueck, 1998; Solh *et al.*, 2008). It is possible that the resulting necrosis of cells caused by these virulence factors recruit an innate immune response for cell clearance, thus resulting in

inflammation that has a significant impact on the prognosis of patients. *P. aeruginosa*, however, can evade such action via the secretion of exoS, which acts as a means to prevent internalisation of bacterial cells (Fleiszig *et al.*, 1997), thus further perpetuating inflammation as it evades cell lysis. As a result, the presence of factors that express the T3SS is often associated with a poor prognosis in general with regards to VAP (Solh *et al.*, 2008).

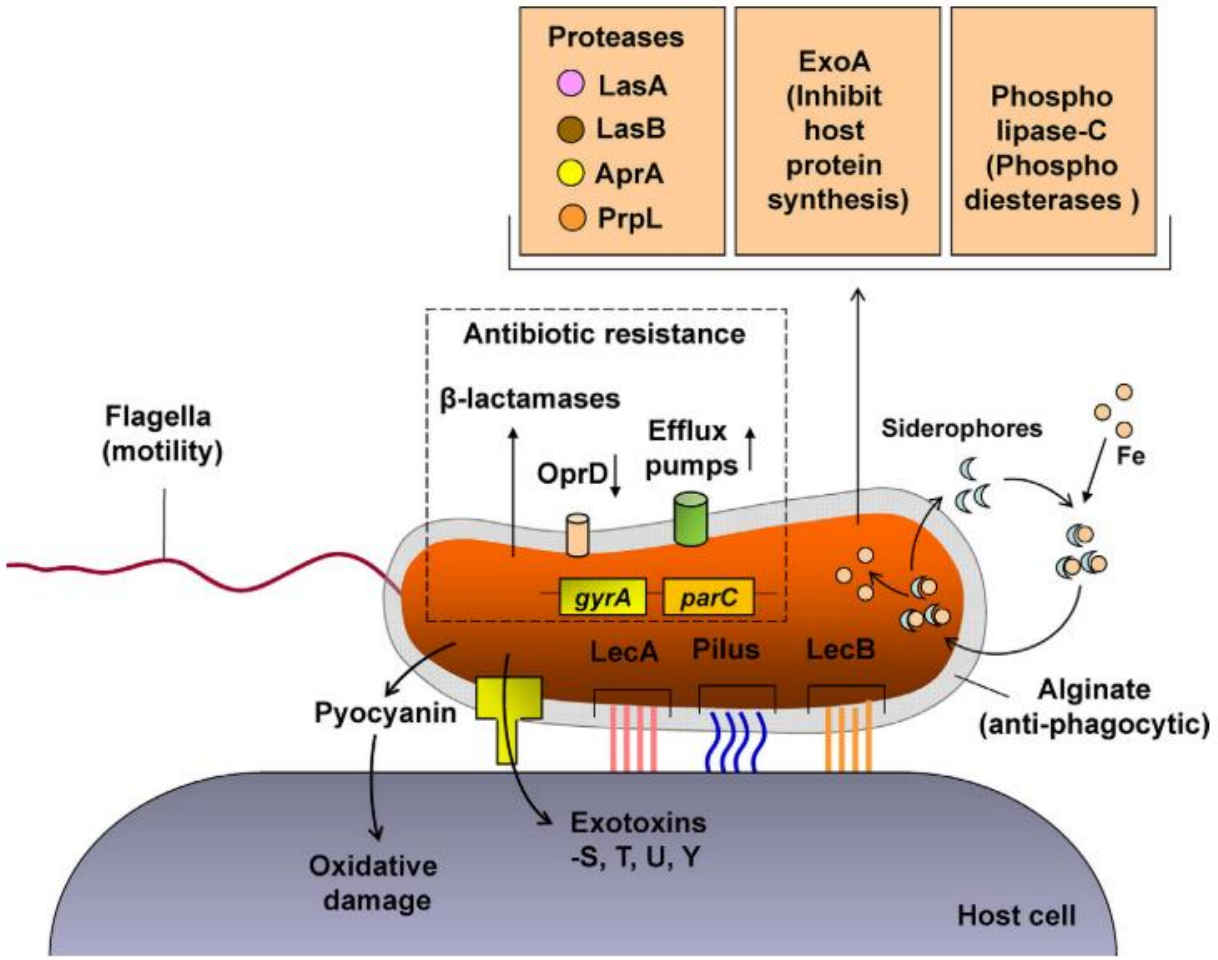

Figure 1.4: A representation of virulence factors produced by *P. aeruginosa* and antibiotic resistance mechanisms (Chatterjee *et al.*, 2016). Major virulence factors produced by *P. aeruginosa* include; exotoxins (A, S, T, U, Y,), pigments and siderophores (pyocyanin and pyoverdine), motility factors (type IV pili, flagella) and biofilms (Phl, Psl and alginate).

When grown in solid medium, such as Mueller-Hinton agar, *P. aeruginosa* can be visibly detected through the means of pigments that they express. Two of these provide a characteristically green colour to the colonies they form, but the shade of such pigmentation depends on which factor is increasingly expressed. These are known as pyoverdine and pyocyanin. Pyoverdine is not only a pigment, but more specifically a siderophore, a molecule that pseudomonads express as a means of securing folic acid from the external environment for metabolism (Budzikiewicz *et al.*, 2007; Schalk & Guillon, 2013). As of reports from 2013, more than 60 pyoverdines have been identified to be secreted by *Pseudomonas* species, and are comprised of three components. The florescence as a result of expression, as seen visibly with the naked eye upon observation of inoculated medium, of one such component, a dihydroquinoline-type chromophore (Schalk & Guillon, 2013). Production of siderophores takes place within the cytosol of the bacterium, before it diffuses out of the cell through means of an efflux pump, into the external environment (Nikaido & Pages, 2012; Schalk & Guillon, 2013). Pyoverdine is not associated with the pathogenicity of *P. aeruginosa*. Pyocyanin, however, is the other green pigment that can be implicated in the development of disease. This blue-green pigment is a redox-active secondary metabolite, thus, it can lead to oxidative stress within the host tissue where the bacteria inhabit, and interfere with cellular functions (Hall *et al.*, 2016; Streeter & Katouli, 2016). From an immunological perspective, the results of such oxidative stress causes the rapid cytokines that block the IL-2 receptors on T-cells, and a deactivation and subsequent decrease in the levels of immunoglobulin production within B-cells (Hall *et al.*, 2016). Further issues occur as not only adaptive immune cells are affected. Neutrophils are affected through apoptotic means, but before such cell destruction occurs, they are attracted to the pyocyanin molecules through chemotaxin secretion, mainly IL-8 and leukotriene B_4 (LTB_4), which then results in apoptosis (Hall *et al.*, 2016; Leidal *et al.*, 2001). With regards to the respiratory system, the activation of factors that lead to pyocyanin expression and secretion can result in large-scale damage to the patient, largely due to the production of free radicals as a result. Interestingly however, apart from large-scale studies into patients with cystic fibrosis, very little information is available regarding pyocyanin and its effect on the human respiratory system (Hall *et al.*, 2016; Hao *et al.*, 2012; Look *et al.*, 2005). The vast majority of information available is largely from *in vitro* studies.

Another important virulence factor is the ability to form biofilms. The formation of these structures is often associated with the presence of environmental stressors, which leads to them undergoing a period of slow development as they try to survive. Figure 1.5 provides further details on the development of biofilms. Bacterial communities living within one environment form a collective matrix of extracellular polymeric structures (EPS), which allows them to adhere to the area that they are colonising (Karatan & Watnick, 2009; Rasamiravaka *et al.*, 2015). EPS is composed of multiple molecules, including exopolysaccharides, extracellular DNA, and protein molecules (Rasamiravaka *et al.*, 2015). This creates a highly hydrophilic, polar environment that contributes to the persistence of the matrix structure (Rasamiravaka *et al.*, 2015). In the case of *P. aeruginosa*, the Pel and Psl polysaccharides are the major contributing unit to biofilms (Ma *et al.*, 2009). Whilst it provides a means of persistence in a sense of "claiming" an area, it also provides a means of protection against certain molecules, such as antibiotics and sterilising agents. Once a biofilm is established, it can provide a means of resistance against natural stressors such as UV light and changes in pH. It also provides a means of added protection against the effects of phagocytosis if exposed to an immune response. Biofilms are also one of the major causes for the increasing prevalence of antibiotic resistance (Høiby *et al.*, 2010; Jamal *et al.*, 2018; Taylor, Yeung, & Hancock, 2014). Planktonic (freely moving) bacteria initiate the development of a biofilm by reversibly adhering to a surface (Bowen *et al.*, 2018). In planktonic form, bacteria are largely susceptible to antibiotics. Under mature biofilm conditions, however, the matrix provides a much higher resistance to antimicrobials by around 10-1000 fold (Taylor *et al.*, 2014). The high level of resistance that is conferred as a result of the presence of a biofilm is thought to arise due to adaptive genetic changes.

A recent study has somewhat questioned the traditional view that biofilms are the true stage of antibiotic resistance, as the evidence suggests that other factors can lead to full resistance regardless of biofilm production. Ahmed *et. al.* (2018) developed an experiment using PAO1 strain P. aeruginosa, in which the isolate was exposed to ever varying concentrations of ciprofloxacin. The isolate was inoculated whilst both in planktonic and biofilm-forming phases. Through genetic sequencing, Ahmed *et. al.* detected that the overall frequency of ciprofloxacin resistant gene expression (CIP) was higher in biofilm forming isolates of PAO1, however, the minimum inhibitory concentration (MIC) of planktonic cultures were much

lower. Thus, it is possible to deduce that planktonic cells are perhaps more resistant towards antibiotic treatment than biofilms. This may, in part, have been due to other means however. For instance, it was found upon further examination of factors expressed by the *P. aeruginosa* samples that there was a general decrease in the expression of type-IV pilus (Ahmed *et. al.*, 2018), which enable the bacteria to move through the environment to which they have infected. When comparing this to other areas of research, such as in Pseudomonas infection in cystic fibrosis patients, there seems to be a consistent trend of reduced motility factors in response to chronic infection (Lebeaux *et al.*, 2014). It is possible that this reduction may be a specific response to external factors that may limit the growth of P. aeruginosa populations, such as the immune response and its recognition of such accessories as a foreign entity. However, there is little evidence to suggest that the loss or increase in expression of motility factors has any correlation towards antibiotic resistance in Pseudomonas spp., and further afield.

Virulence factors that lead to resistance, otherwise coined resistance factors, are genetic factors that are expressed as a result of adaptation towards environmental pressures. Resistance factors are plasmid-transferred, allowing for bacteria in potentially large, varied populations to transfer accessory genes that may well allow for more suitable phenotypes for the area that they have colonised. At a molecular level, plasmid mediated factors are transferred primarily through the means of horizontal transmission, most commonly thrsough conjugation, where individuals within a bacterial population can effectively transfer plasmids to one another by transferring plasmids and other accessory genomes to one another (Bennett, 2008). Other means can be through transformation, where the remains of a lysed bacteria can be endocytosed into a living bacterium, and thus the existing individual can inherit the potential plasmid containing a resistant factor, into their genome. Plasmids exist completely separate from the main chromosome, however, the alleles that they carry are perhaps the most defining feature of a bacterium when it comes to natural selection (Bennett, 2008). These alleles can also provide a means of surviving toxic metals, such as mercury, cadmium and silver (Bennett, 2008), should a colony be exposed to such within their environment, thus further carrying the essential weight that the accessory genome has become in terms of defining resistance to medication.

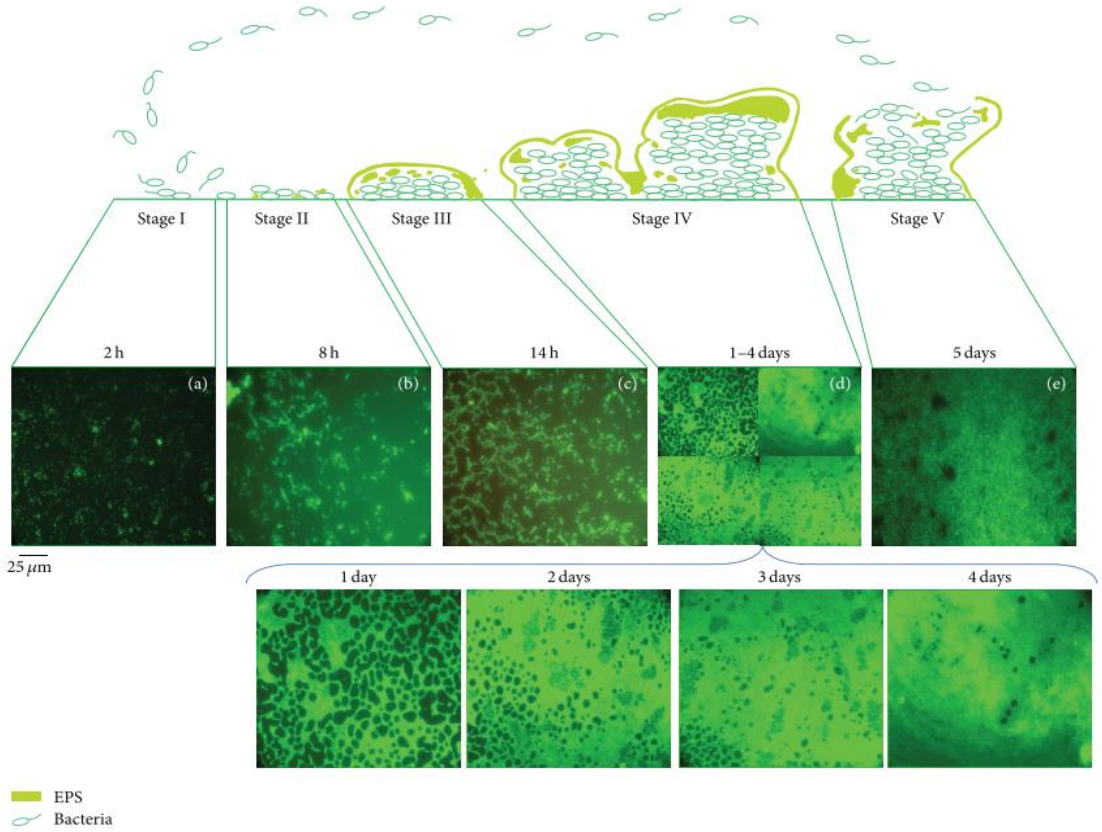

Figure 1.5: The life cycle of biofilm formation, specifically *P. aeruginosa* PAO1 reference strain biofilm grown within glucose minimal media (Rasamiravaka *et al.*, 2015). Stage I depicts the initial colonisation and attachment to a surface by planktonic bacteria, which then becomes irreversible by Stage II. A microcolony subsequently forms (Stage III), before maturing into a biofilm and establishing a 3D-community (Stage IV). Dispersion of the biofilm occurs at Stage V, releasing planktonic bacteria to colonise other surfaces and form further biofilms.

In the case of *P. aeruginosa*, a particular plasmid of interest to research is resistance plasmid RP1, which can be also defined as RP4 or RK4. This plasmid was first discovered in *P. aeruginosa* S8, and was reported to provide factors of resistance against tetracycline, kanamycin, neomycin and carbenicillin (Saunders & Grinsted, 1972). As this report was published back in the 1970's however, and with the ever-increasing use of antibiotics, it is likely that other antibiotics could be part of this plasmid's resistance repertoire, or that more factors are involved. Plasmids can vary in size, from 2-3 genes or to several kilobases (kb), and thus making up a vast sum of the host chromosomal content (Bennett, 2008). One such example of a large scale plasmid can be found in *Escherichia coli*, in which one plasmid comprises of 10% of the overall genetic material contained within the bacterium (Bennett, 2008). Another more recently discovered large-size plasmid variant was found within *S. aureus* ST398, which carries three *ermT* plasmids, each all large in size and carrying resistance genes towards heavy metals, specifically cadmium and copper (Dweba *et al.*, 2018; Gómez-Sanz *et al.*, 2013). Thus, it is highly possible that a significant part of a bacterium's genetic material is partly made up of virulence factors, or perhaps resistance factors. Plasmid-encoded resistance embodies the vast majority of the reasons as to why current medication is rendered ineffective in the presence of infection. However, it is not the plasmid that is the main source of development of potential pathology and resistance per se, rather it is the genes that they carry that leads to an expression of peptides that lead to such.

Whilst plasmids provide bacteria with benefits such as the ability to express genes that confer resistance, they can also be of hinderance to bacteria in the long term. Research has highlighted the existence of a fitness cost; that the host cells, whilst gaining the ability to survive in the presence of heavy metals or antibiotics, will have a reduced capacity to expand as a population (Kottara *et al.*, 2018). In the case of PAO1 strain of *P. aeruginosa*, it has been found that plasmids can affect the growth rate of populations, reducing this rate across a range of environments (San Millan *et al.*, 2018). Intriguingly, plasmid-bearing populations of PAO1 were found to differentially expressed clusters of genes that are responsible for metabolism-related functions (San Millan *et al.*, 2018). Plasmids pAMBL1 and pAMBL2, two plasmids that carry metallo-β-lactamase resistance genes (San Millan *et al.*, 2015; Tato *et al.*, 2010), preferentially alter the expression of metabolic genes within PAO1 (San Millan *et al.*, 2018). pAMBL-1 in particular has been associated with the over-expression of genes related

to glutamine synthesis within the bacteria, and under-expression of genes related to degradation and metabolism of other amino acids, including tyrosine and phenylalanine (San Millan *et al.*, 2018). Whilst it appears that plasmids influence the metabolic ability of each bacterium that possesses resistance factors, the cost that is attributed to possessing these plasmids is somewhat vague. Recent reports have noted that, whilst possessing plasmids leads to high costs, *P. aeruginosa* is perhaps capable of possessing genes that express resistance against external stressors, based on the existence of mutants that exhibit copper resistance (Kottara *et al.*, 2018). To our knowledge, there is little research that focusses on whether accessory gene based resistance factors can be inherited into the core genome of *P. aeruginosa*, even though efflux pumps are an example of factors that are overexpressed to counter antibiotic-related stress.

1.8 - Research Aims and Potential Outcomes

The purpose of this study was to examine the capability of a clinical isolate of *P. aeruginosa* to adapt to various antibiotics that are prescribed to counter infections, which the bacteria is the causative agent. As mentioned, though it is widely known that *P. aeruginosa* is capable of expressing multiple virulence factors that allow types of medication to be rendered null in treatment, there has been little evidence exploring multiple types of antibiotics being tested with a single isolate. This approach would allow us to observe a more complete extent of mutations within the bacterial genome of *Pseudomonas*. The study was composed of multiple aims:

- To examine the effects of adaptation to broad-spectrum antibiotics.
- To gather data on what mutation have occurred by sequencing the genome of the *P. aeruginosa* isolate in comparison to the original parent isolate.
- Whether these mutations have led to a phenotypic change.
- Whether the adaptions have led to advantages or disadvantages in terms of intra/inter-species competition and nutrient metabolism.

The research conducted will provide an early basis of a study, providing information that may be crucial in terms of understanding what factors could be essential regarding the scale of antibiotic resistance within a local ICU. As of present, the evidence surrounding antibiotic

resistance in VAP is somewhat limited, and this study will provide significant information that could contribute to a continuing field of research. The results from this study could be useful in terms of providing a means of further research into ICUs both nationally and internationally with regards to antibiotic resistance in VAP patients. Physicians could use the data to modify current prophylactic regimen regarding *P. aeruginosa* infection in VAP, as the data will display the development of resistance patterns as the bacteria begins to adapt to treatment. Since VAP infections are largely polymicrobial, the focus on one specific bacterial species implicated in lung colonisation and subsequent infection can provide a means as to how genetic expression could spread to other species. The molecular evidence collected from the genomic sequencing could identify potential new target genes for future study, whether certain combinations of alleles lead to a phenotypic change, and whether these selective mutations can be exploited in other ways.

2. METHODS & MATERIALS

2.1.1 - Media Preparation

Laboratory media used were Mueller-Hinton (MH) Agar, and MH Broth (VWR Scientific, Brooklyn, NY), and M9 Broth. All of these materials were prepared according to manufacturer guidelines. All materials were autoclaved prior to use at 121°C for 15 mins.

2.1.2 - Source of Parent Strain

The strain used was a lung clinical isolate collected from Royal Liverpool hospital. Ethical approval was sought before extraction from the patient prior to study. The strain was kept at -80 in 50% Phosphate Buffered Saline (PBS)/50% glycerol prior to use within a 1.5mL cryo-tube.

Cultures were maintained on MH agar.

2.2 - *Pseudomonas aeruginosa* adaptation to antibiotics

2.2.1 - Antibiotics and Disc Diffusion

Disc diffusion experimentation was set out under standard protocol. The antibiotics selected for this adaptation experiment were selected based on the susceptibility profiles listed within EUCAST guidelines (EUCAST, 2019) The following antibiotics, and concentrations, were selected for disk diffusion. Each antibiotic disc was supplied from the same source (Oxoid, Basingstoke, Hampshire, UK) unless stated otherwise:

- Meropenem 10µg
- Doripenem 10µg
- Imipenem 10µg
- Ceftazidime 10µg
- Ceftazidime/Avibactam 10-4µg (MAST, Bootle, Liverpool, UK)
- Colistin 10µg

One loopful of *P. aeruginosa* isolate was placed within PBS (5mL) and vortexed, before 2 drops of suspension was inoculated onto a fresh MH agar plate and spread. One antibiotic disc was applied to a plate using sterile forceps.

In total, 5 replicates were conducted for each antibiotic. Plates were inverted and incubated for 24 hrs at 37°C.

2.2.2 - Examination of Antibiotic Action and Establishment of subsequent passages of *P. aeruginosa*

After incubation, the plates were removed and inhibition zone diameter was measured using a ruler, with measurements recorded in millimetres (mm). A section of colonies found at the edge of the inhibition zone were streaked via a sterile loop and placed within PBS (1mL) and spread onto new plates via the method as previously described with new antibiotic discs and subsequently incubated.

This method was repeated 15 times, resulting in 15 passages. Inhibition zone results were noted at Passages 1, 2, 3, 4, 5, 10, and 15. Frozen glycerol stocks were processed at Passages 1, 2, 3, 4, 5, 10 and 15 for potential future analysis. These samples were made by combining 500uL of PBS/*P. aeruginosa* suspension, before applying remaining suspension to plates, with 500uL Glycerol (VWR Scientific, Brooklyn, NY) in 1.5mL cryovials. A sample of each plate was gram-stained and observed to confirm species identity and rule out contamination.

Experiments were terminated after Passage 15 or upon encountering complete resistance in the form of no observable inhibition zone in the presence of antibiotics.

Table 2.1: Isolates created from the disc diffusion experiment from the original Parent *P. aeruginosa* strain.

Antibiotic	**Passage No.**	1	2	3	4	5	8	10	15	30
Meropenem		PAM1	PAM2	PAM3	PAM4	PAM5	N/A	PAM10	PAM15	N/A
Doripenem		PAD1	PAD2	PAD3	PAD4	PAD5	N/A	PAD10	PAD15	N/A
Imipenem		PAI1	PAI2	PAI3	PAI4	PAI5	N/A	PAI10	PAI15	N/A
Ceftazidime		PACe1	PACe2	PACe3	PACe4	PACe5	PACe8	N/A	N/A	N/A
Ceftazidime/Avibactam		PACeA1	PACeA2	PACeA3	PACeA4	PACeA5	N/A	PACeA10	PACeA15	N/A
Colistin		PACo1	PACo2	PACo3	PACo4	PACo5	N/A	PACo10	PACo15	PACo30

Statistical analysis of results was performed via GraphPad Prism 8 using both Paired T-test (to compare Parent inhibition zone diameter with the inhibition zone recorded at experiment termination), and ANOVA (comparing all passages per antibiotic) tests with additional Tukey's tests.

2.3 Measurement of Growth and Biofilm Production

2.3.1 - Inoculation of Stock culture

Stock cultures of *P. aeruginosa* were setup using adapted isolates that were established from the previous disc diffusion adaptation experiment outlined in Section 2.2.2. The adapted isolates were:

- PAO1
- Parent strain (un-adapted isolate)
- PAM15
- PAD15
- PAI15
- PACe8
- PACeA15
- PACo30

It should be noted that the Colistin-adapted strain that was included as a stock cultures was a strain that had been adapted after 30 passages. The previous experiment (Section 2.2.2) was inconclusive for any evidence of adaptation to Colistin after 15 passages, and the *P. aeruginosa* strain was selected for further disc diffusion adaption.

2.3.2 - Dilution preparations

Overnight cultures of strains listed in Section 2.4.1 were diluted in MH broth to an OD600 of 0.05.

2.3.3 - Growth/Biofilm Assay setup

Cultures were used to inoculate 96 well microtitre assay plates (Thermo Fisher, Waltham, MA) as set out in Figure 7. Sterile controls (MH broth) were also included. All experimentation was conducted within a laminar flow cabinet to minimise chances of contamination.

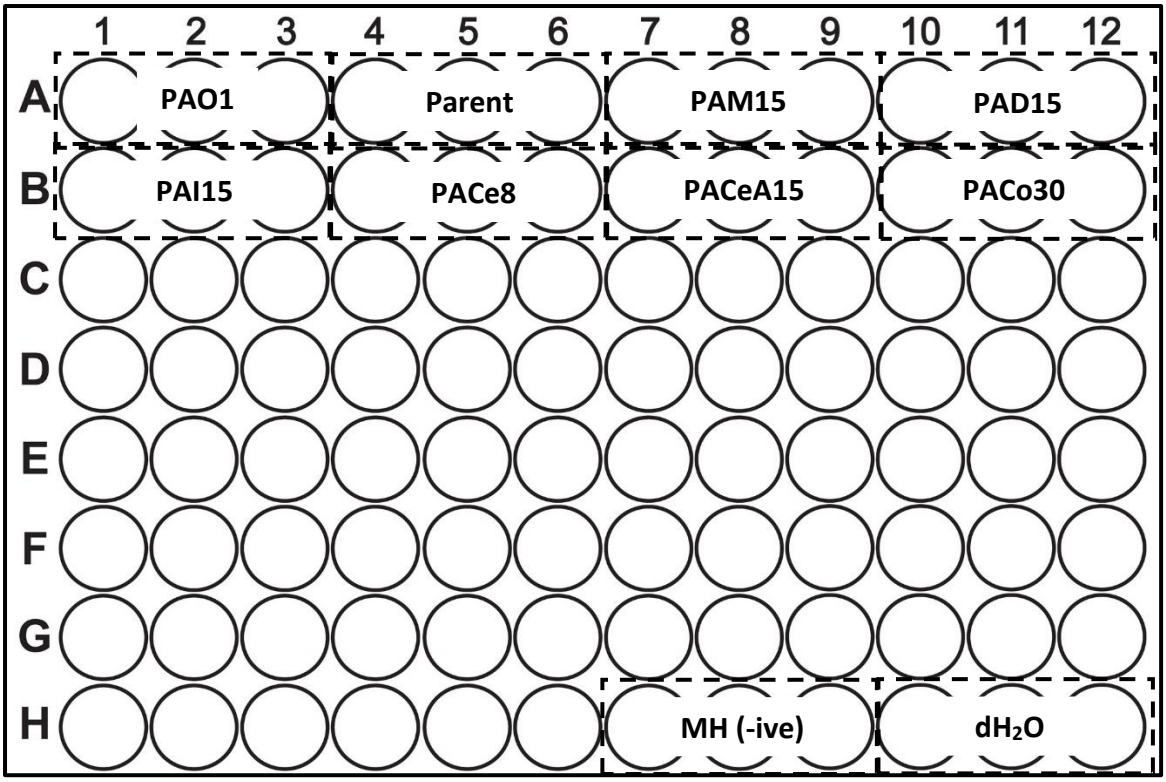

Figure 2.1: Layout of the Growth/Biofilm assay used to measure growth and biofilm production of all strains.

Replicate plates were inoculated to measure planktonic OD600 (0hrs, 3hrs, 6hrs, 12hrs, 24hrs, and 48hrs) and biofilm production (0hrs, 3hrs, 6hrs, 12hrs, 24hrs, 48hrs).

All plates were placed within an orbital shaking incubator at 37°C at a speed of 100 RPM. Each plate was set within a sealed Tupperware container with moist tissue paper in order to minimise potential edge effect; where a combination of increased ventilation around the edge of a well, and evaporation as a result of incubation cause planktonic cells to stick to the edge (Shukla & Rao, In Press). This can present a false reading in relation to crystal violet staining and biofilm biomass.

At each timepoint, relevant plates were removed from the orbital shaking incubator and 3 measures of distilled water (200µL) was injected into three separate wells as a blank measure. The OD was read at 600nm (using a FLUOstar Omega plate reader (BMG LABTECH, Offenburg, Germany)).

2.3.4 - Setup of CFU measurements

Colony Forming Units (CFUs) of each adapted isolate were quantified following a similar method to that outlined by Miles & Misra (Miles & Misra, 1931). Upon completion of plate reading for growth, 1:100 stock dilutions of each isolate were established for preparation of CFUs. A 10-fold dilution technique was established to create subsequent PBS suspensions ranging from 10^{-3} to 10^{-8} in concentration in a fresh 96 well plate. Each dilution (20µL) was dispensed onto a fresh agar plate, in an established sector, to create a spot test assay and left to dry in a laminar flow cabinet to minimise contamination. This was repeated 3 times per isolate, creating in total 3 plates per isolate. The plates were incubated at 37°C for 24hrs before a colony count was then performed. Colonies were counted in the sector where the highest number of full-size discrete colonies was seen, and the dilution was noted. CFUs were calculated via the following method:

$$CFU\ per\ ml\ =\ Average\ number\ of\ colonies\ for\ a\ dilution\ x\ 50\ x\ dilution\ factor$$

2.3.5 - Biofilm staining and measurement

After removal of a sample for CFU calculations, the plate(s) were washed using PBS 3 times, before being stained with 0.1% Crystal Violet (200µL per well). The Crystal Violet suspensions were left for 10 mins, before being removed and washed 3 times with PBS. Plates were then inverted and left to dry in air overnight.

200µL of 70% ethanol was injected into each well to degranulate residual Crystal Violet and left for 10 mins before being read at OD600 using a FLUOstar Omega plate reader.

2.3.6 - Statistical Analyses

Growth curves, biofilm formation curves and CFU charts were plotted using Microsoft Excel. Comparisons between PAO1 and Parent strains for differences in growth and biofilm formation was conducted through Two-way repeated measures ANOVA (and subsequent post-hoc analyses). This was implemented to measure differences in overall growth patterns and at specific timepoints. The same analyses were detected for comparisons between the Parent strain and adapted isolates for detection of changes that correspond to adaptation. All statistical analysis was conducted using GraphPad Prism 8. Specific growth rates (µ) were calculated using data collected from OD600 values at the point of peak growth and calculated CFU/mL.

2.4 - Measurement of Growth under Co-infection conditions

2.4.1 - Inoculation of Stock Culture

Stock was prepared in a similar manner to the previous experimental methods for Biofilm and Growth Curve analysis. Cultures were set up with the following isolates:

- Lab strain *Staphylococcus aureus*
- *Pseudomonas aeruginosa* strain PAO1
- *P. aeruginosa* Parent strain
- PAM15
- PAD15
- PAI15
- PACe8
- PACeA15
- PACo30

A loop-inoculate of each isolate was added to separate MH broth solutions (10mL) within 15mL FALCON tubes. All stock solutions were vortexed for 5 seconds and incubated overnight at 37°C.

2.4.2 - Dilution preparations

All incubated stock broths were removed after overnight incubation and vortexed for 5 seconds. Samples (1mL) were dispensed into separate cuvettes and absorbance of the sample was read at 600nm. The resultant OD600 value was used to dilute stock solutions to 0.05 in 20mL using MH broth as a dilutant.

2.4.3 - Control Plate setup

Similar to the Growth Curve/Biofilm Assay setup, 3 repeat measures of stock culture (200µL) was dispensed into thrsee separate wells within a 96 well microtitre plate. This was repeated for each isolate included within this phase of the experiment. An *S. aureus* control group was included as a positive control to measure against co-infection in the separate co-infection assay. Separate plates were established for separate timepoints; those being 0hrs, 3hrs, 6hrs, 12hrs, 24hrs, and 48hrs. A series of 3 separate wells was filled with MH broth as a negative control, alongside 3 separate wells were spared to use as blanks. Remaining MH stock cultures were then diluted to an OD600 of 0.025 for the co-infection condition.

2.4.4 - Co-infection Plate setup

3 repeat measures of stock culture (100µL), except for *S. aureus*, was added to 3 separate wells within a 96 well microtitre plate. Upon completion, *S. aureus* stock (100µL) was added to each inoculated well to establish a co-infection condition with an overall OD600 of 0.05. 6 separate wells were spared; with 3 being filled with MH broth as a negative control, and 3 others as blanks. A series of co-infection plates were established, with one plate per timepoint. The timepoints that were chosen were as follows; 0hrs, 3hrs, 6hrs, 12hrs, 24hrs, 48hrs.

2.4.5 - Experimental Procedure

All plates, both control and co-infection, were placed within an orbital incubator set at 37°C and a speed of 100RPM. All plates were placed within sealed, sterile Tupperware boxes, with diluted water (dH_2O) soaked paper towels placed below the plates to ensure the assays were within a moist environment. At certain timepoints, corresponding plates were removed and their absorbance read at OD600 using a FLUOstar Omega plate reader. dH_2O (200µL) was used as a blank within each plate.

As with the previous method for Growth Curve and Biofilm analysis, once read, a sample each repeat was removed and a 1:100 dilution of each isolate sample was established for CFU analysis. These PBS stock samples were diluted further in a fresh 96-well microtitre plate to establish separate dilutions ranging from 10^{-5} to 10^{-8}. 20µL of each diluent was dispensed into corresponding sectors on a fresh agar plate to create a spot test assay. This was repeated 3 times to create 3 repeat plates for each time point selected. Once all diluents were dispensed, the plates were left to dry within a laminar flow cabinet for 20 mins, before incubating at 37°C for 24hrss. Resultant colonies were counted after 24hrss, with colonies at the highest concentration noted.

Biofilm analysis was also performed in the same manner as previous. Plates were washed 3 times with PBS and stained using 0.1% Crystal Violet (200µL). The stain was left for 10 mins before being emptied and the plate being washed another 3 times with PBS. These plates were left to dry overnight. 70% ethanol (200µL) was dispensed into each well to degranulate any remaining Crystal Violet stain before each plate was read at OD600.

2.4.6 - Statistical Analysis

Growth curves and biofilm curves were plotted using Microsoft Excel. Statistical tests, namely Two-way repeated measures ANOVA (and subsequent Sidak Post-Hoc) were used to test for significant differences between control and co-infection growth rates using GraphPad Prism 8.

2.5 - Measurement of Growth under restricted carbon resources – 20% Glucose and 20% Alanine

2.5.1 - Setup of carbon-restricted media culture and strain list

The procedure for establishing stock cultures was similar to sub-section 2.3.3 (Standard Growth Curve and Biofilm analysis) though with modifications. All sample stock cultures used the same bacteria as previously mentioned, though the medium used itself was different. The medium consisted of two different types, thus establishing two different experimental conditions. Both stock media were made up with 1X M9 Minimal Medium broth supplemented with either 20% Glucose (Sigma-Aldrich, St. Louis, MI) or 20% Alanine (Sigma-Aldrich, St. Louis, MI). Each sample was inoculated with one loopful of bacteria, in a similar fashion to that of sub-section 2.3.3 The following bacterial isolates were chosen:

- PAO1
- Parent strain (un-adapted isolate)
- PAM15
- PAD15
- PAI15
- PACe8
- PACeA15
- PACo30

Once all stock samples were inoculated, each were vortexed for 5 seconds and incubated overnight at 37°C.

2.5.2 - Dilution preparations

Dilution setup was conducted in a similar conduct to that established during the Growth Curve and Biofilm experimental procedure. Stock samples were removed from incubation after overnight growth, and a sample of each stock was placed within separate cuvettes and their absorbance was read at OD600. Once read, each stock solution, both 20% Glucose and 20% Alanine variants, were diluted to an absorbance value of 0.05 at OD600 using spare M9 broth with respective carbon supplement.

2.5.3 - Growth/Biofilm Assay setup

3 repeat measures of 0.05 (OD600) stock (200µL) was transferred into 3 wells of a sterile 96-well microtitre assay plate. 2 plates were required per timepoint as to separate each stock depending on the carbon supplement that was immersed within the M9 broth solution, that being either 20% Glucose or 20% Alanine. A set of 3 repeats was created per bacterial sample in the microtitre plate(s). As mentioned, sets of two plates with samples were established for each chosen experimental timepoint (0hrss, 3hrss, 6hrss, 12hrss, 24hrss, 48hrss).

A series of three wells were used as a negative control, which were filled with M9 broth with either 20% Glucose supplement, or 20% Alanine supplement. A further 3 wells were allocated as blanks, which would be filled with dH_2O after removal from incubation.

2.5.4 - Experimental Procedure

Just as before with both Growth Curve and Co-infection procedures, each plate was placed within a sealed, sterile Tupperware container, alongside tissues soaked with dH_2O to retain moisture within the container(s). All plates were incubated within an orbital incubator at 37°C operating at 100RPM. Time of condition start was noted, and each plate was removed from incubation upon the arrival of the subsequent timepoint. dH_2O was added to each well allocated as blanks, and the plates absorbance read at OD600.

Upon completion of initial growth readings, samples were removed and each plate washed 3 times with PBS, before 0.1% Crystal Violet was injected into each well and left to stain any remaining bacterial product for 10 mins. The stain was then removed and plate washed a further 3 times before being left overnight to dry at room temperature.

70% Ethanol was dispensed into each well to degranulate any remaining stain and each plate was read at OD600 for biofilm absorbance values.

2.5.5 - Statistical Analysis

Both Growth Curve and Biofilm Growth graphs were plotted and analysed using Microsoft Excel. Subsequent statistical analysis for overall comparison of difference in growth (Two-way repeated measures ANOVA + Sidak Post-Hoc) and comparison between samples and conditions was conducted using GraphPad Prism 8.

2.6 - Analysis of expression of antimicrobial and virulence factor associated genotypes via Whole-Genome Sequencing

2.6.1 DNA sample preparation and extraction

Isolates chosen to be sequenced were selected based on previous results that were collected from both the adaptation and growth curve experiments (I and II). These were selected based on how quickly they became resistant to treatment with the antibiotic they were exposed to, and how growth was affected.

The following isolates were selected for sequencing:

- Parent
- PAM15 (Isolate 4)
- PAD15 (Isolate 4)
- PACe8 (Isolate 2)
- PACeA15 (Isolate 4)
- PACo30 (Isolate 4)

Bacterial samples to be sequenced were prepared by first inoculating one loopful of sample in MH broth immersed within 15mL FALCON tubes. This was conducted following aseptic technique. For further chances for a reduction in contamination, each sample was prepared within a laminar flow cabinet. All MH broth samples were vortexed for 5 seconds, before being incubated overnight at 37°C.

Bacterial inoculates were removed from incubation and vortexed for another 5 seconds, before DNA was extracted from each sample. Extraction was performed using the Zymo Quick-DNA Miniprep kit (Zymo Research, Irvine, CA) and procedure was followed as per manufacturer's instruction.

Upon completion of extraction, each isolate eluted DNA sample was analysed for quality of DNA purity thrsough the use of both the Nanodrop spectrophotometer (Thermo Fisher, Waltham, MA) and Qubit 3.0 fluorometer (Thermo Fisher, Waltham, MA). This was assessed for purity values of approximately 1.8 in absorbance when exposed to 260/280 wavelengths, and 2.0-2.2nm under 260/230. Purified samples were checked via Qubit 3.0 to assess the quantity of DNA within a sample. Upon completion, samples were stored at -20°C for preservation of DNA.

2.6.2 Purified sample fragmentation, ligation and amplification

After assessing the quality and quantity of bacterial DNA extracted, the pooled samples underwent processing to create a pooled library for sequencing using the QIAGEN QIAseq FX DNA Library Kit (QIAGEN, Hilden, Germany). Assembly of the library was conducted as per manufacturer's instructions. Using guidelines included within the protocol, the DNA was fragmented according to an input of 10ng of DNA to create fragments of 350bp. Samples were thawed on ice, and upon completion, each particular sample was then prepared for fragmentation through assembly of an FX reaction mix. The quantity of components was made up to a total of 40µL, as per manufacturer's instruction, with 5µL FX Buffer 10x, 2.5µL FX Enhancer, 16.25µL of purified DNA and 16.25µL of nuclease-free water. FX Enzyme Mix (10µL) was added upon formation of the FX reaction mix, before the mix was immediately transferred to a pre-chilled thermocycler at 4°C, and exposed to the following cycle:

Table 2.1: Procedure for purified DNA fragmentation, as per instruction listed within the handbook for QIAGEN QIAseq FX DNA Library Kit (QIAGEN, Hilden, Germany).

Step	Incubation temperature	Incubation time
1	4°C	1 min
2	32°C	20 min
3	65°C	30 min
4	4°C	Hold

The ligation phase of library preparation included the use of adapters that were part of the QIAseq FX DNA Library Kit, of which 5µL of adapter was added to each 50µL fragmented DNA sample from separate wells. 45µL of pre-prepared ligation master mix was dispensed

additionally into each sample. The samples were then incubated at 20°C for 15 mins to establish ligation.

Sample clean-up occurred after ligation through addition of Agencourt AMPure XP beads (80µL) (Beckman-Coulter, Pasadena, CA). The mixture was left for 5 mins to incubate at room temperature, before being pelleted through the use of a magnetic separation rack for a further 2 mins, with the resultant supernatant being discarded. 200µl of freshly prepared 80% ethanol was dispensed into the individually pelleted samples to wash the beads, before being pelleted once again via magnetic rack and ethanol supernatant removed. This was repeated a further 2 times before the samples were incubated for 5 mins at room temperature to dry the residual DNA. The samples were then eluted by resuspending each one in 52.5µL of Buffer EB (included in the QIAseq FX DNA Library Kit), and pelleted once more. 50µL of resultant supernatant was then transferred to new, sterile Eppendorf tubes, and a second purification stage was commenced. At the end of the second stage, a resultant 23.5µL of purified DNA per sample was generated and transferred to individual LoBind tubes for subsequent amplification.

Amplification proceeded by preparing separate reaction mixes per sample, composed of 25µL of HiFi PCR Master 2x, 1.5µL of Primer Mix and 23.5µL of purified DNA sample. This mix was then placed within a thermocycler to establish reaction using the following programme:

Table 2.2: Procedure for amplication of purified DNA, as per instruction listed within the handbook for QIAGEN QIAseq FX DNA Library Kit (QIAGEN, Hilden, Germany).

Time	Temperature	No. of cycles
2 mins	98°C	1
20 secs	98°C	1
30 secs	60°C	12
30 secs	72°C	1
1 min	72°C	1
∞	4°C	Hold

A further clean-up stage was commenced following amplification in a similar fashion to that mentioned previously following ligation. Following this, a resultant 23µL of eluted, purified DNA was formed per sample. Each 23µL sample was then combined in a fresh, sterile

Eppendorf to assemble a 138µL library sample. This was then assessed for quality via capillary electrophoresis using the Tapestation 4200 system (Agilent Technologies, Santa Clara, CA), to assess that the fragment distribution was centred around 300bp. The quantity of DNA contained within the library was assessed using Qubit 3.0. Upon completion of both assessments, the library was stored at -20°C until needed for whole genome sequencing.

2.6.3 Whole Genome Sequencing of *P. aeruginosa* samples

Before conducting sequencing, the pooled library was thawed in ice before being diluted using nuclease free water to 4nM. The resultant mixture was subsequently diluted further to 20pM, by combining 5µL of 4nM library and 5µL of 0.2N Sodium Hydroxide (NaOH) in a sterile microcentrifuge tube. The combined mixture was vortexed, centrifuged and incubated for 5 mins at room temperature to denature the pool. 990µL of pre-chilled HTI, included as part of the Illumina V2 Nano kit, was added to create a mixture containing 20pM of library.

Due to the fact that during this DNA analysis we would be using the Illumina V2 Nano-kit (300 cycles) (Illumina, San Diego, CA), the library was diluted further to a final mixture of 600µL with a concentration of 8pM using HTI as a diluent. The library was then set aside in ice before proceeding to form the PhiX library necessary for whole-genome sequencing.

2µL of PhiX library stock was added to 3µL of nuclease-free water, to which then the resultant mixture was vortexed and centrifuged to produce a 4nM PhiX library. This was diluted further to 20pM by combining both 5µL of the 4nM PhiX library with 5µL of NaOH in a sterile microcentrifuge tube. As with the DNA library, the PhiX/NaOH mixture was vortexed, centrifuged and left to incubate at room temperature for 5 mins, before 990µL of HTI was added to from 1mL of 20pM PhiX library. The PhiX was diluted once more to form a 600µL solution with a concentration of 8pM.

Within a fresh, sterile microcentrifuge tube, 6µL of 8pM PhiX was combined with 594µL of 8pM DNA library. This mixture was mixed by inverting the solution several times, and then set aside in ice until the Illumina V2 Nano Kit cassette was ready for use. 600µL of the library/PhiX solution was dispensed into the cassette, and sequencing was commenced using the Illumina MiSeq system (Illumina, San Diego, CA).

2.6.4 Whole Genome Sequencing – Earlham Institute

Whole Genome Sequencing was conducted off-site at the Earlham Institute (Colney, Norfolk, UK), who performed subsequent amplification and sequencing steps. Samples were diluted to a total DNA concentration of between 10-50ng/µL as per instruction from the Earlham Institute, and injected into a sterile 96-well microtitre assay plate for transport. Sequencing was performed using an lllumina Novaseq S2 (2x150bp).

2.6.5 Whole Genome Sequencing – SNP analysis

The resultant data collected from sequencing off-site via the Earlham Institute was extracted and interpreted using a series of open source software. Raw fastq data was trimmed using fastp using default parameters (Chen *et. al.*, 2018). Trimmed fastq were mapped against the *P. aeruginosa* PAO1 reference genome (NCBI) using SNIPPY (https://github.com/tseemann/snippy). These SNPs were then interpreted and compared against a *P. aeruginosa* PAO1 reference genome using Artemis software (Sanger Institute, Wellcome Trust, Cambridge, UK).

3. RESULTS

3.1 *Pseudomonas aeruginosa* adapts to repeated exposure to antibiotics

The aims of this study were to examine the effects of antibiotics on a clinical isolate of *Pseudomonas aeruginosa*, a pathogen that is often implicated in Ventilator-associated Pneumonia (VAP), and whether adaptation to antibiotics influences the production of virulence factors. These included a series of adaptation experiments, in order to test and understand the capabilities of the *P. aeruginosa* isolate's ability to adapt to a series of common clinically prescribed antibiotics for *P. aeruginosa* infections within an ICU setting. These antibiotics include Doripenem, Imipenem, Meropenem, Ceftazidime, Ceftazidime/Avibactam and Colistin.

The adaptation experiment phase involved cultivation and repeated exposure of the Parent to different antibiotics as separate isolates. This continued over a period of 15 passages, in order to measure the level of antibiotic action against diameter of inhibition zones newly adapted isolates of the original clinical *P. aeruginosa* isolate.

The adapted isolates indicated a change in their sensitivity towards antibiotics when undergoing continuous application. Figure 3.01 and Table 3.01 displays changes in the average inhibition zone diameter measured per passage, and indicates that all became less sensitive as time progressed, except for the isolate(s) that were exposed to Colistin. The Colistin-adapted isolates showed variable change, that being each repeat would fluctuate in their sensitivity towards Colistin as time progressed. For example, whilst the mean inhibition zone diameter did appear to decrease between Passage 3 and 8, beyond this the mean values appear to increase from 18.5mm to 24.25mm (Table 3.01). The values then continue to fluctuate up until the termination of the experiment at Passage 15.

Table 3.01: Average antimicrobial adaptation (diameter of inhibition zone [mm]) of Parent strain of *Pseudomonas aeruginosa* to chosen antibiotics (Meropenem, Doripenem, Imipenem, Ceftazidime, Ceftazidime/Avibactam and Colistin). Coloured cells indicate resistance according to EUCAST Breakpoint, '*' denotes complete resistance, where no visible inhibition zone was detected upon observation – Updated January 2019 (EUCAST, 2019). '' indicates the need to conduct broth dilution test to establish the minimum inhibitory concentration (MIC) for Colistin, as no inhibition zone breakpoint exists under EUCAST guidelines.**

Antibiotic	**Meropenem**	**Doripenem**	**Imipenem**	**Ceftazidime**	**Ceftazidime/Avibactam**	**Colistin**
Passage						
Parent/1	40.4	41.2	34.4	33.8	33.4	20.6
2	33.2	39.2	29.4	29.4	33.6	14.2
3	24	33.8	29.4	22.2	27.75	15.6
4	15.8	23.4	29.2	14.6	26	16.8
5	18.4	20.6	22.67	10.6	27.25	17.8
6	14.2	18.4	19	9.8	23	15.2
7	9.4	16.8	14	7.4	22.25	15.6
8	8.8	21.2	9	6*	18.5	16.8
9	13.8	20.8	13	6*	24.25	18.4
10	11.2	17.8	12	6*	18.75	14.8
11	13	20.2	13.67	6*	20.75	16.8
12	11	18.4	10.33	6*	24	16.8
13	11.2	17.8	12	6*	24.75	19.8
14	7.2	16.2	11	6*	17.25	13.8
15	8	14	10	6*	16.5	15
EUCAST Breakpoint	**S = ≥24** **R = <18**	**S = ≥25** **R = <22**	**20**	**17**	**17**	****Microdilution needed**

One-way ANOVA tests conducted for each adapted strain displayed clear significant differences between the Parent and each adapted passage (P = <0.05; Figure 3.01). Table 3.01 displays numerical values associated with the average inhibition zone diameters that were recorded per passage in relation to EUCAST breakpoints. The test strain adapted most quickly to Meropenem (Passage 4 = 15.8mm, EUCAST breakpoint for resistance = <18mm; Table 3.01) and Ceftazidime (Passage 4 = 14.6mm, EUCAST breakpoint for resistance = <17mm; Table 3.01). Adaptation to Ceftazidime/Avibactam was the slowest overall (Passage 15 = 16.5mm, EUCAST breakpoint for resistance = 17mm; Table 3.01), but the bacteria developed resistance. Colistin-adapted populations however displayed no resistance, though changes in inhibition zone diameters were noted (Figure 3.01; Table 3.01).

Additional Post-hoc Tukey tests confirmed that the significance of results (Table 3.02) and that the clinical isolate of *P. aeruginosa* did adapt to each antibiotic under mono-therapeutic conditions in comparison to the un-adapted Parent isolate. However, further inspection of the Post-hoc Tukey tests displayed a variance in significance between each adapted strain in comparison to the Parent. All adapted strains, apart from the isolates exposed to Colistin, did not show any significant difference during the early stages of exposure to each antibiotic (Table 3.02). These values differed however as by Passage 3, Meropenem, Doripenem and Ceftazidime isolates appeared to become statistically significant when compared against the Parent inhibition zone diameter values (Table 3.02; P=<0.05). This was followed by Imipenem by Passage 4, and Ceftazidime/Avibactam by Passage 10 (Table 3.02; P=<0.05).

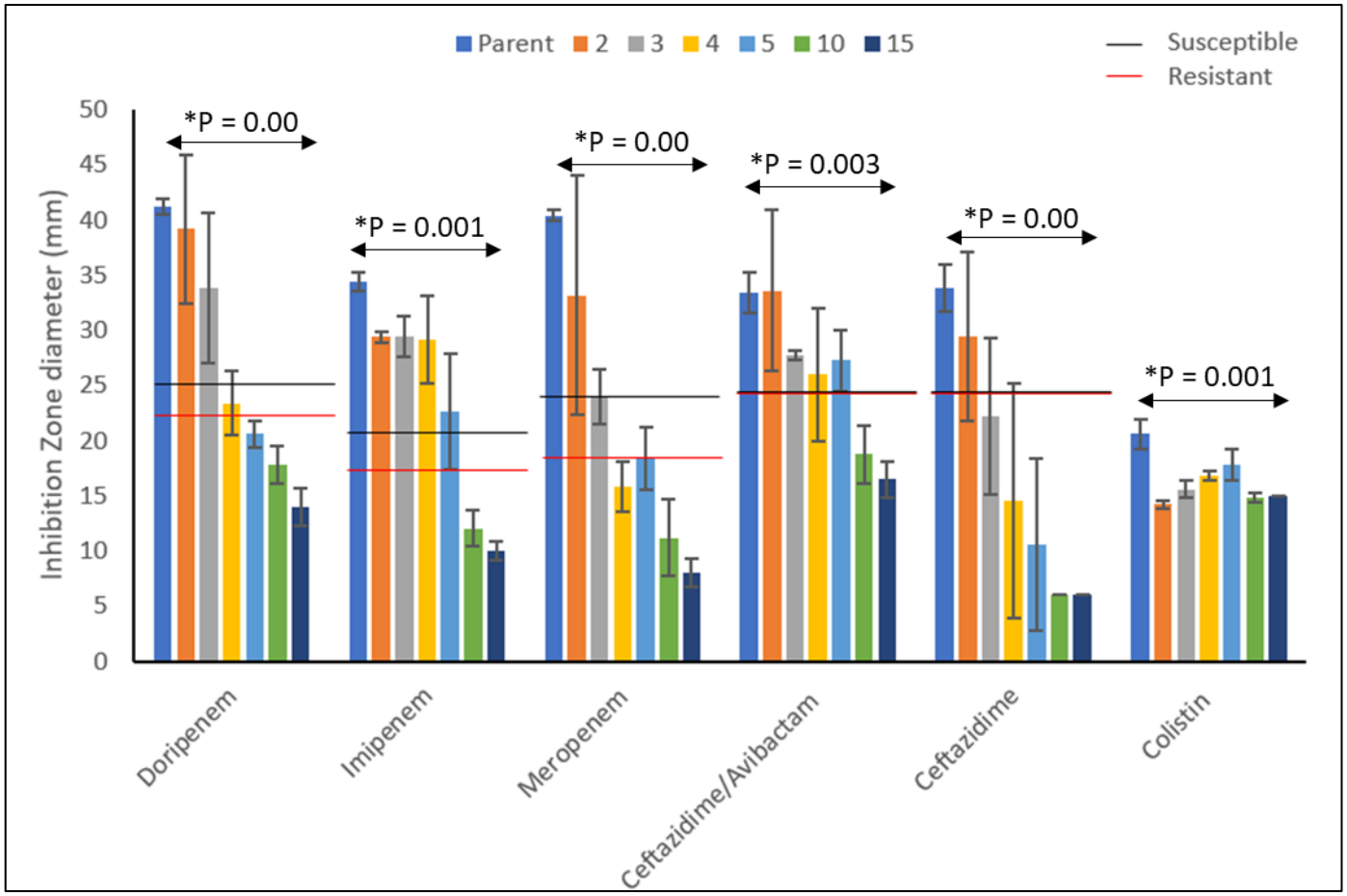

Figure 3.01: Antimicrobial adaptations of Parent strain of *Pseudomonas aeruginosa* tested against 6 different antibiotics over 15 passages. Note: * = One-way ANOVA significance value per average adapted isolate. Each coloured bar represents measurements at each passage (Blue = Parent/Passage 1; Orange = Passage 2; Grey = Passage 3; Yellow = Passage 4; Light Blue = Passage 5; Green = Passage 10; Dark Blue = Passage 15). EUCAST breakpoint guidelines are represented by both black (susceptible to antibiotic) and red (resistant to antibiotic) lines.

Table 3.02: Post-Hoc analysis P-value results associated with comparisons between both the *P. aeruginosa* Parent strain to each adapted isolate(s) mean inhibition zone diameter (mm) when exposed to antibiotics. Each P-value was calculated from comparison between Parent exposure and each subsequent passage that results were recorded (Passage 2, 3, 4, 5, 10 and 15). '*' signifies a significance value (P=<0.05).

Antibiotic	Meropenem	Doripenem	Imipenem	Ceftazidime	Ceftazidime/Avibactam	Colistin
Passage						
Parent /P2	**0.331**	**0.990**	**0.154**	**0.956**	**1.00**	***0.00**
Parent /P3	***0.001**	**0.145**	**0.154**	**0.178**	**0.559**	***0.00**
Parent /P4	***0.00**	***0.00**	**0.126**	***0.004**	**0.259**	***0.00**
Parent /P5	***0.00**	***0.00**	***0.00**	***0.00**	**0.463**	***0.001**
Parent /P10	***0.00**	***0.00**	***0.00**	***0.00**	***0.002**	***0.00**
Parent /P15	***0.00**	***0.00**	***0.00**	***0.00**	***0.00**	***0.00**

3.2 Overall growth and biofilm formation were affected as a result of adaptation to antibiotics

In order to understand the impact of adaptation to antibiotics, experiments measuring both growth and biofilm formation were conducted. Both were monitored over a 48-hour period, with each *P. aeruginosa* isolate (PAO1, Parent and adapted) grown in a nutrient rich medium, MH broth. PAO1 reference strain was implemented as a positive control, as to understand whether specific differences between either Parent or PAO1 occurred in either case that could relate to strain.

Cultures of selected isolates (Parent, PAM15, PAD15, PAI15, PACe8, PACeA15 and PACo30) were read for absorbance for growth, and after removing residue from the plates, read further for biofilm formation analysis. Subsequent comparisons between the Parent, and antibiotic-adapted isolates were carried out, as a means to find out whether adaptations impacted the overall population growth and expression of biofilm.

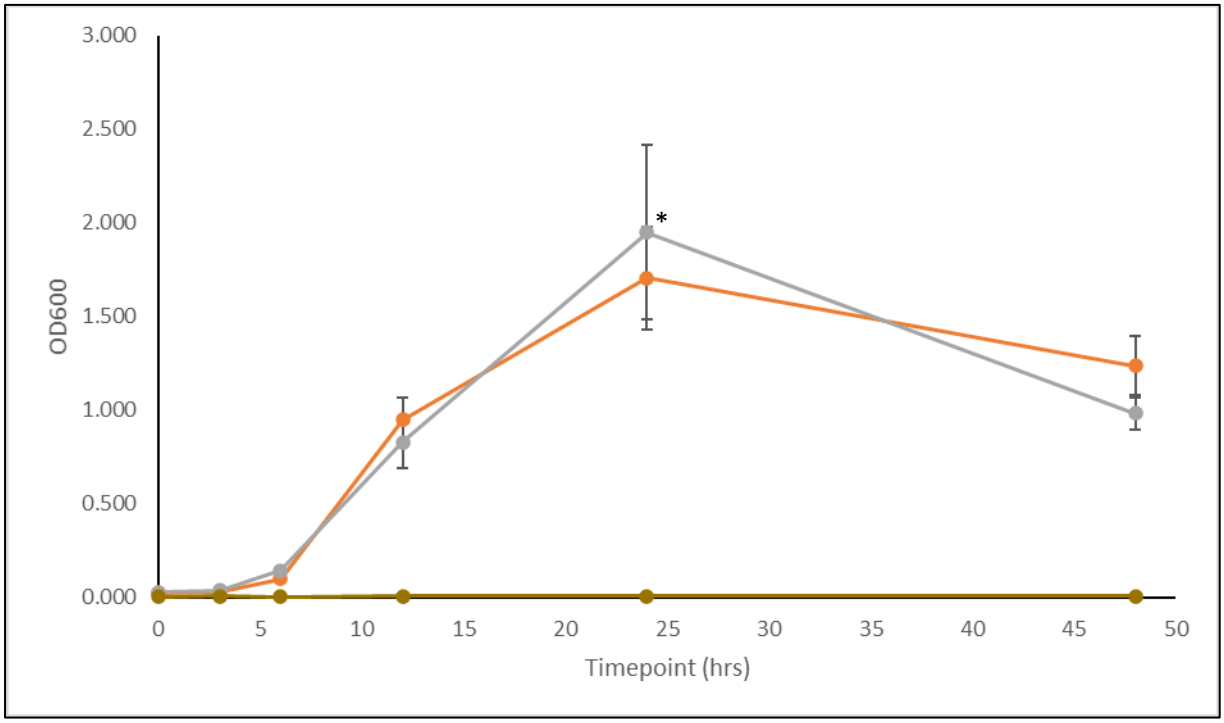

Figure 3.02: Planktonic growth of both *P. aeruginosa* PAO1 (orange) and Parent (grey) strains grown within MH broth over a 48hrs period. *P. aeruginosa* growth absorbance was measured at 600nm (OD600). *P=<0.05; Sidak post-hoc analysis was conducted using GraphPad Prism 8. A negative control (MH broth; dark yellow) was implemented to detect contamination. Error bars represent Standard Error Mean (SEM).

The original clinical strain and PAO1 reference displayed a similar growth pattern over the 48-hour period upon observation of OD600 (Figure 3.02). Both positive control and test strains began growth with a slow lag phase between 0hrss and 6hrs, before a rapid exponential phase occurred between 6-12hrs, as OD readings increased (Figure 3.02). Observable differences in growth, however, were found after 24hrs, as the Parent strain displayed a higher average optical density reading of 1.949 (OD600) (Appendix 1), whereas PAO1 in comparison had a reading of 1.706 (OD600). Both strains entered a decline phase after 24hrs, as readings taken at 48hrs indicate (Figure 3.02). The Parent strain was seen to have entered a much more rapid decline phase as opposed to PAO1, as the OD600 values were much lower than PAO1 (0.983 vs. 1.237, respectively; Appendix 1).

Two-way repeated measures ANOVA analysis indicated that there were significant differences between both PAO1 and the Parent strain in terms of growth within MH broth ($P<0.05$, Table 3.02; Figure 3.02). Subsequent Sidak post-hoc analysis highlighted significant differences ($P=<0.05$) between the PAO1 reference strain (positive control) and the Parent strain, after 24hrs of growth (Figure 3.02; Table 3.03). No other significant difference was detected at any other timepoint.

Comparisons between the Parent strain of *P. aeruginosa* and each of the adapted isolates in terms of whether growth differed upon exposure to antibiotics yielded similar results. All strains entered a rapid exponential phase between 6-12hrs of growth. At 24hrs, however, fluctuations between each of the Carbapenem (PAM15, PAD15, and PAI15) adapted strains and un-adapted Parent were detected, each displaying a visual difference in OD600 absorbance values (Figure 3.03). Whilst the Parent strain continued to display exponential growth, all three carbapenem-adapted strains had displayed lower OD600 values, indicating a slowdown in growth. Both PAI15 and PAM15 appeared to have entered a stationary phase of bacterial growth at this stage (Figure 3.03), with PAM15 displaying the lowest OD600 value (0.978, Appendix 1). By 48hrs, PAI15 of *P. aeruginosa* had entered another exponential phase in growth, whilst PAM15 continued to display a stationary phase, with a slighter higher OD600 value in contrast (Figure 3.03). PAD15 displayed a slight decline in growth by 48hrs, albeit not as dramatically as the un-adapted Parent.

Two-way repeated measures ANOVA tests detected significant differences in each individual strain's growth pattern in comparison to the Parent strain (P=<0.05, Figure 3.03). Subsequent Sidak analysis between each strain and the Parent indicated that there were significant differences in both PAM15's and PAD15's growth in comparison to the Parent at both 3hrs and 24hrs (Table 3.03). PAI15 was found to be significantly different in growth from the Parent at 12rhs, 24hrs and 48hrs of growth.

Comparing each of the carbapenem-adapted strains between each other for individual differences in growth, found that there were significant differences between all three strains (P=<0.05). Tukey's post hoc analysis further indicated PAM15 and PAD15 after 24hrs of growth (Table 3.04; Figure 3.03), and PAI15 in comparison to both carbapenem-adapted strains after 48hrs (Table 3.0; Figure 3.03).

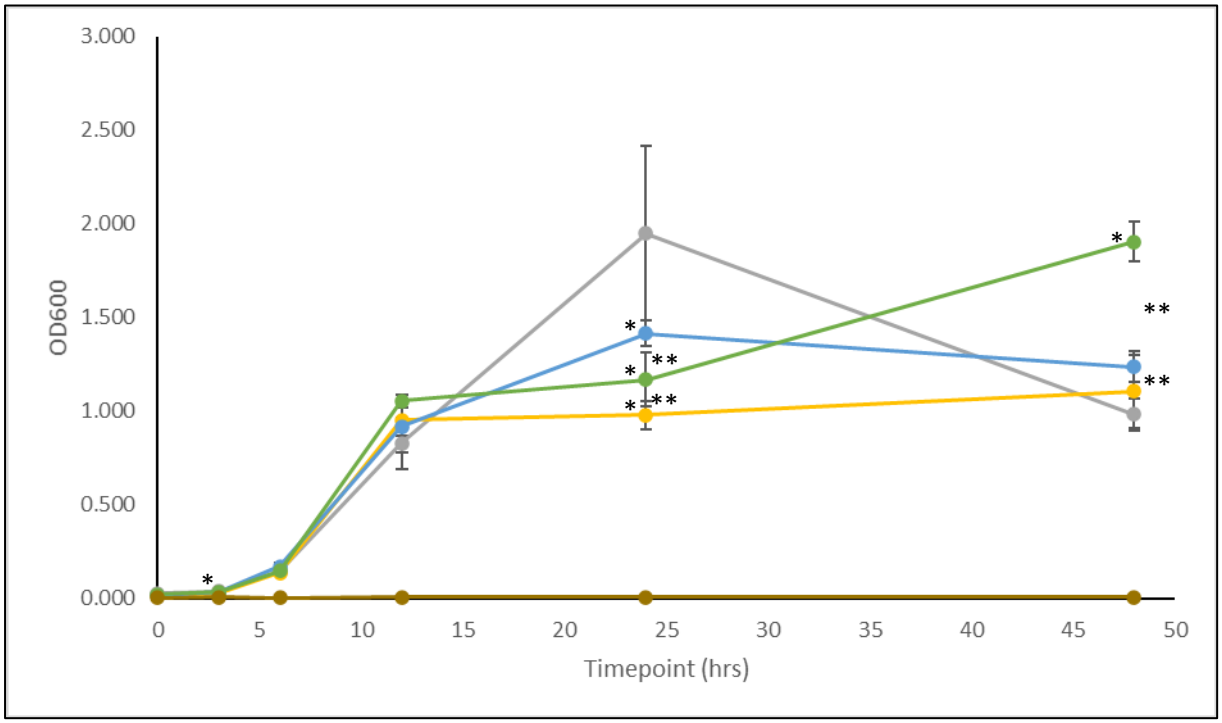

Figure 3.03: Planktonic growth of both Parent (grey) *P. aeruginosa* and Carbapenem-adapted (PAM15 (yellow), PAD15 (light blue) & PAI15 (green)) strains grown within MH broth over a 48hrs period. Growth absorbance was measured at 600nm (OD600). * = significance between carbapenem-adapted strain and Parent (P=<0.05); Sidak post-hoc analysis was conducted using GraphPad Prism 8. ** = significance (P=<0.05) between carbapenem-adapted strains, calculated via Tukey post-hoc analysis. A negative control

(MH broth; dark yellow) was implemented to detect contamination. Error bars represent Standard Error Mean (SEM).

PACe8 and PACeA15 also displayed a similar pattern to the Parent as observed from the carbapenem-adapted strains. Rapid, exponential growth was detected between 6-12hrs, before a slowdown occurred at 24hrs as indicated by their OD600 values (Figure 3.04). The PACe8 had a higher OD600 value (1.283, Appendix 1) at 24 hrs, in comparison to PACeA15 (0.789, Appendix 1). These values indicated that PACe8 had slowed in its growth, whilst not completely entering a stationary phase, unlike PACeA15. At 48hrs, however, both strains had increased in their OD600 values, indicating that the bacteria were continuing population growth unlike the Parent at that point in time (Figure 3.04). PACe8 continued to show a higher average OD600 value at this point (Figure 3.04).

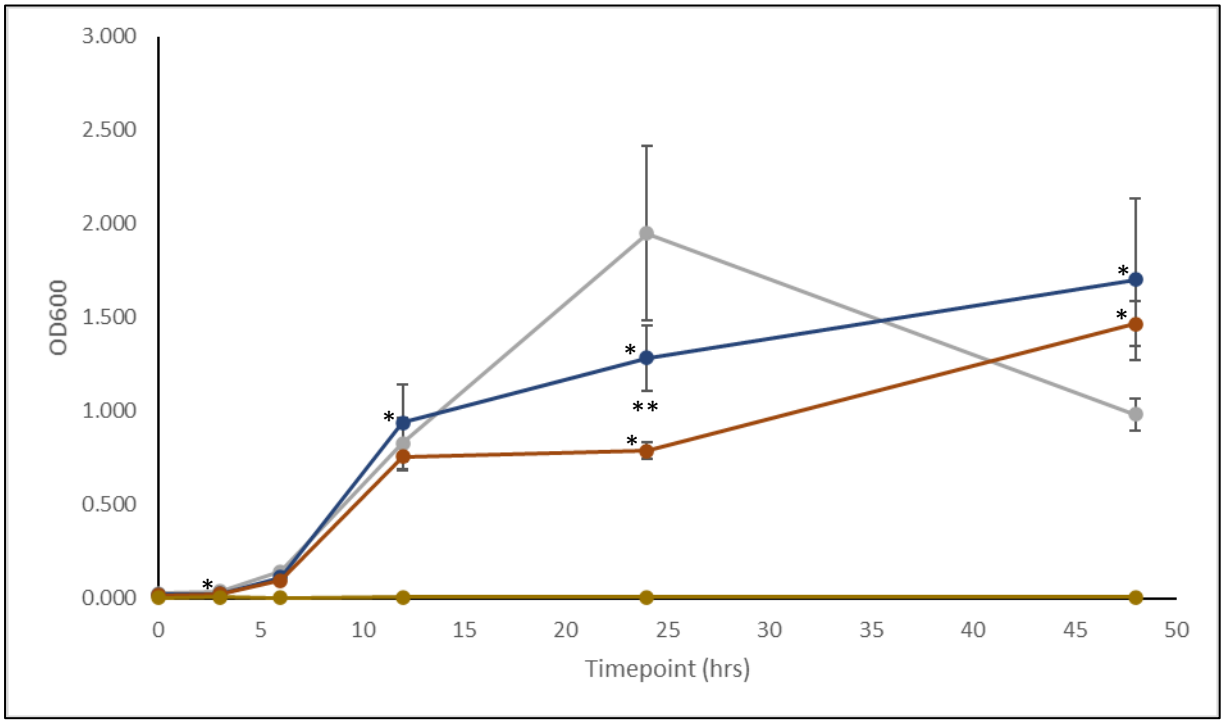

Figure 3.04: Planktonic growth of Parent (grey) *P. aeruginosa,* PACe8 (dark blue), and, PACeA15 (brown) adapted strains grown within MH broth over a 48hrs period. Growth absorbance was measured at 600nm (OD600). * = significance between cephalosporin-adapted strain and the Parent strain (P=<0.05; Sidak post-hoc analysis was conducted using GraphPad Prism 8). ** = significance between PACe8 and PACeA15 (P=<0.05). A negative control (MH broth; dark yellow) was implemented to detect contamination. Error bars represent Standard Error Mean (SEM).

Statistical analysis via Two-way repeated measures ANOVA detected significant differences in both strain's growth patterns in comparison to the Parent strain within MH broth (P=0.05, Figure 3.04; Table 3.03). Additional Sidak post-hoc analysis continued to show significant results between the Parent and adapted *P. aeruginosa* strains in growth within rich medium. Both cephalosporin-adapted strains indicated significant differences between themselves and the Parent after 24hrs and 48hrs of growth (P=<0.05, Table 3.03; Figure 3.04). The strains differed in significance at other timepoints. PACe8 indicated further differences in growth compared to the Parent after 12hrs (P=<0.05, Table 3.03; Figure 3.04). PACeA15, in contrast, displayed a significant difference between itself and the Parent after 3hrs of growth (P=<0.05, Table 3.03; Figure 3.04).

Alongside a significant difference detected from Two-way ANOVA repeated measures analysis, both adapted strains also displayed differences between one another at 2 different timepoints; 12hrs and 24hrs (P=<0.05, Table 3.04; Figure 3.04).

PACo30 had a similar pattern of growth in comparison to the Parent, albeit beyond 12hrs. At 24hrs, the OD600 value for PACo30 was lower than the Parent, indicating that, as with the other adapted strains, growth was entering a slower phase (Figure 3.05). At 48hrs, growth continued at a slow rate, with a higher OD600 value being recorded than the Parent (Figure 3.05).

Two-way repeated measures ANOVA recorded significant differences between growths patterns of both PACo30 and the Parent strain (P=<0.05, Table 3.03; Figure 3.05). Further Sidak post-hoc analysis also indicated significant differences at both 24hrs and 48hrs in comparison to the Parent (P=<0.05, Figure 3.05; Table 3.03).

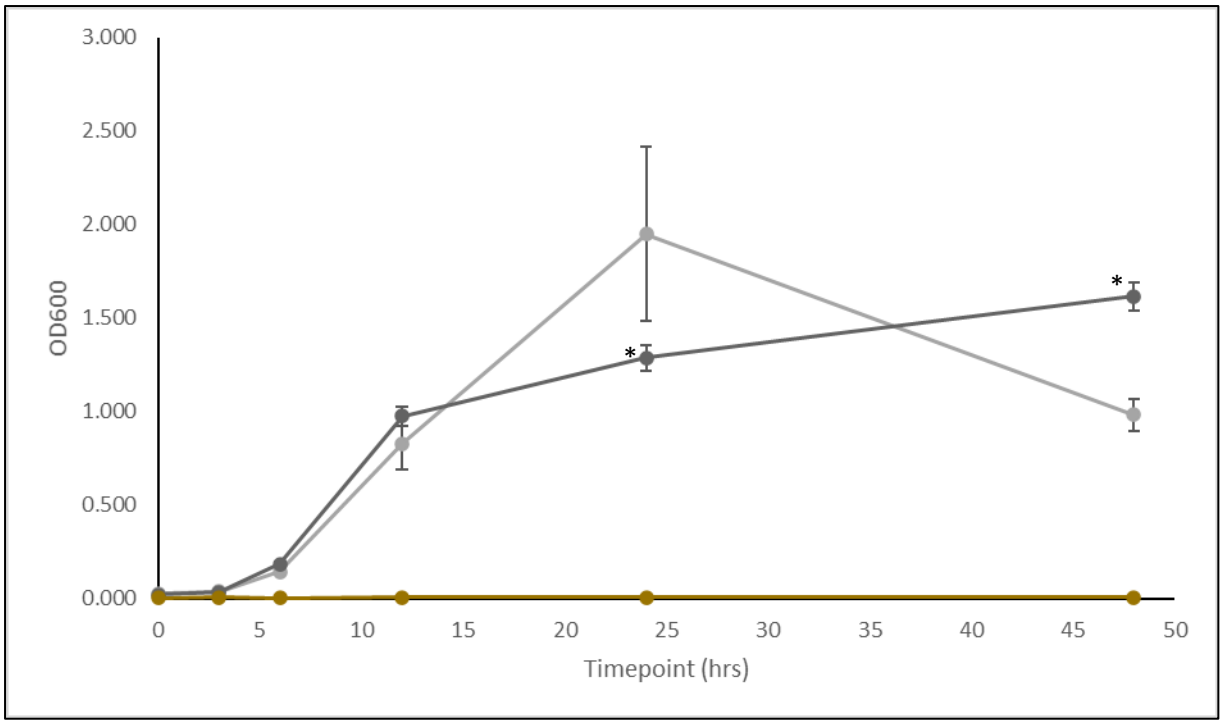

Figure 3.05: Planktonic growth of Parent (grey) *P. aeruginosa* and PACo30 (dark grey) adapted strains grown within MH broth over a 48hrs period. Growth absorbance was measured at 600nm (OD600). * = significance between PACo30 and the Parent strain (P=<0.05; Sidak post-hoc analysis was conducted using GraphPad Prism 8). A negative control (MH broth; dark yellow) was implemented to detect contamination. Error bars represent Standard Error Mean (SEM).

Table 3.03: Calculated significance results of Two-way repeated measures ANOVAs conducted to compare differences in planktonic growth between *P. aeruginosa* Parent strain and each adapted strain. '*' – P=<0.05

Strain	PAO1 vs. Parent	Parent vs. PAM15	Parent vs. PAD15	Parent vs. PAI15	Parent vs. PACe8	Parent vs. PACeA15	Parent vs. PACo30
Timepoint							
2W-RM ANOVA	<0.0001	<0.0001	<0.0001	<0.0001	<0.0001	<0.0001	<0.0001
0hrs							
3hrs	0.0643	*0.0165	*0.0190	>0.9999	0.9993	*0.0008	0.6139
6hrs	0.1813	0.9974	0.5088	0.784	0.9347	0.1702	0.2739
12hrs	0.5644	0.5581	0.7038	*0.022	*0.0241	0.6197	0.7780
24hrs	*0.0450	*0.0008	*0.0006	*0.007	*<0.0001	*0.0052	*0.0009
48hrs	0.1237	0.7322	0.0642	*0.019	*<0.0001	*0.0110	*0.0071

Table 3.04: Calculated significance results of Two-way repeated measures ANOVA s conducted to compares differences in planktonic growth between each adapted strain within antibiotic classes for individual differences. '' – P=<0.05**

Strain	PAM15 vs. PAD15	PAM15 vs. PAI15	PAD15 vs. PAI15	PACe8 vs. PACeA15
Timepoint				
2W-RM ANOVA	<0.0001	<0.0001	<0.0001	<0.0001
0hrs				
3hrs	0.7727	0.7272	0.8068	>0.9999
6hrs	0.0810	0.5623	0.0613	0.8623
12hrs	0.8800	0.3273	0.1636	**0.0110
24hrs	**0.0059	0.1480	**0.0975	**0.0235
48hrs	0.2982	**0.0196	**0.0475	0.1403

3.2.1 Biofilm Formation

Upon completion of bacterial growth assays, any biofilm that remained within each microtitre plate was stained in order to record biofilm formation that occurred during the 48-hour assay. Any differences in biofilm formation between the initial clinical Parent isolate and the PAO1 reference strain was established via Two-way repeated measures ANOVA analysis. A Sidak post-hoc analysis was also conducted to test for any further difference between timepoints. This same method was used to compare any differences in biofilm formation between Parent and adapted strains, as well as any individual differences between antibiotic classes.

Biofilm formation was detected over the 48hrs period. Comparisons between both the PAO1 strain and Parent strain displayed an initial observable difference in biofilm production between 0-3hrs (Figure 3.06). Biofilm continued to be detected, but at a higher volume in accordance to the OD600 values between 3hrss and 6hrs (Figure 3.06). The Parent strain appeared to produce the most biofilm, as the OD600 value that was recorded at 6hrs was much higher (0.867; Appendix 2), in comparison to the PAO1 strain (0.385; Appendix 2). This difference in optical density continued throughout the observed growth period, with the Parent strain producing a much larger value in comparison to the PAO1 strain (Figure 3.06). Both strains appear to enter a stationary phase of biofilm production between 12hrs and 24hrs, with a slight decline occurring with PAO1. Between 24-48hrs, the Parent biofilm OD600 values just above those correlating with PAO1, signalling a decline phase.

When conducting statistical analysis, the Two-way repeated measures ANOVA and Sidak post-hoc indicated only one significant difference in growth. This was at the 6hrs timepoint between both PAO1 and the Parent strain ($P=<0.05$, Table 3.05; Figure 3.06).

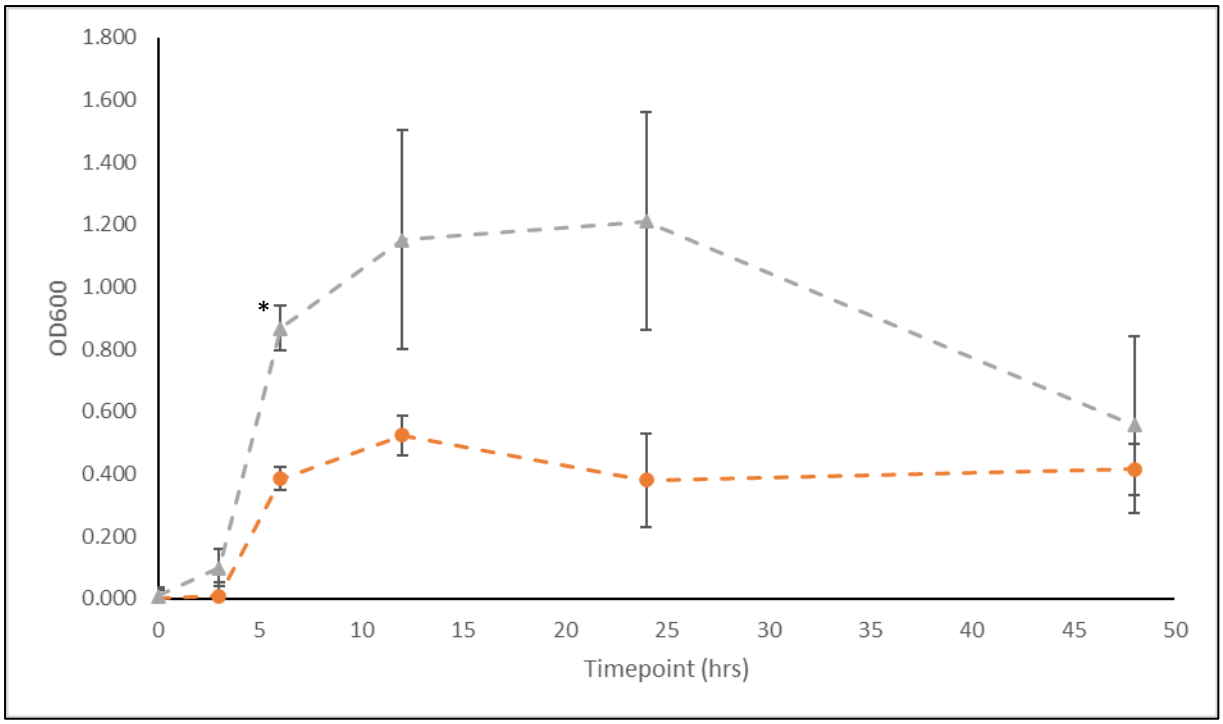

Figure 3.06: Overall biofilm formation of both PAO1 (orange) (positive control) and the un-adapted clinical isolate (Parent) (grey) of *P. aeruginosa* from residual growth in MH broth over a 48-hour period. Biofilm absorbance was measured at 600nm (OD600). * = significance between the Parent strain and PAO1 (P=<0.05; Sidak post-hoc analysis was conducted using GraphPad Prism 8). Error bars represent Standard Error Mean (SEM).

Further comparisons between the Parent and each adapted strain for differences in biofilm formation displayed similar patterns of growth. The carbapenem-adapted strains, when analysed, showed overall fluctuations in biofilm formation, albeit these indicating minor differences in comparison to the Parent (Figure 3.07). All strains showed an initial increase in OD600 value between the 0hrs timepoint and 3hrs timepoint, with a sharp increase between 3hrs and 6hrs (Figure 3.07). This growth levelled off by the 6hrs timepoint, before fluctuations began. All three carbapenem-adapted strains begin a decline phase after 12hrs of biofilm formation, with both PAD15 and PAI15 *P. aeruginosa* isolates displaying a much sharper decline curve in comparison to the PAM15 strain. PAM15 continued a steady decline phase beyond the 24hrs timepoint, whereas PAD15 levelled off in biofilm formation beyond 24hrs. A slight noticeable increase in optical density was noted for PAI15, however, beyond the 24hrs timepoint.

Overall, when conducting Two-way repeated measures ANOVAs, only PAD15 and PAI15 strains indicated a significant difference in biofilm formation patterns in relation to the Parent (P=0.05, Table 3.0; Figure 3.07). No significant differences were detected in biofilm formation pattern from the PAM15. Upon subsequent Sidak post-hoc analysis, however, no significant differences were detected in biofilm formation between the Parent and each carbapenem-adapted strain when comparing optical density at each timepoint.

Significant differences were detected in biofilm formation between any of the carbapenem-adapted strains at any timepoint (Table 3.06; Figure 3.07).

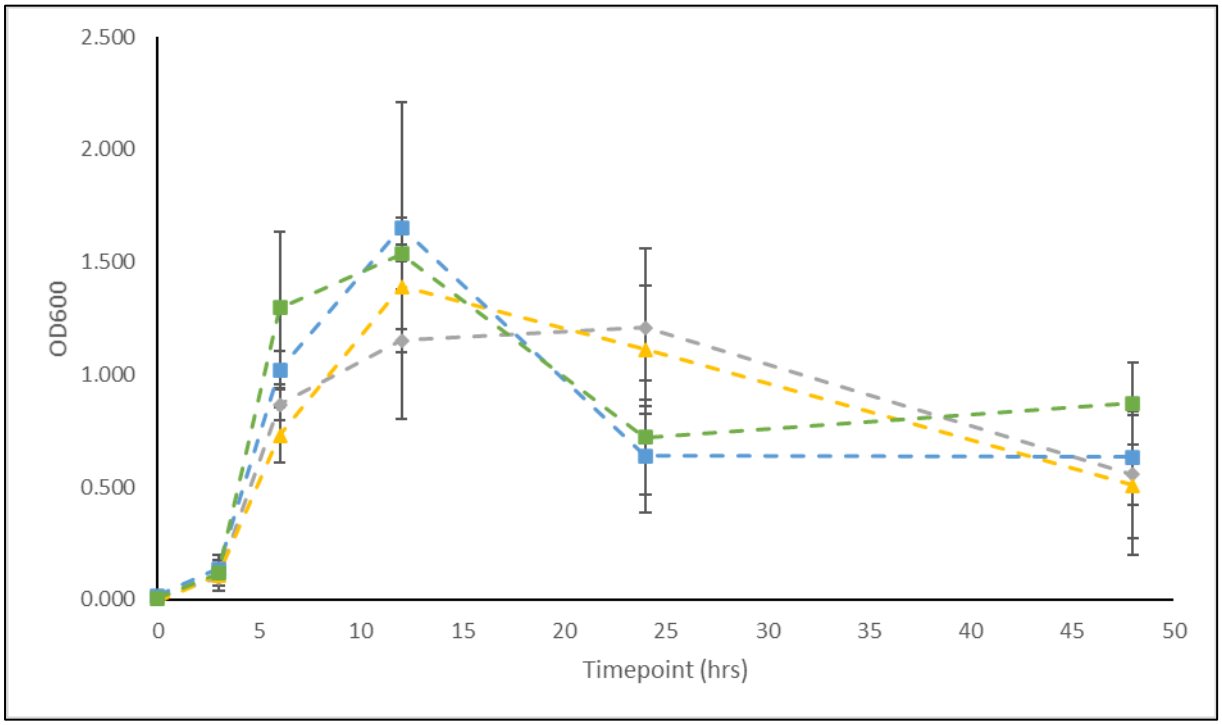

Figure 3.07: Overall biofilm formation of the Parent (grey) and Carbapenem-(PAM15 (yellow), PAD15 (light blue), PAI15 (green) adapted strains of *P. aeruginosa* from residual growth in MH broth over a 48-hour period. Biofilm absorbance was measured at 600nm (OD600). Error bars represent Standard Error Mean (SEM).

Regarding the biofilm formation differences between the cephalosporin-adapted strains, the results differed between each adapted isolate and the Parent. PACe8 displayed a sharp increase in biofilm formation, with regards to the OD600 values detected between 3-12hrss of growth (Figure 3.08). This changed after 12hrs, with a sharp decrease occurring between that timepoint and 24hrs, before a slight increase in optical density after 24hrs. PACeA15,

however, displayed little biofilm formation in comparison to the Parent and PACe8 strains (Figure 3.08).

This was reflected from statistical analysis of the results, as significant differences were detected when comparing PACeA15 with both the un-adapted Parent strain. A significant difference in biofilm formation was noted at 6hrs when comparing PACeA15 with the Parent strain (P=<0.05, Table 3.05; Figure 3.08). Significant differences were noted for the overall biofilm formation pattern via Two-way repeated measures analysis when comparing PACe8 with the Parent (P=<0.05, Table 3.05; Figure 3.08). However, unlike PACeA15, o significant differences were detected when comparing PACe8 with the Parent at any timepoint (P=<0.05, Table 3.05; Figure 3.08).

Significant differences between PACe8 and PACeA15 were found after Two-way ANOVA analysis, and subsequently at 6hrs, 12hrs and 24hrs of biofilm formation from Sidak post-hoc testing (P=<0.05, Table 3.06; Figure 3.08).

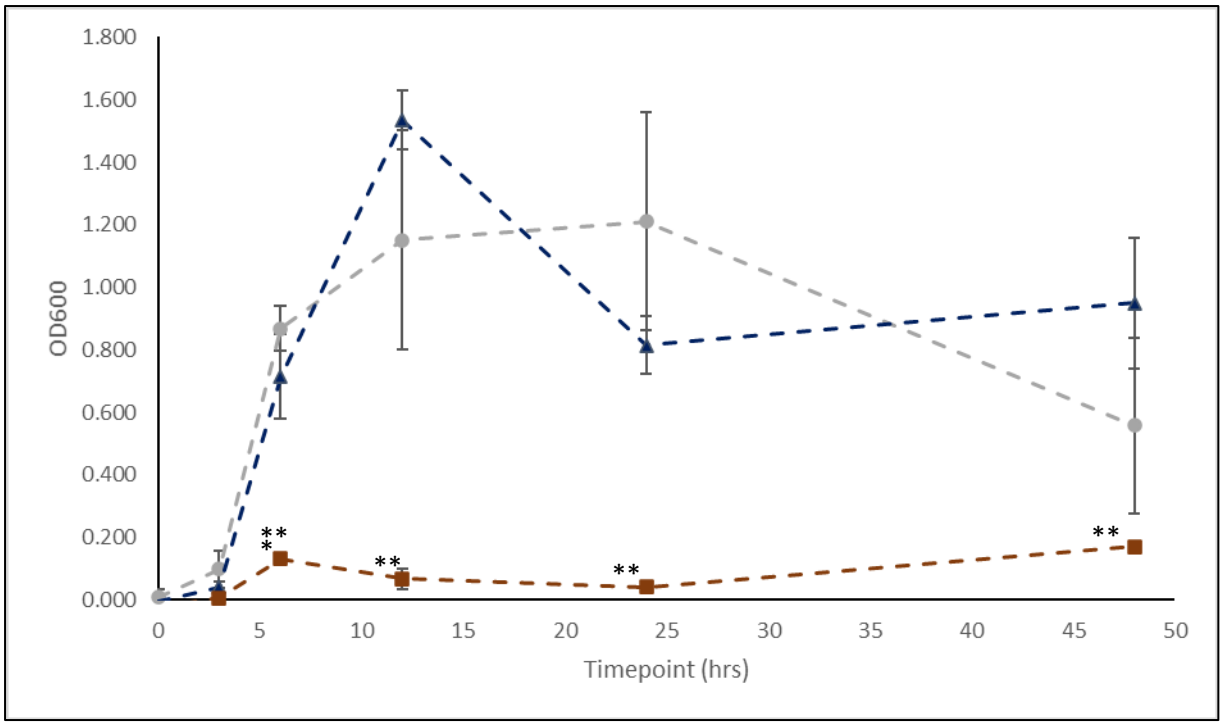

Figure 3.08: Overall biofilm formation of the Parent (grey), Ceftazidime- (dark blue) and Ceftazidime/Avibactam- (brown) adapted strains of *P. aeruginosa* from residual growth in MH broth over a 48-hour period. Biofilm absorbance was measured at 600nm (OD600). * = significance between the cephalosporin-adapted isolates and Parent isolate (P=<0.05; Sidak post-hoc analysis was conducted using GraphPad Prism 8). **P=<0.05 between PACe8 and PACeA15 strains. Error bars represent Standard Error Mean (SEM).

Adaptation to Colistin did not, however, display any major differences between the Parent and any isolates adapted to such in the context of biofilm formation. When comparing both growth patterns, the two isolates display similar changes in biofilm production with regards to the OD600 values detected (Figure 3.09). PACo30 however, did show a much sharper decline in biofilm formation post 12hrs timepoint in comparison to the Parent (Figure 3.09).

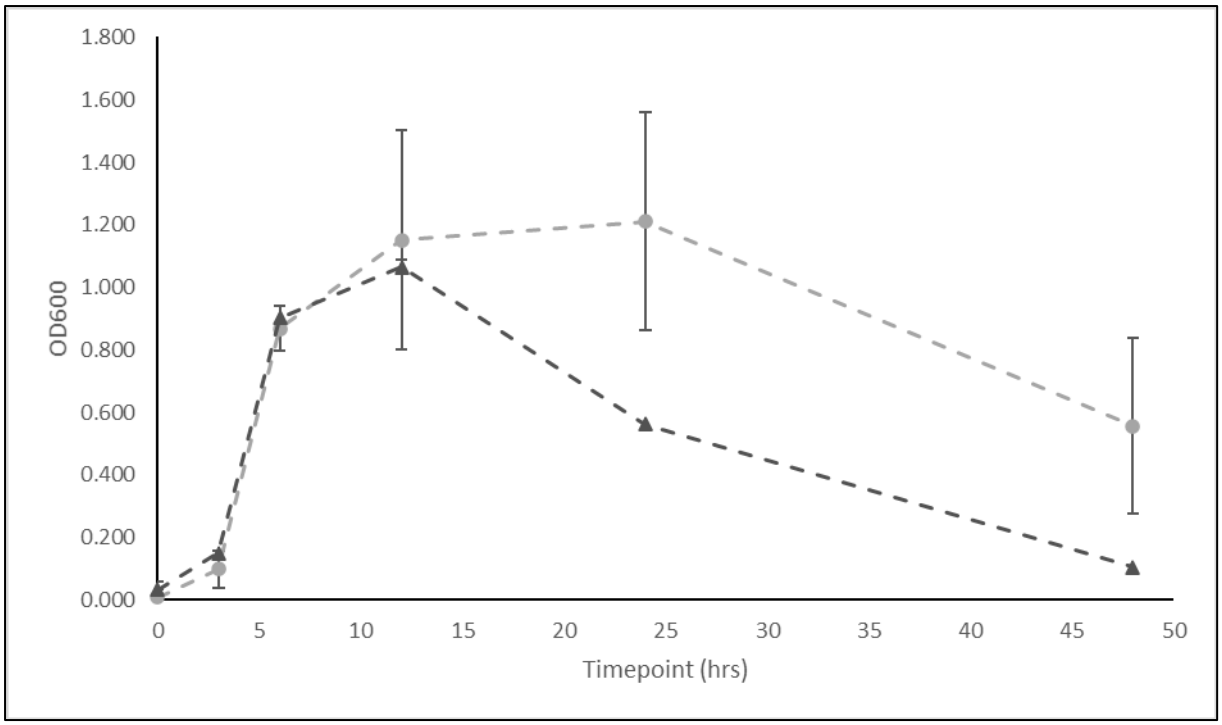

Figure 3.09: Overall biofilm formation of the Parent (grey) and PACo30 (dark grey) adapted strains of *P. aeruginosa* from residual growth in MH broth over a 48-hour period. Error bars represent Standard Error Mean (SEM).

Whilst the growth pattern itself indicated a significant difference upon Two-way repeated measures ANOVA (P=<0.05, Table 3.0; Figure 3.09), no further significant differences in biofilm formation between PACo30 and the Parent were detected at any timepoint from post-hoc analysis.

Table 3.05: Calculated significance results of Two-way repeated measures ANOVAs and post-hoc analyses conducted to compare differences in biofilm formation between *P. aeruginosa* Parent strain and each adapted strain when grown in rich medium (MH broth). '*' - P<0.05

Strain	PAO1 vs. Parent	Parent vs. PAM15	Parent vs. PAD15	Parent vs. PAI15	Parent vs. PACe8	Parent vs. PACeA 15	Parent vs. PACo30
Timepoint							
2W-RM ANOVA	*0.0013	0.7129	*0.0270	*0.0093	*0.0061	*<0.0001	*0.0449
0hrs							
3hrs	0.5079	0.9999	0.9746	0.9991	0.8031	0.4564	0.8370
6hrs	*0.0108	0.7249	0.3829	0.2207	0.6969	*0.0012	0.9859
12hrs	0.4131	0.9391	0.8462	0.7120	0.7230	0.1672	0.9996
24hrs	0.2084	0.9996	0.4298	0.5593	0.6999	0.1505	0.3925
48hrs	0.9806	>0.9999	0.9996	0.7259	0.5708	0.4599	0.9898

Table 3.06: Calculated significance results of Two-way repeated measures ANOVAs and post-hoc analyses conducted to compare differences in biofilm formation between each adapted strain when grown in rich medium (MH broth) within antibiotic classes for individual differences. '' - P<0.05**

Strain	PAM15 vs. PAD15	PAM15 vs. PAI15	PAD15 vs. PAI15	PACe8 vs. PACeA15
Timepoint				
2W-RM ANOVA	0.0825	0.0825	0.0825	**<0.0001
0hrs				
3hrs	0.7480	0.9658	0.9126	0.7095
6hrs	0.0721	0.0517	0.8611	**0.0428
12hrs	0.7450	0.6006	0.9366	**0.0015
24hrs	0.1942	0.2871	0.9157	**0.0100
48hrs	0.8422	0.3163	0.3976	**0.0936

3.2.2 CFU analysis and calculated Growth Rate

In order to decipher whether there are further differences between both the *P. aeruginosa* clinical isolate and PAO1 reference in terms of growth, as well as whether antibiotic-adaptation does impact growth, growth rates of each isolate were calculated. The results were generated through cultivation of a serial-dilution of each isolate tested for growth on agar, and subsequent Colony-Forming Units (CFUs) calculated via the Miles and Misra method (Miles & Misra, 1931).

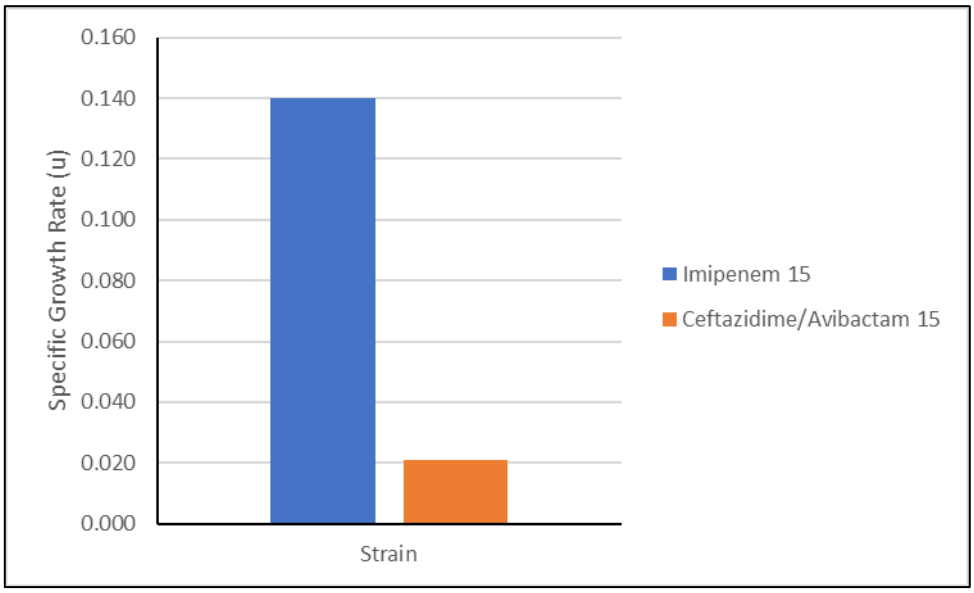

Figure 3.10: Calculated specific growth rate (μ) of individual *P. aeruginosa* growth under MH broth conditions.

Colony-forming units (CFUs) calculated from subsequent PBS dilutions as mentioned within the methodology displayed varied results throughout each adapted and un-adapted strain exposed to experimental conditions. Specific growth rates (μ) that were calculated indicated that the Ceftazidime/Avibactam-population had a lower growth rate in comparison to the Imipenem-adapted population (Figure 3.10; Table 3.07). Specific growth rates relating to other strains were inconclusive, including the Parent and PAO1 strain.

Table 3.07: CFU/mL and Specific Growth Rates of *P. aeruginosa* strains over 48hrs growth period in MH broth medium.

Strain	PAO1	Parent	M15	D15	I15	Cef8	C/A15	Col30
Timepoint 1/Beginning of Exponential Growth	6	6	6	6	6	6	6	6
Timepoint 2/End of Exponential Growth	24	24	12	24	12	48	12	48
CFU/mL Timepoint 1	≥5.0E+08	1.3E+09	≥5.0E+08	N/A	4.0E+09	≥5.0E+08	4.1E+10	≥5.0E+08
CFU/mL Timepoint 2	6.2E+09	≥5.0E+08	7.5E+09	4.6E+09	2.8E+10	2.3E+10	5.5E+10	3.2E+09
Specific Growth Rate μ (g^{-1})	N/A	N/A	N/A	N/A	0.140	N/A	0.021	N/A

3.3 Co-infection with *Staphylococcus aureus* has an effect on the overall population growth and biofilm formation

3.3.1 Interaction of *P. aeruginosa* strains with *S. aureus* control

Because most cases of VAP can be polymicrobial, this experiment observed whether the growth of *P. aeruginosa* in presence of *Staphylococcus aureus*, another causative agent in VAP. The PAO1 control, the Parent clinical strain of *P. aeruginosa*, and antibiotic-adapted isolates were introduced to a similar concentration of *S. aureus*, and growth was measured over 48 hrss. Absorbance was recorded at selected timepoints in order to deduce whether the introduction of *S. aureus* impacted the growth of both un-adapted and antibiotically adapted strains of *P. aeruginosa*.

Initial comparisons of growth between PAO1 and Parent strains under both monoculture and *S. aureus* co-culture conditions displayed little observable difference in growth pattern between both conditions. Under co-culture, the OD600 values detected for the PAO1 strain of *P. aeruginosa* indicated an overall higher level of population growth in comparison to mono-infection conditions (Figure 3.11), whilst following a similar pattern to that detected from mono-infection. The Parent strain, in contrast, displayed a consistent level of growth between both mono- and co-culture conditions, with the only observable differences being a steadier, yet not as expansive, log phase between 3hrs and 24hrs under co-infection conditions. The peak OD600 values, however, associated with peak population growth was slightly lower than that detected under mono-infection (Figure 3.11).

Statistical analysis via Two-way repeated measures ANOVA displayed a significant difference in the growth pattern of both strains when compared against each other ($P=<0.05$, Table 3.0; Figure 3.11). Subsequent post-hoc analysis between both PAO1 and Parent strains identified a significant difference between both strains at 12hrs ($P=<0.05$, Table 3.08; Figure 3.11).

Upon comparisons between monoculture and coculture conditions via Two-way ANOVA with repeated measures, significant differences between the Parent monoculture and co-culture condition ($P<0.05$, Table 3.09; Figure 3.11), specifically at the 6hrs timepoint ($P=<0.05$, Table 3.09; Figure 3.11).

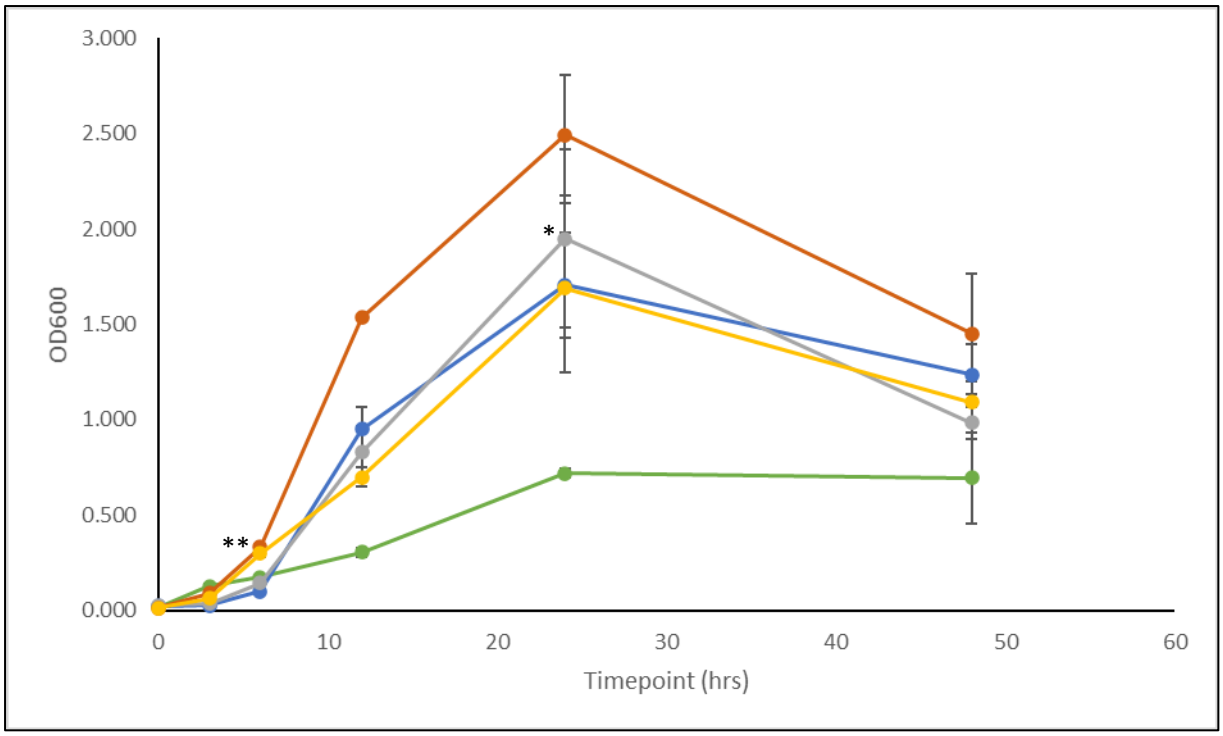

Figure 3.11: Growth Curve of *P. aeruginosa* PAO1 and Parent strains w/ addition of *S. aureus* under co-culture conditions in MH broth over 48hrs. S.aureus mono-culture is highlighted by the green growth curve. Absorbance was measured at 600nm (OD600). * = significance between PAO1 and Parent strain under co-culture conditions (P=<0.05; Sidak post-hoc analyses was conducted using GraphPad Prism 8.) ** significance between monoculture (PAO1 = blue; Parent = grey) and co-culture (PAO1 = orange; Parent = yellow) conditions (P=<0.05; Sidak post-hoc analyses was conducted using GraphPad Prism 8). Error bars represent Standard Error Mean (SEM).

Comparisons between each of the antibiotic-adapted isolates under co-culture displayed a variance in overall growth patterns. The carbapenem-adapted isolates each show a similar trend that was detected within monoculture conditions to begin with. Between 0-12hrs, there was a steep increase in the OD600 readings detected, thus a steep exponential phase during this period of time (Figure 3.12-3.14). Beyond this point, individual differences arise from observation of the results. PAM15 increased in overall population growth in comparison to monoculture conditions at 24hrs, before a moderate decline phase occurs as indicated by the results collected at 48hrs (Figure 3.12). PAD15, in contrast to PAM15, however, enters a stationary phase between 12-48hrs, with slight fluctuations in growth under co-culture conditions (Figure 3.13).

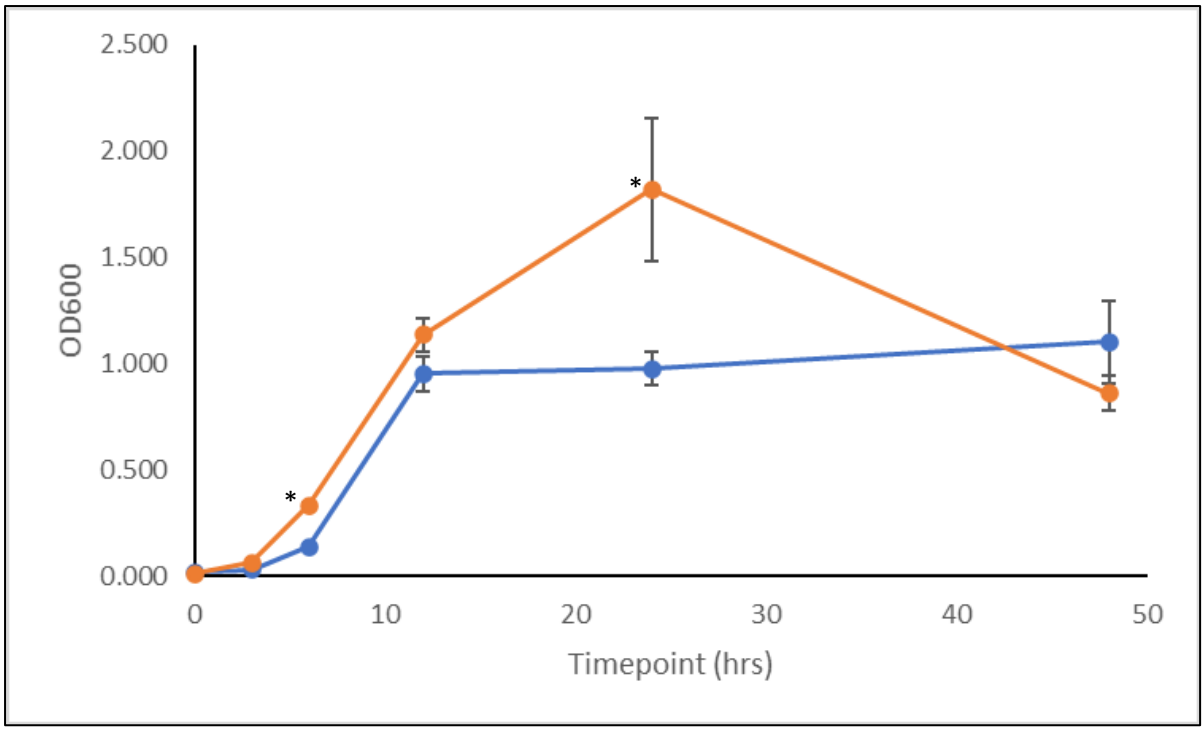

Figure 3.12: Growth Curve of PAM15 monoculture (blue) and w/ addition of *S. aureus* under co-culture (orange) conditions in MH broth over 48hrs. Absorbance was measured at 600nm (OD600). * = significance between monoculture and co-culture conditions (P=<0.05; Sidak post-hoc analysis was conducted using GraphPad Prism 8). Error bars represent Standard Error Mean (SEM).

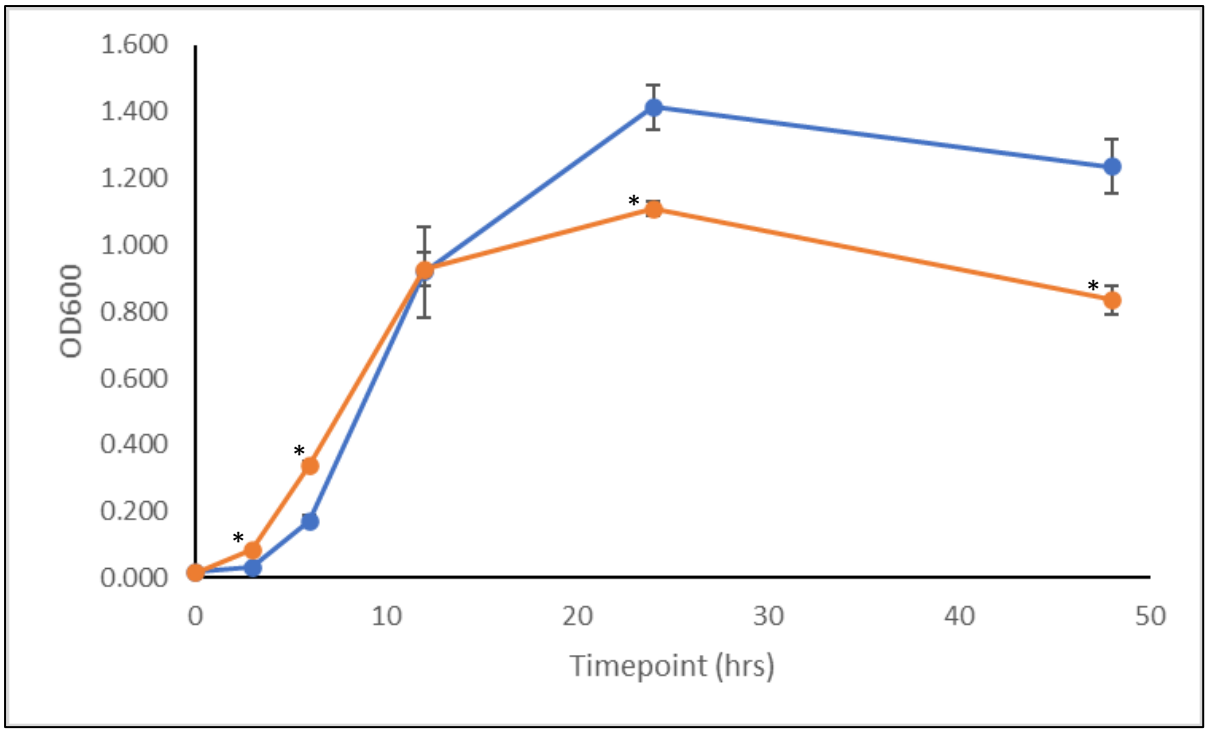

Figure 3.13: Growth Curve of PAD15 monoculture (blue) and w/ addition of *S. aureus* under co-culture (orange) conditions in MH broth over 48hrs. Absorbance was measured at 600nm (OD600). * = significance between monoculture and co-culture conditions (P=<0.05; Sidak post-hoc analysis was conducted using GraphPad Prism 8). Error bars represent Standard Error Mean (SEM).

PAI15 displayed a much different pattern to what had previously been observed under monoculture conditions. Population growth, as signified by the OD600 values, continued to steeply increase until peaking at 24hrs, at a much higher reading than what was found under monoculture (Figure 3.14). In contrast once again to the previous condition, the strain then entered a steep decline phase after 24hrs. Both growth patterns (monoculture and co-culture) displayed higher OD600 values in comparison to the Parent strain (Figure 3.14).

Each of the three *P. aeruginosa* strains displayed significant differences in growth patterns in comparison to monoculture conditions upon application of Two-way repeated measures ANOVA (P=<0.05, Table 3.09; Figure 3.12-3.14). Subsequent Sidak post-hoc analysis indicated significant differences at various timepoints between carbapenem-adapted strains upon comparing *S. aureus* co-culture conditions with monoculture patterns. All three adapted isolates displayed significance in growth after 6hrs (P=<0.05, Table 3.09; Figure 3.12-3.14). Differences between isolates, however, were detected when comparing these isolates against

OD600 values at later timepoints. For PAM15, significance was only detected after 24hrs of growth when compared against monoculture (P=<0.05, Table 3.09; Figure 3.12). PAD15 was similar in that there was significance detected at 24hrs, whilst also displaying a significant difference at 3hrs and 48hrs (P=<0.05, Table 3.09; Figure 3.13). PAI15 had further significant variance in growth detected at 3hrs and 48hrs timepoints (P=<0.05, Table 3.09; Figure 3.14), sharing one similar finding with PAD15.

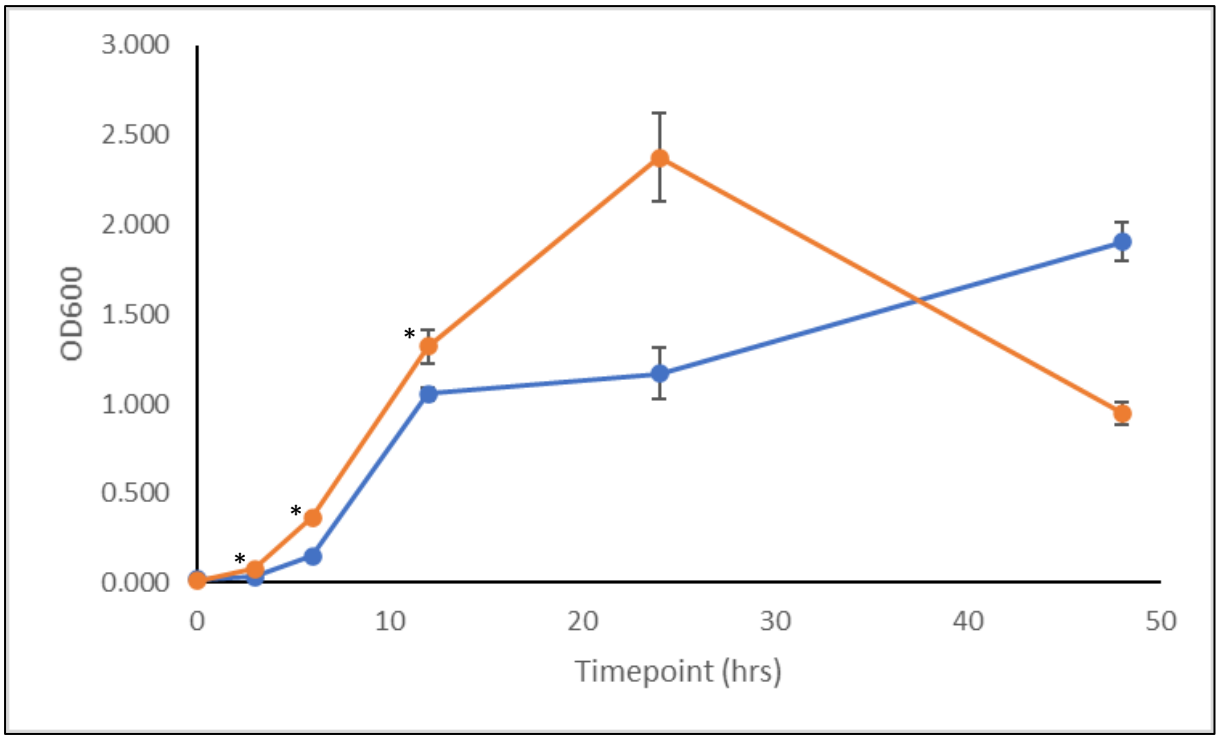

Figure 3.14: Growth Curve of PAI15 monoculture (blue) and w/ addition of *S. aureus* under co-culture (orange) conditions in MH broth over 48hrs. Absorbance was measured at 600nm (OD600). * = significance between monoculture and co-culture conditions (P=<0.05; Sidak post-hoc analysis was conducted using GraphPad Prism 8). Error bars represent Standard Error Mean (SEM).

The cephalosporin-adapted strains also displayed variance in overall growth patterns when exposed to co-culture with *S. aureus*. Growth within the PACe8 population rose sharply between 6hrs-24hrs timepoints, in contrast to the original timepoint, which exhibited a sharp exponential phase at first, before a slow, gradual increase after 12hrs of growth (Figure 3.15). Peak growth was detected at 24hrs under co-culture conditions, before a sharp decline phase

occurred.

PACeA15 displayed little change in comparison to the pattern detected under mono-infection conditions, albeit with a slight increase in optical density detected at the 24hrs timepoint, indicating a slow, gradual exponential phase beginning at the 12hrs timepoint (Figure 3.16).

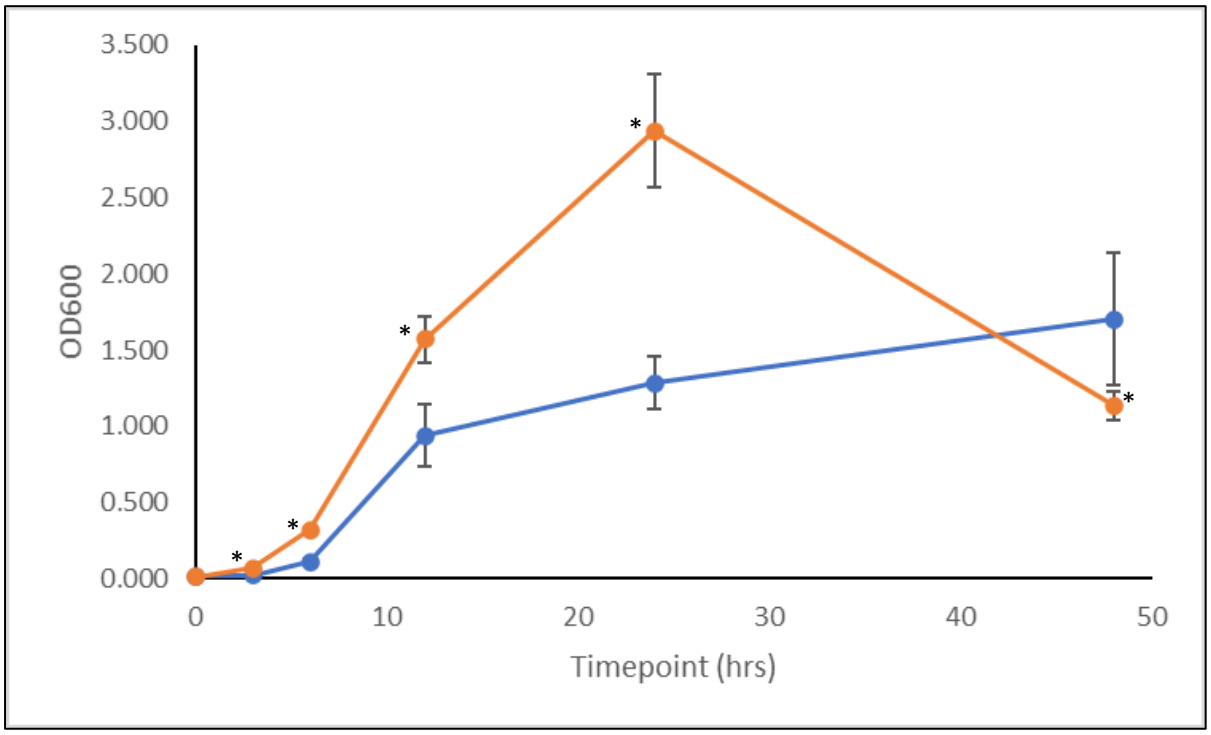

Figure 3.15: Growth Curve of PACe8 monoculture (blue) and w/ addition of *S. aureus* under co-culture (orange) conditions in MH broth over 48hrs. Absorbance was measured at 600nm (OD600). * = significance between monoculture and co-culture conditions (P=<0.05; Sidak post-hoc analysis was conducted using GraphPad Prism 8). Error bars represent Standard Error Mean (SEM).

Significance values were detected from Two-way repeated measures ANOVA analyses of both cephalosporins in comparison to their monoculture patterns (P=<0.05, Table 3.09; Figure 3.15-3.16). Sidal post-hoc analysis found that PACe8 displayed significances at all timepoints measured (3hrs, 6hrs, 12hrs, 24hrs, 48hrs) (P=<0.05, Table 3.09; Figure 3.15). In contrast, only two timepoints exhibited significant differences when comparing both PACeA15 growth conditions; at both 3hrs and 6hrs (P=<0.05, Table 3.09; Figure 3.16).

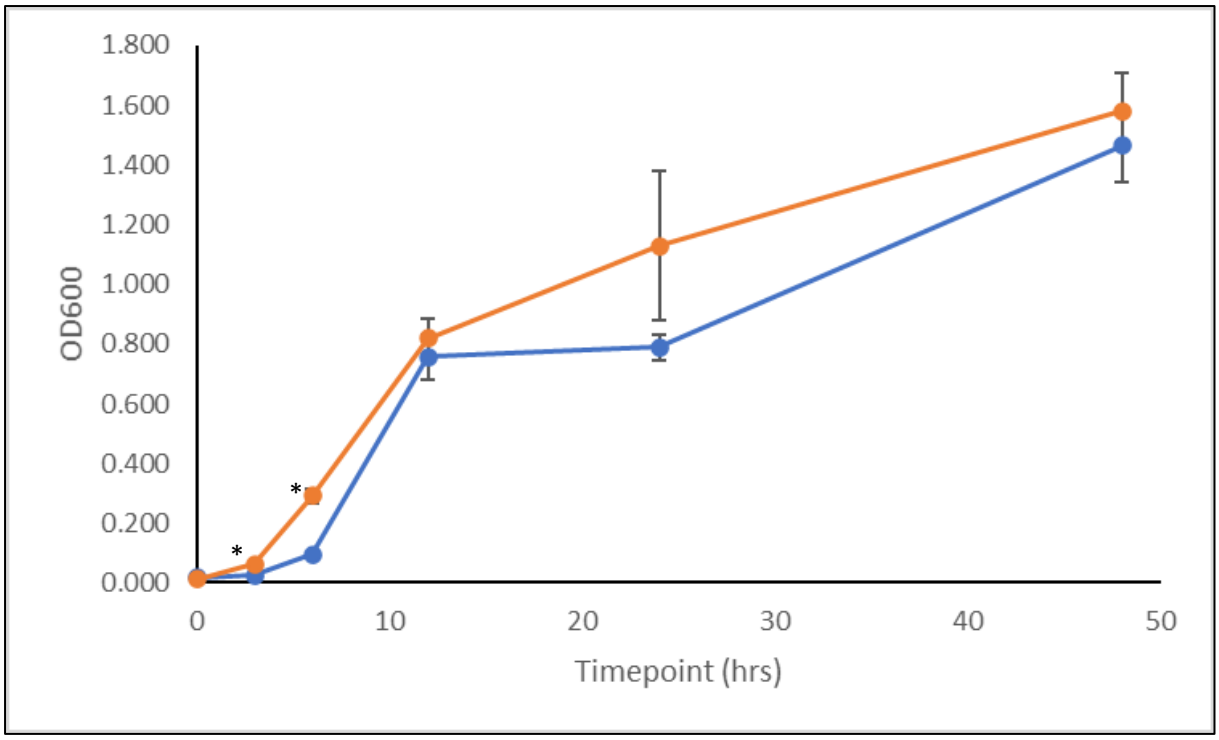

Figure 3.16: Growth Curve of PACeA15 monoculture (blue) and w/ addition of *S. aureus* under co-culture (orange) conditions in MH broth over 48hrs. Absorbance was measured at 600nm (OD600). * = significance between monoculture and co-culture conditions (P=<0.05; Sidak post-hoc analysis was conducted using GraphPad Prism 8). Error bars represent Standard Error Mean (SEM).

PACo30 diverted from its original growth pattern under co-culture conditions according to the recorded OD600 values. When combined with *S. aureus*, this strain of *P. aeruginosa* displayed a sharper exponential growth phase as the values increased between 3hrs and 12hrss timepoints (Figure 3.17). Population growth peaked at 24hrs, before entering a gradual decline phase (Figure 3.17).

Two-way repeated measures ANOVA found that there was a significant difference in growth patterns between both PACo30/*S. aureus* co-culture and monoculture (P=0.05, Table 3.09; Figure 3.16). Significant differences between co-culture with *S. aureus* and monoculture were detected at 3hrs and 6hrs timepoints for PACo30 (P=<0.05, Table 3.09; Figure 3.17).

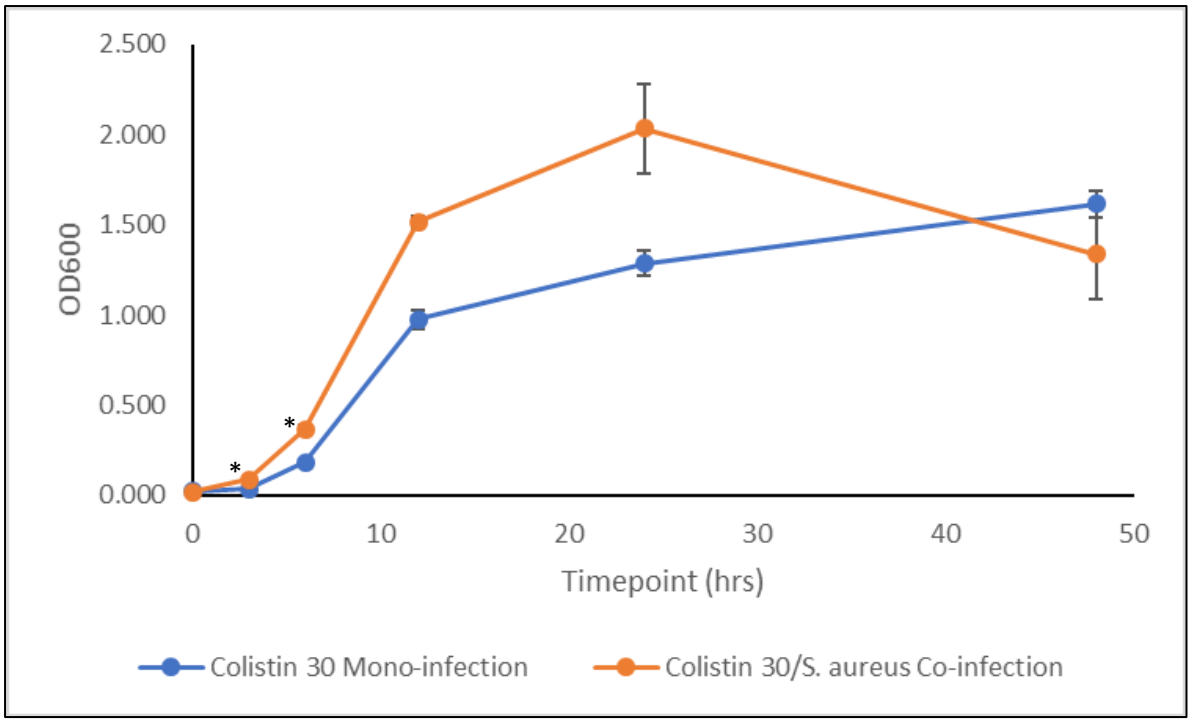

Figure 3.17: Growth Curve of PACo30 monoculture (blue) and w/ addition of *S. aureus* under co-culture (orange) conditions in MH broth over 48hrs. Absorbance was measured at 600nm (OD600). * = significance between monoculture and co-culture conditions (P=<0.05; Sidak post-hoc analysis was conducted using GraphPad Prism 8). Error bars represent Standard Error Mean (SEM).

Further detailed results regarding the growth of each *P. aeruginosa* isolate when exposed to *S. aureus* can be found in Appendix 3.

Table 3.08: Calculated significance results of Two-way repeated measures ANOVA analysis between both PAO1 control and Parent *P. aeruginosa* strains to compare differences in planktonic growth under *S. aureus* co-culture in MH broth. '*' – P=<0.05

Strain	Timepoint	2W-RM ANOVA	0hrs	3hrs	6hrs	12hrs	24hrs	48hrs
PAO1 vs. Parent		*<0.0001		0.0872	0.4195	*0.0001	0.2046	0.8184

Table 3.09: Calculated significance results of Paired T-tests conducted to compare differences in *P. aeruginosa* strain planktonic growth under monoculture and *S. aureus* co-culture in MH broth. '*' – P=<0.05

Strain	Parent	PAM15	PAD15	PAI15	PACe8	PACeA15	PACo30
2W-RM ANOVA	*0.0219	*<0.0001	*<0.0001	*<0.0001	*<0.0001	0.0869	*<0.0001
Timepoint							
0hrs							
3hrs	0.0885	0.0529	*0.0449	*0.0057	*0.0010	*0.0386	*0.0002
6hrs	*0.0018	*0.0004	*0.0023	*<0.0001	*0.0019	*0.0312	*0.0017
12hrs	0.2155	0.2841	>0.9999	*0.0263	*0.0001	0.2913	0.1239
24hrs	0.8882	*0.0248	*0.0158	0.4710	*0.0022	0.7371	0.0533
48hrs	0.5094	0.2238	*0.0038	0.0803	*0.0011	0.6036	0.5440

3.3.2 Biofilm Formation under *S. aureus* co-culture conditions

Biofilm formation analysis was also conducted within the co-culture experiment to understand whether the presence of another species influences the amount of biofilm produced by *P. aeruginosa*. Absorbance values were recorded from any biofilm left after washing the microtitre assays and staining residual biofilm with Crystal Violet. Both PAO1 and the clinical sample were compared against one another to compare differences in biofilm expression under co-culture conditions, as well as in comparison under solo growth conditions to understand any effect *S. aureus* had on secretion.

Each *P. aeruginosa* antibiotically-adapted strain undergoing exposure to *S. aureus* were also compared with monoculture conditions, as to understand whether adaptation had an effect on whether biofilm formation would have changed under co-culture conditions as a means to understand whether this could be a potential fitness cost as a result of adaptation.

Both the PAO1 strain and Parent strain of *P. aeruginosa* have an observable difference in biofilm production when comparing both monoculture and co-culture conditions. The initial readings from 0hrs timepoints for both PAO1 and the Parent both indicate observable biofilm formation upon contact with *S. aureus* (Figure 3.18). In contrast to monoculture, a steep exponential growth was displayed by PAO1 from the 6hrs to 12hrs timepoints (Figure 3.18). This then is contrasted by a sharp decrease leading to the 24hrs timepoint, before biofilm formation reaches a stationary phase beyond 24hrss (Figure 3.18).

The Parent, in comparison to monoculture, also experienced a sharp increase in biofilm formation, before reaching a peak at 12hrs (Figure 3.18). This peak, however, is at a smaller value than that detected from monoculture, as indicated by OD600 values recorded at 6hrss. OD600 values dip lightly between 6-12hrs of infection, before a steep decline phase in biofilm production occurs between 12-24hrs (Figure 3.18). As with PAO1, the Parent strain enters a stationary phase in biofilm formation between 24-48hrs (Figure 3.18), albeit recording a lower OD600 value than PAO1 at 48hrs.

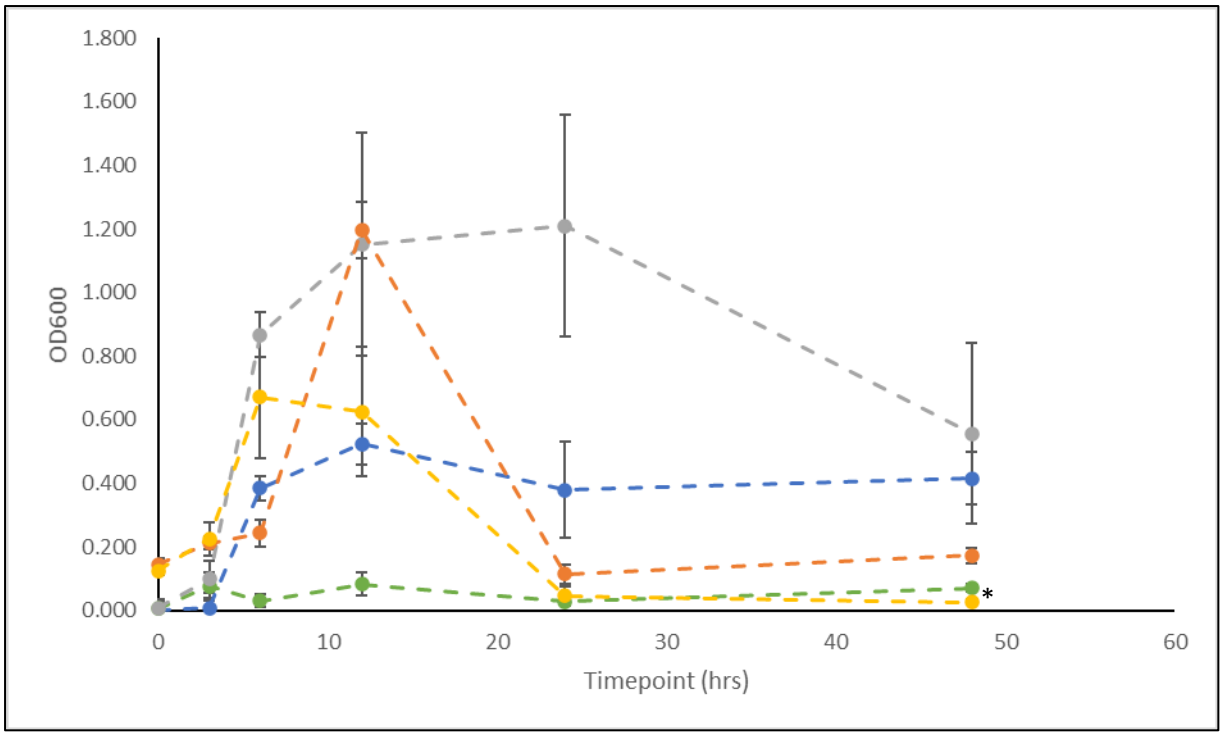

Figure 3.18: Biofilm Formation of PAO1 and Parent strains of *P. aeruginosa* monoculture (PAO1 = blue; Parent = grey) and w/ addition of *S. aureus* under co-culture (PAO1 = orange; Parent = yellow) conditions in MH broth over 48hrs. *S. aureus* biofilm is represented by the green growth curve. Absorbance was measured at 600nm (OD600). * = significance between PAO1 and Parent under *S. aureus* co-infection (P=<0.05; Sidak post-hoc analysis was conducted using GraphPad Prism 8). Error bars represent Standard Error Mean (SEM).

Two-way repeated measures ANOVA indicated that significant differences were present between both PAO1 and the Parent strain within *S. aureus* co-culture (P=<0.05, Table 3.10; Figure 3.18). Sidak post-hoc analysis further demonstrated that a significant difference between both PAO1 and the Parent strain under co-culture was found after 48hrs of growth (P=<0.05, Table 3.10; Figure 3.18). Upon comparing both strains against optical density values detected within monoculture, PAO1 displayed significant differences at 3hrs and 12hrs timepoints (P=<0.05, Table 3.11; Figure 3.18). The Parent strain, in contrast, indicated no significant differences in biofilm formation throughout the entire period of growth (Table 3.11; Figure 3.18).

Examination of each of the antibiotic-adapted strains under *S. aureus* co-culture conditions also displayed a different effect on biofilm formation over 48hrs.

The carbapenem-adapted strains all differed in their secretion in various ways. Both PAM15 and PAD15 display similar patterns of biofilm production to one another over the experimental period. Both strains display an initial increase in biofilm production at the beginning of growth at 0hrs (Figure 3.19-3.20), before displaying sharp increases in biofilm production between 0hrs and 6hrs of growth (Figure 3.19-3.20). Overall biofilm formation peaks at 6hrs for both PAM15 and PAD15. A sharp decline occurs between 6hrs and 24hrs timepoints for PAM15 before biofilm production levels out between 24-48hrs (Figure 3.19). PAD15 differs slightly in this pattern, in that there is a slow decrease in biofilm production between 6-12hrs, before entering a sharp decline phase between 12hrs-24hrs of growth (Figure 3.20).

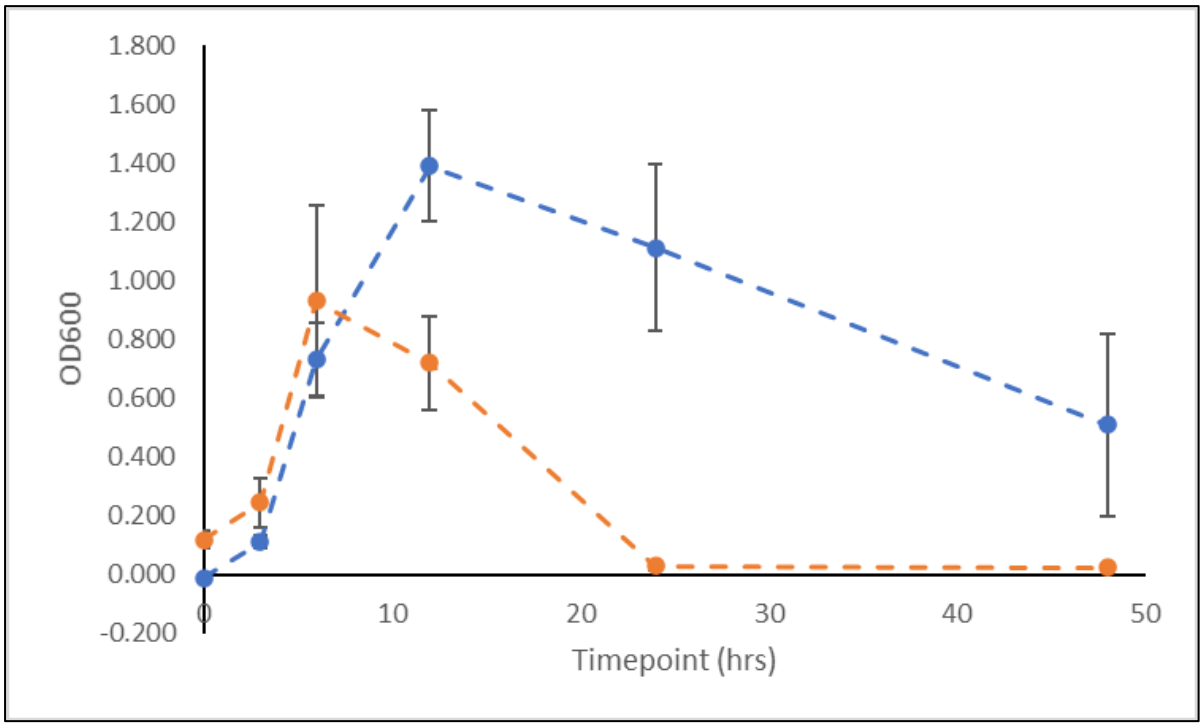

Figure 3.19: Biofilm Formation of PAM15 monoculture (blue) and w/ addition of *S. aureus* under co-culture (orange) conditions in MH broth over 48hrs. Absorbance was measured at 600nm (OD600). Error bars represent Standard Error Mean (SEM).

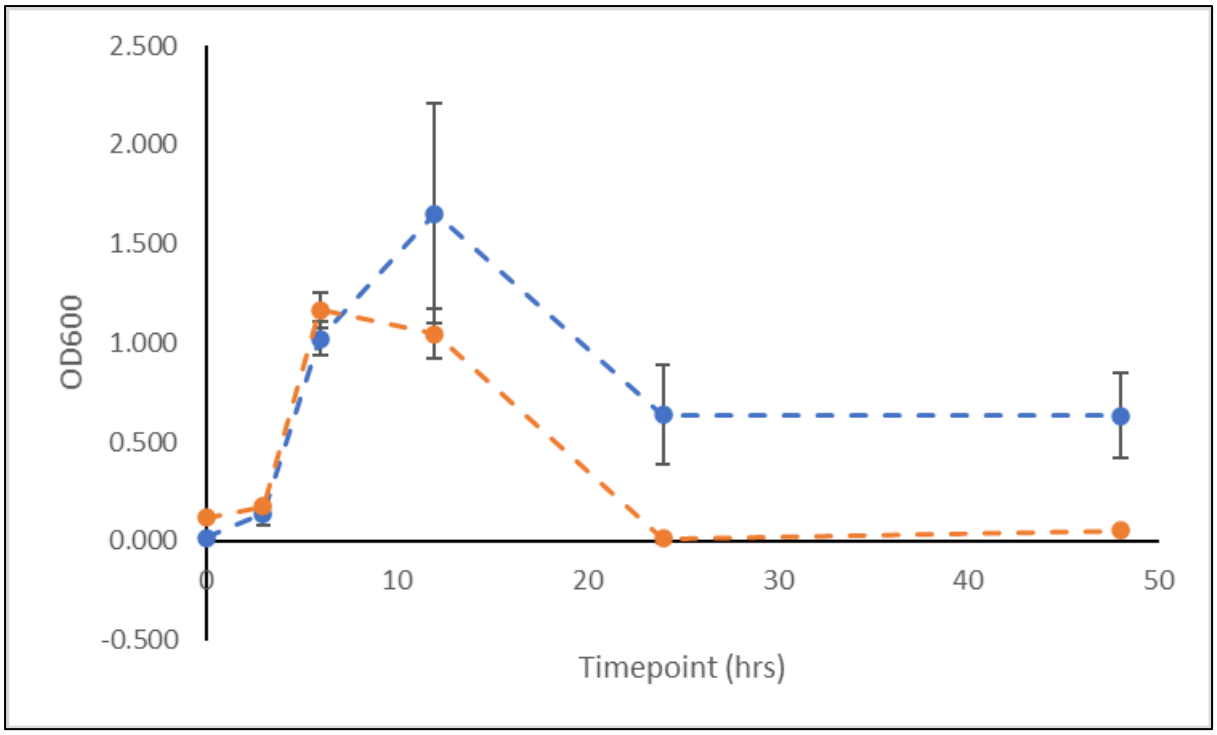

Figure 3.20: Biofilm Formation of PAD15 monoculture (blue) and w/ addition of *S. aureus* under co-culture (orange) conditions in MH broth over 48hrs. Absorbance was measured at 600nm (OD600). Error bars represent Standard Error Mean (SEM).

PAI15, in contrast, displays a much different pattern when biofilm formation occurs in the presence of *S. aureus*. Whilst a higher optical density was detected at 0hrss, a sharp rise in growth occurs before 3hrs of growth (Figure 3.21). A slight decline occurs before biofilm formation once again rises and peaks at 12hrs of growth (Figure 3.21). The Imipenem-adapted strain then follows a similar formation pattern as with the other carbapenems; a sharp decline in the presence of biofilm between 12-24hrs before growth becomes stationary (Figure 3.21).

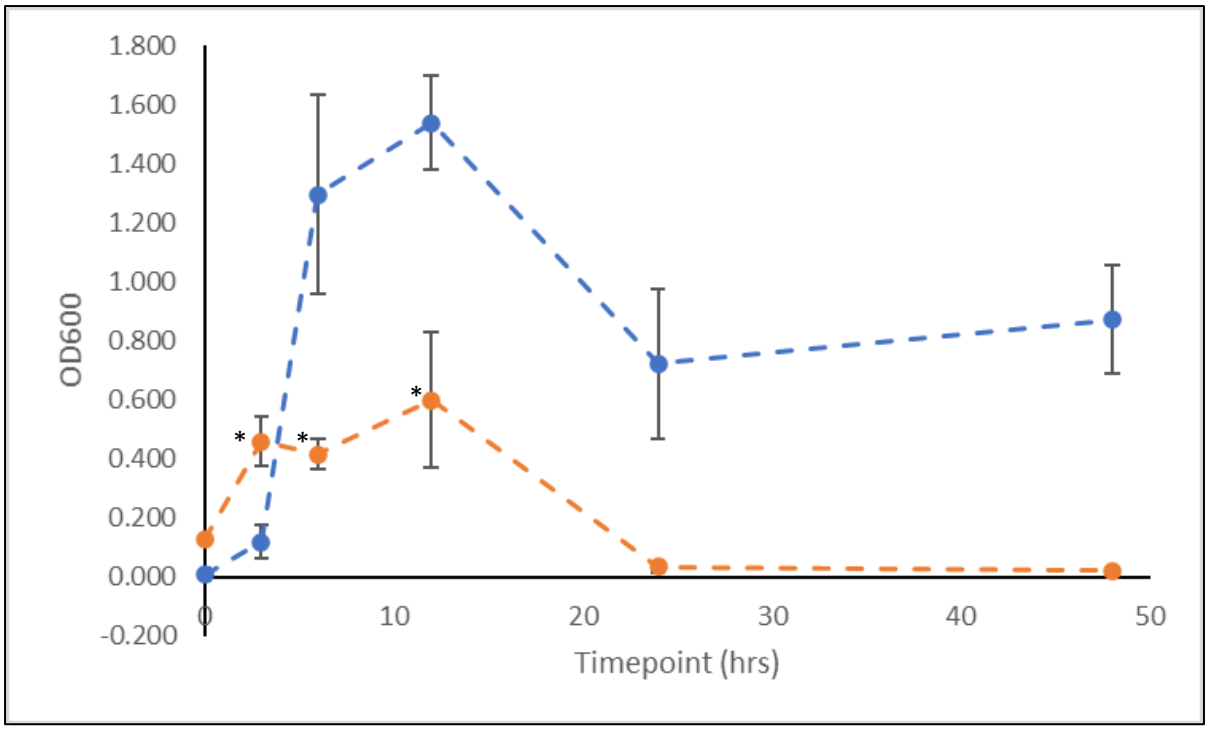

Figure 3.21: Biofilm Formation of PAI15 monoculture (blue) and w/ addition of *S. aureus* under co-culture (orange) conditions in MH broth over 48hrs. Absorbance was measured at 600nm (OD600). * = significance between monoculture and co-culture conditions (P=<0.05; Sidak post-hoc analysis was conducted using GraphPad Prism 8). Error bars represent Standard Error Mean (SEM).

Statistical analysis between these carbapenem-adapted isolates when comparing biofilm formation with that encountered from monoculture indicated significant differences significant differences within their respective growth patten (P=<0.05, Table 3.11; Figure 3.19-3.21). From post-hoc analysis, however, both PAM15 and PAD15 reported no significant differences in biofilm formation in comparison to monoculture at specific timepoints (Table 3.11; Figure 3.19). PAI15, in contrast, displayed significant differences in biofilm formation when exposed to co-culture at 3hrs, 6hrs and 12hrs (P=<0.05, Table 3.11; Figure 3.21).

Cephalosporin-adapted *P. aeruginosa* strains also displayed some difference in biofilm secretion in comparison to the levels detected from monoculture. The PACe8 displayed a similar pattern to what was originally observed (Figure 3.22). The differences, however, were that initial optical density detected at 0hrs was at a higher reading compared to mono-

infection (Figure 3.22). Peak biofilm formation was observed at 12hrs, albeit at a lower reading to that encountered in the monoculture condition. A much steeper decline phase was noted between 12hrs and 24hrs timepoints, before slowing down between 24-48hrs.

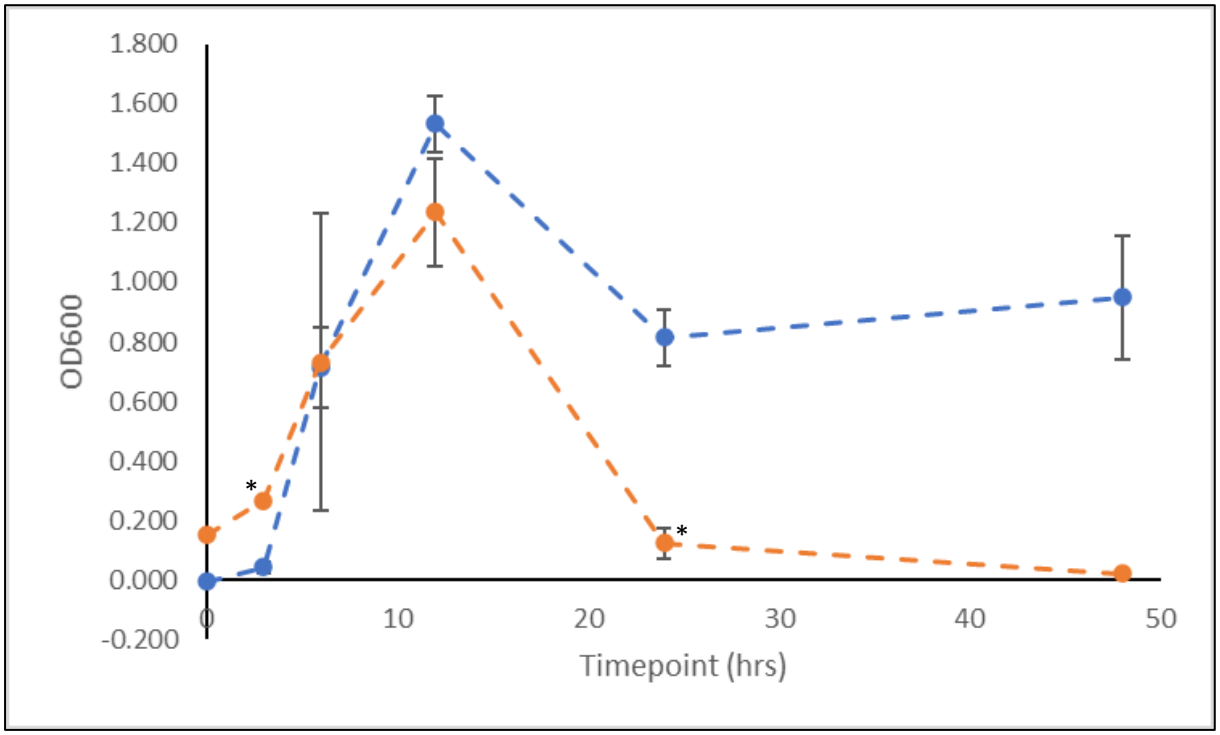

Figure 3.22: Biofilm Formation of PACe8 monoculture (blue) and w/ addition of *S. aureus* under co-culture (orange) conditions in MH broth over 48hrs. Absorbance was measured at 600nm (OD600). * = significance between monoculture and co-culture conditions (P=<0.05; Sidak post-hoc analysis was conducted using GraphPad Prism 8). Error bars represent Standard Error Mean (SEM).

In contrast to monoculture PACeA15 displayed a similar pattern to that shown from PACe8 co-culture (Figure 3.23). Biofilm formation initially began at a higher optical density, before then entering a sharp exponential phase peaking at 12hrs (Figure 3.23). A sharp decline was then noted between 12-24hrs before biofilm formation remained stationary (Figure 3.23).

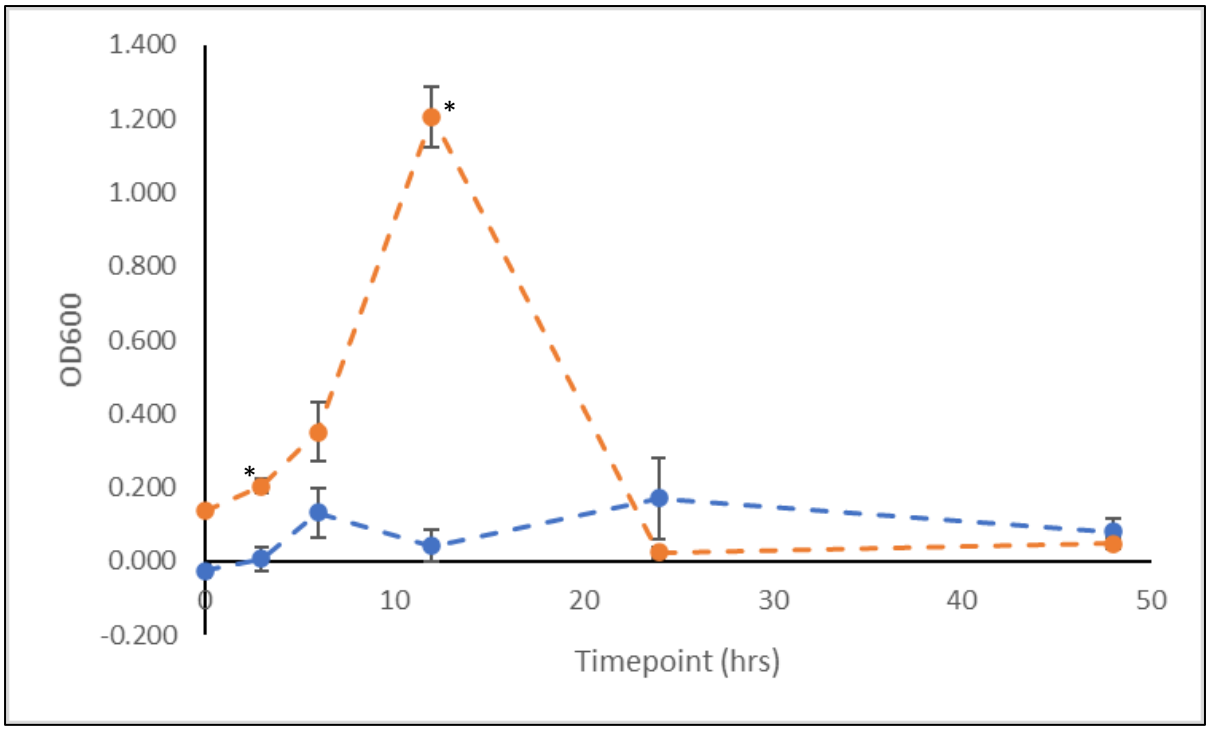

Figure 3.23: Biofilm Formation of PACeA15 monoculture (blue) and w/ addition of *S. aureus* under co-culture (orange) conditions in MH broth over 48hrs. Absorbance was measured at 600nm (OD600). * = significance between monoculture and co-culture conditions (P=<0.05; Sidak post-hoc analysis was conducted using GraphPad Prism 8). Error bars represent Standard Error Mean (SEM).

Significant differences in biofilm formation between monoculture and co-culture with *S. aureus* were noted from Two-way repeated measures ANOVA (P=<0.05, Table 3.11; Figure 3.22-3.23), specifically at 3hrs for both cephalosporin-adapted isolates (P=<0.05, Table 3.11; Figure 3.22-3.23). Contrasts, however, were found upon comparing OD600 values at other timepoints, with one additional significant difference occurring after 24hrs of growth for PACe8 (P=<0.05, Table 3.11; Figure 3.22), and after 12hrs for PACeA15 (P=<0.05, Table 3.11; Figure 3.23).

PACo30 when exposed to a growth medium with *S. aureus* showed some variation in comparison to monoculture. As with all other adapted strains, a higher OD600 value was detected at the 0hrs timepoint (Figure 3.24). Steep exponential biofilm formation occurred afterwards, until reaching a peak at 24hrs (Figure 3.24). After 12hrs of growth, biofilm formation enters a sharp decline phase, before slowing down, with biofilm reaching lower levels than that observed from the monoculture. Though significant differences were detected in comparison to PACo30 monoculture (P=<0.05, Table 3.11; Figure 3.24), this was only found have occurred at 6hrs (P=<-0.05, Table 3.11; Figure 3.24).

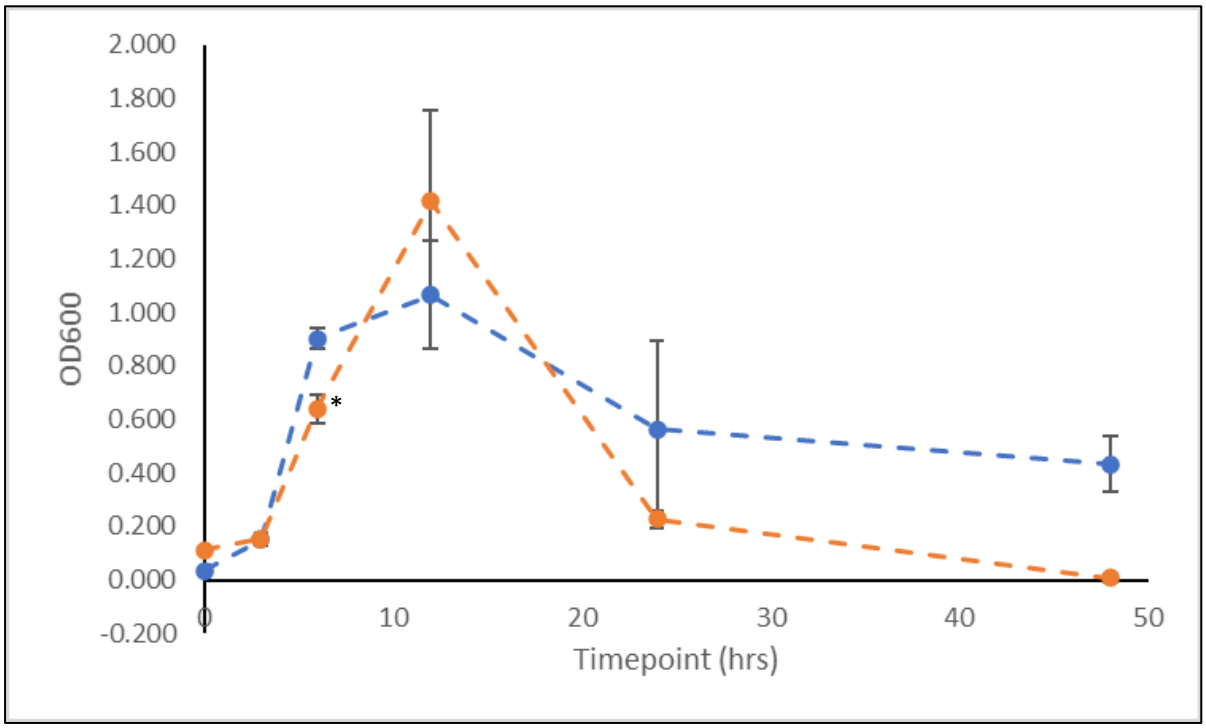

Figure 3.24: Biofilm Formation of PACo30 (blue) and w/ addition of *S. aureus* under co-culture (orange) conditions in MH broth over 48hrs. Absorbance was measured at 600nm (OD600). * = significance between monoculture and co-culture conditions (P=<0.05; Sidak post-hoc analysis was conducted using GraphPad Prism 8). Error bars represent Standard Error Mean (SEM).

Further detailed results regarding OD600 values collected from the co-culture biofilm formation condition are displayed within Appendix 4.

Table 3.10: Calculated significance results of Two-way repeated measures ANOVA analysis between both PAO1 control and Parent *P. aeruginosa* strains to compare differences in biofilm formation under *S. aureus* co-culture in MH broth. '*' – P=<0.05

Strain	2W-RM ANOVA	Timepoint	0hrs	3hrs	6hrs	12hrs	24hrs	48hrs
PAO1 vs. Parent	*<0.0001			0.9993	0.2844	0.1444	0.2637	*0.0298

Table 3.11: Calculated significance results of Two-way repeated measures ANOVA, and subsequent Sidak post-hoc analysis, conducted to compare differences in *P. aeruginosa* strain biofilm formation under monoculture and *S. aureus* co-culture in MH broth. '*' – P=<0.05

Strain	Parent	PAM15	PAD15	PAI15	PACe8	PACeA15	PACo30
2W-RM ANOVA	*<0.0001	*<0.0001	*0.0010	*<0.0001	*<0.0001	*<0.0001	*0.0025
Timepoint							
0hrs							
3hrs	0.2591	0.4808	0.9545	*0.0384	*0.0035	*0.098	>0.9999
6hrs	0.7512	0.9564	0.4988	*0.0051	0.2380	0.1330	*0.0209
12hrs	0.4823	0.0579	0.7259	*0.0362	0.4179	*0.0014	0.7691
24hrs	0.1558	0.1251	0.2615	0.2231	*0.0077	0.6049	0.7733
48hrs	0.4055	0.5140	0.2305	0.0867	0.0939	0.8585	0.1000

3.4 Growth within restricted carbon media has a drastic effect on the *P. aeruginosa* growth and biofilm formation universally

3.4.1 Growth of *P. aeruginosa* strains

In order to understand whether antibiotic adaptation created a fitness cost regarding the growth of *P. aeruginosa* when exposed to different environmental conditions, namely in an environment that has a limited number of carbon metabolites needed to sustain growth. The next set of experiments involved each strain being grown within M9 minimal media, a growth medium that has little metabolic content, whilst being exposed to different specific carbon sources.

Each *P. aeruginosa* strain was cultured in M9 minimal media, which was supplemented with either 20% Glucose or 20% Alanine, both of which are known elements that bacteria use as a source of carbon. A growth curve analysis was conducted over a period of 48 hrs, and absorbance values recorded during this period at an optical density of 600nm.

Initial differences between PAO1 and the clinical isolate were established through statistical analyses, namely through a Paired T-test, in order to establish whether there was difference in growth patterns between the two strains when exposed to minimal media, and whether the difference in genetics affected their ability to grow in an environment with restricted sources of carbon.

Further comparisons between the un-adapted clinical isolate and antibiotically adapted isolates differed in growth pattern as a result of adaptation mutations. This would provide potential explanations as to whether a fitness cost may have been induced due to adaptation.

All strain absorbance values were also compared with previous growth under nutrient-rich conditions, namely MH broth, to understand whether a lack of nutrients was a limiting factor in growth.

Initial observations of growth under Minimal Media conditions and their impact on bacterial growth of both the PAO1 control, and the Parent strain of *P. aeruginosa* indicated very little distinction in the pattern of growth between either strain over the 48hrs period.

The PAO1 growth pattern when cultured M9 Minimal Media supplemented with either 20% Glucose or 20% Alanine displayed little growth between 0-12hrs (Figure 3.25). After 12hrs, a

rapid spike in growth occurred, peaking at 24hrs (Figure 3.25), before entering a rapid decline phase after 24hrs of growth. This rapid decline, highlighted by the OD600 value detected after 48hrs of growth (Figure 3.25), may have been due to the depletion of nutrient within each well the bacteria was contained within. As a result, growth will have reduced, and eventually led to population decrease.

The Parent strain exhibited similar growth, albeit with minor differences in comparison to PAO1. Minor growth was detected between 6hrs and 12hrs, before spiking at 24hrs (Figure 3.26), though at a lower detected OD600 value to both PAO1 in minimal media, and Parent growth in rich MH broth medium. Growth with 20% Glucose supplement produced a slighter higher growth peak in comparison to medium supplemented with 20% Alanine (Figure 3.26).

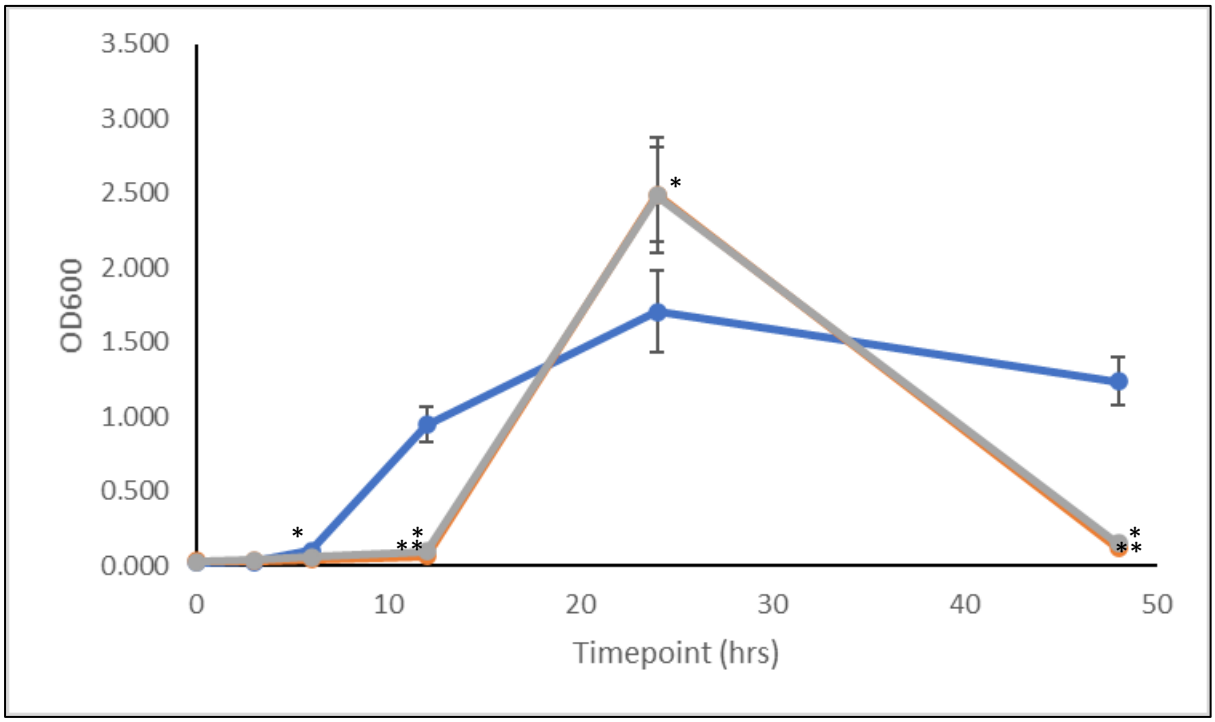

Figure 3.25: Planktonic growth of PAO1 *P. aeruginosa* grown within three separate media; Mueller-Hinton (blue) and M9 Minimal Media supplemented with 20% Glucose (grey) or 20% Alanine (orange) over a 48hrs period. Growth absorbance was measured at 600nm (OD600). * = significant differences between rich media (Mueller-Hinton) and restricted carbon sources (M9 Minimal Media supplemented with 20% Glucose/Alanine) (P=<0.05; Sidak post-hoc analysis was conducted using GraphPad Prism 8). Error bars represent Standard Error Mean (SEM).**

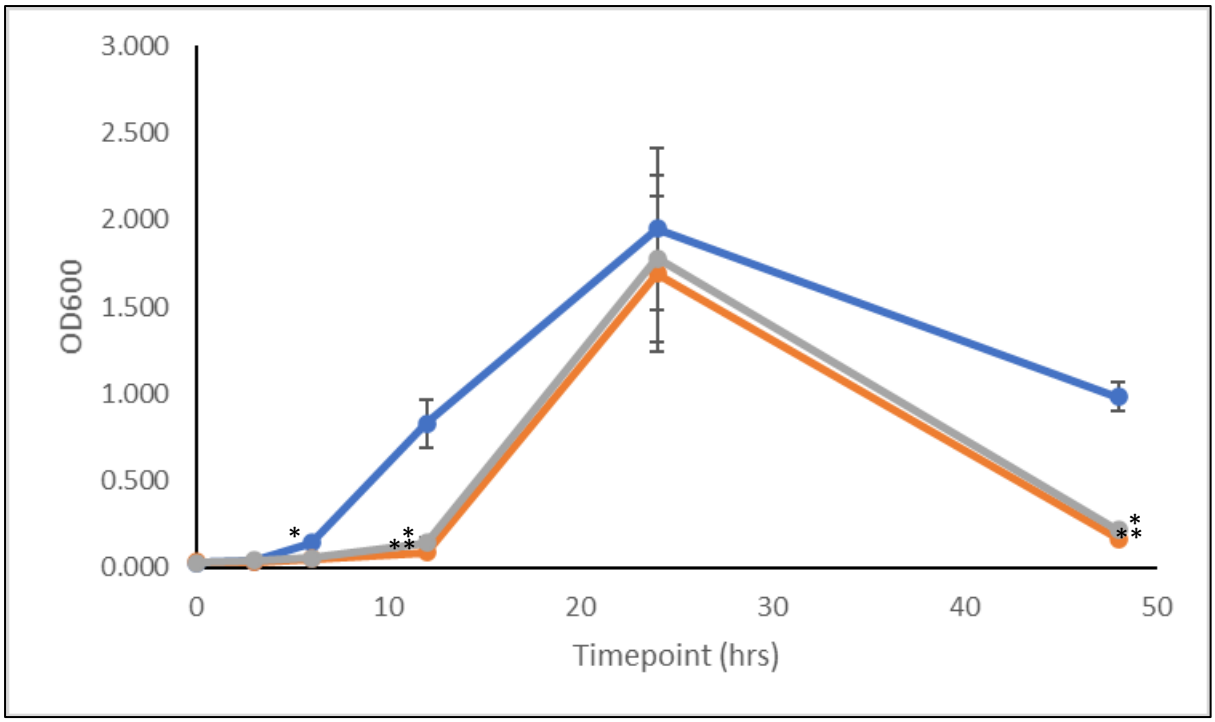

Figure 3.26: Planktonic growth of Parent strain *P. aeruginosa* grown within three separate media; Mueller-Hinton (blue) and M9 Minimal Media supplemented with 20% Glucose (grey) or 20% Alanine (orange) over a 48hrs period. Growth absorbance was measured at 600nm (OD600). * = significant differences between rich media (Mueller-Hinton) and restricted carbon sources (M9 Minimal Media supplemented with 20% Glucose/Alanine) (P=<0.05; Sidak post-hoc analysis was conducted using GraphPad Prism 8). Error bars represent Standard Error Mean (SEM).**

Two-way repeated measures ANOVA found that there were significant differences between MH and M9 Minimal Media growth supplemented with either 20% Alanine or 20% Glucose (P=<0.05, Table 3.12-3.13; Figure 3.26). Specifically, after Sidak post-hoc analysis, this significance was found at 6hrs, 12hrs, 24hrs, and 48hrs timepoints for PAO1 in 20% Alanine (P=<0.05, Table 3.12; Figure 3.26). In contrast, significance was recorded at 12hrs and 48hrs of growth when PAO1 was grown in 20% Glucose supplemented media (P=<0.05, Table 3.13; Figure 3.26). Significance in OD600 results were also found for the Parent strain of *P. aeruginosa* between MH and M9 minimal media growth at 6hrs, 12hrs and 48hrs with 20% Alanine supplement (P=<0.05, Table 3.12; Figure 3.26). Points of significance reduced, however, for Parent growth within 20% Glucose supplemented media, with significant growth only reported at both 12hrs and 24hrs timepoints (P=<0.05, Table 3.13; Figure 3.26).

When comparing between either supplement, no significant differences in growth were found at any timepoint between M9 media supplemented with either 20% Alanine or 20% Glucose (Table 3.14), based on both Two-way ANOVA and post-hoc analysis.

Similar patterns were found when comparing each adapted strains' growth pattern within different media. The carbapenems exhibited a near identical growth pattern to what was described for both PAO1 and Parent strains, albeit with minor differences in optical density values. Both PAM15 and PAI15 displayed higher peaks in growth at 24hrss in comparison to the Parent (Figure 3.27; Figure 3.29). PAD15 in contrast, had a lower OD600 value recorded at peak growth at 24hrs (Figure 3.28). Slight growth was also detected from the Doripenem-adapted strain between 3-12hrs in both minimal media conditions.

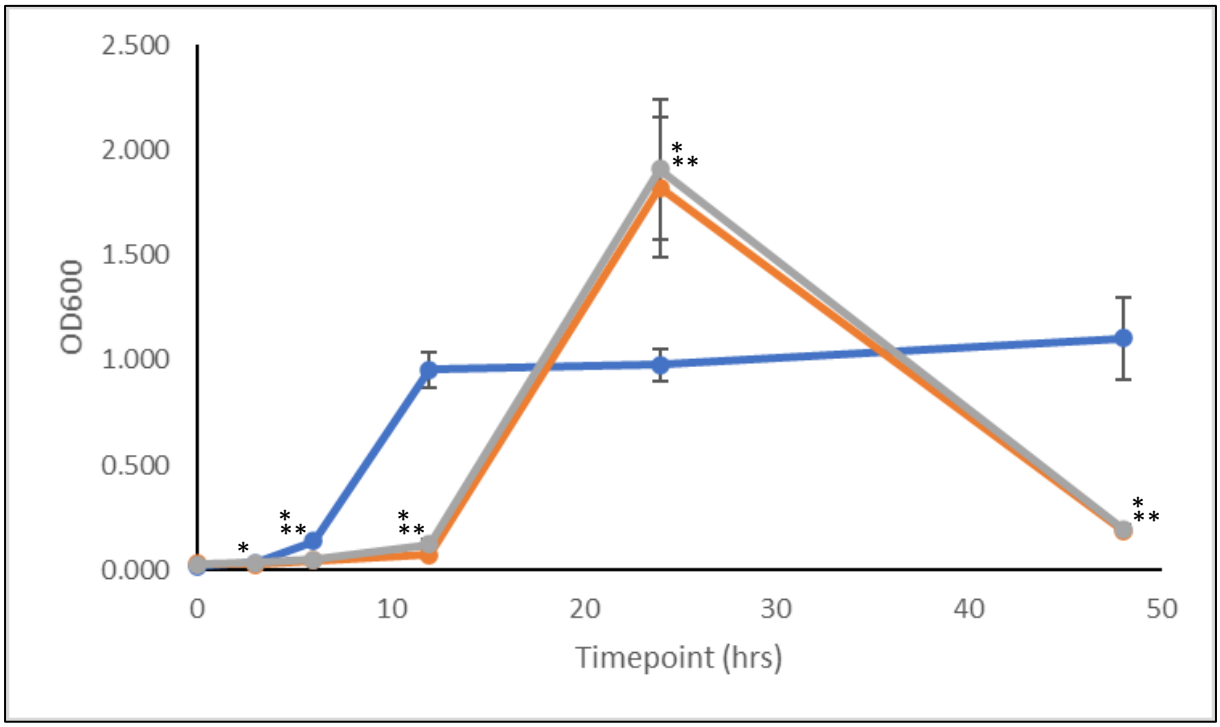

Figure 3.27: Planktonic growth of PAM15 grown within three separate media; Mueller-Hinton (blue) and M9 Minimal Media supplemented with 20% Glucose (grey) or 20% Alanine (orange) over a 48hrs period. Growth absorbance was measured at 600nm (OD600). * = significant differences between rich media (Mueller-Hinton) and restricted carbon sources (M9 Minimal Media supplemented with 20% Glucose/Alanine) (P=<0.05; Sidak post-hoc analysis was conducted using GraphPad Prism 8). Error bars represent Standard Error Mean (SEM).**

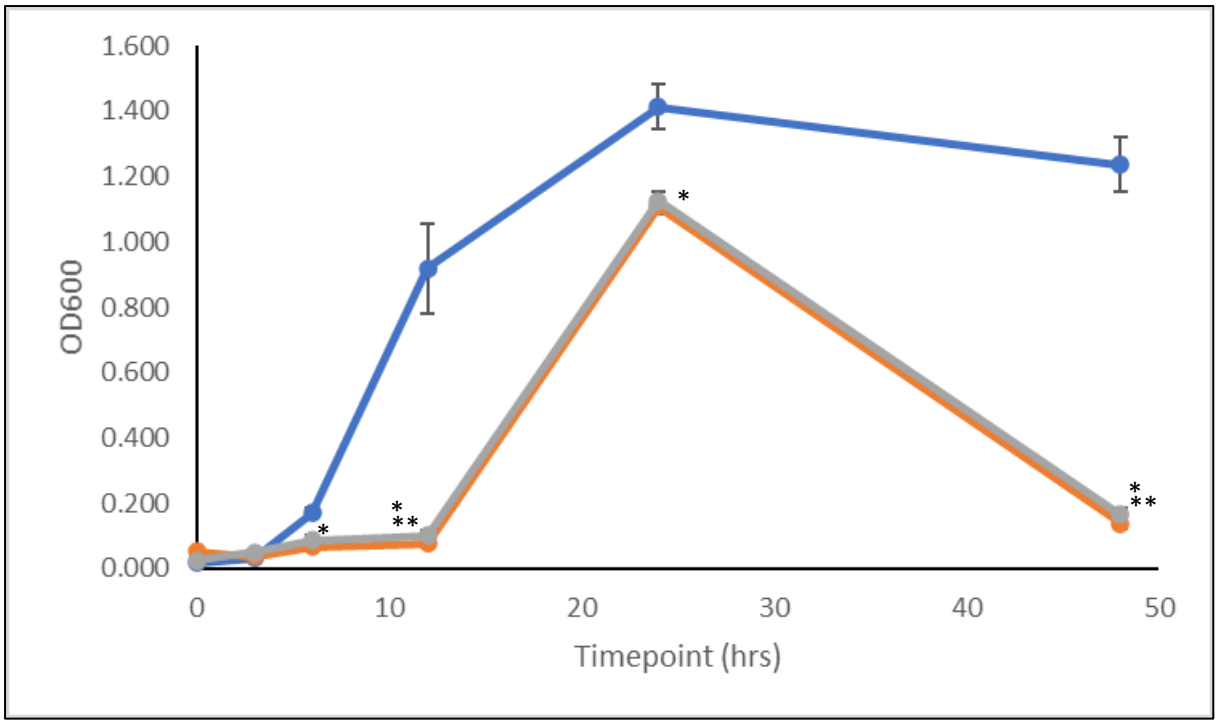

Figure 3.28: Planktonic growth of PAD15 grown within three separate media; Mueller-Hinton (blue) and M9 Minimal Media supplemented with 20% Glucose (grey) or 20% Alanine (orange) over a 48hrs period. Growth absorbance was measured at 600nm (OD600). * = significant differences between rich media (Mueller-Hinton) and restricted carbon sources (M9 Minimal Media supplemented with 20% Glucose/Alanine) (P=<0.05; Sidak post-hoc analysis was conducted using GraphPad Prism 8). Error bars represent Standard Error Mean (SEM).**

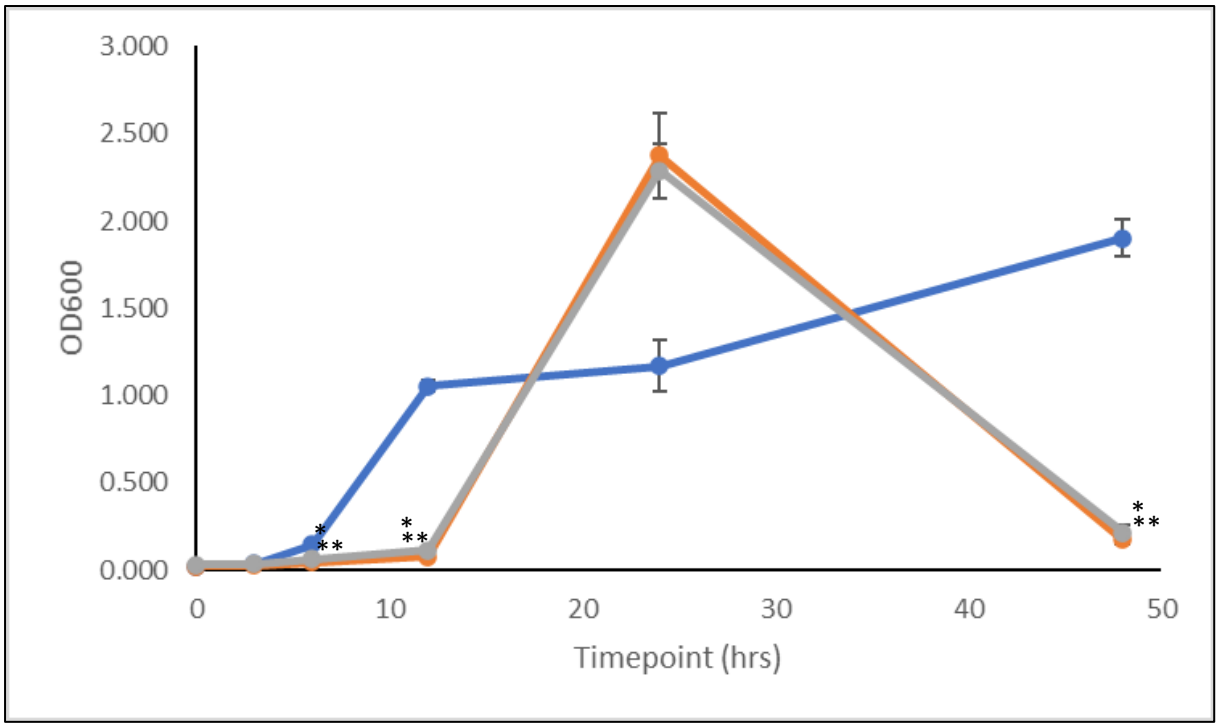

Figure 3.29: Planktonic growth of PAI15 grown within three separate media; Mueller-Hinton (blue) and M9 Minimal Media supplemented with 20% Glucose (grey) or 20% Alanine (orange) over a 48hrs period. Growth absorbance was measured at 600nm (OD600). * = significant differences between rich media (Mueller-Hinton) and restricted carbon sources (M9 Minimal Media supplemented with 20% Glucose/Alanine) (P=<0.05; Sidak post-hoc analysis was conducted using GraphPad Prism 8). Error bars represent Standard Error Mean (SEM).**

Significant differences were detected in both minimal media conditions from all carbapenem-adapted strains (P=0.05, Table 3.12-13; Figure 3.27-3.29), but with individual differences between them. From M9 minimal media supplemented with 20% Alanine, PAM15 had significant differences in growth in comparison to nutrient rich MH media at all timepoints (P=<0.05, Table 3.12; Figure 3.27). The PAD15 exhibited significant differences at 6hrs, 12hrs, 24hrs and 48hrs timepoints (P=<0.05, Table 3.12; Figure 3.28), whilst the PAI15 displayed significant differences at 6hrs, 12hrs and 48hrs timepoints (P=<0.05, Table 3.12; Figure 3.29).

When cultured in M9 minimal media supplemented with 20% Glucose, PAM15 exhibited significant results at 6hrs, 12hrs, 24hrs and 48hrs timepoints (P=<0.05, Table 3.13; Figure 3.27), whilst the PAD15 at 12hrs and 48hrs (P=<0.05, Table 3.13; Figure 3.28). PAI15 displayed different variation in significance values, with differences being recorded at 6hrs, 12hrs, and

48hrs timepoints (P=<0.05, Table 3.13; Figure 3.29). All of these significant differences indicate that the difference in growth detected was due to the variation in adaptations present as a result of prior exposure to specific carbapenems.

No significant differences were detected when comparing carbapenem-adapted growth patterns between either minimal media conditions (Table 3.14).

Once more, similar growth patterns to the PAO1 and Parent strain were displayed from the PACe8 population, albeit that peak growth was detected at a higher OD600 value (Figure 3.30).

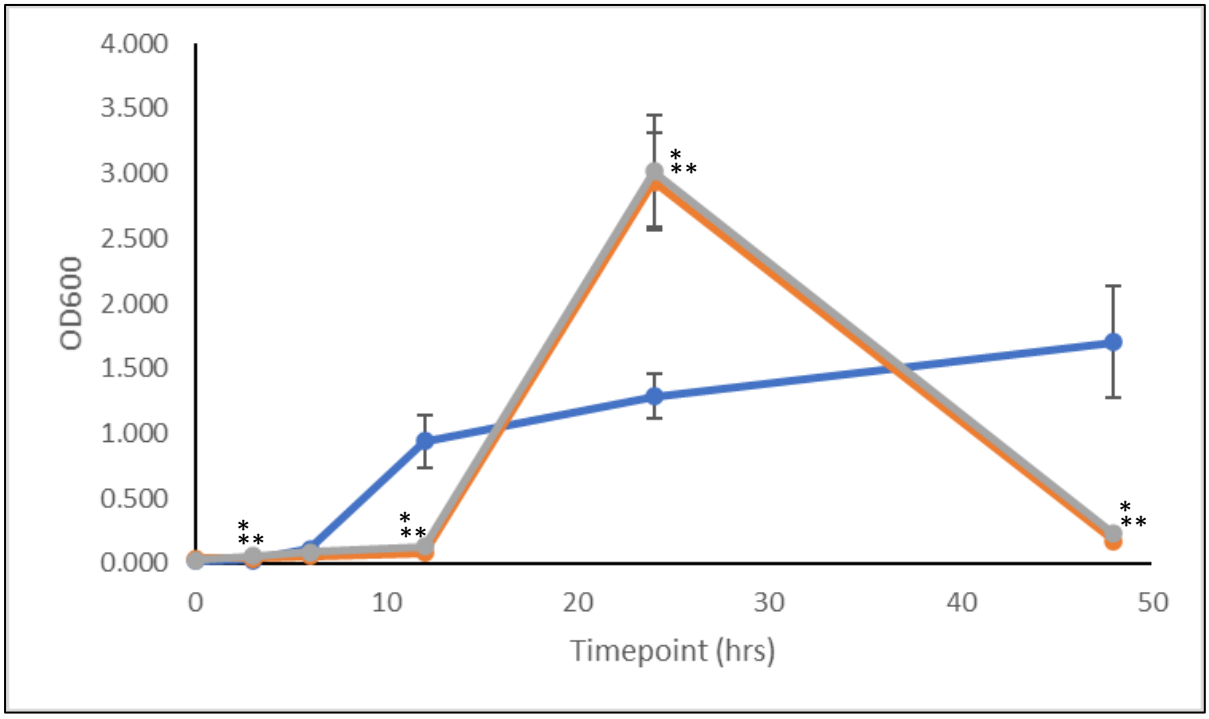

Figure 3.30: Planktonic growth of PACe8 grown within three separate media; Mueller-Hinton (blue) and M9 Minimal Media supplemented with 20% Glucose (grey) or 20% Alanine (orange) over a 48hrs period. Growth absorbance was measured at 600nm (OD600). * = significant differences between rich media (Mueller-Hinton) and restricted carbon sources (M9 Minimal Media supplemented with 20% Glucose/Alanine) (P=<0.05; Sidak post-hoc analysis was conducted using GraphPad Prism 8). Error bars represent Standard Error Mean (SEM).**

PACeA15, however, whilst it indicated another similar pattern, exhibited higher growth when exposed to 20% Alanine in contrast to PACe8, and peak growth was detected at a lower reading (Figure 3.31). Growth, however, in both conditions at 24hrs of growth was higher than that recorded in nutrient rich MH media, albeit not as high as that displayed at peak growth in MH broth (Figure 3.31).

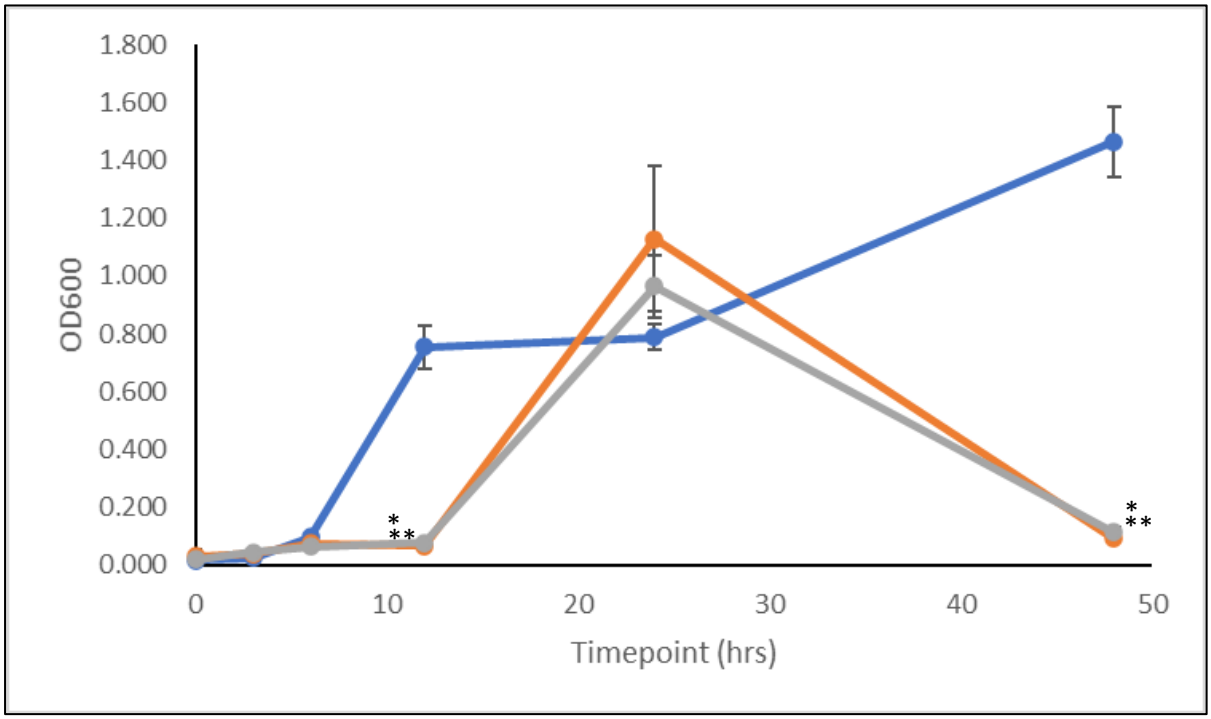

Figure 3.31: Planktonic growth of PACeA15 grown within three separate media; Mueller-Hinton (blue) and M9 Minimal Media supplemented with 20% Glucose (grey) or 20% Alanine (orange) over a 48hrs period. Growth absorbance was measured at 600nm (OD600). * = significant differences between rich media (Mueller-Hinton) and restricted carbon sources (M9 Minimal Media supplemented with 20% Glucose/Alanine) (P=<0.05; Sidak post-hoc analysis was conducted using GraphPad Prism 8). Error bars represent Standard Error Mean (SEM).**

Application of Two-way repeated-measures ANOVA found that both cephalosporin-adapted strains had significant differences in growth patterns between both M9 supplemented media conditions in comparison to rich MH media conditions (P=0.05, Table 3.12-13; Figure 3.30-3.31).

PACe8 exhibited significance difference in growth compared to growth in rich medium at 3hrs, 12hrs, 24hrs, and 48hrs timepoints when exposed to minimal medium with 20% Alanine supplement (P=<0.05, Table 3.12; Figure 3.30). When exposed to 20% Glucose, a similar pattern of significant differences were found at 3hrs, 12hrs, 24hrs and 48hrs timepoints (P=<0.05, Table 3.13; Figure 3.30).

When grown in minimal medium supplemented with 20% Alanine, the PACeA15 isolate was found to exhibit significant differences at 12hrs and 48hrs of growth when compared against growth in MH broth (P=<0.05, Table 3.12; Figure 3.31). The same pattern of significant differences also occurred when comparing growth in rich medium to that detected in minimal media supplemented with 20% Glucose (P=<0.05, Table 3.13; Figure 3.31).

No significant differences in growth was found for either cephalosporin-adapted strain when comparing growth in either supplemented minimal media (Table 3.14).

PACo30 displayed little-to-no deviation in any growth pattern when observing for differences between both minimal media supplement conditions, whilst following a similar growth pattern to that of PAO1 and the Parent (Figure 3.32). A slightly higher peak was detected for growth at 24hrs in 20% Alanine supplement in comparison to growth in minimal media supplemented with 20% Glucose (Figure 3.32).

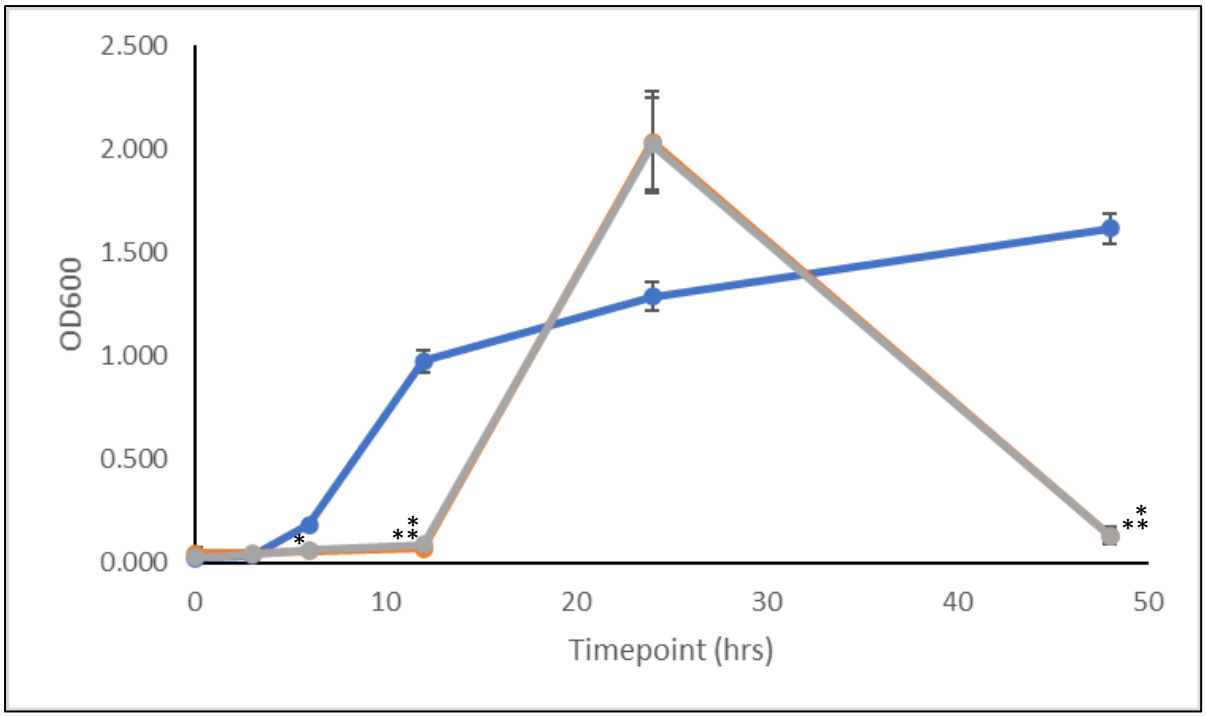

Figure 3.32: Planktonic growth of PACo30 grown within three separate media; Mueller-Hinton and M9 Minimal Media supplemented with 20% Glucose or 20% Alanine over a 48hrs period. Growth absorbance was measured at 600nm (OD600). * = significant differences between rich media (Mueller-Hinton) and restricted carbon sources (M9 Minimal Media supplemented with 20% Glucose/Alanine) (P=<0.05; Sidak post-hoc analysis was conducted using GraphPad Prism 8). Error bars represent Standard Error Mean (SEM).**

Two-way repeated measures ANOVA indicated that there were significant differences in PACo30's patterns of growth when exposed to either minimal media in comparison to rich MH media (P=<0.05, Table 3.12-3.13; Figure 3.32). Sidak post-hoc analysis further highlighted deviations at 6hrs 12hrs, and 48hrs timepoints when grown in 20% Alanine (P=<0.05, Table 3.12; Figure 3.32). When grown in minimal media with 20% Glucose supplement, the number of significant values reduced, being detected at 6hrs and 48hrs (P=<0.05, Table 3.12; Figure 3.32).

No significant difference in growth between either supplemented minimal media condition was found for Colistin-adapted *P. aeruginosa* (Table 3.14).

Further detailed results can be found in Appendices 5 (20% Alanine) and 6 (20% Glucose).

Table 3.12: Calculated significance results of Two-way repeated measures ANOVA, and subsequent Sidak post-hoc analyses, conducted to compare differences in *P. aeruginosa* strain planktonic growth when cultivated in M9 Minimal Media w/ 20% Alanine supplement against growth in rich MH media. '*' – P=<0.05

Strain	PAO1	Parent	PAM15	PAD15	PAI15	PACe8	PACeA15	PACo30
2W-RM ANOVA	*<0.0001	*<0.0001	*<0.0001	*<0.0001	*<0.0001	*<0.0001	*<0.0001	*<0.0001
Timepoint								
0hrs								
3hrs	0.1565	0.9301	*0.0009	0.7034	0.8820	*0.0353	0.0748	0.0798
6hrs	*0.0110	*0.0114	*0.0101	*0.0274	*0.0096	0.1171	0.1340	*<0.0001
12hrs	*0.0054	*0.0007	*0.0068	*0.0046	*0.0026	*0.0004	*0.0008	*0.0467
24hrs	*0.0214	0.8882	*0.0248	*0.0158	0.4710	*0.0022	0.7371	0.0533
48hrs	*0.0090	*0.0145	*0.0270	*0.0006	*0.0252	*<0.0001	*0.0066	*<0.0001

Table 3.13: Calculated significance results of Two-way repeated measures ANOVA, and subsequent Sidak post-hoc analyses, conducted to compare differences in *P. aeruginosa* strain planktonic growth when cultivated in M9 Minimal Media w/ 20% Glucose supplement against growth in rich MH media. '*' – P=<0.05

Strain	PAO1	Parent	PAM15	PAD15	PAI15	PACe8	PACeA15	PACo30
2W-RM ANOVA	*<0.0001	*<0.0001	*<0.0001	*<0.0001	*<0.0001	*<0.0001	*<0.0001	*<0.0001
Timepoint								
0hrs								
3hrs	0.0795	>0.9999	>0.9999	0.1820	0.9899	*0.0311	0.7541	0.1374
6hrs	0.1487	0.0779	*0.0320	0.4710	*0.0080	0.8169	0.9076	*0.0001
12hrs	*0.0186	*0.0134	*0.0128	*0.0168	*0.0231	*0.0130	*0.0007	0.0541
24hrs	0.4366	0.9985	*0.0019	0.3460	0.9316	*0.0294	0.9664	0.5049
48hrs	*0.0138	*0.0053	*0.0252	*0.0016	*0.0276	*0.0001	*0.0032	*0.0008

Table 3.14: Calculated significance results of Two-way repeated measures ANOVA, and subsequent Sidak post-hoc analyses, conducted to compare differences in *P. aeruginosa* strain planktonic growth when cultivated in M9 Minimal Media w/ either 20% Alanine or 20% Glucose supplement.

Strain	PAO1	Parent	PAM15	PAD15	PAI15	PACe8	PACeA15	PACo30
2W-RM ANOVA	0.9973	0.9972	0.7217	0.6805	0.9997	0.8672	0.8322	0.9978
Timepoint								
0hrs								
3hrs	0.5819	0.9565	0.9811	0.5787	0.7446	0.7611	0.9942	0.7348
6hrs	0.5722	0.7316	0.6677	0.7836	0.6462	0.7970	0.9988	0.8593
12hrs	0.8465	0.7938	0.6032	0.8260	0.9414	0.5981	0.9817	0.8928
24hrs	>0.9999	>0.9999	0.9654	>0.9999	>0.9999	0.9949	0.9908	>0.9999
48hrs	0.7396	0.9265	>0.9999	0.5247	0.5432	0.5900	0.8990	0.8674

3.4.2 Biofilm Formation under Minimal Medium conditions

As with previous experiments, a biofilm assay was also conducted at the same time as growth curve analysis, in order to understand whether a difference in supplemented carbon source had an effect on biofilm production within *P. aeruginosa*. All isolates were exposed to growth within M9 Minimal Media, supplemented with either 20% Glucose or 20% Alanine. All samples were statistically tested via Two-way repeated measures ANOVA, with additional post-hoc analysis, against one another for any differences in biofilm formation under these conditions compared to biofilm formation when grown in rich media (MH broth). Further testing was implemented to compare differences in biofilm formation when grown in minimal media with either carbon source.

Upon examination of both the PAO1 and Parent strain of *P. aeruginosa*, clear differences were observed between biofilm formation when exposed to either carbon source supplement. In comparison to growth in nutrient-rich MH broth, initial biofilm detection was found to be higher at initial readings (0hrs), with biofilm production detected at a higher reading when exposed to Glucose-supplemented media (Figure 3.33; Figure 3.34). For PAO1, biofilm formation enters an exponential phase from 3-6hrs when cultivated in minimal media supplemented with 20% Alanine, peaking at 6hrs of growth (Figure 3.33). In contrast, the Parent strain appears to produce biofilm from initial cultivation in M9 minimal media with 20% Alanine, as exponential growth was detected between 0-6hrs of growth (Figure 3.34). As with PAO1, Parent biofilm production in 20% Alanine supplemented media peaked at 6hrss (Figure 3.34), but the optical density at peak was at a higher reading to that of PAO1 (Figure 3.33; Figure 3.34). Both strains experience a sharp decrease in biofilm formation post-6hrss timepoint, before a slow, gradual decrease is noted between 24-48hrs of growth (Figure 3.33; Figure 3.34). At the 12hrs timepoint, a higher amount of biofilm was detected being produced by the Parent strain in comparison to PAO1 (Figure 3.33; Figure 3.34).

When exposed to 20% Glucose supplement, the *P. aeruginosa* strains produced less overall biofilm formation in comparison to both MH broth and minimal media supplemented with 20% Alanine (Figure 3.33; Figure 3.34). The PAO1 strain displays little production up until 3hrs timepoint, where a slight increase in biofilm formation was observed between 3-12hrs, peaking at 12hrs and remaining in a stationary phase before the end of the experiment (Figure

3.33). In contrast, a slight increase in biofilm production was noted from the Parent strain from the beginning of growth at 0hrs until the 6hrs timepoint (Figure 3.34). This formation begins to even out slightly, entering a stationary phase between 6-12hrs of growth, before entering a decline phase after 12hrs of growth (Figure 3.34). As experienced in all growth conditions, the Parent strain produced more biofilm in contrast to the PAO1 control at observed peak biofilm formation (Figure 3.33; Figure 3.34).

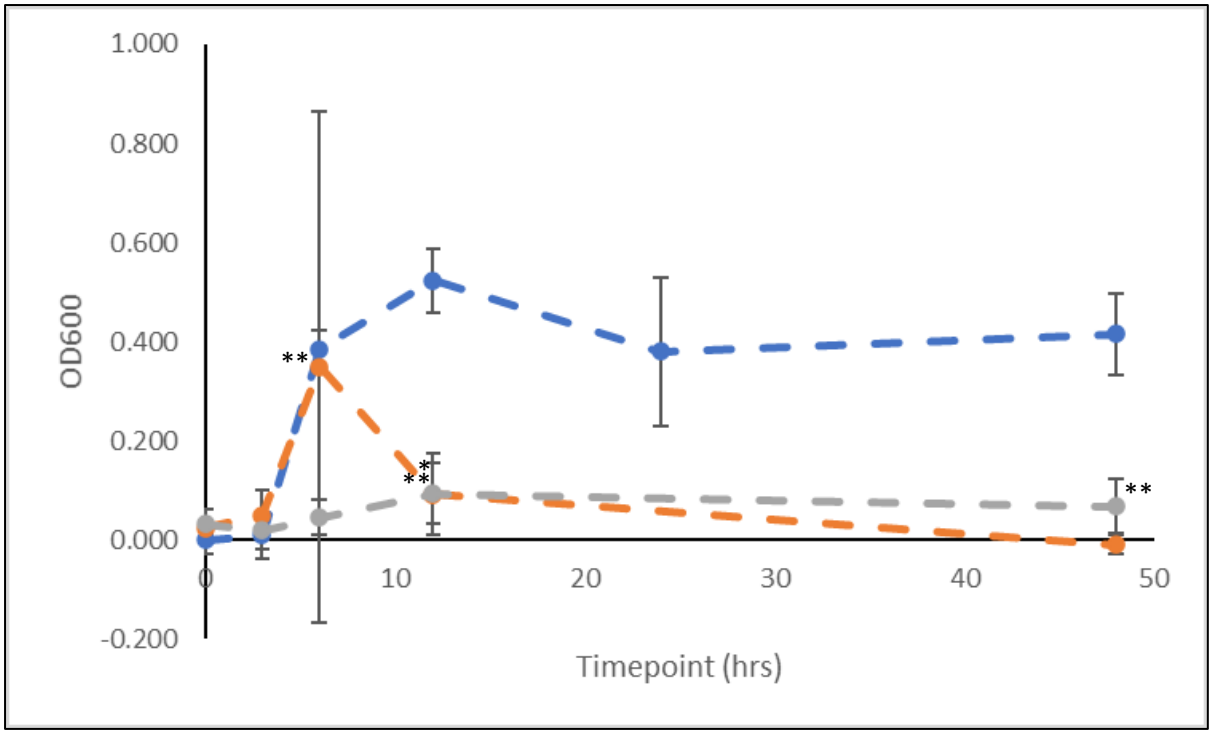

Figure 3.33: Biofilm formation of PAO1 strain *P. aeruginosa* grown within three separate media; Mueller-Hinton (blue) and M9 Minimal Media supplemented with 20% Glucose (grey) or 20% Alanine (orange) over a 48hrs period. Growth absorbance was measured at 600nm (OD600). * = significant differences between rich media (Mueller-Hinton) and restricted carbon sources (M9 Minimal Media supplemented with 20% Glucose/Alanine) (P=<0.05; Sidak post-hoc analyses were conducted using GraphPad Prism 8). Error bars represent Standard Error Mean (SEM).**

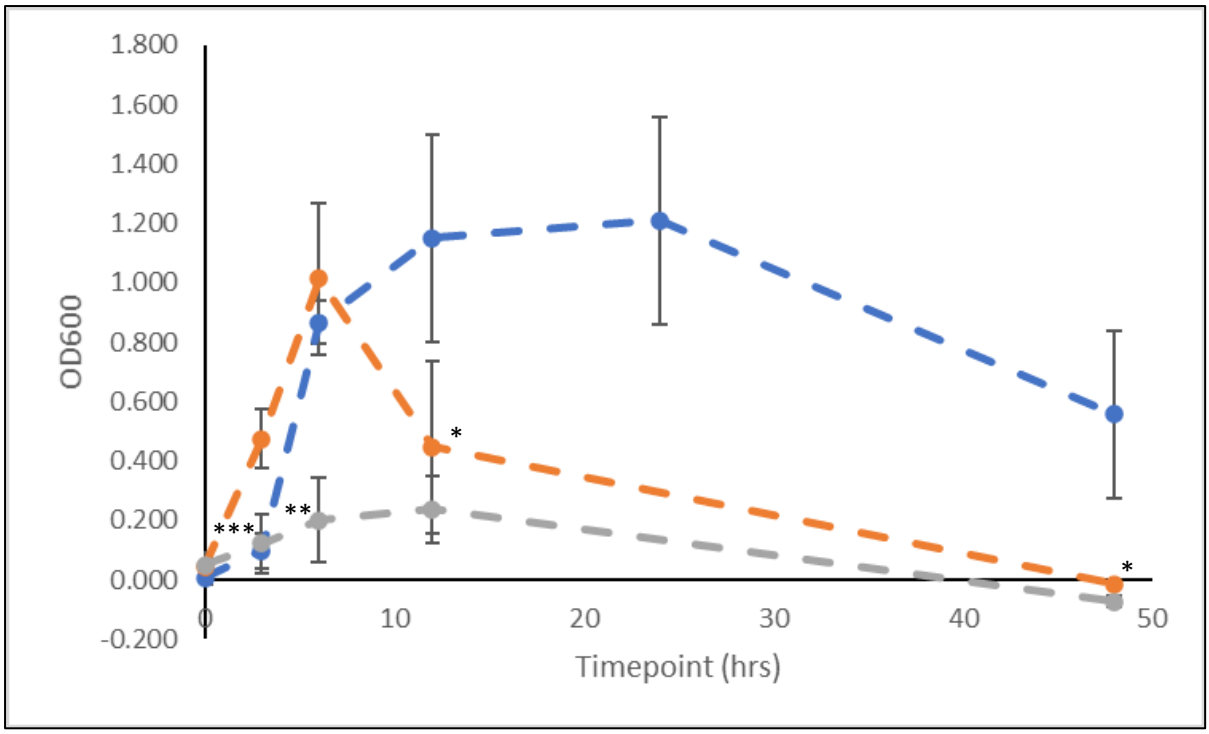

Figure 3.34: Biofilm formation of Parent strain *P. aeruginosa* grown within three separate media; Mueller-Hinton (blue) and M9 Minimal Media supplemented with 20% Glucose (grey) or 20% Alanine (orange) over a 48hrs period. Growth absorbance was measured at 600nm (OD600). * = significant differences between rich media (Mueller-Hinton) and restricted carbon sources (M9 Minimal Media supplemented with 20% Glucose/Alanine) (P=<0.05; Sidak post-hoc analyses were conducted using GraphPad Prism 8). *** = Significant differences in biofilm formation between both sets of minimal media (P=<0.05). Error bars represent Standard Error Mean (SEM).**

Significant differences in biofilm formation between growth in rich MH medium and supplemented M9 medium were found at various timepoints for both strains (P=0.05, Table 3.15-3.16; Figure 3.33-3.34). In the case of PAO1, only one significant difference was detected after 12hrs of growth with 20% Alanine (P=<0.05, Table 3.15; Figure 3.33). When grown with 20% Glucose supplement, these differences increased, with significance being found at 6hrs, 12hrs, and 48hrs timepoints (P=<0.05, Table 3.16; Figure 3.33). The Parent strain displayed significant differences to biofilm formation in nutrient-rich medium at 12hrs and 48hrs when cultivated in minimal media with 20% Alanine (P=<0.05, Table 3.15; Figure 3.34), and 6hrs when supplemented with 20% Glucose (P=<0.05, Table 3.16; Figure 3.34).

When comparing biofilm formation in both supplemented forms of minimal media, whilst

both strain had displayed significant differences according to Two-way ANOVA analysis (P=<0.05, Table 3.17; Figure 3.33; Figure 3.34), subsequent Sidak post-hoc only detected a point of significance at 3hrs for the Parent strain. No additional significance was detected beyond that stage.

Upon initial observations of the carbapenem-adapted strains of *P. aeruginosa*, there was little deviation in the biofilm formation pattern that was observed from the Parent strain (Figure 3.35-3.37). Both PAM15 and PAD15 populations followed the same pattern of growth, peaking after 6hrs of growth in 20% Alanine supplemented media, and 12hrs in 20% Glucose supplemented media (Figure 3.35; Figure 3.36).

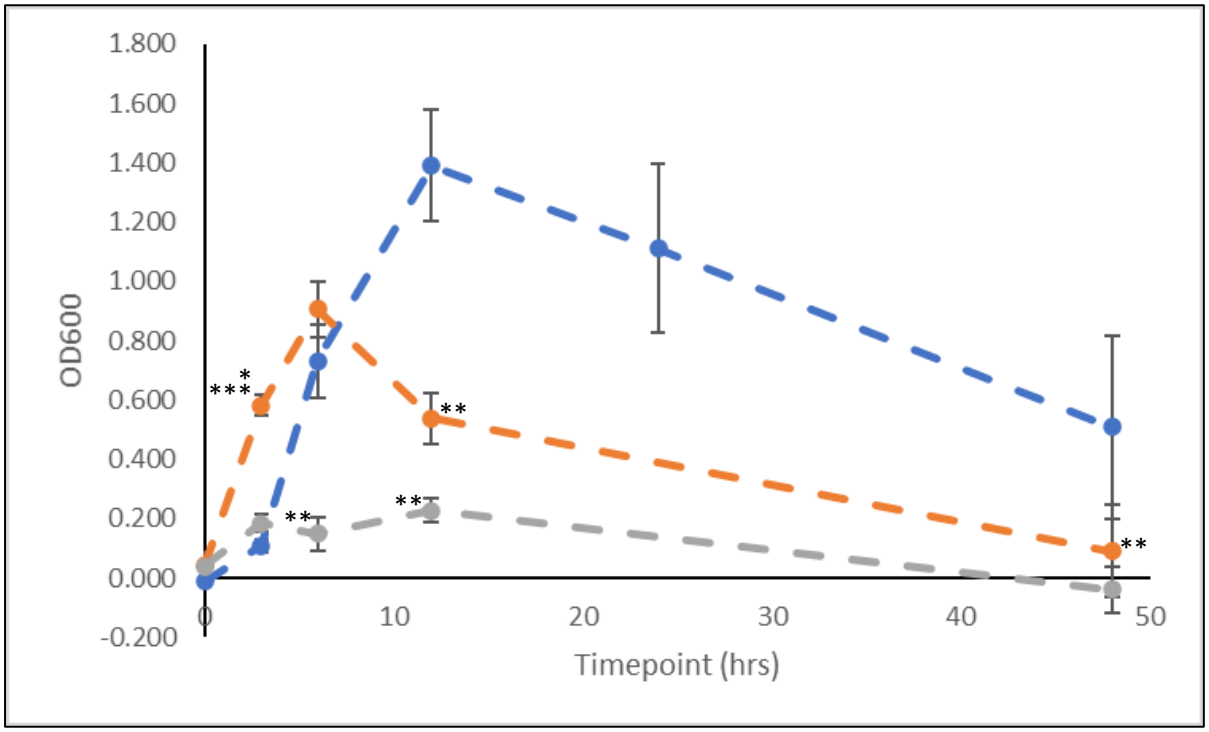

Figure 3.35: Biofilm formation of PAM15 grown within three separate media; Mueller-Hinton (blue) and M9 Minimal Media supplemented with 20% Glucose (grey) or 20% Alanine (orange) over a 48hrs period. Growth absorbance was measured at 600nm (OD600). * = significant differences between rich media (Mueller-Hinton) and restricted carbon sources (M9 Minimal Media supplemented with 20% Glucose/Alanine) (P=<0.05; Sidak post-hoc analyses were conducted using GraphPad Prism 8). *** = Significant differences in biofilm formation between both sets of minimal media (P=<0.05). Error bars represent Standard Error Mean (SEM).**

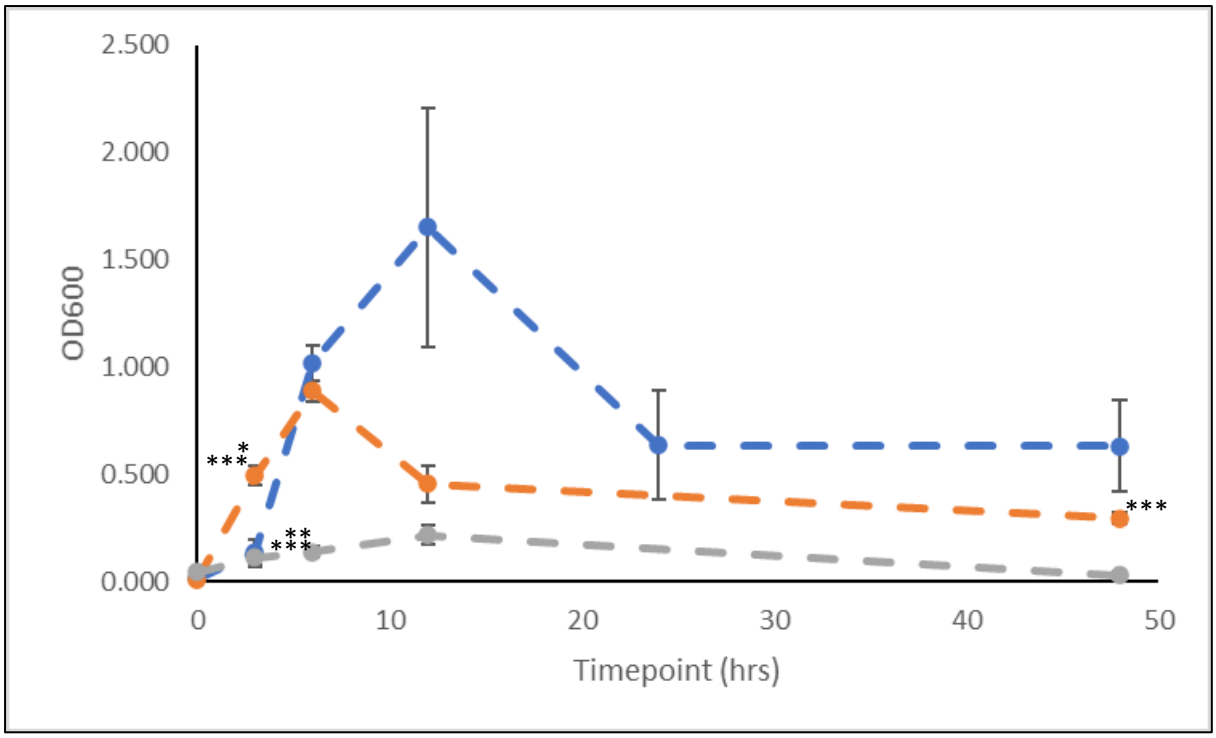

Figure 3.36: Biofilm formation of PAD15 grown within thrsee separate media; Mueller-Hinton (blue) and M9 Minimal Media supplemented with 20% Glucose (grey) or 20% Alanine (orange) over a 48hrs period. Growth absorbance was measured at 600nm (OD600). * = significant differences between rich media (Mueller-Hinton) and restricted carbon sources (M9 Minimal Media supplemented with 20% Glucose/Alanine) (P=<0.05; Sidak post-hoc analyses were conducted using GraphPad Prism 8). *** = Significant differences in biofilm formation between both sets of minimal media (P=<0.05). Error bars represent Standard Error Mean (SEM).**

Slight deviations to this pattern was found from the readings associated with PAI15 (Figure 3.37). Within Alanine-supplemented M9 broth, the bacteria displayed slight production of biofilm between 0-3hrs of growth, before an exponential increase occurred before the 6hrs timepoint (Figure 3.37). Peak biofilm production in 20% Glucose supplemented media also occurred at the 6hrs timepoint, as opposed to 12hrs in contrast to both PAM15 and PAD15 (Figure 3.37).

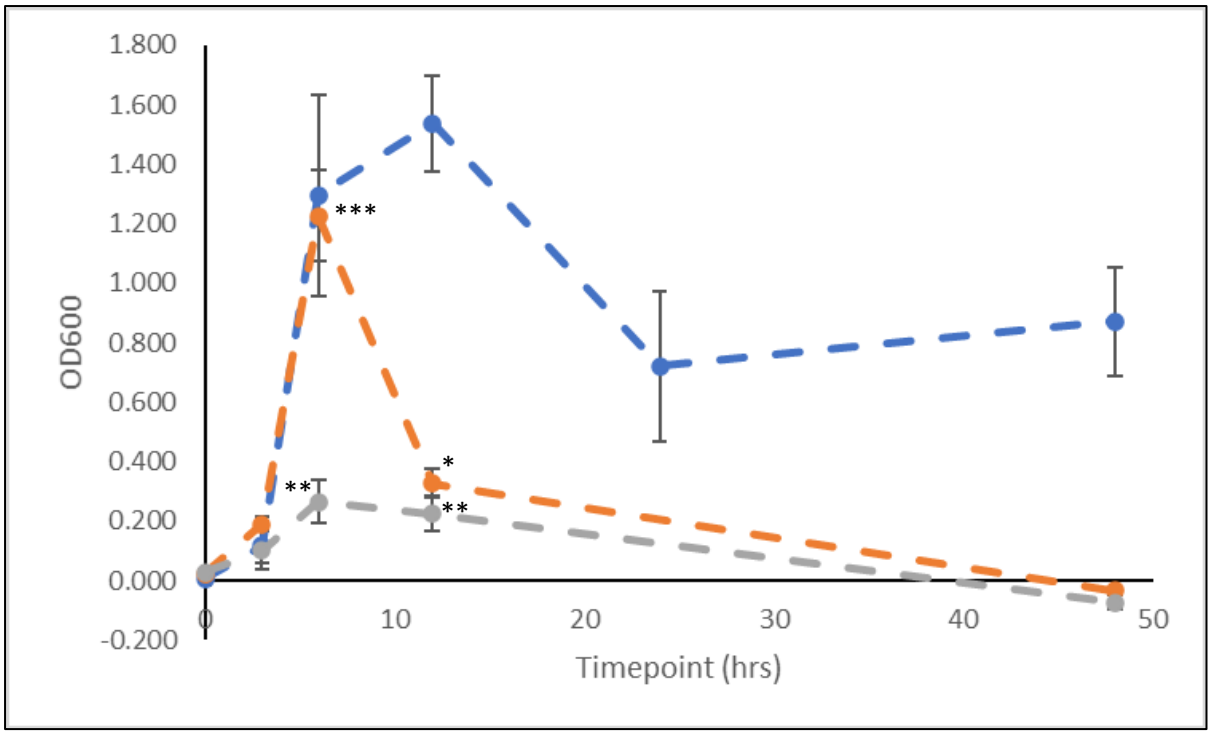

Figure 3.37: Biofilm formation of PAI15 grown within three separate media; Mueller-Hinton (blue) and M9 Minimal Media supplemented with 20% Glucose (grey) or 20% Alanine (orange) over a 48hrs period. Growth absorbance was measured at 600nm (OD600). * = significant differences between rich media (Mueller-Hinton) and restricted carbon sources (M9 Minimal Media supplemented with 20% Glucose/Alanine) (P=<0.05; Sidak post-hoc analyses were conducted using GraphPad Prism 8). *** = Significant differences in biofilm formation between both sets of minimal media (P=<0.05). Error bars represent Standard Error Mean (SEM).**

Significant differences were found in each biofilm formation pattern after conducting Two-way repeated measures ANOVA in both conditions against MH broth growth for all strains (P=0.05, Table 3.15-3.16; Figure 3.35-3.37). Variations were detected at different timepoints when comparing growth between each supplemented medium. PAM15 displayed significant differences in the presence of biofilm at 3hrs and 12hrs within the 20% Alanine condition (P=<0.05, Table 3.15; Figure 3.35). When cultivated in 20% Glucose, M15 displayed significant differences in biofilm formation at both 6hrs and 12hrs of growth (P=<0.05, Table 3.16; Figure 3.35). PAD15 also displayed significant differences in biofilm formation at 3hrs when cultivated in M9 broth supplemented with 20% Alanine (P=<0.05, Table 3.15; Figure 3.36; Figure 3.37). However, when cultivated 20% Glucose minimal media, D15 had recorded a

significant difference after 6hrs (P=<0.05, Table 3.16; Figure 3.36). PAI15 had additional significance in biofilm formation detected after 12hrs of growth in 20% Alanine (P=<0.05, Table 3.15; Figure 3.37). Under 20% Glucose supplement growth conditions, however, this variation was detected at two separate timepoints, at both 6hrs and 12hrs of growth in comparison to biofilm formation in MH media (P=<0.05, Table 3.16; Figure 3.37).

All three strains also displayed significant differences in biofilm formation patterns when comparing formation between both 20% Alanine and 20% Glucose supplemented media conditions (P=<0.05, Table 3.17; Figure 3.35-3.37). Further calculations found that both PAM15 and PAD15 *P. aeruginosa* strains had significant biofilm formation growth after 3hrs in this comparison (P=<0.05, Table 3.17; Figure 3.35; Figure 3.36). Additional differences were detected within the PAD15 strain, at both 6hrs and 48hrs of growth (P=<0.05, Table 3.17; Figure 3.36). Only at peak growth (6hrs) was there a significant variation in biofilm detected in PAI15 when comparing between both supplemented growth media (P=<0.05, Table 3.17; Figure 3.37).

The cephalosporin-adapted strains were found to have different growth patterns to each other when observed. The Ceftazidime-adapted population was found to follow a similar biofilm formation pattern to what the Imipenem-adapted strain displayed under both growth media (Figure 3.38).

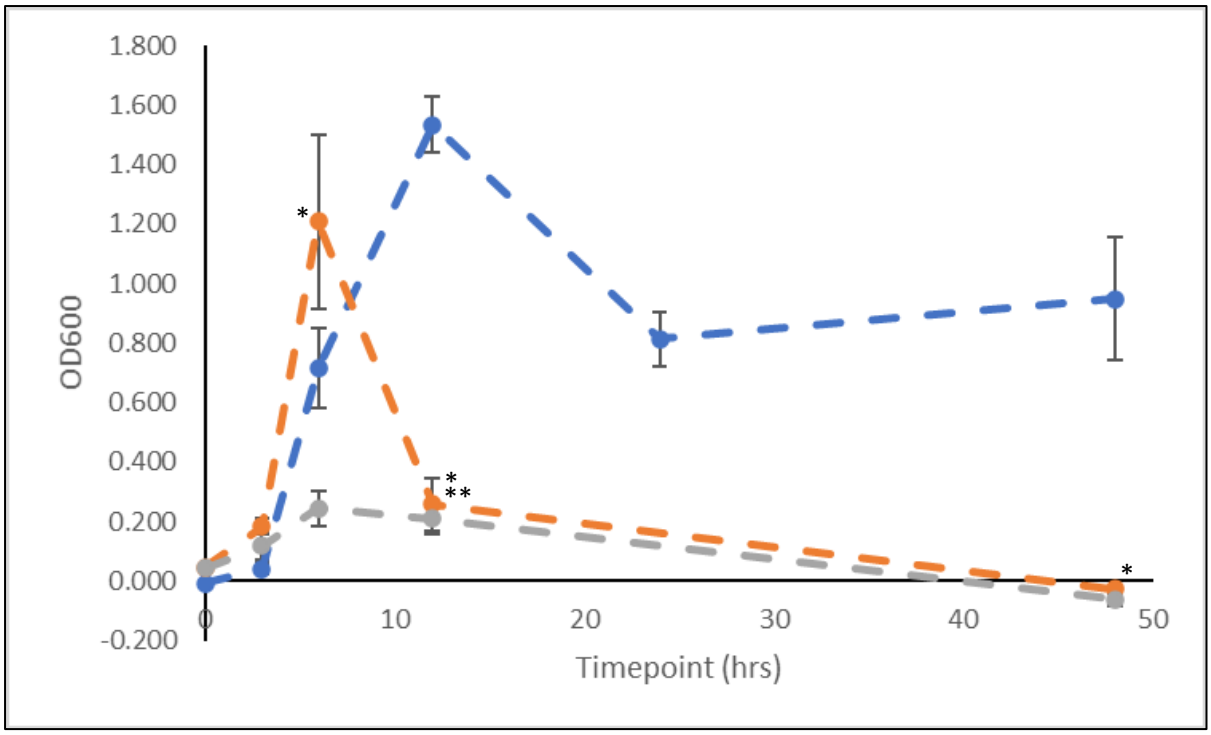

Figure 3.38: Biofilm formation of PACe8 grown within three separate media; Mueller-Hinton (blue) and M9 Minimal Media supplemented with 20% Glucose (grey) or 20% Alanine (orange) over a 48hrs period. Growth absorbance was measured at 600nm (OD600). * = significant differences between rich media (Mueller-Hinton) and restricted carbon sources (M9 Minimal Media supplemented with 20% Glucose/Alanine) (P=<0.05; Sidak post-hoc analyses were conducted using GraphPad Prism 8). Error bars represent Standard Error Mean (SEM).**

In contrast, under 20% Alanine supplemented conditions, PACeA15 displayed an exponential phase of biofilm production between 0-3hrs of growth, reaching peak biofilm at 3hrs (Figure 3.39), before entering a steady decline phase throughout the rest of the experiment. Under these conditions, PACeA15 also produced biofilm at much lower levels than PACe8 (OD600 = 0.115 vs. 1.208; Appendix 8) at respective peak levels (Figure 3.38; Figure 3.39). Under 20% Glucose conditions, however, PACeA15 had little difference in biofilm formation compared to that produced by the population adapted to Ceftazidime alone.

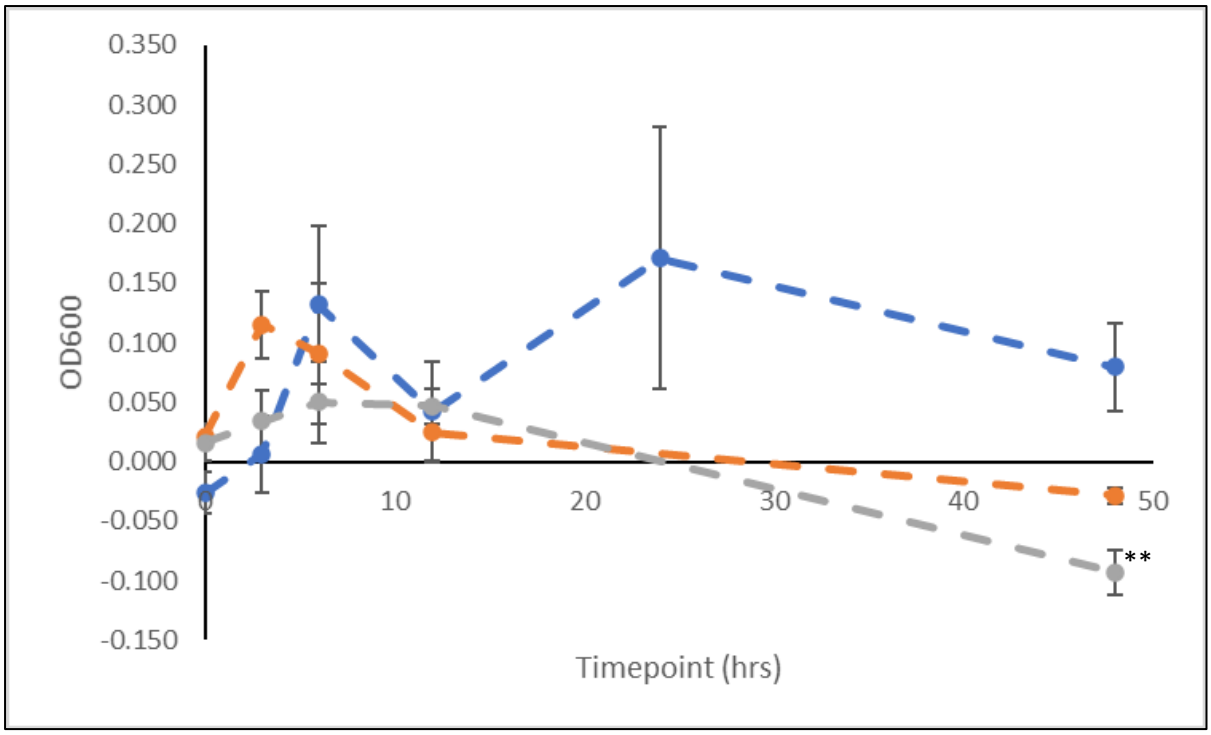

Figure 3.39: Biofilm formation of PACeA15 *P. aeruginosa* grown within three separate media; Mueller-Hinton (blue) and M9 Minimal Media supplemented with 20% Glucose (grey) or 20% Alanine (orange) over a 48hrs period. Growth absorbance was measured at 600nm (OD600). ** = significant differences between rich media (Mueller-Hinton) and restricted carbon sources (M9 Minimal Media supplemented with 20% Glucose (P=<0.05; Sidak post-hoc analyses were conducted using GraphPad Prism 8). Error bars represent Standard Error Mean (SEM).

When Two-way repeated measures ANOVA tests were implemented to test for significant differences between either minimal media condition in comparison to biofilm formation in MH media, both strains were found to have significant variations at different timepoints (P=0.05, Table 3.15-3.16; Figure 3.38-3.39). Under 20% Alanine-supplement conditions, PACe8 produced a significant variation in biofilm at 6hrs, 12hrs, and 48hrs (P=<0.05, Table 3.15; Figure 3.38). Under 20% Glucose, significant differences in biofilm detected was found only at 12hrs for the Ceftazidime-population (P=0.05, Table 3.16; Figure 3.38). PACeA15, however, produced no significant differences in biofilm formation at any timepoint under 20% Alanine conditions (Table 3.15; Figure 3.39), but did indicate a significant difference, at 48hrs, when cultured in 20% Glucose (P=0.05, Table 3.16; Figure 3.39).

Only PACe8 had a significant variation in biofilm formation when comparing both minimal

media conditions against each other (P=0.05, Table 3.17; Figure 3.38). Subsequent post-hoc analysis, however, does not display any significant timepoints of biofilm formation, which could cast doubt on the previous figure (Table 3.17; Figure 3.38).

PACo30 shared a similar pattern of biofilm formation described for the Parent (Figure 3.40) under both minimal media conditions. Although Two-way ANOVA analysis did indicate significant differences in biofilm formation patterns (P=<0.05, Table 3.15; Figure 3.40), post-hoc analysis found no significant contrast in biofilm formation was detected at any timepoint under 20% Alanine supplementation (Table 3.15; Figure 3.40). There was, however, a significant deviation in biofilm formation, in comparison to what was recorded within nutrient-rich MH media, at 6hrs within the 20% Glucose supplemented media (P=<0.05, Table 3.16; Figure 3.40).

Significant differences in biofilm formation pattern was found for PACo30 when comparing either minimal media condition against each other (P=<0.05, Table 3.17; Figure 3.40), however, subsequent post-hoc analysis did not detect any significant growth variation at each timepoint analysed.

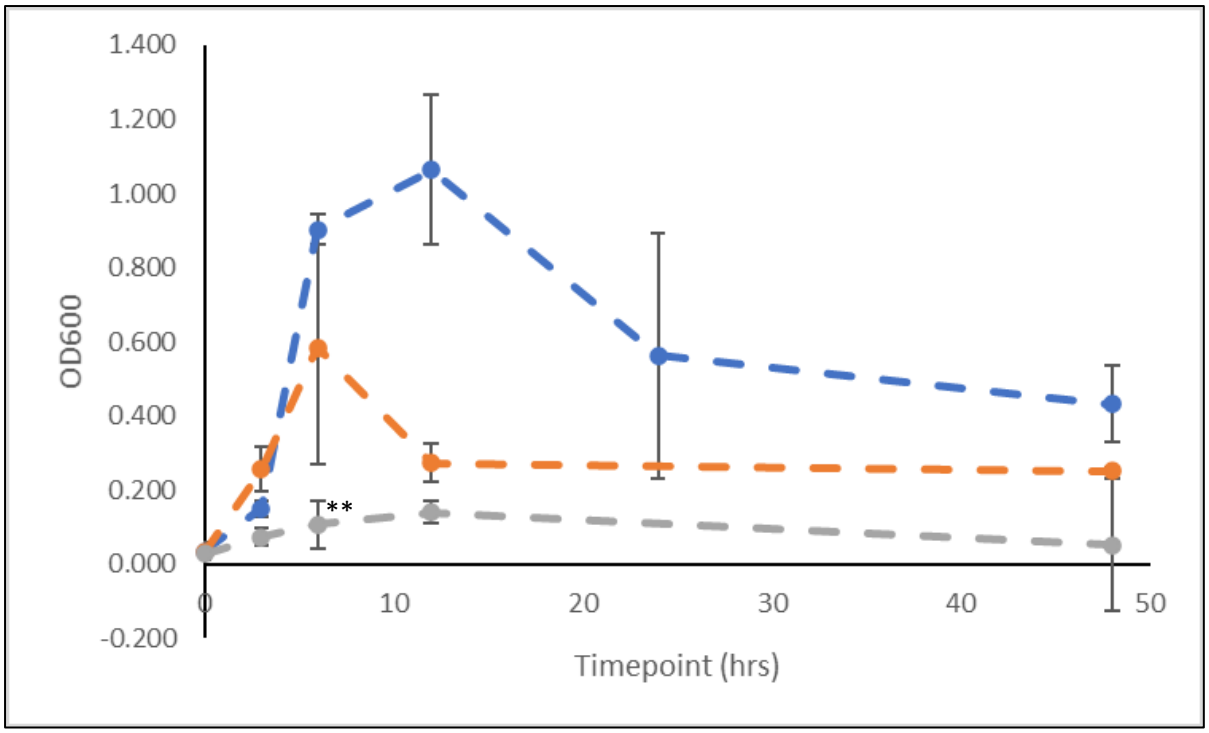

Figure 3.40: Biofilm formation of PACo30 grown within three separate media; Mueller-Hinton (blue) and M9 Minimal Media supplemented with 20% Glucose (grey) or 20% Alanine (orange) over a 48hrs period. Growth absorbance was measured at 600nm (OD600). ** = significant differences between rich media (Mueller-Hinton) and restricted carbon sources (M9 Minimal Media supplemented with 20% Glucose) (P=<0.05; Sidak post-hoc analyses were conducted using GraphPad Prism 8). Error bars represent Standard Error Mean (SEM).

Table 3.15: Calculated significance results of Two-way repeated measures ANOVA, and subsequent Sidak post-hoc analyses, conducted to compare differences in *P. aeruginosa* strain biofilm formation when cultivated in M9 Minimal Media w/ 20% Alanine supplement against growth in rich MH media. '*' – P=<0.05

Strain	PAO1	Parent	PAM15	PAD15	PAI15	PACe8	PACeA15	PACo30
2W-RM ANOVA	*<0.0001	*<0.0001	*<0.0001	*<0.0001	*<0.0001	*<0.0001	*0.0071	*<0.0001
Timepoint								
0hrs								
3hrs	0.3044	0.1214	*0.0008	*0.0089	0.5608	0.6551	0.1139	0.3458
6hrs	0.1395	0.8161	0.6132	0.4083	0.6484	*0.0007	0.0578	0.7450
12hrs	*0.0060	*0.0001	*0.0317	0.2729	*0.0079	*<0.0001	>0.9999	0.0797
24hrs	N/A	N/A	N/A	N/A	N/A	N/A	N/A	N/A
48hrs	0.0536	*0.0036	0.4233	0.4466	0.0662	*<0.0001	0.1521	0.3909

Table 3.16: Calculated significance results of Two-way repeated measures ANOVA, and subsequent Sidak post-hoc analyses, conducted to compare differences in *P. aeruginosa* strain biofilm formation when cultivated in M9 Minimal Media w/ 20% Glucose supplement against growth in rich MH media. '*' – P=<0.05

Strain	PAO1	Parent	PAM15	PAD15	PAI15	PACe8	PACeA15	PACo30
2W-RM ANOVA	*<0.0001	*<0.0001	*<0.0001	*<0.0001	*<0.0001	*<0.0001	*0.0002	*<0.0001
Timepoint								
0hrs								
3hrs	0.9774	>0.9999	0.1288	0.9880	0.9986	0.3779	0.8463	0.0670
6hrs	*0.0137	*0.0042	*0.0357	*0.0072	*0.0013	0.0728	0.7302	*0.0007
12hrs	*0.0409	0.1801	*0.0148	0.2083	*0.0104	*0.0008	>0.9999	0.0684
24hrs	N/A	N/A	N/A	N/A	N/A	N/A	N/A	N/A
48hrs	*0.0461	0.2665	0.3471	0.1791	0.0556	0.0644	*0.0271	0.2047

Table 3.17: Calculated significance results of Two-way repeated measures ANOVA, and subsequent Sidak post-hoc analyses, conducted to compare differences in *P. aeruginosa* strain biofilm formation when cultivated in M9 Minimal Media w/ either 20% Alanine or 20% Glucose supplement.

Strain	PAO1	Parent	PAM15	PAD15	PAI15	PACe8	PACeA15	PACo30
2W-RM ANOVA	*<0.0001	*<0.0001	*<0.0001	*<0.0001	*<0.0001	*<0.0001	0.0684	*0.0001
Timepoint								
0hrs								
3hrs	0.4732	*0.0162	*0.0008	*0.0022	0.4843	0.4524	0.1017	0.1138
6hrs	0.0735	0.1065	0.0798	*0.0006	*0.0139	0.1223	0.8583	0.0512
12hrs	0.9756	0.7383	0.1021	0.1113	0.3515	0.9643	0.7521	0.1201
24hrs	N/A	N/A	N/A	N/A	N/A	N/A	N/A	N/A
48hrs	0.1688	0.0611	0.1042	*0.0014	0.4260	0.3661	0.0895	0.6546

3.5 Changes in SNP frequency and layout was detected between each adapted strain of *P. aeruginosa* in response of antibiotic exposure

In order to understand whether antibiotic adaptation are associated with genetic polymorphisms in *P. aeruginosa*, selected complete adapted strains were whole genome sequenced, and Single Nucleotide Polymorphisms (SNPs) extracted to observe whether single mutations had occurred in contrast to the parental strain.

The first task regarding observing differences in SNPs was to understand any change in nucleotide sequence between the Parent and subsequent antibiotic-adapted strain against the PAO1 reference genome. This allowed us to understand whether any mutation that had occurred prior to experimentation pre-disposed the bacteria to potentially display certain phenotypical characteristics.

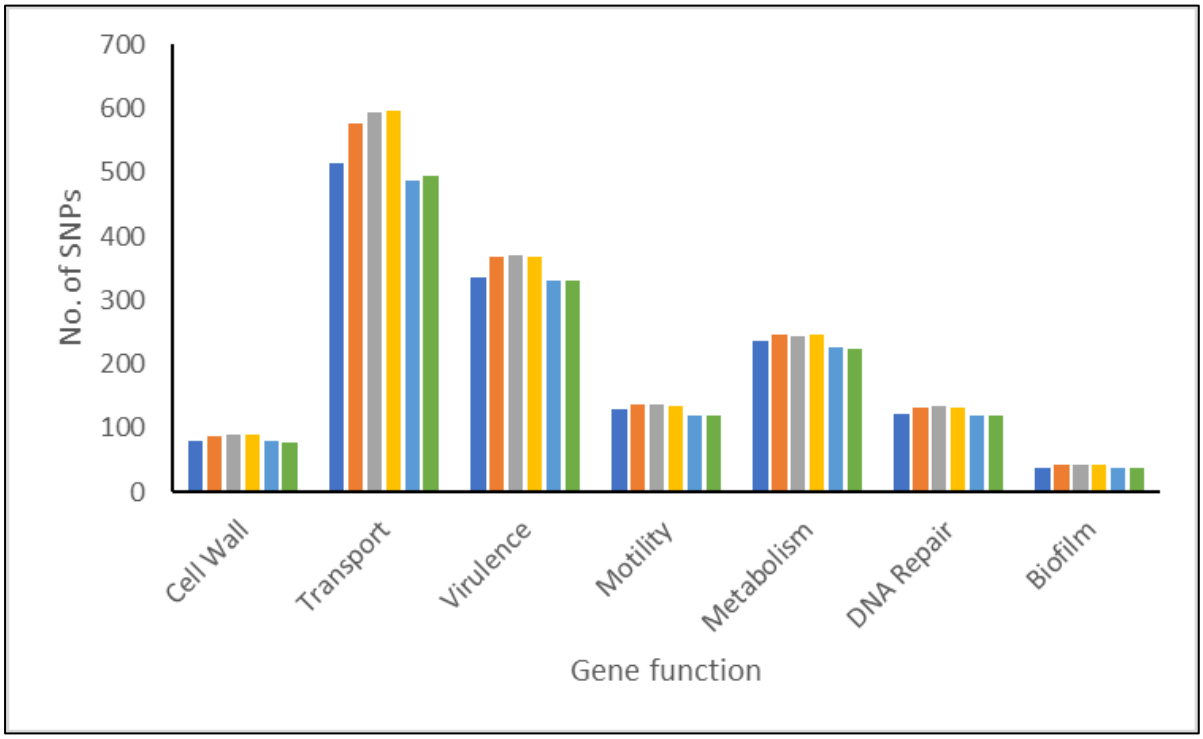

Figure 3.41: The total number of Single Nucleotide Polymorphisms (SNPs) that were detected as a result of WGS of both Parent (blue) and selected antibiotic-adapted (PAM15 = orange; PAD15 = grey; PACe8 = yellow; PACeA15 = light blue; PACo30 = green) variants of *P. aeruginosa* in comparison to the PAO1 reference genome.

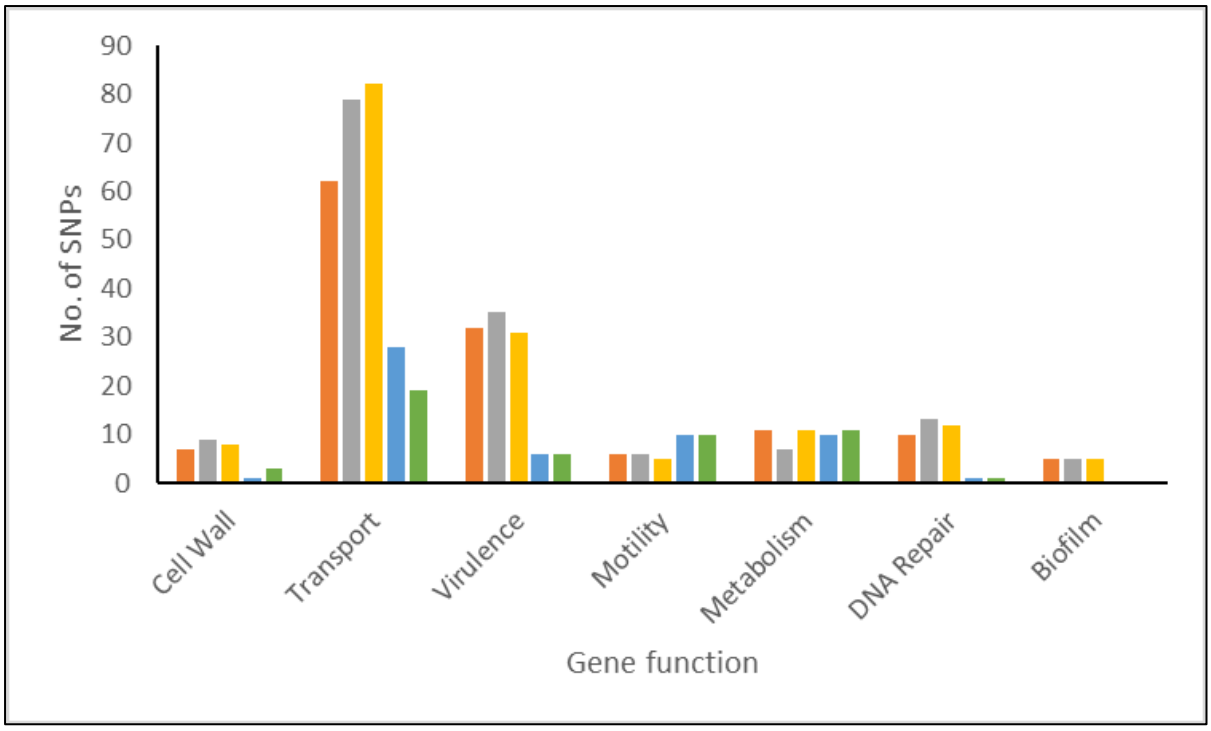

Figure 3.42: The total difference in the number of SNPs detected as a result of WGS in each selected antibiotically-adapted variant (PAM15 = orange; PAD15 = grey; PACe8 = yellow; PACeA15 = light blue; PACo30 = green) of Parent strain *P. aeruginosa* in comparison to the original un-adapted Parent.

Table 3.18: Number of total SNPs detected in each sequenced *P. aeruginosa* strain in comparison to the PAO1 reference genome.

Strain	Cell Wall	Transport	Virulence	Motility	Metabolism	DNA Repair	Biofilm	TOTAL
Parent	81	514	336	130	236	121	37	**1455**
PAM15	88	576	368	136	247	131	42	**1588**
PAD15	90	593	371	136	243	134	42	**1609**
PACe8	89	596	367	135	247	133	42	**1609**
PACeA15	80	486	330	120	226	120	37	**1399**
PACo30	78	495	330	120	225	120	37	**1405**

Table 3.19: Number of total SNPs detected in each sequenced antibiotic-adapted *P. aeruginosa* genome in comparison to the Parent strain.

Strain	Cell Wall	Transport	Virulence	Motility	Metabolism	DNA Repair	Biofilm	TOTAL
PAM15	7	62	32	6	11	10	5	**133**
PAD15	9	79	35	6	7	13	5	**154**
PACe8	8	82	31	5	11	12	5	**154**
PACeA15	1	28	6	10	10	1	0	**56**
PACo30	3	19	6	10	11	1	0	**50**

Upon further review of the genetic data available, comparing the original Parent strain with the antibiotic-adapted variants indicated further changes to their genetic structure. All, but two variants, increased greatly in their frequency of SNPs in comparison to the original Parent strain (Meropenem, Doripenem and Ceftazidime adapted strains; Figure 3.42). The antibiotic-adapted populations with the greatest number of SNPs in comparison to the Parent *P. aeruginosa* were both Doripenem- and Ceftazidime-adapted populations, with a total of 154 (Figure 3.42; Table 3.21). These SNPs were, once more, largely located in genes that have functions related to transport or virulence. Overall, genes related to transport functions were found to have the highest number of nucleotide variations, both in comparison to the PAO1 reference genome (Figure 3.41) and the Parent genome (Figure 3.42). Genes related to biofilm function were found to have the least number of SNPs when comparing for mutations against the PAO1 reference (Table 3.18) and Parent genome (Table 3.19).

Among the genes of note that displayed modifications included those related to porins. In comparison to the PAO1 genome, these series of genes displayed an array of SNPs. Upon closer examination of SNP differentiation that were detected within the adapted strains, however, there were further modifications, albeit, not as great a number to the Parent. The Doripenem-adapted strain displayed the greatest number of nucleotide changes related to these groups of genes in comparison to the Parent (Figure 3.44; Figure 3.46). Ceftazidime/Avibactam-adapted bacteria, in contrast, displayed no change in SNP arrangement in comparison to the Parent genome between these two porin-related gene groups (OprD and nicP) (Figure 3.44; Figure 3.46).

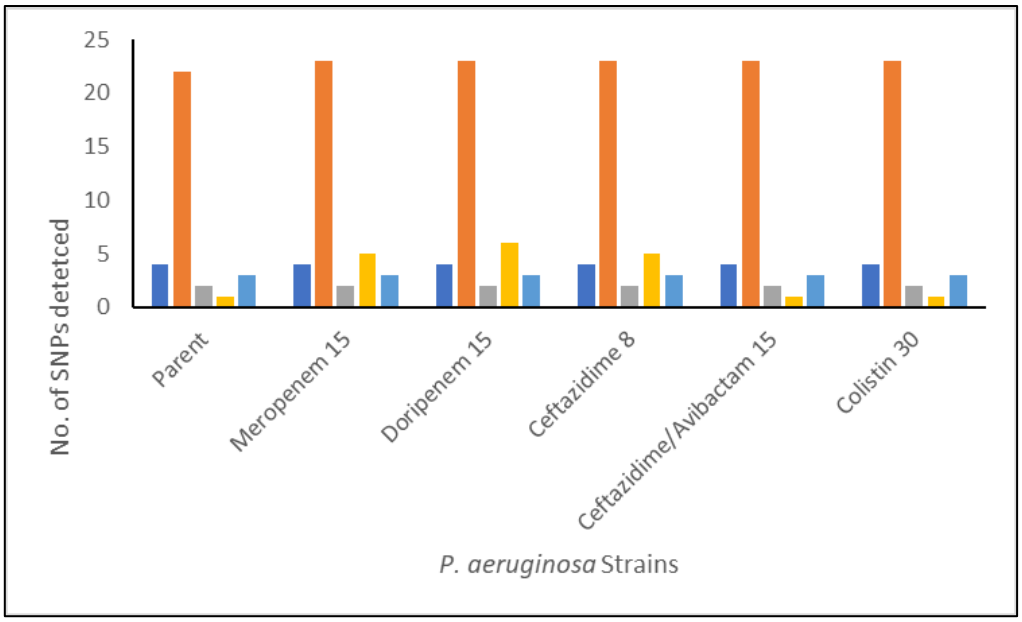

Figure 3.43: The total number of Single Nucleotide Polymorphisms (SNPs) in the OprD gene group (OprD_1 = blue; OprD_3 = orange; OprD_4 = grey; OprD_5 = yellow; OprD_7 = light blue) where SNPs were detected as a result of WGS of both Parent and selected antibiotic-adapted variants of *P. aeruginosa* in comparison to the PAO1 reference genome.

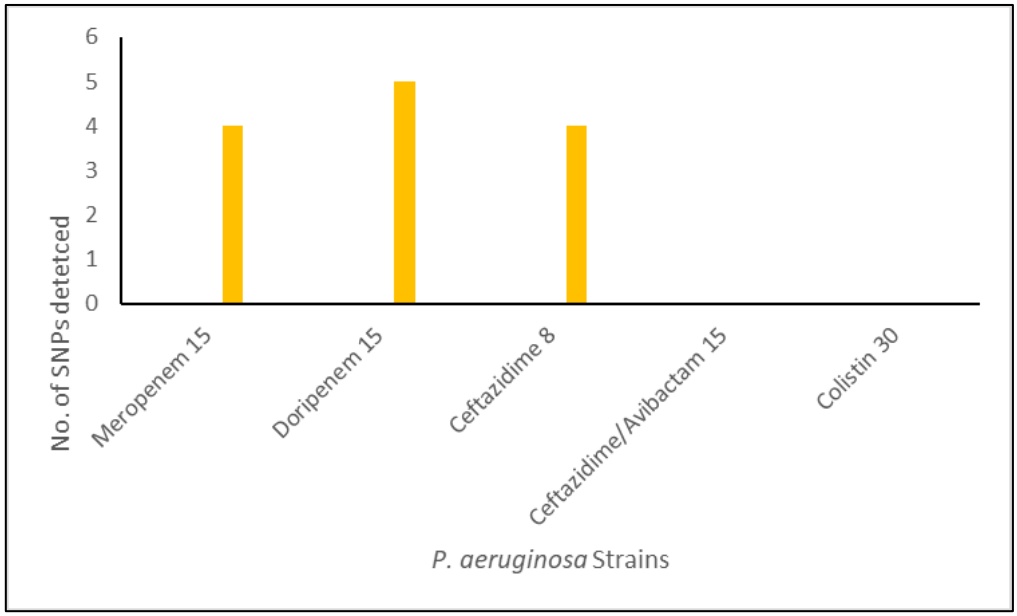

Figure 3.44: The total number of Single Nucleotide Polymorphisms (SNPs) in the OprD gene group (OprD_1 = blue; OprD_3 = orange; OprD_4 = grey; OprD_5 = yellow; OprD_7 = light blue) where SNPs were detected as a result of WGS of the antibiotic-adapted strains in relation to the Parent genome.

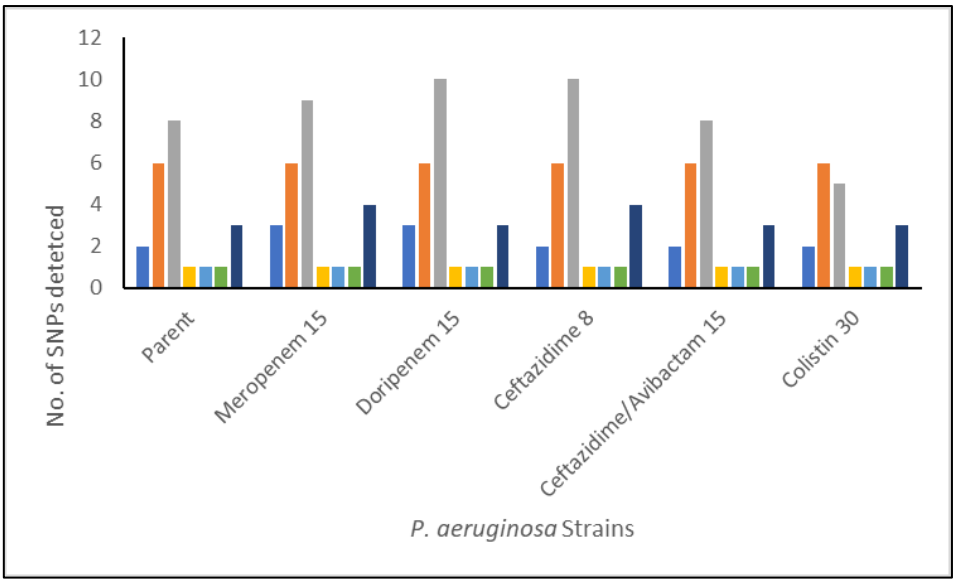

Figure 3.45: The total number of Single Nucleotide Polymorphisms (SNPs) in the nicP gene group (nicP_2 = blue; nicP_3 = orange; nicP_4 = grey; nicP_6 = yellow; nicP_8 = light blue; nicP_9 = green; nicP_11 = dark blue) where SNPs were detected as a result of WGS of both Parent and selected antibiotic-adapted variants of *P. aeruginosa* in comparison to the PAO1 reference genome.

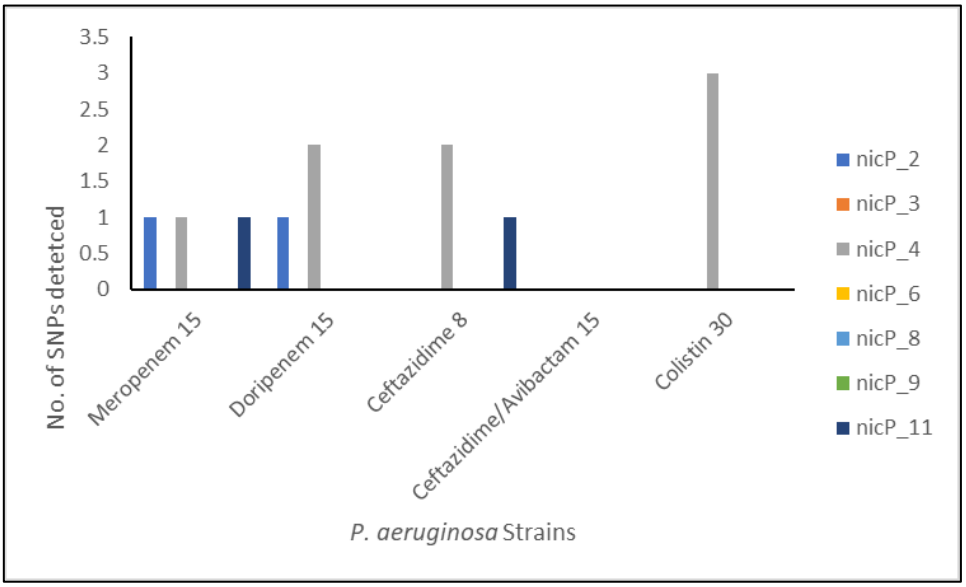

Figure 3.46: The total number of Single Nucleotide Polymorphisms (SNPs) in the nicP gene group (nicP_2 = blue; nicP_3 = orange; nicP_4 = grey; nicP_6 = yellow; nicP_8 = light blue; nicP_9 = green; nicP_11 = dark blue) where SNPs were detected as a result of WGS of the antibiotic-adapted strains in relation to the Parent genome.

Biofilm-related genes that displayed SNPs in comparison to the PAO1 genome indicated some minor differentiation to the Parent. The Doripenem-adapted strain comprised of the greatest number of SNPs in comparison to the Parent in relation to biofilm production (Table 3.20). In contrast, both Ceftazidime/Avibactam- and Colistin-adapted population genomes contain the least number of SNPs relative to the Parent within the group of genes with SNPs recognised based on comparison to the PAO1 genome.

Table 3.20: Number of total SNPs detected in biofilm-related genes in each sequenced antibiotic-adapted *P. aeruginosa* genome compared to the Parent strain.

Strain	PAM15	PAD15	PACe8	PACeA15	PACo30
EpsE	0	0	0	0	0
alyA_1	0	1	0	0	0
bdlA_1	0	0	0	1	1
alyA_2	0	0	0	0	0
algA_1	0	1	0	0	0
algA_2	1	1	1	1	1
algA_3	1	1	1	0	0
icaR	0	0	0	0	0
algB_1	2	2	2	1	1
alg8	0	0	0	0	0
algG	0	0	0	0	0
algX	1	1	1	1	1
kinB	0	0	0	0	0
TOTAL	**5**	**7**	**5**	**4**	**4**

Other genes of note with SNP in comparison to the Parent genome included the penicillin binding protein 2X (pbpX), vitamin B12 transporter (btuB), and flagellar hook-associated protein 1 (flgK) genes (Table 3.21).

Table 3.21: Number of total SNPs detected in each sequenced antibiotic-adapted *P. aeruginosa* genome within other genes with notable nucleotide changes compared to the Parent strain.

Strain	PAM15	PAD15	PACe8	PACeA15	PACo30
pbpX	3	3	1	1	1
btuB_1	1	1	1	1	1
btuB_3	3	3	1	1	3
flgK	1	1	1	4	4

4. DISCUSSION

Bacteria are adapting to the pressures forced upon them as a result of the prescription of antibiotics. Adaptations to such have been well documented. The purpose of this study has been to examine adaptations within one species, *Pseudomonas aeruginosa*, which is known to produce numerous factors to combat antimicrobials (Ciofu *et. al.*, 2015; Jagadevi *et al.*, 2018). Specifically, *P. aeruginosa* has been implicated in various nosocomial infections, including one that has been a focus of this research, Ventilator-associated pneumonia (VAP) (Ali *et. al.*, 2016; Hurley, 2019). *P. aeruginosa* has been one of several pathogens listed as research priorities by the World Health Organisation in terms of treatment (Jagadevi *et al.*, 2018; WHO, 2017), as the scale of resistance and global prevalence creates a large thrseat in terms of patient morbidity and strain on the medical economy.

The key aim of this study was to further understand the way in which *P. aeruginosa* adapts to antibiotics. To do this, a VAP clinical strain of *P. aeruginosa* was exposed to six antibiotics (Meropenem, Doripenem, Imipenem, Ceftazidime, Ceftazidime/Avibactam and Colistin) via disk diffusion over a series of 15 passages. Adapted variants were then tested in terms of their capability of growth and biofilm production under rich nutrient medium, co-infection, and restricted carbon source growth conditions. Whole genome sequencing was performed to observe whether changes in the genetic structure of this bacteria may explain their response to the antibiotic they have adapted to, as well as the type of media the bacteria were grown within. This would provide the basis of further epidemiological study as to understand the capability of *P. aeruginosa* to adapt to antibiotics that are typically prescribed against it, due to their effectiveness against the bacteria, and the conditions in which VAP cases are often treated in.

4.1 *Pseudomonas aeruginosa* adapts to a wide range of currently prescribed antibiotics

P. aeruginosa is a species of gram-negative bacteria that has an extensive genetic structure which can allow it to adapt to various antibiotics (Lambert, 2002; López-Causapé *et. al.*, 2018).

Following exposure, isolates of the Parent clinical strain of *P. aeruginosa* developed resistance to all but one antibiotic. The antibiotic to which the *P. aeruginosa* strain most quickly developed resistance was Ceftazidime. Resistance to this type of antimicrobial agent has been

well publicised, including within VAP cases (Rhodes *et al.*, 2019) . Recent experimental analysis using similar culturing methodology, albeit using E-test antibiotic strips, found that 20 out of 24 tested isolates of *P. aeruginosa* developed resistance, with 9 of these cultures becoming resistant to a concentration of 256µg of Ceftazidime (Zamudio *et al.*, 2019). Resistance to this agent has been highlighted in experimental studies as early as 2001 (Dancer, 2001; Henwood *et al.*, 2001), and the proportion to which *P. aeruginosa* isolates are resistant to Ceftazidime have increased since then, such as in the case of Zamudio *et. al.* Ceftazidime itself, is a third-generation cephalosporin, a group of antibiotics that are often prescribed due to their effectiveness against gram-negative bacteria, such as *P. aeruginosa* (Dancer, 2001). Cephalosporins are often prescribed for VAP due to previously recorded effectiveness against various agents of respiratory pathogenesis, such as coagulase-negative *Staphylococci* and Methicillin-resistant *Staphylococcus aureus* (MRSA) (Dancer, 2001). However, since treatment, and consequently resistance, has advanced (Wright *et al.*, 2017), certain antibiotics, as is the case with Ceftazidime, are rarely prescribed as a mono-therapeutic option. This has led to the development of new options.

One of these options, the recently developed combination drug, Ceftazidime/Avibactam, has been used as part of this study. Ceftazidime/Avibactam combines the known effects of Ceftazidime with that of a β-lactamase inhibitor, Avibactam, which proceeds to impede the activity of β-lactamase enzymes bacteria produce to counter the effects of the cephalosporin (Koulenti *et al.*, 2019; Livermore *et al.*, 2018; Zasowski *et al.*, 2015). Clinical trials testing this drug have displayed promising effects against infections, such as VAP and other nosocomial infections, with a 77.4% cure rate in patients with VAP itself (Koulenti *et al.*, 2019; Torres *et al.*, 2017). Whilst clinically this combination is promising, our data demonstrates *P. aeruginosa* can adapt following exposure. This is supported by further studies (Livermore *et al.*, 2018; Winkler *et al.*, 2015). In contrast to the mono-therapeutic option, the *P. aeruginosa* isolate was more susceptible to this form of treatment. The strain used in this study, however, did become resistant to Ceftazidime/Avibactam by Passage 10, and the bacteria adapted to treatment. Whilst this particular drug has been only recently prescribed within the United Kingdom (ECDC, 2018; Hawkes, 2017; Koulenti *et al.*, 2019), this study provides evidence that potentially strains of *P. aeruginosa* within the UK could adapt to this new combination. A UK study reviewing the activity of Ceftazidime/Avibactam against *P. aeruginosa* isolates collected

from clinical cases in 2015-16 found that treatment with this antibiotic against *P. aeruginosa* was effective, particularly against those with derepressed AmpC, a well-characterised β-lactamase (Livermore *et al.*, 2018). Ceftazidime/Avibactam was not as effective, however, with isolates displaying efflux-mediated resistance (Livermore *et al.*, 2018). Little other evidence before 2018 demonstrates any significant level of resistance to the author's knowledge, other than one study conducted in 2015 (Winkler *et al.*, 2015). Winkler *et. al.* conducted both MIC tests and genetic sequencing on 54 clinical isolates of *P. aeruginosa* in the U.S., where Ceftazidime/Avibactam has been licensed for use since 2015 (Winkler *et al.*, 2015). They found that 18.5% of the isolates were resistant as a result of efflux pump overexpression (Winkler *et al.*, 2015). More alarmingly, however, a more recent review from the UK reported that in some cases, only 44.1% *P. aeruginosa* isolates from UK origin were susceptible to Ceftzidime/Avibactam combination (Livermore *et al.*, 2018). Some of these strains were known to contain features that convey widespread resistance, including efflux pumps (Livermore *et al.*, 2018). Whilst in this study, and within literature, Ceftazidime/Avibactam has indicated being a more successful mode of treatment in comparison to Ceftazidime alone, *P. aeruginosa* does wield capabilities that allow it to become resistant to this as well.

Interestingly, there was a varied response in terms of how well carbapenem-variant antibiotics worked against the clinical strain of *P. aeruginosa*. Meropenem was the first of the three carbapenems tested that *P. aeruginosa* became resistant, followed by Doripenem, and Imipenem. According to one review, Doripenem has been found to have lower Minimum Inhibitory Concentrations (MICs) than both Meropenem and Imipenem (Codjoe & Donkor, 2017) when applied against *P. aeruginosa* infection. A Phase III trial found similar results, that Doripenem was less likely to select for resistance than Imipenem (Hawkey & Livermore, 2012). Whilst we did not conduct any testing that would attribute an MIC to the *in-vitro* growth present, we did establish that through disk diffusion, the last carbapenem that the strain we tested did establish resistance against was Imipenem. This could, if applied to the review, establish a difference to what is commonly reported in literature, however, we would need to conduct a broth dilution methodology to accurately measure whether the result carries any weight.

Broth dilution uses a doubling-dilution protocol, where the antibiotic of interest would be set at certain concentrations that an inoculum of bacteria would be tested against. This would allow for a more accurate representation of the concentration where resistance had been established. Such a method, however, should be implemented potentially alongside the disk diffusion method, as colonies closest to the inhibition zone from disk diffusion could be selected to be exposed to broth dilution to understand the extent of the clinical strain's resistance. In contrast to most articles, however, it is possible to argue Doripenem resistance being more prevalent due to extensive use. One study investigating the use of carbapenem-based antibiotics, and appropriateness of such, found that 84 patients at Hartford Hospital in 2014 had received carbapenem-based treatment as part of empiric therapy (Goodlet & Nailor, 2017). 52 of these patients received Doripenem as their course of carbapenem, which was the most widely prescribed within the study group (Goodlet & Nailor, 2017). By applying this to this study, it would be likely that the clinical strain had prior exposure to Doripenem treatment. This interpretation however is likely to be subjective, as prescription data or patient data was not available during the time of study, and special permission was required. Carbapenems themselves are considered to be "antibiotics of last resort" due to their broad-spectrum of activity (Papp-Wallace *et. al.*, 2011). As a result, they are often set aside for extreme cases, where the patient is in critical health or when bacteria are resistant to extensive numbers of commonly prescribed antibiotics (Crandon *et al.*, 2016; Papp-Wallace *et al.*, 2011). Considering this, it is often the case that these antibiotics are applied to combat such conditions as VAP (Crandon *et al.*, 2016; Mustafa *et al.*, 2016; Trinh *et al.*, 2017), and adaptation to such would be expected as a result.

The data collected from the Colistin-adapted strain of *P. aeruginosa* provided little evidence to suggest that the bacteria had indeed adapted to the antibiotic. EUCAST does recommend that in order to generate evidence for such, a broth dilution test would be needed to calculate an MIC (EUCAST, 2019). Thus, the disk diffusion method is not suitable to test the full extent of adaptation towards such. To test whether this strain was resistant to concentrations of Colistin, a broth dilution test would have needed to be conducted in future.

Evidence of *P. aeruginosa* resistance against Colistin, and by extension polymixins, is limited (Landman *et. al.*, 2005; Pedersen *et. al.*, 2018). The use of Colistin as a treatment option remains to be controversial, even as antimicrobial resistance increases globally, due to the

well-known issues of neurotoxicity and nephrotoxicity towards patients (Goli *et. al.*, 2016). The extensive use of broad spectrum agents, however, has encouraged the use of Colistin as a measure of last resort due to the emergence of MDR pathogens (Goli *et al.*, 2016; Landman *et al.*, 2005; Mustafa *et al.*, 2016; Palavutitotai *et al.*, 2018). The record of activity against *P. aeruginosa* has been successful to a large extent with Colistin treatment (El-Nawawy *et. al.*, 2019; Jain *et al.*, 2014; Mustafa *et al.*, 2016), however the pattern of resistance has increased as a result of use (Du *et. al.*, 2016; Pedersen *et al.*, 2018). The result of this is characterised by the expression of certain genes, which will be discussed later in this section. It is likely, however, that the strain of *P. aeruginosa* that we tested is susceptible to Colistin-based therapy based on the evidence from disc diffusion, albeit without MIC data.

Whilst the experimental method used to test how the *P. aeruginosa* strain adapted to antibiotic exposure indicated that all of the adaptations were significant, further experimentation focussing on the concentration of antibiotic is needed to assume as to whether this resistance is universal. Testing for the MICs of each strain would have allowed for further clarification as to whether the bacteria have adapted to the antibiotic, and at a certain concentration. Since the disk diffusion method incorporates antibiotic-impregnated paper discs at a set concentration, it is not possible to determine as a to whether *P. aeruginosa* in this study would be able to adapt to varied measures of antimicrobial compound. This can be easily amended in future experiments, with the use of other methods such as the E-test strip or through the means of broth dilution. The means of accurately measuring the adaptation to MICs would be achieved primarily through broth dilution, however, as there is a large amount of subjectivity when it comes to accurately measuring where the resulting inhibition zone border lies with respect the concentration of antibiotic on the E-strip (White *et al.*, 2001).

The disk diffusion method is also open to subjectivity, as the only way of measuring the impact of antibiotic action was through measuring the diameter of the inhibition zone, and correlating it's size with that mentioned within the EUCAST guidelines (EUCAST, 2019). Interpretation of these inhibition zones may vary based on the interpreter's measurement of the area, but this type of error can be reduced. One way is to measure the inhibition zone multiple times and record the average of these multiple measurements. Another, which has been conducted in this study, is to collect data from multiple populations of the same

bacterial strain, exposed to the same antibiotic. This allows for a means as to identify a representative measure of antimicrobial action, and as to whether, as time progresses, the bacteria grown on specific medium is adapting to the repeated measures of medication. The issue with this particular mode of representation, however, is that new isolates, and potentially new strains of bacteria, are created in effect as a result of the difference in certain variables that each one was exposed to.

A standing hypothesis when it comes to considering how resistance occurs is proposes that bacteria are able to adapt to treatment, but a fitness cost is imposed as a result (Amini *et. al.*, 2011; Gerrish & García-Lerma, 2003; Melnyk, Wong, & Kassen, 2014). These fitness costs can vary with some, which can convey genuinely successful resistance, but at a high price to the microorganism in some other way (Melnyk *et al.*, 2014). Because our method implemented 5 repeats; 5 total populations exposed to one antibiotic, the likelihood is that the each of these repeats could have evolved their own separate way of resistance through a multitude of mutations and fitness costs. It can also be deduced that *P. aeruginosa* also has a high rate of mutation, as reported within research examining the genome of PAO1 reference strain (Klockgether *et al.*, 2010, 2011). Thus, if applying such a mutation rate and variable genome to these repeats, it is likely that a genetic bottleneck event may have occurred because of this experiment in each repeat population. This does, however, provide an average inhibition zone result that could be more representative of the strain testing, given that there was an increased chance to introduce a wide variety of mutations that this strain would be able to display.

4.2 *Pseudomonas aeruginosa* AMR adaptations create differences in growth patterns

The second part of this overall study was an investigation on how adaptation to antibiotics impacted planktonic growth of the *P. aeruginosa* strain. Antibiotics can impact bacteria in multiple ways, which can include disruption of cell wall assembly, inhibiting metabolic processes and blocking DNA replication mechanisms (Kapoor *et al.*, 2017). As a result of antibiotic action, the bacteria can either be prevented from further population expansion (bacteriostatic) or be killed outright (bactericidal).

We investigated this by growing a selected population of the Parent strain of *P. aeruginosa* and each antibiotically adapted isolate in growth medium over a period of 48 hrs. This allowed for observations to effectively measure whether each adaptation would impact the rate of

growth, within a medium that contains no antibiotic. A 96-well microtitre method was used. Separate assays were implemented to remove each plate at a set timepoint they were selected for without disturbing each of the other cultures once that timepoint had been reached for analysis.

The results from these sets of experiments indicated that overall growth was affected by antimicrobial exposure when comparing all antibiotic-adapted strains against the un-adapted Parent clinical strain. Two-way repeated measures ANOVA analyses found significant differences between each strain tested in terms of growth in Mueller-Hinton broth medium at various timepoints. Perhaps the most clearly defining difference was that there were differences at the 24hrs timepoint when comparing both the Parent strain with the adapted strains. This timepoint was identified to be the point at which the Parent population was at peak population growth. In contrast, all antibiotic-adapted strains appeared to reach peak growth at a later point in time, all except PAD15. The Doripenem-adapted strain did achieve peak growth at 24hrs, similar to the Parent, however in accordance to the optical density recorded, the population was much less dense in comparison. It is likely that the mutations that occurred to allow the adapted strains to survive antimicrobial action led to change in their growth pattern.

To suggest that a fitness cost to growth may have occurred as a result of antibiotic adaptation was inconclusive, due to issues regarding growth rate calculations. Not all growth rates as a result of CFU calculations could be defined unfortunately, as some of the adapted strains produced dense colonies that could not be accurately counted at the dilutions that were set following the methodology outlined by Miles & Misra, one example being PAD15. This included the Parent strain as well, thus comparisons to explain whether the overall rate of population growth would be impacted because of antibiotic adaptation was difficult to deduce. A repeat of this protocol could not be conducted due to the time restrictions of the overall study.

Between the evidence that was available, however, it was clear that potential differences in antibiotic resistance generation may affect growth rate. This assumption can be based on the overall growth rates that were calculated from both the Imipenem-adapted strain and the Ceftazidime/Avibactam-adapted strain. PAI15 indicated that it grew at a faster rate in

comparison to PACeA15, which indicates that the specific modes of action of antibiotic affected *P. aeruginosa* differently. Both of these antibiotics are bactericidal in purpose, with Imipenem inhibiting cell wall synthesis by targeting penicillin-binding proteins (PBPs) (Rodloff *et al.*, 2006). Ceftazidime/Avibactam works in combination between a cephalosporin (Ceftazidime) and a β-lactamase inhibitor (Avibactam), with the latter component inhibiting the action of β-lactamase enzymes that render antibiotics, such as Imipenem, ineffective as they belong to the β-lactam family of agents (Lahiri *et al.*, 2014). It is perhaps the fact that *P. aeruginosa* was being targeted by two antibiotic components, with the addition of Ceftazidime/Avibactam, the other target as the focus of Ceftazidime application being cell wall formation by inhibiting PBPs similar to Imipenem (Hayes & Orr, 1983), leads to the bacteria a reduced growth rate in comparison to a mono-therapeutic option.

Mueller-Hinton is a medium that is widely used in microbiological research for antimicrobial susceptibility experiments (Jones *et. al.*, 1987; Mattei *et. al.*, 2014; Rimek, Fehse, & Go, 2007). It contains a wide variety of amino acids to ensure that there is continuous growth over a long period of time, but perhaps one variable that has had an effect on previous research was the concentration of magnesium, calcium and zinc cations contained within the media (Kenny *et al.*, 1980; Pollock *et. al.*, 1978). These particular elements have been reported to increase the potential for *P. aeruginosa* to develop increased resistance towards antibiotics such as Gentamicin (Kenny *et al.*, 1980), mainly influencing porin and efflux pump expression and activity (Lister *et al.*, 2009). As a result of this, it would be important to observe in future how the levels of these cations may potentially affect antimicrobial activity with the agents selected. Perhaps more interestingly, when these cations are applied individually in a restricted growth medium such as M9 Growth Media.

4.3 Biofilm formation is affected as a result of adaptation to antibiotics

Alongside growth, biofilm formation was assessed through the means of using a microtitre assay, which was then subsequently washed and stained with 0.1% Crystal Violet to pick up any biofilm that was left behind from *P. aeruginosa* growth.

Based on observations and the significance of the results, the Parent strain produced more biofilm in comparison to the PAO1 reference. The potential causes behind this are speculative without further genetic data, which will be discussed later in the discussion. The genome of *P. aeruginosa* in general, is subject to change. A sub-strain of PAO1, PAO1-UW, was found to

contain 2.2Mb inversion in contrast to the original PAO1 strain (Klockgether *et al.*, 2010, 2011), indicating that laboratory strains across the globe are more diverse than the original reference. A more recent study comparing 10 PAO1 laboratory isolates found that whilst a total number of 5,434 out of 5,682 genes were conserved between each of the strains, variability in secreted molecules from each of these strains was observed (Chandler *et al.*, 2019). These variations included differences in the secretions of virulence factors such as pyocyanin, *Pseudomonas* quinolone signal (PQS) and rhamnolipids, however biofilm formation profiles remained similar across all ten strains (Chandler *et al.*, 2019). Because of this, it was likely that the values relating to biofilm formation in the case of the reference PAO1 laboratory strain we used would be similar in profile. With that in mind, the results that was collected with respect to the Parent strain indicates that it is of a different strain to PAO1.

Differing results were observed in relation to biofilm formation between each antibiotic-adapted strain to the Parent. The results in relation to the carbapenem-adapted strains indicated that there were significant differences between both PAD15 and PAI15 in comparison to the Parent, based on ANOVA analysis. Further post-hoc analyses, however, did not display any specific timepoint where there was a difference. When comparing each strain to each other thus any difference that was recorded was likely due to random formation as opposed to being due to antibiotic adaptation. Upon further review of the data, the biofilm formation values, for the most part, displayed similar formation patterns. To our knowledge, there is little evidence that studies incorporate a design in which different carbapenem class antibiotics are compared against each other on their effects on biofilm formation. This has made it difficult to draw any comparison as to whether there are key differences between each of these medications on how they impact bacteria in this manner.

The adapted strains also produced their own differences in relation to the un-adapted Parent, with the carbapenem-adapted strains each indicating that their biofilm formation was affected in some way. Carbapenems, within research, have been compared as a sum when comparing their effects on biofilm formation to other antimicrobial agents. To the writer's knowledge, based on scrutiny of research papers regarding carbapenems and their effect on biofilm formation in general, there was little evidence that even carbapenems affect *P. aeruginosa* biofilm formation. One study has examined the effects of carbapenems on the biofilm formation ability of *Klebsiella pneumoniae* (Cusumano *et al.*, 2019). *K. pneumoniae* is

another species of gram-negative bacteria that is implicated in many nosocomial infections, including VAP, and is a species of bacteria that has become increasingly resistant to many forms of antibiotics (Ferreira *et. al.*, 2016; Jagadevi *et. al.*, 2018; Santajit & Indrawattana, 2016). Cusumano *et. al.* employed a similar *in vitro* biofilm assay to investigate multiple clinical strains of *K. pneumoniae* and their biofilm formation activity in relation to application of various antibiotics. Upon application of carbapenem antibiotics, out of a total of 70 isolates exposed to such, 43 of these strains were found to form weak biofilms, as opposed to 26 that formed strong biofilms (Cusumano *et al.*, 2019). Weak biofilm formation was defined as absorbance values being recorded at less than 0.2 when exposed to a wavelength at 570nm. By applying Cusomano *et. al.'s* research, all of the *P. aeruginosa* isolates, in regard to biofilm formation, did not match the definition of a "weak biofilm", as all were recorded to have an OD600 absorbance value above 0.2. With reference to VAP, this research can perhaps be further questioned when trying to apply results to *P. aeruginosa*, as *K. pneumoniae* is largely implicated within cases of early-onset VAP, as opposed to late-onset (Patil & Patil, 2017; Restrepo *et al.*, 2013). A large proportion of microbiota that are involved in early-onset VAP are associated with being more susceptible to antibiotics (Golia *et al.*, 2013; R. Khan *et al.*, 2016; Patil & Patil, 2017). One reason why this may be is that these pathogens may well produce less-persistent biofilm than those implicated in late-onset VAP. Further study into how organisms that are typically implicated in late-onset VAP should be considered. As with regard to the impact of carbapenems on biofilm formation, more work is needed to understand the individual modes of action on other species, and how they may play a role in such, though the results included in this study are insignificant.

Although adaptation to Ceftazidime did not influence biofilm formation, based on subsequent post-hoc analysis, Ceftazidime/Avibactam adaptation did result in significantly impaired biofilm growth. This assumption, however, was based on the evidence presented from both sets of statistical analysis that was conducted. The Sidak post-hoc analysis did detect one point of significant growth, at 6hrs, between PACeA15 and the Parent *P. aeruginosa*. When comparing the significance values to the growth curve graphs, however, the other results appear to be at a much lower OD value in comparison to the Parent strain. It is likely that the other timepoints were not significant due to the statistical mode that was implemented. Intriguingly, the addition of a β-lactamase inhibitor did influence biofilm formation, however,

when comparing both PACe8 and PACeA15 strains and their biofilm formation patterns. Significant differences were found at multiple timepoints, and potentially indicates that adaptations towards PACeA15 does potentially reduce the amount of biofilm produced by *P. aeruginosa*.

This is the first report of such an adaptation affecting biofilm formation. A similar Ceftazidime/β-lactamase inhibitor combination, Ceftazidime/Tazobactam, has been noted to have an effect on biofilm production within PAO1 cultures based on time-dependent killing (H. Wang *et al.*, 2015). Thus, it is able to penetrate through and impact the target bacterial population, and does provide evidence that could extend to the effects of the Ceftazidime/Avibactam based on our results. Further research, however, is needed to investigate whether this effect is repeated in future, regarding both PAO1 cultures and MDR cultures. This would allow further evidence for consolidation whether the combination of cephalosporin and β-lactamase inhibitor provides an effective treatment in the presence of biofilm. This, however, should be treated with caution, as with previous evidence that this study has provided, resistance to Ceftazidime/Avibactam can occur due to continuous use.

Whilst the Colistin-adapted strain displayed significant differences in biofilm formation patterns, it is unclear based on post-hoc analysis at what timepoint. Though the growth curve indicates that the Colistin-adapted sample does display lower OD600 absorbance values in comparison to the Parent itself beyond the 12hrs timepoint, based on the statistical analysis, the results may not be as a direct result of antibiotic adaptation. Combining this with the need of broth dilution test to analyse for adaptation, the strength of any conclusion relating to antibiotic adaptation is limited.

Colistin itself has been proven to have a bactericidal effect on biofilm formation, though these effects have varied depending on the concentration of medication that was applied (Klinger-Strobel *et. al.*, 2016). Nonetheless, the effects of the application still stand that when applied as therapy, Colistin does reduce the overall build-up of biofilm against *P. aeruginosa* strains (Klinger-Strobel *et al.*, 2016; Kolpen *et al.*, 2015; Pompilio *et. al.*, 2015). This also extends to other species of bacteria, including *Escherichia coli* and *Staphylococcus aureus* (Klinger-Strobel *et. al.*, 2017), although evidence of action against MRSA indicated that Colistin had little effect on such, though the overall cell density within the biofilm was reduced (Klinger-

Strobel *et al.*, 2017). A future implication would be to investigate the effects of combination therapy, with Colistin being one of the principal agents, and whether this form of combined treatment has an influence on both biofilm and cell density. On a similar theme, another combination, which has been proposed as an alternative due to its reduced effects on host neurology, could be tested, with the principal agent being Rifampicin (Hu *et al.*, 2016) in comparison to Colistin combination therapy.

The experimental design indicated that the bacteria did grow over a period of 48 hrs whilst contained within microtitre wells of a fixed volume. However, this fixed volume; 200µL of medium, provided some issues. Because of this fixed volume, the amount of nutrient contained within the medium during the experiment was restricted to that within the well. This would not be replenished over time, in comparison to what may occur in natural cases. Within *in vivo* environments, infections can persist within environments for long periods of time due to continuous dynamics within the microbiome. In the case of VAP, *P. aeruginosa* is one such agent associated with chronic, or late-onset VAP, thus persisting within patient lungs over a long period of time, likely due to the dynamics within this environment. Late-onset VAP is characterised by the resultant VAP condition occurring after 5 days of intubation, and is more likely to be caused by microorganisms that are associated as multi-drug resistant (MDR) (Golia *et al.*, 2013; Nair & Niederman, 2015). To clarify whether this may have been due to a decline in nutrient levels within the medium, or through some other means, another in-vitro based system could well be created. Through the means of a chemostat or other apparatus, that could allow a continuous system of metabolites to be supplied over a long period of time. Such a model, however, would need conditions to match similar levels of certain other variables, such as pH, temperature and O_2/CO_2 levels, within the infected lungs, which would be difficult to control or interpret due to potential individual differences, alongside other issues. To the author's knowledge, no such system exists at present, and should be considered in future.

A similar issue as encountered with the growth rate experiment relating to the microtitre assay method could have also played a role in relation to biofilm formation. Whilst the microtitre assay is a widely-applied method (Welch *et al.*, 2012), it relies on the bacteria being grown in a medium with a fixed concentration of nutrient. A continuous flow-based method could be implemented in future to resolve this issue, as a continuous nutrient supply would

maintain a constant environment for the bacteria *in vitro*. Whilst there was evidence of absorbance associated with biofilm production according to this method, the likelihood that we could apply such results to a living VAP case could be disputed. The diseased lung environment, in which these microorganisms infect and thrive in, contains a wide variety of potential metabolic material that the bacteria will take in and compete against species for, in order to continue population expansion. Some of these molecules have been highlighted in papers, such as the host molecules haemoglobin and transferrin (Nguyen & Oglesby-Sherrouse, 2016), which are used by *P. aeruginosa* as alternative sources of iron. Other factors that play a key role in biofilm formation, such as host immunity (Jamal *et al.*, 2018; Kovach *et al.*, 2017), further add to the issue that such a model cannot be applied fully to a wider context. An ex-vivo model would provide an excellent means of adding additional variables, such as residual innate immune cells, that could impact the experimental biofilm formation. However, quantification of biofilm would remain a challenge.

The use of Crystal Violet as a method of quantifying biofilm was another issue that could well have affected the validity of our findings. This is largely due to fact that what was stained may have not been residual biofilm, but potentially other particles associated with bacterial growth, such as dead bacterial cells (Merritt *et al.*, 2005). This would result in an overestimate in the amount of biofilm present. The implementation of a microscopic, cover-slip based method could counter this (Merritt *et al.*, 2005), as the coverslip interacting with the culture would provide a sample interface that provides a representation of current growth within the culture at time of sampling. This would also create a more qualitative means of both measuring biofilm, whilst also acting as a quality control, as biofilm and free-swimming planktonic bacteria can be clearly defined and interpreted through interpretation via microscope.

4.4 *Pseudomonas aeruginosa* adaptation to antibiotics affects growth within *S. aureus* co-culture

A further growth and biofilm formation experiment was conducted in a similar manner to the MH broth condition as part of the overall study. In this case, the strains of *P. aeruginosa* were tested against an equal concentration and volume of *S. aureus*. *S. aureus* was chosen due to

its association with late-onset VAP (García-Leoni *et. al.*, 2010; Park, 2005), alongside the fact that in most VAP cases, infections are often polymicrobial in nature (Joseph *et al.*, 2010).

The results collected from this set of experiments indicated that throughout each comparison, there were significant differences detected in growth in comparison to previous growth under monoculture. Considering that differences were detected at peak growth in most cases, there was an apparent effect that antibiotics may lead to *P. aeruginosa* growth being affected under co-infection circumstances. In most cases, the growth that was detected was at a higher density in comparison to the mono-infection conditions, albeit from PAD15, which displayed a decrease in density. This may suggest that the Doripenem-adapted strain of *P. aeruginosa* may have been either affected by the presence of *S. aureus*, however, to understand whether *P. aeruginosa* or *S. aureus* was the dominant species requires further examination. It has been documented that *P. aeruginosa* exploits the presence of bacteria, such as *S. aureus*, as a means of a source of iron, parasitising the species by harvesting the iron *S. aureus* has (Barnabie & Whiteley, 2015). This knowledge has largely been known as a result of studying the behaviour of these two species within cystic fibrosis patients, of which *P. aeruginosa* is a well-known pathogen to colonise the mucus-lined lungs (Mulcahy *et al.*, 2013; Nguyen & Oglesby-Sherrouse, 2016). The Doripenem-adapted strain was found have a less dense OD value at peak growth (24hrs) in comparison to the mono-infection, which may hint that the antibiotic may have created a fitness cost, where resistance to the antibiotic came at a cost of being less able to grow in the presence of *S. aureus*, potentially due to competition for nutrient. More evidence, however, would be needed to substantiate this assumption, possible through means of assessing growth or viability in restricted media conditions with iron supplement. On top of this, it is not understood whether the species present within the medium at the end of the experiment, or at peak, was either dominated by *P. aeruginosa* or *S. aureus*, thus future experiments should include a means to observe if either species was present at each timepoint, further emphasising the need for a CFU count.

Co-infection conditions caused by both *P. aeruginosa* and *S. aureus* have been studied over the years, with particular emphasis under *in vitro* conditions (Hotterbeekx *et. al.*, 2017; Limoli *et. al.*, 2016; Limoli & Hoffman, 2019; Nguyen & Oglesby-Sherrouse, 2016). This is largely due to the fact that large numbers of respiratory infections, including VAP, have often been diagnosed and treated with a combination of aetiological agents (Patil & Patil, 2017; Walkey

et al., 2009). These two pathogens are of particular interest in VAP research due to their extensive resistance profile. (Limoli *et al.*, 2016). Most of the evidence supporting this particular association has been isolated from cystic fibrosis patients, however. (Kahl, 2018; Limoli & Hoffman, 2019; Nguyen & Oglesby-Sherrouse, 2016). The interactions between both *S. aureus* and *P. aeruginosa* are poorly understood when it comes to *in vitro* culture. This is perhaps due to the difficulty of replicating conditions within the impaired lung; conditions that both species thrive in. Defining the interactions between these two species can differ, due to conflicting evidence. One such interaction that has been reported is that both species act synergistically, such as certain virulence factors being expressed by one species that benefits the other (Murray *et. al.*, 2014; Nguyen & Oglesby-Sherrouse, 2016). This particular behaviour has been observed in multiple models of *S. aureus*/*P. aeruginosa* co-infection, such as the production of Small Colony Variants (SCVs) within *P. aeruginosa* when exposed to *S. aureus* (Michelsen *et. al.*, 2014; Nguyen & Oglesby-Sherrouse, 2016), increasing the chance of colony survival and antimicrobial tolerance. This may explain why VAP is often quite difficult to treat and leads to the patient being contained within the ICU for weeks whilst being mechanically ventilated. Other models, such as a mammalian model-based experiment that mixed poly-microbial *in vitro* cultures into the wounds of mice, found that the outcomes of infection led to delayed wound closure, and reduced effectiveness of antimicrobial therapy (Dalton *et al.*, 2011). This suggests that co-infection with these two pathogens leads to an increase in virulence factor expression.

Evidence from this study does indicate that virulence factors were indeed expressed as part of co-infection, as results relating to biofilm production did indicate the microtitre assay cultures did produce what may be potential biofilm. The OD600 absorbance values, however, were smaller in all cases, apart from the PAO1 reference control sample. This may be due to the source of the Parent strain itself, as being it was a clinical strain, this *P. aeruginosa* strain may well have been exposed prior to *S. aureus* at one stage. All samples were found to produce significantly less biofilm in response to co-infection, apart from both Ceftazidime/Avibactam- and Colistin-adapted samples, which produced significantly more. This suggests that the adaptation to either of the two antibiotic combinations contributes to biofilm formation, however, as stated before, more evidence is needed to understand whether the biofilm produced was from *P. aeruginosa*, and not as a result of *S. aureus*.

In most cases when it comes to co-infection relating to both *P. aeruginosa* and *S. aureus*, biofilm production has been reported to increase alongside other virulence factors (Dalton *et al.*, 2011; DeLeon *et al.*, 2014; Nguyen & Oglesby-Sherrouse, 2016). This contrasts what has been observed from all strains apart from the PAO1 control. The decrease in relation to the Parent and antibiotically-adapted strains requires further examination into what virulence factors may well have been present. The interactions that both bacteria display under co-infection can be defined as synergistic or antagonistic. In this case, *P. aeruginosa* and *S. aureus* may well have been antagonistic towards one another. Evidence from previous studies, with particular focus on Cystic Fibrosis cases, highlight that *P. aeruginosa* can become highly prevalent as the disease progresses into chronic cases, a change from the highly diverse makeup found in acute cases (Foundation, 2018; Nguyen & Oglesby-Sherrouse, 2016). Of note, however, due to possible improvements in diagnostics for gram-positive bacteria, *S. aureus* has been found to be the most commonly isolated organism in Cystic Fibrosis cases, thus potentially outcompeting *P. aeruginosa*. (Foundation, 2018). The changes in nutrient availability and reaction from host immunity has been proposed to be driving forces in competition between both species (Bhagirath *et al.*, 2016). The availability of iron plays a key role with particular regard to *P. aeruginosa* (Barnabie & Whiteley, 2015). Host proteins, including haemoglobin, transferrin and lactoferrin, provide bacteria a means to acquire iron for metabolism (Nairz *et. al.*, 2010), which *P. aeruginosa* exploits by secreting a wide variety of virulence factors. These factors include the use of siderophores (A. Khan *et al.*, 2018; Streeter & Katouli, 2016), and heme transport and degradation system molecules (Barker *et al.*, 2012). These factors are also found to be agents that *S. aureus* can excrete and activate (Cassat & Skaar, 2012; Hammer & Skarr, 2011). Because of this, it is likely that both species may compete for iron resources, should this be a limiting factor within the environment that they occupy. However, in the case of this particular form of competition, biofilm production has been found to increase due to the sequestration of iron from both the host environment, and in some cases, *S. aureus* (Mashburn *et. al.*, 2005). In this case, *P. aeruginosa* acts as a parasite towards the gram-positive bacterium. This evidence has been gathered from *in vivo* mouse studies (Mashburn *et al.*, 2005), which may explain how certain forms of pathogenesis can occur within nosocomial cases. To our knowledge, however, there is little evidence of any form of biofilm reduction occurring between both species within host lung environments in

relation to *S. aureus* exploitation by *P. aeruginosa*. As previously described, *in vitro* studies have provided evidence that biofilm formation is increased as a result of coinfection, but the exact ratio and interactions involved in the production of such and whether it is as a direct consequence of one another needs further investigation.

4.5 Under limited carbon sources, *P. aeruginosa* displays a variation in both growth and biofilm formation against nutrient rich conditions

In the case of growth within restricted media using different carbon sources, in the vast majority of cases, significant differences were found comparing growth between both rich nutrient media, in this case being Mueller-Hinton, and growth in limited carbon medium. There were significant differences reported between all of the strains when it comes to growth in M9 medium with either 20% Glucose or 20% Alanine supplementation in comparison to MH medium. This also included a noticeable difference in growth pattern, being that the growth of each strain, both Parent and adapted, featured a population density spike at 24hrss of growth in both limited media. Comparison for differences between both media found no significant differences in growth. This would suggest that the antibiotic adaptations that have occurred was not associated with any fitness cost that could relate to growth in either Alanine or Glucose. Further tests should be conducted observing whether other specific carbon sources have an effect on growth. Perhaps more so, observing whether the presence of iron displays differences in the growth within antibiotically-adapted populations, considering the evidence displayed from the coinfection conditions.

With regards to biofilm production with either supplement, the Paired T-tests accounting for individual differences between presence of biofilm in rich or carbon source deprived medium found significant differences at multiple timepoints. All strains appeared to display decreased biofilm formation in either of these conditions in comparison to growth in rich medium. Comparing between both growth supplements, all displayed an increased amount of biofilm produced when grown with 20% Alanine, in comparison to Glucose. Perhaps more intriguingly, the Ceftazidime/Avibactam population was found to produce peak biofilm formation at a different timepoint to all others, at 3hrs as opposed to 6hrs. To our knowledge, this is the first evidence of any difference in biofilm formation displayed by *P. aeruginosa* in this way regarding antibiotic-adapted populations. This difference, however, is only related

to the time that peak biofilm formation occurred, as with comparison to all other adapted strains, and the time of each peak, all displayed a significant difference at that point. Interestingly, however, peak biofilm formation for each strain occurred before all strains reached peak population density at 24hrs, thus this may signify that the bacteria may have undergone a morphological change in order to survive within this medium. *P. aeruginosa*, under 20% Alanine supplement conditions, have switched from a largely biofilm dependent form of colonisation to that which is free-swimming. Evidence from previous studies does suggest that this may have occurred, as *P. aeruginosa* is found to vary in biofilm density depending on the carbon source available (Shrout et al., 2006). In order to examine this further, future experimentation would be needed to examine swimming/swarming motility within either supplemented medium. A limitation, however, to note was that due to human error encountered during the study, a 24hrs timepoint analysis of biofilm formation in either case was not possible, thus it is likely that a potential spike in biofilm production alongside the population density spike as seen at 24hrs could have been missed.

Upon further review of literature in relation to biofilms, *P. aeruginosa* morphology may differ depending on the type of medium it is grown in. Under liquid conditions, PAO1 strain bacteria have been documented to form cellular aggregates during growth, where the biomass contained within these aggregates measure in size between 5-600µm (Schleheck *et al.*, 2009). This dynamic changes as the population reached a stationary phase, the biomass within these aggregates decreased in size, and the number of planktonic single cells increased (Schleheck *et al.*, 2009), in response to reduction in the amount of nutrients available. It was likely, considering that we used a method that implemented liquid-broth based medium, that the majority of bacteria that grew remained mostly in a planktonic state. This would be more so in the case of 20% Glucose supplement, rather than the 20% Alanine condition, as upon examination of the Figures, the OD600 values contained within each 20% Glucose supplement graph was lower than those values associated with 20% Alanine (Appendix 7; Appendix 8). Thus, there is suggestion that Glucose-based medium is more likely to be hostile towards overall population growth, in comparison to amino acid-based medium. Evidence relating to testing *E. coli* growth in rich vs. Glucose-based minimal medium would suggest this pattern (Tao *et. al.*, 1999). A more accurate qualitative-based method, such as the one implemented in Seneviratne *et. al.*'s (2013) method, which included both laser-diffraction and microscopy,

would allow for further analysis as to whether the reported aggregates exist in restricted growth settings.

Whilst there does not seem to be any study that relates to this where research specifically measures the level of *P. aeruginosa* biofilm within different nutrient conditions, other studies have examined these effects on other species. *Enterococcus faecalis*, a gram-positive microorganism that that is implicated as a causative species of endodontic infections (Seneviratne *et. al.*, 2013), was subject to growth within 3 different liquid media within a 96-well microtitre based method, and analysed for biofilm growth (Seneviratne *et al.*, 2013). These media, however, were all rich nutrient media, including Tryptic Soy broth, BHI broth and a modified version of Tryptic Soy broth named "pg broth" (Seneviratne *et al.*, 2013). Additions of 2% glucose supplement to such broths caused biofilms to display a much thicker biofilm, but only in relation to cell density (Seneviratne *et al.*, 2013). In relation to our study, future work would need to highlight whether the growth we have detected, albeit insignificant in the case of statistical calculations, are indeed as a result of cell density, or whether it is extracellular polysaccharide secretion.

4.6 Whole genome sequencing detected variations in SNPs as *P. aeruginosa* developed resistance to antibiotics

Whole genome sequencing of these samples was implemented as a means to provide further explanation as to whether *P. aeruginosa* samples differed in comparison to the Parent, and if so, to formulate assumptions as to whether these changes, if present, were as a result of antibiotic adaptation. Whether these affect the pathology of VAP and other nosocomial conditions would be subject to debate.

Each of the samples sequenced displayed a variety of differences in relation to the PAO1 genome. The number of SNPs detected from whole genome sequencing increased in relation to PAO1, and the levels of such were roughly similar throughout all genes identified and categorised. The most SNPs detected were in relation to transport genes, whilst the least linked to biofilm production. This includes comparison of each adapted strain against the Parent strain, where in most cases, there was an increase in the number of SNPs present in all carbapenem strains tested (PAM15 and PAD15) and PACe8. In the case of both Ceftazidime/Avibactam and Colistin-adapted strains, however, the number of SNPs in

comparison to the Parent genome was not as pronounced as the other adapted strains sequenced.

The presence of SNPs can affect the functionality of genes within the bacterial genome. The mutations that arise because of this can either be synonymous or non-synonymous, with the latter form of mutation creating a potentially drastic change in the expression of a gene. Based on prior evidence within cystic fibrosis (CF) patients, SNPs within specific locis can occur at least once in 7.1% of each loci (Greipel *et al*., 2016). The proportion of synonymous to non-synonymous SNPs can differ in clinical isolates, with convergent mutations independent from the strain background being 80% synonymous, and 20% nonsynonymous (Muthukumarasamy *et al*., 2020). This would suggest, based on the use of a clinical isolate in our study, that many SNPs that were detected were synonymous, and would potentially not result in a drastic change in phenotypic expression.

From whole genome sequencing, several genes were identified to have had SNPs present within them. One set of genes that was found have had a prolific number of SNPs was the OprD gene subset. OprD is a porin that is expressed by *P. aeruginosa*, which expedites compounds in relation to metabolism and nutrient uptake (Tamber *et al*., 2006). SNPs that are associated with deletions within the OprD subset are associated with increased antibiotic resistance, in particularly those associated with OprD_2 and OprD_3 (Chevalier *et al*., 2007, 2017). These two domains have been intensively studied, and are associated with resistance to a wide spectrum of antibiotics, including carbapenems, β-lactams, and tetracyclines (Chevalier *et al*., 2017; Pirnay *et al*., 2002). Whilst OprD_2 was not detected from the analysis, the Parent strain of *P. aeruginosa*, alongside each of the adapted strains that were sequenced, were found to have had 22-23 SNPs in the OprD_3 gene in comparison to the PAO1 reference gene. Whilst further work is needed to clarify whether these SNPs resulted in a deletion within the OprD_3 domain, it is possible that the resistance that was encountered during experimentation was due to these mutations within the gene. Interestingly, however, when comparing all the sequenced adapted strains against the Parent genome, no further SNP mutations were detected within the OprD_3 domain. Considering that the bacteria developed resistance, as opposed to already being resistant to each antibiotic before experimental exposure, it is unlikely that the SNPs that were detected within the OprD_3 domain resulted in resistance. Alongside this, since the OprD_2 domain was not detected from whole genome

sequence analysis, it is difficult to associate any antibiotic resistance that occurred to this. Intriguingly, however, one domain where further changes to the genome were detected in contrast the un-adapted Parent strain was within OprD_5. Both PAM15 and PAD15 carbapenem stains, and PACe8 were found to have had 4-5 SNPs detected in comparison to the Parent in this domain, indicating that this occurred whilst undergoing experimentation. OprD_5 has been associated with an entirely opposite effect, with deletions occurring due to the presence of SNPs resulting in increased susceptibility to antibiotics, including carbapenems, chloramphenicol and β-lactams (Li *et al*., 2012). Considering the implications from this, and the evidence from the adaptation experiments, it was likely that the SNPs that occurred here did not result in a deleterious effect to OprD, and instead may have resulted in a mutation that conferred resistance. This could potentially mean that the mutations that occurred in this domain would be synonymous or silent, as the potential impact that a nonsynonymous mutation would lead to conformational change in the phenotype. There is, however, a contrasting explanation for this, as the mutations that occurred within the OprD_5 domain could have nonsynonymous, conveying a change to the phenotype. Considering that both PACeA15 and PACo30 did not also display SNPs in this loci, however, this conclusion is perhaps unlikely. More evidence is needed to fully conclude whether SNPs in this region resulted in changes to the OprD phenotype overall.

Other genes that appeared to indicate several polymorphisms in comparison to PAO1 was the nicP subset of genes. These genes correspond to a porin-like protein, however, to our knowledge, there is no literature at the time of study that highlighted mutations to this gene associated with antibiotic resistance. Considering this, and further evidence that this could have also been influenced by adaptation, based on evidence that all sequenced strains, apart from PACeA15, had SNPs present in relation to the Parent strain. Once more, further work would be needed to elucidate whether these genes play a key role in the acquisition of antibiotic resistance.

Because biofilm production-related genes contained the least number of SNPs, it is likely to explain why there was little significant data in relation to biofilm formation when comparing the Parent to adapted strains. Observing the individual genes that were detected, however, there was no clear indicative mutation that may have related to why PACeA15 produced the least amount of biofilm overall. There was, however, one gene of interest which, in theory,

may explain the potential reduction in biofilm, though this same gene also indicated the presence of a SNP within the Colistin-adapted population. bdlA (Biofilm dispersion locus A) is a protein that is associated with the dispersion of biofilms (Li *et al.,* 2014). Depending upon the type of infections, mutations that confer inactivation of this protein can reduce dispersal and overall virulence within an acute infection setting. Under chronic conditions, this inactivation produces a contrasting effect, allowing *P. aeruginosa* to persist within the lungs, based on evidence from a murine pneumonia model (Li *et al*., 2014). This impairment of dispersion allows the bacteria to accumulate biofilm biomass within the area they persist within, which could explain why chronic VAP infections are more difficult to treat. Species, such as *P. aeruginosa*, are associated with chronic VAP cases, and thus may explain part of the reason. This, however, could not explain PACeA15, as it produced the least amount of biofilm in comparison to all other strains. Overall, with the genetic evidence present, the mutations that were detected were perhaps unlikely to affect the overall production of biofilm, without further genetic analysis. Thus, it is more likely that the non-significance may apply to investigations in other areas, such as implementing designs that test the metabolic efficiency of these bacterial strains. As highlighted with both rich media and limited media experiment discussions, the ability of bacteria to collect and metabolise key nutrients plays a key role in both growth (Nucleo *et al.*, 2009) and biofilm production (Seneviratne *et al.*, 2013). Whether any of these SNPs play a role in the ability of each strain's metabolic activity should be investigated further in future through both *in vitro* and transcriptomic experimental studies. Previous studies have identified the role of non-synonymous SNPs playing a role in modifying biofilm formation. Structural amino acid changes in the LasR protein has been found to lead to certain strains of *P. aeruginosa* to form less biofilm (Lima *et al*., 2018). These changes can include an insertion at position 53, which corresponded to a valine amino acid, within LasR prevented the formation of a hydrogen bond, subsequently preventing biofilm formation.

Whether any of these findings were indeed related to adaptation to antibiotic resistance is perhaps debatable, as no expression data was generated as a result of whole genome sequencing. To generate such data, and to examine whether certain genes were indeed present and in what form, further investigations implementing both 16s RNA and transcriptomics would be suitable. This data would allow us to examine whether certain genes

associated with antibiotic resistance, and virulence, were active in expression or not, and to what extent, because of adaptation to each antibiotic tested. This would then allow us to compare this with studies on VAP-related MDR *P. aeruginosa* or other nosocomial cases, such as cystic fibrosis, to determine whether the same patterns of virulence factors were observed as a result of adaptation to antibiotics commonly prescribed to ICU patients. It would allow for further clarification as to whether certain genetic elements originated from other origins as a result of horizontal gene transfer or are enteric DNA elements. Horizontal gene transfer plays a key role in the spread of resistance (Colomer-Lluch *et. al.*, 2011; Potter, D'Souza, & Dantas, 2016; Schrsoeder, Brooks, & Brooks, 2017), and the means of detecting such mobile elements within clinical samples would allow researchers and clinicians to establish a means of tracing which species of bacteria are key issues when it comes to the dissemination of such elements. One such set of genes that has come to light as a key mobile element of antimicrobial resistance are *Klebsiella pneumoniae* Carbapenemases (KPCs), (Shields *et. al.*, 2017) which originate from *K. pneumoniae* strains, and have recently been isolated from *P. aeruginosa* strains in the US (Poirel *et. al.*, 2010) and elsewhere. These elements have the ability to counter recently prescribed antibiotics, such as Ceftazidime/Avibactam (Shields *et al.*, 2017) and thus cause further complications when it comes to prescribing appropriate treatment, particularly in sensitive cases such as VAP.

5 CONCLUSION

Antibiotic resistance is one of the biggest issues when it comes to medical treatment, and continues to complicate measures in combating infection. It is important to study key bacterial species that could further increase either mortality or morbidity as a result of ongoing evolution and adaptation to antimicrobials, particularly with regard to conditions where the patient is severely compromised, as is the case with VAP. In this study, we have adapted and tested a clinical strain of *P. aeruginosa*, isolated from a patient diagnosed with VAP, against several conditions, including measuring how it's growth and biofilm formation is affected when it has adapted to several key antimicrobial agents. The clinical strain adapted to all antimicrobials supplied mono-therapeutically, and whilst in most cases there was no clear evidence that these adaptations affected either growth or biofilm formation under different growth conditions, it was clear that Ceftazidime/Avibactam has an effect on the growth of *P. aeruginosa* as well as biofilm formation. Whilst the evidence gathered from the study supports this, caution should be taken in any case when applying Ceftazidime/Avibactam antibiotic therapy, as resistance towards this antibiotic was encountered under continuous application. The genetic evidence did indicate that genes related to transport and metabolism were largely affected as a result of a build up of resistance towards antibiotic, though further testing regarding expression of such factors should be conducted to understand whether these nucleotide changes result in overexpression characterised as part of resistance.

6 REFERENCES

Abdel-Gawad, T. A., El-Hodhod, M. A., Ibrahim, H. M., & Michael, Y. W. (2009). Gastroesophageal reflux in mechanically ventilated pediatric patients and its relation to ventilator-associated pneumonia. *Critical Care*, *13*(5), 1–5. https://doi.org/10.1186/cc8134

Abdelrazik Othman, A., & Salah Abdelazim, M. (2017). Ventilator-associated pneumonia in adult intensive care unit prevalence and complications. *The Egyptian Journal of Critical Care Medicine*, *5*(2), 61–63. https://doi.org/10.1016/j.ejccm.2017.06.001

Ali, H. S., Khan, F. Y., George, S., Shaikh, N., & Al-Ajmi, J. (2016). Epidemiology and outcome of ventilator-associated pneumonia in a heterogeneous ICU population in Qatar. *BioMed Research International*, *2016*(December 2012). https://doi.org/10.1155/2016/8231787

Alp, E., Cookson, B., Erdem, H., Rello, J., & Group, S. (2019). Infection control bundles in intensive care : an international cross-sectional survey in low- and middle-income countries. *Journal of Hospital Infection*, *101*, 248–256. https://doi.org/10.1016/j.jhin.2018.07.022

Amini, S., Hottes, A. K., Smith, L. E., & Tavazoie, S. (2011). Fitness landscape of antibiotic tolerance in pseudomonas aeruginosa biofilms. *PLoS Pathogens*, *7*(10). https://doi.org/10.1371/journal.ppat.1002298

Aminov, R. (2017). History of antimicrobial drug discovery: Major classes and health impact. *Biochemical Pharmacology*, *133*, 4–19. https://doi.org/10.1016/j.bcp.2016.10.001

Aminov, R. (2010). A brief history of the antibiotic era: Lessons learned and challenges for the future. *Frontiers in Microbiology*, *1*, 1–7. https://doi.org/10.3389/fmicb.2010.00134

Baltrus, D. A. (2013). Exploring the costs of horizontal gene transfer. *Trends in Ecology and Evolution*, *28*(8), 489–495. https://doi.org/10.1016/j.tree.2013.04.002

Barker, K. D., Barkovits, K., & Wilks, A. (2012). Metabolic Flux of Extracellular Heme Uptake in Pseudomonas aeruginosa Is Driven by the Iron-regulated Heme Oxygenase. *The Journal of Biological Chemistry*, *287*(22), 18342–18350. https://doi.org/10.1074/jbc.M112.359265

Barnabie, P. M., & Whiteley, M. (2015). Iron-Mediated Control of Pseudomonas aeruginosa-Staphylococcus aureus Interactions in the Cystic Fibrosis Lung. *Journal of Bacteriology*, *197*(14), 2250–2251. https://doi.org/10.1128/JB.00303-15

Baron, S. A., Diene, S. M., & Rolain, J. M. (2018). Human microbiomes and antibiotic resistance. *Human Microbiome Journal*, *10*(November), 43–52. https://doi.org/10.1016/j.humic.2018.08.005

Bashir, M. E. H., Louie, S., Shi, H. N., & Nagler-Anderson, C. (2004). Toll-Like Receptor 4 Signaling by Intestinal Microbes Influences Susceptibility to Food Allergy. *The Journal of Immunology*, *172*(11), 6978–6987. https://doi.org/10.4049/jimmunol.172.11.6978

Bekaert, M., Timsit, J. F., Vansteelandt, S., Depuydt, P., Vésin, A., Garrouste-Orgeas, M.,

Decruyenaere, J., Clec'h, C., Azoulay, E., & Benoit, D. (2011). Attributable mortality of ventilator-associated pneumonia: A reappraisal using causal analysis. *American Journal of Respiratory and Critical Care Medicine*, *184*(10), 1133–1139. https://doi.org/10.1164/rccm.201105-0867OC

Bennett, P. M. (2008). Plasmid encoded antibiotic resistance: Acquisition and transfer of antibiotic resistance genes in bacteria. *British Journal of Pharmacology*, *153*(SUPPL. 1), 347–357. https://doi.org/10.1038/sj.bjp.0707607

Beuscart, J. B., Genin, M., Dupont, C., Verloop, D., Duhamel, A., Defebvre, M. M., & Puisieux, F. (2017). Potentially inappropriate medication prescribing is associated with socioeconomic factors: A spatial analysis in the French Nord-Pas-de-Calais Region. *Age and Ageing*, *46*(4), 607–613. https://doi.org/10.1093/ageing/afw245

Bhagirath, A. Y., Li, Y., Somayajula, D., Dadashi, M., Badr, S., & Duan, K. (2016). Cystic fibrosis lung environment and Pseudomonas aeruginosa infection. *BMC Pulmonary Medicine*, *16*(174), 1–22. https://doi.org/10.1186/s12890-016-0339-5

Bisgaard, H., Hermansen, M., & Buchvald, F. (2007). Childhood Asthma after Bacterial Colonization of the Airway in Neonates Childhood Asthma after Bacterial Colonization of the Airway in Neonates. *New England Journal of Medicine*, *357*(15), 1487–1495. https://doi.org/10.1056/NEJMoa052632

Boissy, R., Ahmed, A., Janto, B., Earl, J., Hall, B. G., Hogg, J. S., Pusch, G. D., Hiller, L. N., Powell, E., Hayes, J., Yu, S., Kathju, S., Stoodley, P., Post, J. C., Ehrlich, G. D., & Hu, F. Z. (2011). Comparative supragenomic analyses among the pathogens Staphylococcus aureus, Streptococcus pneumoniae, and Haemophilus influenzae Using a modification of the finite supragenome model. *BMC Genomics*, *12*(187). https://doi.org/10.1186/1471-2164-12-187

Bonten, M. J. M., Kollef, M. H., & Hall, J. B. (2004). Risk Factors for Ventilator-Associated Pneumonia: From Epidemiology to Patient Management. *Clinical Infectious Diseases*, *38*(8), 1141–1149. https://doi.org/10.1086/383039

Botelho, J., Grosso, F., & Peixe, L. (2019). Antibiotic resistance in Pseudomonas aeruginosa – mechanisms, epidemiology and evolution. *Drug Resistance Updates*, *44*, 100640. https://doi.org/10.1016/j.drup.2019.07.002

Bouza, E., Brun-Buisson, C., Chastre, J., Ewig, S., Fagon, J.-Y., Marquette, C. H., Munoz, P., Niederman, M. S., Papazian, L., Rello, J., Rouby, J.-J., Van-Saene, H., & Welte, T. (2001). Ventilator-associated pneumonia. *European Respiratory Journal*, *17*(5), 1034–1045.

Bowen, W. H., Burne, R. A., Wu, H., & Koo, H. (2018). Oral Biofilms: Pathogens, Matrix, and Polymicrobial Interactions in Microenvironments. *Trends in Microbiology*, *26*(3), 229–242. https://doi.org/10.1016/j.tim.2017.09.008

Browne, E., Hellyer, T. P., Baudouin, S. V, Conway Morris, A., Linnett, V., McAuley, D. F., Perkins, G. D., & Simpson, A. J. (2014). A national survey of the diagnosis and management of suspected ventilator-associated pneumonia. *BMJ Open Respiratory Research*, *1*(1), e000066. https://doi.org/10.1136/bmjresp-2014-000066

Brusselaers, N., Shrestha, S., van de Wijgert, J., & Verstraelen, H. (2019). Vaginal dysbiosis

and the risk of human papillomavirus and cervical cancer: systematic review and meta-analysis. *The American Journal of Obstetrics & Gynecology*, *221*(1), 9-18.e8. https://doi.org/10.1016/j.ajog.2018.12.011

Budzikiewicz, H., Schäfer, M., Fernández, D. U., Matthijs, S., & Cornelis, P. (2007). Characterization of the chromophores of pyoverdins and related siderophores by electrospray tandem mass spectrometry. *BioMetals*, *20*(2), 135–144. https://doi.org/10.1007/s10534-006-9021-3

Cassat, J. E., & Skaar, E. P. (2012). Metal ion acquisition in Staphylococcus aureus : overcoming nutritional immunity. *Seminars in Immunopathology*, *34*, 215–235. https://doi.org/10.1007/s00281-011-0294-4

Castanheira, M., Deshpande, L. M., Costello, A., Davies, T. A., & Jones, R. N. (2014). Epidemiology and carbapenem resistance mechanisms of carbapenem-non-susceptible pseudomonas aeruginosa collected during 2009-11 in 14 european and mediterranean countries. *Journal of Antimicrobial Chemotherapy*, *69*(7), 1804–1814. https://doi.org/10.1093/jac/dku048

Chandler, C. E., Horspool, A. M., Hill, P. J., Wozniak, D. J., Schertzer, J. W., Rasko, D. A., & Ernst, R. K. (2019). Genomic and Phenotypic Diversity among Ten Laboratory Isolates of Pseudomonas aeruginosa PAO1. *Journal of Bacteriology*, *201*, e00595-18. https://doi.org/10.1128/JB.00595-18

Chastre, J., & Fagon, J.-Y. (2002). Ventilator-associated Pneumonia. *American Journal of Respiratory and Critical Care Medicine*, *165*(7), 867–903. https://doi.org/10.1164/ajrccm.165.7.2105078

Chatterjee, M., Anju, C. P., Biswas, L., Anil Kumar, V., Gopi Mohan, C., & Biswas, R. (2016). Antibiotic resistance in Pseudomonas aeruginosa and alternative therapeutic options. *International Journal of Medical Microbiology*, *306*(1), 48–58. https://doi.org/10.1016/j.ijmm.2015.11.004

Chen, S., Zhou, Y., Chen, Y., & Gu, J. (2018). fastp : an ultra-fast all-in-one FASTQ preprocessor. *Bioinformatics*, *34*, 884–890. https://doi.org/10.1093/bioinformatics/bty560

Chen, Y., & Blaser, M. J. (2008). Helicobacter pylori Colonization Is Inversely Associated with Childhood Asthma. *The Journal of Infectious Diseases*, *198*(4), 553–560. https://doi.org/10.1086/590158

Chevalier, S., Bodilis, J., Jaouen, T., Barray, S., Feuilloley, M. G. J., & Orange, N. (2007). Sequence diversity of the OprD protein of environmental Pseudomonas strains: Brief report. *Environmental Microbiology*, *9*(3), 824–835. https://doi.org/10.1111/j.1462-2920.2006.01191.x

Chevalier, S., Bouffartigues, E., Bodilis, J., Maillot, O., Lesouhaitier, O., Feuilloley, M. G. J., Orange, N., Dufour, A., & Cornelis, P. (2017). Structure, function and regulation of Pseudomonas aeruginosa porins. *FEMS Microbiology Reviews*, *41*(5), 698–722. https://doi.org/10.1093/femsre/fux020

Cilloniz, C., Martin-Loeches, I., Garcia-Vidal, C., Jose, A. S., & Torres, A. (2016). Microbial

etiology of pneumonia: Epidemiology, diagnosis and resistance patterns. *International Journal of Molecular Sciences*, *17*(12). https://doi.org/10.3390/ijms17122120

Ciofu, O., Tolker-Nielsen, T., Jensen, P. Ø., Wang, H., & Høiby, N. (2015). Antimicrobial resistance, respiratory tract infections and role of biofilms in lung infections in cystic fibrosis patients. *Advanced Drug Delivery Reviews*, *85*, 7–23. https://doi.org/10.1016/j.archoralbio.2016.10.028

Codjoe, F. S., & Donkor, E. S. (2017). Carbapenem Resistance : A Review. *Medical Sciences*, *6*(1), 1–28. https://doi.org/10.3390/medsci6010001

Colomer-Lluch, M., Imamovic, L., Jofre, J., & Muniesa, M. (2011). Bacteriophages carrying antibiotic resistance genes in fecal waste from cattle, pigs, and poultry. *Antimicrobial Agents and Chemotherapy*, *55*(10), 4908–4911. https://doi.org/10.1128/AAC.00535-11

Coussens, N. P., Molinaro, A. L., Culbertson, K. J., Peryea, T., Zahoránszky-Köhalmi, G., Hall, M. D., & Daines, D. A. (2018). Better living through chemistry: Addressing emerging antibiotic resistance. *Experimental Biology and Medicine*, *243*(6), 538–553. https://doi.org/10.1177/1535370218755659

Crandon, J. L., Luyt, C. E., Aubry, A., Chastre, J., & Nicolau, D. P. (2016). Pharmacodynamics of carbapenems for the treatment of Pseudomonas aeruginosa ventilator-associated pneumonia: associations with clinical outcome and recurrence. *The Journal of Antimicrobial Chemotherapy*, *71*(9), 2534–2537. https://doi.org/10.1093/jac/dkw200

Craven, D. E., & Hjalmarson, K. I. (2010). Ventilator-Associated Tracheobronchitis and Pneumonia: Thinking Outside the Box. *Clinical Infectious Diseases*, *51*(S1), S59–S66. https://doi.org/10.1086/653051

Cusumano, J. A., Caffrey, A. R., Daf, K. E., Luther, M. K., Lopes, V., & Laplante, K. L. (n.d.). Weak biofilm formation among carbapenem-resistant Klebsiella pneumoniae☆. *Diagnostic Microbiology and Infectious Disease*. https://doi.org/10.1016/j.diagmicrobio.2019.114877

Dalton, T., Dowd, S. E., Wolcott, R. D., Sun, Y., Watters, C., Griswold, J. A., & Rumbaugh, K. P. (2011). An In Vivo Polymicrobial Biofilm Wound Infection Model to Study Interspecies Interactions. *PLoS ONE*, *6*(11), e27317. https://doi.org/10.1371/journal.pone.0027317

Dancer, S. J. (2001). The problem with cephalosporins. *Journal of Antimicrobial Chemotherapy*, *48*(4), 463–478.

Dang, A. T., & Marsland, B. J. (2019). Microbes, metabolites, and the gut–lung axis. *Mucosal Immunology*, *December 2018*. https://doi.org/10.1038/s41385-019-0160-6

Davies, J., & Davies, D. (2010). Origins and Evolution of Antibiotic Resistance. *Microbiology and Molecular Biology Reviews*, *74*(3), 417–433. https://doi.org/10.1128/MMBR.00016-10

DeGruttola, A. K., Low, D., Mizoguchi, A., & Mizoguchi, E. (2016). Current understanding of dysbiosis in disease in human and animal models. *Inflammatory Bowel Diseases*, *22*(5), 1137–1150. https://doi.org/10.1097/MIB.0000000000000750.Current

DeLeon, S., Clinton, A., Fowler, H., Everett, J., Horswill, A. R., & Rumbaugh, P. (2014).

Synergistic Interactions of Pseudomonas aeruginosa and Staphylococcus aureus in an In Vitro Wound Model. *Infection and Immunity*, *82*(11), 4718–4728. https://doi.org/10.1128/IAI.02198-14

Denis, J. B., Lehingue, S., Pauly, V., Cassir, N., Gainnier, M., Léone, M., Daviet, F., Coiffard, B., Baron, S., Guervilly, C., Forel, J. M., Roch, A., & Papazian, L. (2019). Multidrug-resistant *Pseudomonas aeruginosa* and mortality in mechanically ventilated ICU patients. *American Journal of Infection Control*, *47*(9), 1059-1064. https://doi.org/10.1016/j.ajic.2019.02.030

Dettman, J. R., Rodrigue, N., Aaron, S. D., & Kassen, R. (2013). Evolutionary genomics of epidemic and nonepidemic strains of Pseudomonas aeruginosa. *Proceedings of the National Academy of Sciences*, *110*(52), 21065–21070. https://doi.org/10.1073/pnas.1307862110

Dickson, R. P., Erb-Downward, J. R., & Huffnagle, G. B. (2013). The Role of the Bacterial Microbiome in Lung Disease. *Expert Review of Resipiratory Medicine*, *7*(3), 245–257. https://doi.org/10.1586/ers.13.24.The

Djordjevic, Z. M., Folic, M. M., & Jankovic, S. M. (2017). Distribution and antibiotic susceptibility of pathogens isolated from adults with hospital-acquired and ventilator-associated pneumonia in intensive care unit. *Journal of Infection and Public Health*, *10*(6), 740–744. https://doi.org/10.1016/j.jiph.2016.11.016

Dodds, D. R. (2017). Antibiotic resistance: A current epilogue. *Biochemical Pharmacology*, *134*, 139–146. https://doi.org/10.1016/j.bcp.2016.12.005

Driscoll, J. A., Brody, S. L., & Kollef, M. H. (2007). The Epidemiology, Pathogenesis and Treatment of Pseudomonas aeruginosa Infections. *Drugs*, *67*(3), 351–368.

Du, H., Chen, L., Tang, Y. W., & Kreiswirth, B. N. (2016). Emergence of the mcr-1 colistin resistance gene in carbapenem-resistant Enterobacteriaceae. *The Lancet Infectious Diseases*, *16*(3), 287–288. https://doi.org/10.1016/S1473-3099(16)00056-6

Durand, G. A., Raoult, D., & Dubourg, G. (2019). Antibiotic discovery: history, methods and perspectives. *International Journal of Antimicrobial Agents*, *53*(4), 371–382. https://doi.org/10.1016/j.ijantimicag.2018.11.010

Dweba, C. C., Zishiri, O. T., & Zowalaty, M. E. El. (2018). Methicillin-resistant Staphylococcus aureus: livestock-associated, antimicrobial, and heavy metal resistance. *Infection and Drug Resistance*, *11*, 2497–2509.

ECDC. (2017). *Healthcare-associated infections acquired in intensive care units*. https://ecdc.europa.eu/en/publications-data/healthcare-associated-infections-acquired-intensive-care-units-annual (Accessed: 01/04/2020).

El-Nawawy, A., Ramadan, M. A.-F., Antonios, M. A.-M., Arafa, S. A.-F., & Hamza, E. (2019). Bacteriologic Profile and Susceptibility Pattern of Mechanically - Ventilated Pediatric Patients with Pneumonia. *Journal of Global Antimicrobial Resistance*. https://doi.org/10.1016/j.jgar.2019.01.028

Estella, A., & Álvarez-Lerma, F. (2011). Should the diagnosis of ventilator associated

pneumonia be improved ? &. *Medicina Intensiva (English Edition)*, *35*(9), 578–582. https://doi.org/10.1016/j.medine.2012.01.004

EUCAST. (2019). *Breakpoint tables for interpretation of MICs and zone diameters. Version 9.0, Valid from 01-01-19.* https://www.eucast.org/fileadmin/src/media/PDFs/EUCAST_files/Breakpoint_tables/v_9.0_Breakpoint_Tables.pdf (Retrieved 02/02/19).

Fàbregas, N., Ewig, S., Torres, A., El-ebiary, M., & Ramirez, J. (1999). *Clinical diagnosis of ventilator associated pneumonia revisited : comparative validation using immediate post-mortem lung biopsies Clinical diagnosis of ventilator associated pneumonia revisited : comparative validation using immediate post-mortem lung bi*. *September 2007*, 867–873.

Fabregas, N., Torres, A., El-Ebiary, M., Ramírez, J., Hernández, C., González, J., de la Bellacasa, J. P., de Anta, J., & Rodríguez-Roisin, R. (1996). Histopathologic and Microbiologic Aspects of Ventilator-associated Pneumonia. *Anethesiology*, *84*, 760–771.

Fair, R. J., & Tor, Y. (2014). Perspectives in Medicinal Chemistry Antibiotics and Bacterial Resistance in the 21st Century. *Perspectives in Medicinal Chemistry*, *6,* 25–64. https://doi.org/10.4137/PMC.S14459.Received

Ferreira, T. de O., Koto, R. Y., Leite, G. F. da C., Klautau, G. B., Nigro, S., Silva, C. B. da, Souza, A. P. I. da F., Mimica, M. J., Cesar, R. G., & Salles, M. J. C. (2016). Microbial investigation of biofilms recovered from endotracheal tubes using sonication in intensive care unit pediatric patients. *Brazilian Journal of Infectious Diseases*, *20*(5), 468–475. https://doi.org/10.1016/j.bjid.2016.07.003

Ferrer, M., Difrancesco, L. F., Liapikou, A., Rinaudo, M., Carbonara, M., Li Bassi, G., Gabarrus, A., & Torres, A. (2015). Polymicrobial intensive care unit-acquired pneumonia - prevalence, microbiology and outcome. *Critical Care*, *19*, 450.

Fleming, A. (1929). On antibacterial action of culture of Penicillium, with special reference to their use in isola- tion of B. influenzae. *Br J Exp Pathol*, *1923*, 226–236. https://www.ncbi.nlm.nih.gov/pmc/articles/PMC2048009/pdf/brjexppathol00255-0037.pdf

Fletcher, S. (2015). Understanding the contribution of environmental factors in the spread of antimicrobial resistance. *Environmental Health and Preventive Medicine*, *20*(4), 243–252. https://doi.org/10.1007/s12199-015-0468-0

Forsgård, R. A. (2019). Lactose digestion in humans: intestinal lactase appears to be constitutive whereas the colonic microbiome is adaptable. *The American Journal of Clinical Nutrition*, *110*(2), 273–279. https://doi.org/10.1093/ajcn/nqz104

Cystic Fibrosis Foundation (2018). *2017 PATIENT REGISTRY ANNUAL DATA REPORT*. https://www.cff.org/Research/Researcher-Resources/Patient-Registry/2017-Patient-Registry-Annual-Data-Report.pdf (Retrieved: 03/02/2019)

Fourie, & Pohl. (2019). Beyond Antagonism: The Interaction Between Candida Species and Pseudomonas aeruginosa. *Journal of Fungi*, *5*(2), 34.

https://doi.org/10.3390/jof5020034

Fourie, R., Ells, R., Swart, C. W., Sebolai, O. M., Albertyn, J., & Pohl, C. H. (2016). Candida albicans and Pseudomonas aeruginosa interaction, with focus on the role of eicosanoids. *Frontiers in Physiology*, *7,* 64. https://doi.org/10.3389/fphys.2016.00064

García-Leoni, M. E., Moreno, S., García-Garrote, F., & Cercenado, E. (2010). Ventilator-associated pneumonia in long-term ventilator-assisted individuals. *Spinal Cord*, *48*(12), 876–880. https://doi.org/10.1038/sc.2010.43

Gerrish, P. J., & García-Lerma, J. G. (2003). Mutation rate and the efficacy of antimicrobial drug treatment. *The Lancet Infectious Diseases*, *3*, 28–32.

Giard, M., Lepape, A., Allaouchiche, B., Guerin, C., Lehot, J. J., Robert, M. O., Fournier, G., Jacques, D., Chassard, D., Gueugniaud, P. Y., Artru, F., Petit, P., Robert, D., Mohammedi, I., Girard, R., Cêtre, J. C., Nicolle, M. C., Grando, J., Fabry, J., & Vanhems, P. (2008). Early- and late-onset ventilator-associated pneumonia acquired in the intensive care unit: comparison of risk factors. *Journal of Critical Care*, *23*(1), 27–33. https://doi.org/10.1016/j.jcrc.2007.08.005

Gillet, Y., Lorrot, M., Cohena, R., Hau, I., Grimprel, E., & Gras-Le Guen, C. (2017). Antibiotic treatment of skin and soft tissue infections. *Archives de Pédiatrie*, *24*(12), S30–S35. https://doi.org/10.1016/S0929-693X(17)30516-X

Gnb, M. M. D. R. (2018). *Emergence of resistance to ceftazidime-avibactam in carbapenem-resistant Enterobacteriaceae*. *June*.

Goel, V., Gupta, S., & Goel, T. (2016). Ventilator-associated pneumonia: A review of the clinically relevant challenges in diagnosis and prevention. *British Journal of Medical Practitioners*, *9*(2), a910.

Goli, H. R., Nahaei, M. R., Rezaee, M. A., & Hasani, A. (2016). Emergence of colistin resistant Pseudomonas aeruginosa at Tabriz hospitals , Iran. *Iranian Journal of Microbiology*, *8*(1), 62–69.

Golia, S., Sangeetha, K. T., & Vasudha, C. L. (2013). Microbial Profile of Early and Late Onset Ventilator Associated Pneumonia in The Intensive Care Unit of A Tertiary Care Hospital in Bangalore, India. *Journal of Clinical and Diagnostic Research*, *7*(11), 2462–2466. https://doi.org/10.7860/JCDR/2013/6344.3580

Gómez-Sanz, E., Kadlec, K., Feßler, A. T., Zarazaga, M., Torres, C., & Schwarz, S. (2013). Novel erm(T)-Carrying Multiresistance Plasmids from Porcine and Human Isolates of Methicillin-Resistant Staphylococcus aureus ST398 That Also Harbor Cadmium and Copper Resistance Determinants. *Antimicrobial Agents and Chemotherapy*, *57*(7), 3275–3282. https://doi.org/10.1128/AAC.00171-13

Goodlet, K. J., & Nailor, M. D. (2017). Necessity of carbapenem use when prescribed per infectious diseases specialists. *Diagnostic Microbiology & Infectious Disease*, *88*(1), 41–46. https://doi.org/10.1016/j.diagmicrobio.2017.02.013

Greipel, L., Fischer, S., Klockgether, J., Dorda, M., Mielke, S., Cramer, N., & Tümmler, B. (2016). Molecular Epidemiology of Mutations in Antimicrobial Resistance of

Pseudomonas aeruginosa Isolates from Airways of Cystic Fibrosis Patients. *Antimicrobial Agents and Chemotherapy*, *60*(11), 6726–6734. https://doi.org/10.1128/AAC.00724.16

Gunasekera, P., & Gratrix, A. (2016). Ventilator-associated pneumonia. *BJA Education*, *16*(6), 198–202. https://doi.org/10.1093/bjaed/mkv046

Gupta, N., Limbago, B. M., Patel, J. B., & Kallen, A. J. (2011). Carbapenem-Resistant Enterobacteriaceae: Epidemiology and Prevention. *Clinical Infectious Diseases*, *53*(1), 60–67. https://doi.org/10.1093/cid/cir202

Haas, H., Launay, E., Minodier, P., Cohen, R., & Gras-Le Guen, C. (2017). Surgical and medical antibiotic prophylaxis. *Archives de Pédiatrie*, *24*(12), S46–S51. https://doi.org/10.1016/S0929-693X(17)30519-5

Hall, S., McDermott, C., Anoopkumar-Dukie, S., McFarland, A. J., Forbes, A., Perkins, A. V., Davey, A. K., Chess-Williams, R., Kiefel, M. J., Arora, D., & Grant, G. D. (2016). Cellular effects of pyocyanin, a secreted virulence factor of Pseudomonas aeruginosa. *Toxins*, *8*(8), 1–14. https://doi.org/10.3390/toxins8080236

Hammer, N. D., & Skarr, E. P. (2011). Molecular mechanisms of Staphylococcus aureus iron acquisition. *Annual Review of Microbiology*, *65*, 129–147. https://doi.org/10.1146/annurev-micro-090110-102851.Molecular

Hao, Y., Kuang, Z., Walling, B. E., Bhatia, S., Sivaguru, M., Chen, Y., Gaskins, H. R., & Lau, G. W. (2012). Pseudomonas aeruginosa pyocyanin causes airway goblet cell hyperplasia and metaplasia and mucus hypersecretion by inactivating the transcriptional factor FoxA2. *Cellular Microbiology*, *14*(3), 401–415. https://doi.org/10.1111/j.1462-5822.2011.01727.x

Harriott, M. M., & Noverr, M. C. (2011). Importance of Candida-bacterial polymicrobial biofilms in disease. *Trends in Microbiology*, *19*(11), 557–563. https://doi.org/10.1016/j.tim.2011.07.004

Hawkes, N. (2017). Sixty seconds on . . . Zavicefta. *BMJ*, *356*(j1409), 2017. https://doi.org/10.1136/bmj.j1409

Hawkey, P. M., & Livermore, D. M. (2012). Carbapenem antibiotics for serious infections. *BMJ (Online)*, *344*(7863), 1–7. https://doi.org/10.1136/bmj.e3236

Hayes, M. V, & Orr, D. C. (1983). Mode of action of ceftazidime: affinity for the penicillin-binding proteins of Escherichia coli K12, Pseudomonas aeruginosa and Staphylococcus aureus. *Journal of Antimicrobial Chemotherapy*, *12*(2), 119–126.

He, S., Chen, B., Li, W., Yan, J., Chen, L., Wang, X., & Xiao, Y. (2014). Ventilator-associated pneumonia after cardiac surgery: A meta-analysis and systematic review. *Journal of Thoracic and Cardiovascular Surgery*, *148*(6), 3148–3155. https://doi.org/10.1016/j.jtcvs.2014.07.107

Henwood, C. J., Livermore, D. M., James, D., Warner, M., & Group, P. S. (2001). Antimicrobial susceptibility of Pseudomonas aeruginosa : results of a UK survey and evaluation of the British Society for Antimicrobial Chemotherapy disc susceptibility

test. *Journal of Antimicrobial Chemotherapy*, *47*, 789–799.

Hilty, M., Burke, C., Pedro, H., Cardenas, P., Bush, A., Bossley, C., Davies, J., Ervine, A., Poulter, L., Pachter, L., Moffatt, M. F., & Cookson, W. O. C. (2010). Disordered Microbial Communities in Asthmatic Airways. *PLoS ONE*, *5*(1), e8578. https://doi.org/10.1371/journal.pone.0008578

Høiby, N., Bjarnsholt, T., Givskov, M., Molin, S., & Ciofu, O. (2010). Antibiotic resistance of bacterial biofilms. *International Journal of Antimicrobial Agents*, *35*(4), 322–332. https://doi.org/10.1016/j.ijantimicag.2009.12.011

Holloway, B. W. (1955). Genetic recombination in Pseudomonas aeruginosa. *Journal of General Microbiology*, *13*(3), 572–581. https://doi.org/10.1099/00221287-13-3-572

Hortal, J., Giannella, M., Pérez, M. J., Barrio, J. M., Desco, M., Bouza, E., & Muñoz, P. (2009). Incidence and risk factors for ventilator-associated pneumonia after major heart surgery. *Intensive Care Medicine*, *35*(9), 1518–1525. https://doi.org/10.1007/s00134-009-1523-3

Hortal, J., Muñoz, P., Cuerpo, G., Litvan, H., Rosseel, P. M., Bouza, E., Mares, P., Eliasen, K., Michel, D., Bonato, R., Moreno, J. A., Colmenero, M., Berceruelo, A., Maruenda, A., Arribas, P., Voces, R., Borrallo, J. M., Marcos, R. C., Reyes, A., … Francioli, P. (2009). Ventilator-associated pneumonia in patients undergoing major heart surgery: An incidence study in Europe. *Critical Care*, *13*(3), 1–10. https://doi.org/10.1186/cc7896

Hotterbeekx, A., Kumar-Singh, S., Goossens, H., & Maddocks, S. (2017). In vivo and In vitro Interactions between Pseudomonas aeruginosa and Staphylococcus spp. *Frontiers in Cellular and Infection Microbiology*, *7*(106), 1–13. https://doi.org/10.3389/fcimb.2017.00106

Hu, Y.-F., Liu, C.-P., Wang, N.-Y., & Shih, S.-C. (2016). In vitro antibacterial activity of rifampicin in combination with imipenem , meropenem and doripenem against multidrug-resistant clinical isolates of Pseudomonas aeruginosa. *BMC Infectious Diseases*, *16*(444), 1–10. https://doi.org/10.1186/s12879-016-1785-7

Hunter, J. D. (2006). Ventilator associated pneumonia. *Postgraduate Medical Journal*, *82*(965), 172–178. https://doi.org/10.1136/pgmj.2005.036905

Hurley, J. C. (2019). Worldwide variation in Pseudomonas associated ventilator associated pneumonia. A meta-regression. *Journal of Critical Care*, *51*, 88–93. https://doi.org/10.1016/j.jcrc.2019.02.001

Ioanas, M., Ferrer, R., Angrill, J., Ferrer, M., & Torres, A. (2001). Microbial investigation in ventilator-associated pneumonia. *European Respiratory Journal*, *17*(1), 791–801.

Jagadevi, B. S., Shubha, D. S., Sudhindra, K. S., Sumantha, A., & Madhuri, K. R. (2018). Clinical Importance of Emerging ESKAPE Pathogens and Antimicrobial Susceptibility Profile from a Tertiary Care Centre. *International Journal of Current Microbiology and Applied Sciences*, *7*(5), 2881–2891. https://doi.org/10.20546/ijcmas.2018.705.336

Jain, A., Hopkins, K. L., Turton, J., Doumith, M., Hill, R., Loy, R., Meunier, D., Pike, R., Livermore, D. M., & Woodford, N. (2014). NDM carbapenemases in the United

Kingdom: An analysis of the first 250 cases. *Journal of Antimicrobial Chemotherapy*, *69*(7), 1777–1784. https://doi.org/10.1093/jac/dku084

Jamal, M., Ahmad, W., Andleeb, S., Jalil, F., Imran, M., Nawaz, M. A., Hussain, T., Ali, M., Rafiq, M., & Kamil, M. A. (2018). Bacterial biofilm and associated infections. *Journal of the Chinese Medical Association*, *81*(1), 7–11. https://doi.org/10.1016/j.jcma.2017.07.012

Jeukens, J., Boyle, B., Kukavica-Ibrulj, I., Ouellet, M. M., Aaron, S. D., Charette, S. J., Fothergill, J. L., Tucker, N. P., Winstanley, C., & Levesque, R. C. (2014). Comparative genomics of isolates of a Pseudomonas aeruginosa epidemic strain associated with chronic lung infections of cystic fibrosis patients. *PLoS ONE*, *9*(2), 1–15. https://doi.org/10.1371/journal.pone.0087611

Johnson, E. L., Heaver, S. L., Walters, W. A., & Ley, R. E. (2017). Microbiome and metabolic disease: revisiting the bacterial phylum Bacteroidetes. *Journal of Molecular Medicine*, *85*(1), 1–8. https://doi.org/10.1007/s00109-016-1492-2

Jones, R. N., Thornsberry, C., Neu, H. C., & Young, L. S. (1987). Implementation of the Mueller- Reference Standard Program. *The Antimicrobic Newsletter*, *4*(5), 37–46.

Joseph, N. M., Sistla, S., Dutta, T. K., Badhe, A. S., & Parija, S. C. (2010). Ventilator-associated pneumonia: a review. *European Journal of Internal Medicine*, *21*(5), 360–368. https://doi.org/10.3810/hp.2012.02.950

Kahl, B. C. (2018). *Staphylococcus aureus* and *Pseudomonas aeruginosa* Respiratory Tract Coinfection - What Can We Learn from Animal Models? *Journal of Infectious Diseases*, *217*(6), 854–856. https://doi.org/10.1093/infdis/jix624

Kalil, A. C., Metersky, M. L., Klompas, M., Muscedere, J., Sweeney, D. A., Palmer, L. B., Napolitano, L. M., O'Grady, N. P., Bartlett, J. G., Carratalà, J., El Solh, A. A., Ewig, S., Fey, P. D., File, T. M., Restrepo, M. I., Roberts, J. A., Waterer, G. W., Cruse, P., Knight, S. L., & Brozek, J. L. (2016). Management of Adults With Hospital-acquired and Ventilator-associated Pneumonia: 2016 Clinical Practice Guidelines by the Infectious Diseases Society of America and the American Thoracic Society. *Clinical Infectious Diseases*, *63*(5), e61–e111. https://doi.org/10.1093/cid/ciw353

Kapoor, G., Saigal, S., & Elongavan, A. (2017). Action and resistance mechanisms of antibiotics: A guide for clinicians. *Journal of Anaesthesiology Clinical Pharmacology*, *33*, 300–305. https://doi.org/10.4103/joacp.JOACP

Karatan, E., & Watnick, P. (2009). Signals, Regulatory Networks, and Materials That Build and Break Bacterial Biofilms. *Microbiology and Molecular Biology Reviews*, *73*(2), 310–347. https://doi.org/10.1128/MMBR.00041-08

Katayama, Y., Minami, H., Enomoto, M., Takano, T., Hayashi, S., & Lee, Y. K. (2010). Usefulness of gram staining of tracheal aspirates in initial therapy for ventilator-associated pneumonia in extremely preterm neonates. *Journal of Perinatology*, *30*(4), 270–274. https://doi.org/10.1038/jp.2009.144

Kenny, M. A., Pollock, H. M., Minshew, B. H., Casillas, E., Schoenknecht, F. D., & Al, K. E. T. (1980). Cation Components of Mueller-Hinton Agar Affecting Testing of Pseudomonas

aeruginosa Susceptibility to Gentamicin. *Antimicrobial Agents and Chemotherapy*, *17*(1), 55–62.

Khan, A., Singh, P., & Srivastava, A. (2018). Synthesis, nature and utility of universal iron chelator – Siderophore: A review. *Microbiological Research*, *212–213*, 103–111. https://doi.org/10.1016/j.micres.2017.10.012

Khan, R., Al-Dorzi, H. M., Tamim, H. M., Rishu, A. H., Balkhy, H., El-Saed, A., & Arabi, Y. M. (2016). The impact of onset time on the isolated pathogens and outcomes in ventilator associated pneumonia. *Journal of Infection and Public Health*, *9*(2), 161–171. https://doi.org/10.1016/j.jiph.2015.09.002

Klein, E. Y., Boeckel, T. P. Van, Martinez, E. M., Pant, S., Gandra, S., & Levin, S. A. (2018). Global increase and geographic convergence in antibiotic consumption between 2000 and 2015. *Proceedings of the National Academy of Sciences*, *115*(15), 3463–3470. https://doi.org/10.1073/pnas.1717295115

Klinger-Strobel, M., Stein, C., Forstner, C., & Makarewicz, O. (2017). Effects of colistin on biofilm matrices of *Escherichia coli* and *Staphylococcus aureus*. *International Journal of Antimicrobial Agents*, *49*(4), 472–479. https://doi.org/10.1016/j.ijantimicag.2017.01.005

Klinger-Strobel, M., Suesse, H., Fischer, D., & Pletz, M. W. (2016). A Novel Computerized Cell Count Algorithm for Biofilm Analysis. *PLoS ONE*, *11*(5), e0154937. https://doi.org/10.1371/journal.pone.0154937

Klockgether, J., Cramer, N., Wiehlmann, L., Davenport, C. F., & Tümmler, B. (2011). *Pseudomonas aeruginosa* genomic structure and diversity. *Frontiers in Microbiology*, *2*(JULY), 1–18. https://doi.org/10.3389/fmicb.2011.00150

Klockgether, J., Munder, A., Neugebauer, J., Davenport, C. F., Stanke, F., Larbig, K. D., Heeb, S., Schöck, U., Pohl, T. M., Wiehlmann, L., & Tümmler, B. (2010). Genome diversity of *Pseudomonas aeruginosa* PAO1 laboratory strains. *Journal of Bacteriology*, *192*(4), 1113–1121. https://doi.org/10.1128/JB.01515-09

Koenig, S. M., & Truwit, J. D. (2006). Ventilator-associated pneumonia: Diagnosis, treatment, and prevention. *Clinical Microbiology Reviews*, *19*(4), 637–657. https://doi.org/10.1128/CMR.00051-05

Koerner, R. J. (1997). Contribution of endotracheal tubes to the pathogenesis of ventilator-associated pneumonia. *Journal of Hospital Infection*, *35*(2), 83–89. https://doi.org/10.1016/S0195-6701(97)90096-7

Kohanski, M. A., Dwyer, D. J., & Collins, J. J. (2010). How antibiotics kill bacteria: from targets to networks. *Nat Rev Microbiol*, *8*(6), 423–435. https://doi.org/10.1038/nrmicro2333.How

Kolpen, M., Appeldorff, C. F., Brandt, S., Mousavi, N., Kragh, K. N., Bjarnsholt, T., Ciofu, O., Høiby, N., & Jensen, P. Ø. (2015). WS02.6 Increased bactericidal activity of colistin on *Pseudomonas aeruginosa* biofilms in anaerobic conditions. *Journal of Cystic Fibrosis*, *14*(Supplement 1), S4. https://doi.org/10.1016/S1569-1993(15)30012-6

Kottara, A., Hall, J. P. J., Harrison, E., & Brockhurst, M. A. (2018). Variable plasmid fitness effects and mobile genetic element dynamics across Pseudomonas species. *FEMS Microbiology Ecology*, *94*(1), 1–8. https://doi.org/10.1093/femsec/fix172

Koulenti, D., Song, A., Ellingboe, A., Abdul-aziz, M. H., Harris, P., Gavey, E., & Lipman, J. (2019). Infections by multidrug-resistant Gram-negative Bacteria : What's new in our arsenal and what's in the pipeline ? *International Journal of Antimicrobial Agents*, *53*(3), 211–224. https://doi.org/10.1016/j.ijantimicag.2018.10.011

Kourkouta, L., Tsaloglidou, A., Koukourikos, K., Iliadis, C., Plati, P., & Dimitriadou, A. (2018). History of Antibiotics. *Sumerianz Journal of Medical and Healthcare*, *1*(2), 51–54.

Kovach, K., Davis-Fields, M., Irie, Y., Jain, K., Doorwar, S., Vuong, K., Dhamani, N., Mohanty, K., Touhami, A., & Gordon, V. D. (2017). Evolutionary adaptations of biofilms infecting cystic fibrosis lungs promote mechanical toughness by adjusting polysaccharide production. *Npj Biofilms and Microbiomes*, *3*(1), 0–1. https://doi.org/10.1038/s41522-016-0007-9

Kung, V. L., Ozer, E. A., & Hauser, A. R. (2010). The Accessory Genome of *Pseudomonas aeruginosa*. *Microbiology and Molecular Biology Reviews*, *74*(4), 621–641. https://doi.org/10.1128/mmbr.00027-10

Lahiri, S. D., Johnstone, M. R., Ross, P. L., Mclaughlin, R. E., Olivier, N. B., & Alm, R. A. (2014). Avibactam and Class C β-Lactamases: Mechanism of Inhibition, Conservation of the Binding Pocket, and Implications for Resistance. *Antimicrobial Agents and Chemotherapy*, *58*(10), 5704–5713. https://doi.org/10.1128/AAC.03057-14

Lambert, P. A. (2002). Mechanism of antibiotic resistance in *Pseudomonas aeruginosa*. *J R Soc Med*, *95*(41), S22-26.

Landman, D., Bratu, S., Alam, M., & Quale, J. (2005). Citywide emergence of Pseudomonas aeruginosa strains. *Journal of Antimicrobial Chemotherapy*, *55*, 954–957. https://doi.org/10.1093/jac/dki153

Lederberg, J. (1955). *Mechanism of Action of Penicillin*. *73*(1), 144–144. https://www.ncbi.nlm.nih.gov/pmc/articles/PMC289761/pdf/jbacter00519-0162.pdf

Lee, H. (2013). Procalcitonin as a biomarker of infectious diseases. *Korean Journal of Internal Medicine*, *28*(3), 285–291. https://doi.org/10.3904/kjim.2013.28.3.285

Leidal, K. G., Munson, K. L., & Denning, G. M. (2001). Small molecular weight secretory factors from Pseudomonas aeruginosa have opposite effects on IL-8 and RANTES expression by human airway epithelial cells. *American Journal of Respiratory Cell and Molecular Biology*, *25*(2), 186–195. https://doi.org/10.1165/ajrcmb.25.2.4273

Levy, S. B., & Bonnie, M. (2004). Antibacterial resistance worldwide: Causes, challenges and responses. *Nature Medicine*, *10*(12S), S122–S129. https://doi.org/10.1038/nm1145

Li, B., Qiu, Y., Song, Y., Lin, H., & Yin, H. (2019). Dissecting horizontal and vertical gene transfer of antibiotic resistance plasmid in bacterial community using micro fluidics. *Environment International*, *131*, 105007. https://doi.org/10.1016/j.envint.2019.105007

Li, H., Luo, Y.-F., Williams, B. J., Blackwell, T. S., & Xie, C.-M. (2012). Structure and function of OprD protein in *Pseudomonas aeruginosa*: From antibiotic resistance to novel therapies. *International Journal of Medical Microbiology*, *302*(2), 63–68. https://doi.org/10.1016/j.ijmm.2011.10.001.

Li, Y., Petrova, O. E., Su, S., Lau, G. W., Panmanee, W., Na, R., Hassett, D. J., Davies, D. G., & Sauer, K. (2014). BdlA, DipA and Induced Dispersion Contribute to Acute Virulence and Chronic Persistence of *Pseudomonas aeruginosa*. *PLoS Pathogens*, *10*(6), e1004168. https://doi.org/10.1371/journal.ppat.1004168

Lima, J. L. da C., Alves, L. R., Jacomé, P. R. L. de A., Bezerra Neto, J. P., Maciel, M. A. V., & Morais, M. M. C. de. (2018). Biofilm production by clinical isolates of *Pseudomonas aeruginosa* and structural changes in LasR protein of isolates non biofilm-producing. *Brazilian Journal of Infectious Diseases*, *22*(2), 129–136. https://doi.org/10.1016/j.bjid.2018.03.003

Limoli, D H, Yang, J., Khansaheb, M. K., Helfman, B., & Peng, L. (2016). *Staphylococcus aureus* and *Pseudomonas aeruginosa* co-infection is associated with cystic fibrosis-related diabetes and poor clinical outcomes. *European Journal of Clinical Microbiology & Infectious Diseases*, 947–953. https://doi.org/10.1007/s10096-016-2621-0

Limoli, Dominique Hope, & Hoffman, L. R. (2019). Help, hinder, hide and harm: What can we learn from the interactions between *Pseudomonas aeruginosa* and *Staphylococcus aureus* during respiratory infections. *Thorax*, *74*(7), 684–692. https://doi.org/10.1136/thoraxjnl-2018-212616

Lin, L., Xie, F., Sun, D., Liu, J., Zhu, W., & Mao, S. (2019). Ruminal microbiome-host crosstalk stimulates the development of the ruminal epithelium in a lamb model. *Microbiome*, *7*(83).

Lister, P. D., Wolter, D. J., & Hanson, N. D. (2009). Antibacterial-resistant Pseudomonas aeruginosa: Clinical impact and complex regulation of chromosomally encoded resistance mechanisms. *Clinical Microbiology Reviews*, *22*(4), 582–610. https://doi.org/10.1128/CMR.00040-09

Livermore, D. M., Hopkins, K. L., Doumith, M., Hill, R., Pike, R., Staves, P., & Woodford, N. (2018). Activity of ceftazidime/avibactam against problem Enterobacteriaceae and *Pseudomonas aeruginosa* in the UK, 2015–16. *Journal of Antimicrobial Chemotherapy*, *73*, 648–657. https://doi.org/10.1093/jac/dkx438

Llor, C., & Bjerrum, L. (2014). Antimicrobial resistance: Risk associated with antibiotic overuse and initiatives to reduce the problem. *Therapeutic Advances in Drug Safety*, *5*(6), 229–241. https://doi.org/10.1177/2042098614554919

Long, H., Miller, S. F., Strauss, C., Zhao, C., Cheng, L., Ye, Z., & Griffin, K. (2016). Antibiotic treatment enhances the genome-wide mutation rate of target cells. *PNAS*, E2498–E2505. https://doi.org/10.1073/pnas.1601208113

Look, D. C., Stoll, L. L., Romig, S. A., Humlicek, A., Britigan, B. E., & Denning, G. M. (2005). Pyocyanin and its precursor phenazine-1-carboxylic acid increase IL-8 and intercellular adhesion molecule-1 expression in human airway epithelial cells by oxidant-dependent

mechanisms. *J Immunol*, *175*(6), 4017–4023. https://doi.org/10.4049/jimmunol.175.6.4017

López-Causapé, C., Cabot, G., del Barrio-Tofiño, E., & Oliver, A. (2018). The versatile mutational resistome of *Pseudomonas aeruginosa*. *Frontiers in Microbiology*, *9*, 1–9. https://doi.org/10.3389/fmicb.2018.00685

Lorente, L., Blot, S., & Rello, J. (2007). Evidence on measures for the prevention of ventilator-associated pneumonia. *European Respiratory Journal*, *30*(6), 1193–1207. https://doi.org/10.1183/09031936.00048507

Lu, Q., Eggimann, P., Luyt, C.-E., Wolff, M., Tamm, M., François, B., Mercier, E., Garbino, J., Laterre, P.-F., Koch, H., Gafner, V., Rudolf, M. P., Mus, E., Perez, A., Lazar, H., Chastre, J., & Rouby, J.-J. (2014). *Pseudomonas aeruginosa* serotypes in nosocomial pneumonia: prevalence and clinical outcomes. *Critical Care*, *18*(1), R17. https://doi.org/10.1186/cc13697

Luyt, C.-E., Bréchot, N., Trouillet, J.-L., & Chastre, J. (2014). Antibiotic stewardship in the intensive care unit. *Critical Care*, *18*, 480.

Ma, L., Conover, M., Lu, H., Parsek, M. R., Bayles, K., & Wozniak, D. J. (2009). Assembly and Development of the *Pseudomonas aeruginosa* Biofilm Matrix. *PLoS Pathogens*, *5*(3), e1000354. https://doi.org/10.1371/journal.ppat.1000354

Marquette, C. H., Wallet, F., Nevière, R., Copin, M.-C., Saulnier, F., & Drault, J. N. (1994). Diagnostic value of direct examination of the protected specimen brush in ventilator-associated pneumonia. *European Respiratory Journal*, *7*, 105–113. https://doi.org/10.1183/09031936.94.07010105

Mashburn, L. M., Jett, A. M., Akins, D. R., & Whiteley, M. (2005). *Staphylococcus aureus* Serves as an Iron Source for *Pseudomonas aeruginosa* during In Vivo Coculture. *Journal of Bacteriology*, *187*(2), 554–566. https://doi.org/10.1128/JB.187.2.554

Mattei, A. S., Alves, S. H., Severo, C. B., & Guazzelli, S. (2014). Use of Mueller-Hinton Broth and Agar in the Germ Tube Test. *Revista Do Instituto de Medicina Tropical de São Paulo*, *56*(6), 483–485. https://doi.org/10.1590/S0036-46652014000600005

Melnyk, A. H., Wong, A., & Kassen, R. (2014). The fitness costs of antibiotic resistance mutations. *Evolutionary Applications*, *8*(3), 273–283. https://doi.org/10.1111/eva.12196

Merritt, J. H., Kadouri, D. E., & O'Toole, G. A. (2005). Growing and Analysing Static Biofilms. *Current Protocols in Microbiology*, *00*(1), 1–29. https://doi.org/10.1002/9780471729259.mc01b01s00.Growing

Micek, S. T., Wunderink, R. G., Kollef, M. H., Chen, C., Rello, J., Chastre, J., Antonelli, M., Welte, T., Clair, B., Ostermann, H., Calbo, E., Torres, A., Menichetti, F., Schramm, G. E., & Menon, V. (2015). An international multicenter retrospective study of *Pseudomonas aeruginosa* nosocomial pneumonia: Impact of multidrug resistance. *Critical Care*, *19*(1), 1–8. https://doi.org/10.1186/s13054-015-0926-5

Michelsen, C. F., Christensen, A. J., Bojer, S., Høiby, N., & Ingmer, H. (2014). Antibiotic

Tolerance in a Human Host-Adapted *Pseudomonas aeruginosa* Lineage. *Journal of Bacteriology*, *196*(22), 3903–3911. https://doi.org/10.1128/JB.02006-14

Miles, B. Y. A. A., & Misra, S. S. (1931). The Estimation of the Bactericidal Power of the Blood. *The Journal of Hygiene*, *38*(6), 732–749. https://doi.org/10.1017/S002217240001158X

Mölter, A., Belmonte, M., Palin, V., Mistry, C., Sperrin, M., White, A., Welfare, W., & Van Staa, T. (2018). Antibiotic prescribing patterns in general medical practices in England: Does area matter? *Health and Place*, *53*, 10–16. https://doi.org/10.1016/j.healthplace.2018.07.004

Montiel-Castro, A. J., Gonzalez-Cervantes, R. M., Bravo-Ruiseco, G., & Pacheco-Lopez, G. (2013). The microbiota–gut–brain axis: neurobehavioral correlates, health and sociality. *Frontiers in Integrative Neuroscience*, *7*(70). https://doi.org/10.3389/fnint.2013.00070

Mosca, A., Leclerc, M., & Hugot, J. P. (2016). Gut Microbiota Diversity and Human Diseases: Should We Reintroduce Key Predators in Our Ecosystem? *Frontiers in Microbiology*, *7*(455). https://doi.org/10.3389/fmicb.2016.00455

Mulcahy, L. R., Isabella, V. M., & Lewis, K. (2013). *Pseudomonas aeruginosa* biofilms in disease. *Microbial Ecology*, *68*(1), 1–12. https://doi.org/10.1007/s00248-013-0297-x

Mulcahy, M. E., & Mcloughlin, R. M. (2016). Host–Bacterial Crosstalk Determines *Staphylococcus aureus* Nasal Colonization. *Trends in Microbiology*, *24*(11), 872–886. https://doi.org/10.1016/j.tim.2016.06.012

Murray, J. L., Connell, J. L., Stacy, A., Turner, K. H., & Whiteley, M. (2014). Mechanisms of Synergy in Polymicrobial Infections. *Journal of Microbiology*, *52*(3), 188–199. https://doi.org/10.1007/s12275-014-4067-3

Muscedere, J. G., Martin, C. M., & Heyland, D. K. (2008). The impact of ventilator-associated pneumonia on the Canadian health care system. *Journal of Critical Care*, *23*(1), 5–10. https://doi.org/10.1016/j.jcrc.2007.11.012

Mustafa, M.-H., Chalhoub, H., Denis, O., Deplano, A., Vergison, A., Rodriguez-Villalobos, H., Tunney, M. M., Elborn, J. S., Kahl, B. C., Traore, H., Vanderbist, F., Tulkens, P. M., & Bambeke, F. Van. (2016). Antimicrobial susceptibility of *Pseudomonas aeruginosa* isolated from Cystic Fibrosis patients in northern Europe. *Antimicrobial Agents and Chemotherapy*, *60*(11), 6735–6741. https://doi.org/10.1128/AAC.01046-16

Muthukumarasamy, U., Preusse, M., Kordes, A., Koska, M., Schniederjans, M., Khaledi, A., & Häussler, S. (2020). Single-Nucleotide Polymorphism-Based Genetic Diversity Analysis of Clinical *Pseudomonas aeruginosa* Isolates. *Genome Biology and Evolution*, *12*(4), 396–406. https://doi.org/10.1093/gbe/evaa059

Nair, G. B., & Niederman, M. S. (2015). Ventilator-associated pneumonia: present understanding and ongoing debates. In *Intensive Care Medicine* (Vol. 41, Issue 1). https://doi.org/10.1007/s00134-014-3564-5

Nairz, M., Schroll, A., Sonnweber, T., & Weiss, G. (2010). The struggle for iron – a metal at the host – pathogen interface. *Cellular Microbiology*, *12*(12), 1691–1702.

https://doi.org/10.1111/j.1462-5822.2010.01529.x

Naylor, N. R., Atun, R., Zhu, N., Kulasabanathan, K., Silva, S., Chatterjee, A., Knight, G. M., & Robotham, J. V. (2018). Estimating the burden of antimicrobial resistance: a systematic literature review. *Antimicrobial Resistance & Infection Control*, *7*(1), 58. https://doi.org/10.1186/s13756-018-0336-y

Nelson, M. L., Dinardo, A., Hochberg, J., & Armelagos, G. J. (2010). Brief communication: Mass spectroscopic characterization of tetracycline in the skeletal remains of an ancient population from Sudanese Nubia 350-550 CE. *American Journal of Physical Anthropology*, *143*(1), 151–154. https://doi.org/10.1002/ajpa.21340

Nguyen, A. T., & Oglesby-Sherrouse, A. G. (2016). Interactions between *Pseudomonas aeruginosa* and *Staphylococcus aureus* during co-cultivations and polymicrobial infections. *Applied Microbiology and Biotechnology*, 6141–6148. https://doi.org/10.1007/s00253-016-7596-3

Niederman, M. S., Craven, D. E., Bonten, M. J., Chastre, J., Craig, W. A., Fagon, J.-Y., Hall, J., Jacoby, G. A., Kollef, M. H., Luna, C. M., Mandell, L. A., Torres, A., & Wunderink, R. G. (2005). Guidelines for the management of adults with hospital-acquired, ventilator-associated, and healthcare-associated pneumonia. *Guidelines for the Management of Adults with Hospital-Acquired, Ventilator-Associated, and Healthcare-Associated Pneumonia*, *171*(4), 388–416. https://doi.org/10.1164/rccm.200405-644ST

Nikaido, H., & Pages, J.-M. (2012). Broad Speicificity Efflux pumps and Their Role in Multidrug Resistance of Gram Negative Bacteria. *FEMS Microbiology Reviews*, *36*(2), 340–363. https://doi.org/10.1111/j.1574-6976.2011.00290.x.

Niu, C., Yu, D., Wang, Y., Ren, H., Jin, Y., Zhou, W., Li, B., Cheng, Y., Yue, J., Gao, Z., & Liang, L. (2013). Common and pathogen-specific virulence factors are different in function and structure. *Virulence*, *4*(6), 473–482. https://doi.org/10.4161/viru.25730

Nucleo, E., Steffanoni, L., Fugazza, G., Migliavacca, R., Giacobone, E., Navarra, A., Pagani, L., & Landini, P. (2009). Growth in glucose-based medium and exposure to subinhibitory concentrations of imipenem induce biofilm formation in a multidrug-resistant clinical isolate of Acinetobacter baumannii. *BMC Microbiology*, *9*(270). https://doi.org/10.1186/1471-2180-9-270

O'Neill, J. (2014). *Antimicrobial Resistance: Tackling a Crisis for the Health and Wealth of Nations, 2014*. https://doi.org/10.1038/510015a (Retrieved: 30/11/2018).

Oliveira, P. H., Touchon, M., Cury, J., & Rocha, E. P. C. (2017). The chromosomal organization of horizontal gene transfer in bacteria. *Nature Communications*, *8*(1), 1–10. https://doi.org/10.1038/s41467-017-00808-w

Palavutitotai, N., Jitmuang, A., Tongsai, S., Kiratisin, P., & Angkasekwinai, N. (2018). Epidemiology and risk factors of extensively drug-resistant Pseudomonas aeruginosa infections. *PLoS ONE*, *13*(2), 1–13. https://doi.org/10.1371/journal.pone.0193431

Papp-Wallace, K. M., Endimiani, A., Taracila, M. A., & Bonomo, R. A. (2011). Carbapenems: Past, present, and future. *Antimicrobial Agents and Chemotherapy*, *55*(11), 4943–4960. https://doi.org/10.1128/AAC.00296-11

Park, D. R. (2005). The microbiology of ventilator-associated pneumonia. *Respiratory Care*, *50*(6), 742–763.

Patil, H., & Patil, V. (2017). Incidence, bacteriology, and clinical outcome of ventilator-associated pneumonia at tertiary care hospital. *Journal of Natural Science, Biology and Medicine*, *8*(1), 46. https://doi.org/10.4103/0976-9668.198360

Pedersen, M. G., Olesen, H. V, Jensen-Fangel, S., Nørskov-Lauritsen, N., & Wang, M. (2018). Colistin resistance in *Pseudomonas aeruginosa* and *Achromobacter* spp . cultured from Danish cystic fibrosis patients is not related to plasmid--mediated expression of mcr-1. *Journal of Cystic Fibrosis*, *17*(2), e22–e23. https://doi.org/10.1016/j.jcf.2017.12.001

Pirnay, J. P., De Vos, D., Mossialos, D., Vanderkelen, A., Cornelis, P., & Zizi, M. (2002). Analysis of the *Pseudomonas aeruginosa* oprD gene from clinical and environmental isolates. *Environmental Microbiology*, *4*(12), 872–882. https://doi.org/10.1046/j.1462-2920.2002.00281.x

Poirel, L., Nordmann, P., Lagrutta, E., Cleary, T., & Munoz-Price, L. S. (2010). Emergence of KPC-Producing *Pseudomonas aeruginosa* in the United States. *Antimicrobial Agents and Chemotherapy*, *54*(7), 33136. https://doi.org/10.1128/AAC.00513-10

Pollock, H. M., Minshew, B. H., Kenny, M. A., & Fritz, D. (1978). Effect of Different Lots of Mueller-Hinton Agar on the Interpretation of the Gentamicin Susceptibility of *Pseudomonas aeruginosa*. *Antimicrobial Agents and Chemotherapy*, *14*(3), 360–367.

Pompilio, A., Crocetta, V., Pomponio, S., Fiscarelli, E., & Di Bonaventura, G. (2015). In vitro activity of colistin against biofilm by *Pseudomonas aeruginosa* is significantly improved under “cystic fibrosis – like” physicochemical conditions. *Diagnostic Microbiology & Infectious Disease*, *82*(4), 318–325. https://doi.org/10.1016/j.diagmicrobio.2015.01.006

Potter, R. F., D’Souza, A. W., & Dantas, G. (2016). The rapid spread of carbapenem-resistant Enterobacteriaceae. *Drug Resistance Updates*, *29*, 30–46. https://doi.org/10.1016/j.drup.2016.09.002

Public Health England. (2018). English surveillance programme for antimicrobial utilisation and resistance (ESPAUR) Report 2018. https://doi.org/2014362

Ramírez-Estrada, S., Borgatta, B., & Rello, J. (2016). Pseudomonas aeruginosa ventilator-associated pneumonia management. *Infection and Drug Resistance*, *9*, 7–18. https://doi.org/10.2147/IDR.S50669

Rankin, D. J., McGinty, S. E., Nogueira, T., Touchon, M., Taddei, F., Rocha, E. P. C., & Brown, S. P. (2011). Bacterial cooperation controlled by mobile elements: Kin selection and infectivity are part of the same process. *Heredity*, *107*(3), 279–281. https://doi.org/10.1038/hdy.2011.59

Rasamiravaka, T., Labtani, Q., Duez, P., & El Jaziri, M. (2015). The Formation of Biofilms by *Pseudomonas aeruginosa* : A Review of the Natural and Synthetic Compounds Interfering with Control Mechanisms. *BioMed Research International*, *2015*, 1–17. https://doi.org/10.1155/2015/759348

Rello, J., & Bunsow, E. (2016). What is the Research Agenda in Ventilator-associated

Pneumonia? *International Journal of Infectious Diseases*, *51*, 110–112. https://doi.org/10.1016/j.ijid.2016.09.019

Restrepo, M. I., Peterson, J., Fernandez, J. F., Qin, Z., Fisher, A. C., & Nicholson, S. C. (2013). Comparison of the bacterial etiology of early-onset and late-onset ventilator-associated pneumonia in subjects enrolled in 2 large clinical studies. *Respiratory Care*, *58*(7), 1220–1225. https://doi.org/10.4187/respcare.02173

Rhodes, N. J., Cruce, C. E., O'Donnell, J. N., Wunderink, R. G., & Hauser, A. R. (2019). Resistance trends and treatment options in Gram-negative ventilator-associated pneumonia. *Current Infectious Disease Reports*, *20*(2), 3. https://doi.org/10.1007/s11908-018-0609-x.Resistance

Rimek, D., Fehse, B., & Go, P. (2007). Evaluation of Mueller-Hinton-agar as a simple medium for the germ tube production of *Candida albicans* and *Candida dubliniensis*. *Mycoses*, *51*, 205–208. https://doi.org/10.1111/j.1439-0507.2007.01469.x

Rodloff, A. C., Goldstein, E. J. C., & Torres, A. (2006). Two decades of imipenem therapy. *Journal of Antimicrobial Chemotherapy*, *58*, 916–929. https://doi.org/10.1093/jac/dkl354

Rodrigues, M. E., Lopes, S. P., Pereira, C. R., Azevedo, N. F., Lourenï¿½o, A., Henriques, M., & Pereira, M. O. (2017). Polymicrobial ventilator-associated pneumonia: Fighting in vitro *Candida albicans-Pseudomonas aeruginosa* biofilms with antifungal-antibacterial combination therapy. *PLoS ONE*, *12*(1), 1–19. https://doi.org/10.1371/journal.pone.0170433

Rosa, C. P., Brancaglion, G. A., Miyauchi-Tavares, T. M., Corsetti, P. P., & de Almeida, L. A. (2018). Antibiotic-induced dysbiosis effects on the murine gastrointestinal tract and their systemic repercussions. *Life Sciences*, *207*, 480–491. https://doi.org/10.1016/j.lfs.2018.06.030

Rosenthal, Victor D., Maki, D. G., Jamulitrat, S., Medeiros, E. A., Todi, S. K., Gomez, D. Y., Leblebicioglu, H., Abu Khader, I., Miranda Novales, M. G., Berba, R., Ramírez Wong, F. M., Barkat, A., Pino, O. R., Dueñas, L., Mitrev, Z., Bijie, H., Gurskis, V., Kanj, S. S., Mapp, T., … Guzmán Siritt, M. E. (2010). International Nosocomial Infection Control Consortium (INICC) report, data summary for 2003-2008, issued June 2009. *American Journal of Infection Control*, *38*(2). https://doi.org/10.1016/j.ajic.2009.12.004

Rosenthal, Victor Daniel. (2016). International Nosocomial Infection Control Consortium (INICC) resources: INICC multidimensional approach and INICC surveillance online system. *American Journal of Infection Control*, *44*(6), e81–e90. https://doi.org/10.1016/j.ajic.2016.01.005

San Millan, A., Toll-Riera, M., Escudero, J. A., Cantón, R., Coque, T. M., & Craig MacLean, R. (2015). Sequencing of plasmids pAMBL1 and pAMBL2 from *Pseudomonas aeruginosa* reveals a blaVIM-1 amplification causing high-level carbapenem resistance. *Journal of Antimicrobial Chemotherapy*, *70*(11), 3000–3003. https://doi.org/10.1093/jac/dkv222

San Millan, A., Toll-Riera, M., Qi, Q., Betts, A., Hopkinson, R. J., McCullagh, J., & MacLean, R. C. (2018). Integrative analysis of fitness and metabolic effects of plasmids in

Pseudomonas aeruginosa PAO1. *ISME Journal*, *12*(12), 3014–3024. https://doi.org/10.1038/s41396-018-0224-8

Santajit, S., & Indrawattana, N. (2016). Mechanisms of Antimicrobial Resistance in ESKAPE Pathogens. *BioMed Research International*, *2016*, 1–8. https://doi.org/10.1155/2016/2475067

Saunders, J. R., & Grinsted, J. (1972). Properties of RP4, an R factor which originated in *Pseudomonas aeruginosa* S8. *Journal of Bacteriology*, *112*(2), 690–696.

Schalk, I. J., & Guillon, L. (2013). Pyoverdine biosynthesis and secretion in *Pseudomonas aeruginosa*: Implications for metal homeostasis. *Environmental Microbiology*, *15*(6), 1661–1673. https://doi.org/10.1111/1462-2920.12013

Schick, A., & Kassen, R. (2018). Rapid diversification of *Pseudomonas aeruginosa* in cystic fibrosis lung-like conditions . *Proceedings of the National Academy of Sciences*, *115*(42), 10714–10719. https://doi.org/10.1073/pnas.1721270115

Schleheck, D., Barraud, N., Klebensberger, J., Webb, J. S., Mcdougald, D., Rice, S. A., & Kjelleberg, S. (2009). *Pseudomonas aeruginosa* PAO1 Preferentially Grows as Aggregates in Liquid Batch Cultures and Disperses upon Starvation. *PLoS ONE*, *4*(5), e5513. https://doi.org/10.1371/journal.pone.0005513

Schroeder, M., Brooks, B. D., & Brooks, A. E. (2017). The complex relationship between virulence and antibiotic resistance. *Genes*, *8*(1). https://doi.org/10.3390/genes8010039

Seneviratne, C. J., Yip, J. W. Y., Chang, J. W. W., Zhang, C. F., & Samaranayake, L. P. (2013). Effect of culture media and nutrients on biofilm growth kinetics of laboratory and clinical strains of *Enterococcus faecalis*. *Archives of Oral Biology*, *58*(10), 1327–1334. https://doi.org/10.1016/j.archoralbio.2013.06.017

Shields, R. K., Chen, L., Cheng, S., Chavda, K. D., & Press, E. G. (2017). Emergence of Ceftazidime-Avibactam Resistance Due to Plasmid-Borne blaKPC-3 Mutations during Treatment of Carbapenem-Resistant Klebsiella pneumoniae Infections. *Antimicrobial Agents and Chemotherapy, 61*, e02097-16. https://doi.org/10.1128/AAC.02097-16

Shorr, A. F., Chan, C. M., & Zilberberg, M. D. (2011). Diagnostics and epidemiology in ventilator-associated pneumonia. *Therapeutic Advances in Respiratory Disease*, *5*(2), 121–130. https://doi.org/10.1177/1753465810390262

Shrout, J. D., Chopp, D. L., Just, C. L., Hentzer, M., Givskov, M., & Parsek, M. R. (2006). The impact of quorum sensing and swarming motility on *Pseudomonas aeruginosa* biofilm formation is nutritionally conditional. *Molecular Microbiology*, *62*(5), 1264–1277.

Shukla, S. K., & Rao, T. S. (n.d.). An Improved Crystal Violet Assay for Biofilm Quantification in 96-Well Microtitre Plate. *BioRxiv*, 100214. https://doi.org/10.1101/100214

Solh, A. A. El, Akinnusi, M. E., Wiener-Kronish, J. P., Lynch, S. V, & Pineda, L. A. (2008). Persistent Infection with Pseudomonas aeruginosa in Ventilator-associated Pneumonia. *AMERICAN JOURNAL OF RESPIRATORY AND CRITICAL CARE MEDICINE*, *178*(5), 513–519. https://doi.org/10.1164/rccm.200802-239OC

Sosa-Hernandez, O., Matías-Tellez, B., Estrada-Hernandez, A., Cureno-Diaz, M. A., & Bello-

Lopez, J. M. (2019). Incidence and costs of ventilator-associated pneumonia in the adult intensive care unit of a tertiary referral hospital in Mexico. *American Journal of Infection Control*, *47*(9), e21–e25. https://doi.org/10.1016/j.ajic.2019.02.031

Stover, C. K., Pham, X. Q., Erwin, A. L., Mizoguchi, S. D., Warrener, P., Hickey, M. J., Brinkman, F. S. L., Hufnagle, W. O., Kowalik, D. J., Lagrou, M., Garber, R. L., Goltry, L., Tolentino, E., Yuan, Y., Brody, L. L., Coulter, S. N., Folger, K. R., Kas, A., Larbig, K., … West, E. A. (2000). Complete genome sequence of Pseudomonas aeruginosa PAO1 , an opportunistic pathogen. *Nature, 406*, 959–964.

Streeter, K., & Katouli, M. (2016). *Pseudomonas aeruginosa:* A review of their Pathogenesis and Prevalence in Clinical Settings and the Environment. *Infection, Epidemiology and Medicine*, *2*(1), 25–32. https://doi.org/10.18869/modares.iem.2.1.25

Tamber, S., Ochs, M. M., & Hancock, R. E. W. (2006). Role of the Novel OprD Family of Porins in Nutrient Uptake in *Pseudomonas aeruginosa*. *Journal of Bacteriology*, *188*(1), 45–54. https://doi.org/10.1128/JB.188.1.45

Tao, H., Bausch, C., Richmond, C., Blattner, F. R., & Conway, T. (1999). Functional Genomics : Expression Analysis of Escherichia coli Growing on Minimal and Rich Media. *Journal of Bacteriology*, *181*(20), 6425–6440.

Tato, M., Coque, T. M., Baquero, F., & Cantón, R. (2010). Dispersal of carbapenemase blaVIM-1 gene associated with different Tn402 variants, mercury transposons, and conjugative plasmids in Enterobacteriaceae and *Pseudomonas aeruginosa. Antimicrobial Agents and Chemotherapy*, *54*(1), 320–327. https://doi.org/10.1128/AAC.00783-09

Taylor, P. K., Yeung, A. T. Y., & Hancock, R. E. W. (2014). Antibiotic resistance in *Pseudomonas aeruginosa* biofilms: Towards the development of novel anti-biofilm therapies. *Journal of Biotechnology*, *191*, 121–130. https://doi.org/10.1016/j.jbiotec.2014.09.003

Tedja, R., Nowacki, A., Fraser, T., Fatica, C., Griffiths, L., Gordon, S., Isada, C., & Van Duin, D. (2014). The impact of multidrug resistance on outcomes in ventilator-associated pneumonia. *American Journal of Infection Control*, *42*(5), 542–545. https://doi.org/10.1016/j.ajic.2013.12.009

Torres, A., Zhong, N., Pachl, J., Timsit, J. F., Kollef, M., Chen, Z., Song, J., Taylor, D., Laud, P. J., Stone, G. G., & Chow, J. W. (2017). Ceftazidime-avibactam versus meropenem in nosocomial pneumonia, including ventilator-associated pneumonia (REPROVE): A randomised, double-blind, phase 3 non-inferiority trial. *The Lancet Infectious Diseases*, 285–295. https://doi.org/10.1016/S1473-3099(17)30747-8

Trejo-Hernández, A., Andrade-Domínguez, A., Hernández, M., & Encarnación, S. (2014). Interspecies competition triggers virulence and mutability in *Candida albicans – Pseudomonas aeruginosa* mixed biofilms. *The ISME Journal*, *8*, 1974–1988. https://doi.org/10.1038/ismej.2014.53

Trinh, T. D., Zasowski, E. J., Claeys, K. C., Lagnf, A. M., Kidambi, S., Davis, S. L., & Rybak, M. J. (2017). Multidrug-resistant *Pseudomonas aeruginosa* lower respiratory tract infections

in the intensive care unit: Prevalence and risk factors. *Diagnostic Microbiology and Infectious Disease*, *89*(1), 61–66. https://doi.org/10.1016/j.diagmicrobio.2017.06.009

Trubiano, J. A., & Padiglione, A. A. (2015). Nosocomial infections in the intensive care unit. *Anaesthesia and Intensive Care Medicine*, *16*(12), 598–602. https://doi.org/10.1016/j.mpaic.2015.09.010

Tuon, F. F., Graf, M. E., Merlini, A., Rocha, J. L., Stallbaum, S., Arend, L. N., & Pecoit-Filho, R. (2017). Risk factors for mortality in patients with ventilator-associated pneumonia caused by carbapenem-resistant Enterobacteriaceae. *Brazilian Journal of Infectious Diseases*, *21*(1), 1–6. https://doi.org/10.1016/j.bjid.2016.09.008

Ubeda, C., & Pamer, E. G. (2012). Antibiotics, microbiota, and immune defense. *Trends in Immunology*, *33*(9), 459–466. https://doi.org/10.1016/j.it.2012.05.003.Antibiotics

Valot, B., Guyeux, C., Rolland, J. Y., Mazouzi, K., Bertrand, X., & Hocquet, D. (2015). What it takes to be a *Pseudomonas aeruginosa*? The core genome of the opportunistic pathogen updated. *PLoS ONE*, *10*(5), 1–15. https://doi.org/10.1371/journal.pone.0126468

Walkey, A. J., Reardon, C. C., Sulis, C. A., Nace, R. N., & Joyce-Brady, M. (2009). Epidemiology of Ventilator-Associated Pneumonia in a Long-Term Acute Care Hospital. *Infection Control & Hospital Epidemiology*, *30*(4), 319–324. https://doi.org/10.1086/596103

Wang, H., Jørgensen, C., Ciofu, O., Christophersen, L., Kolpen, M., Jensen, P. Ø., Song, Z., Moser, C., & Høiby, N. (2015). WS02.5 Pharmacodynamics of ceftazidime combined with beta-lactamase inhibitors in biofilm *Pseudomonas aeruginosa* in vitro. *Journal of Cystic Fibrosis*, *14*(Supplement 1), S4. https://doi.org/10.1016/S1569-1993(15)30011-4

Wang, L., Alammar, N., Singh, R., Nanavati, J., Song, Y., Chaudhary, R., & Mullin, G. E. (2019). Gut Microbial Dysbiosis in the Irritable Bowel Syndrome: A Systematic Review and Meta-Analysis of Case-Control Studies. *Journal of the Academy of Nutrition and Dietetics*. https://doi.org/10.1016/j.jand.2019.05.015

Watanabe, J., Fujiwara, R., Jima, N. S., & Ito, S. (2010). Administration of Antibiotics during Infancy Promoted the Development of Atopic Dermatitis-Like Skin Lesions in NC/Nga Mice. *Bioscience, Biotechnology and Biochemistry*, *74*(2), 358–363. https://doi.org/10.1271/bbb.90709

Weinstein, R. A., Gaynes, R., Edwards, J. R., & System, N. N. I. S. (2005). Overview of Nosocomial Infections Caused by Gram-Negative Bacilli. *Clinical Infectious Diseases*, *41*(6), 848–854.

Welch, K., Cai, Y., & Strømme, M. (2012). A Method for Quantitative Determination of Biofilm Viability. *Journal of Functional Biomaterials*, *3*(2), 418–431. https://doi.org/10.3390/jfb3020418

White, D. G., Acar, J., Anthony, F., Franklin, A., Gupta, R., Nicholls, T., Tamura, Y., Thompson, S., Threlfall, E. J., Vose, D., van Vuuren, M., Wegener, H. C., & Costarrica, M. L. (2001). Antimicrobial resistance: standardisation and harmonisation of laboratory methodologies for the detection and quantification of antimicrobial resistance. *Revue Scientifique et Technique*, *20*(3), 849–858.

WHO. (2017). *Global priority list of antibiotic-resistant bacteria to guide research, discovery, and development of new antibiotics*. https://www.who.int/medicines/publications/global-priority-list-antibiotic-resistant-bacteria/en/ (Retrieved 30/10/2018).

WHO. (2017). *Global Antimicrobial Resistance Surveillance System (GLASS) Report*. https://www.who.int/glass/resources/publications/early-implementation-report/en/ (Retrieved: 30/10/2018).

Wilkins, L. J., Monga, M., & Miller, A. W. (2019). Defining Dysbiosis for a Cluster of Chronic Diseases. *Scientific Reports*, *9*(12918). https://doi.org/10.1038/s41598-019-49452-y

Wilson, I. D., & Nicholson, J. K. (2017). Gut microbiome interactions with drug metabolism, efficacy, and toxicity. *Translational Research*, *179*, 204–222. https://doi.org/10.1016/j.trsl.2016.08.002

Winkler, M. L., Papp-Wallace, K. M., Hujer, A. M., Domitrovic, T. N., Hujer, K. M., Hurless, K. N., Tuohy, M., Hall, G., & Bonomo, R. A. (2015). Unexpected Challenges in Treating Multidrug-Resistant Gram- Negative Bacteria : Resistance to Ceftazidime-Avibactam in Archived Isolates of *Pseudomonas aeruginosa*. *Antimicrobial Agents and Chemotherapy*, *59*(2), 1020–1029. https://doi.org/10.1128/AAC.04238-14

Wistrand-Yuen, E., Knopp, M., Hjort, K., Koskiniemi, S., Berg, O. G., & Andersson, D. I. (2018). Evolution of high-level resistance during low-level antibiotic exposure. *Nature Communications*, *9*(1). https://doi.org/10.1038/s41467-018-04059-1

Woodford, N., & Ellington, M. J. (2007). The emergence of antibiotic resistance by mutation. *Clinical Microbiology and Infection*, *13*(1), 5–18. https://doi.org/10.1111/j.1469-0691.2006.01492.x

Wright, H., Bonomo, R. A., & Paterson, D. L. (2017). New agents for the treatment of infections with Gram-negative bacteria : restoring the miracle or false dawn? *Clinical Microbiology and Infection*, *23*(10), 704–712. https://doi.org/10.1016/j.cmi.2017.09.001

Zakharkina, T., Martin-Loeches, I., Matamoros, S., Povoa, P., Torres, A., Kastelijn, J. B., Hofstra, J. J., De Wever, B., De Jong, M., Schultz, M. J., Sterk, P. J., Artigas, A., & Bos, L. D. J. (2017). The dynamics of the pulmonary microbiome during mechanical ventilation in the intensive care unit and the association with occurrence of pneumonia. *Thorax*, *72*(9), 803–810. https://doi.org/10.1136/thoraxjnl-2016-209158

Zamudio, R., Hijazi, K., Joshi, C., Aitken, E., Oggioni, M. R., & Gould, I. M. (2019). Phylogenetic analysis of resistance to ceftazidime/ avibactam, ceftolozane/ tazobactam and carbapenems in piperacillin/ tazobactam-resistant *Pseudomonas aeruginosa* from cystic fibrosis patients. *International Journal of Antimicrobial Agents*, *53*(6), 774–780. https://doi.org/10.1016/j.ijantimicag.2019.02.022

Zasowski, E. J., Rybak, J. M., & Rybak, M. J. (2015). The β-Lactams Strike Back: Ceftazidime-Avibactam. *Pharmacotherapy*, *35*(8), 755–770. https://doi.org/10.1002/phar.1622.

Zhang, Y.-Z. (2015). Antibiotic stewardship programmes in intensive care units: Why, how, and where are they leading us. *World Journal of Critical Care Medicine*, *4*(1), 13.

https://doi.org/10.5492/wjccm.v4.i1.13

Zilahi, G., McMahon, M. A., Povoa, P., & Martin-Loeches, I. (2016). Duration of antibiotic therapy in the intensive care unit. *Journal of Thoracic Disease*, *8*(12), 3774–3780. https://doi.org/10.21037/jtd.2016.12.89

7 APPENDICES

Appendix 1: Table containing the average results of all strains of *P. aeruginosa* growth within MH broth medium. Note: "SD" = Standard Deviation.

Strain	PAO1	Parent	Meropenem 15	Doripenem 15	Imipenem 15	Ceftazidime 8	Ceftazidime /Avibactam 15	Colistin 30	Negative (MH)
Timepoint									
0hrs	0.023	0.027	0.019	0.018	0.022	0.020	0.016	0.022	0.004
SD 0hrs	0.011	0.002	0.001	0.001	0.005	0.002	0.001	0.001	0.002
3hrs	0.027	0.039	0.032	0.033	0.034	0.026	0.026	0.036	0.006
SD 3hrs	0.004	0.006	0.003	0.004	0.003	0.004	0.002	0.006	0.002
6hrs	0.101	0.145	0.139	0.171	0.148	0.113	0.096	0.184	0.003
SD 6hrs	0.006	0.005	0.006	0.016	0.013	0.015	0.005	0.015	0.002
12hrs	0.949	0.829	0.953	0.919	1.054	0.940	0.756	0.976	0.008
SD 12hrs	0.118	0.136	0.085	0.137	0.033	0.205	0.074	0.053	0.003
24hrs	1.706	1.949	0.978	1.413	1.169	1.283	0.789	1.287	0.006
SD 24hrs	0.274	0.467	0.076	0.069	0.147	0.173	0.044	0.069	0.004
48hrs	1.237	0.983	1.104	1.236	1.903	1.703	1.465	1.615	0.008
SD 48hrs	0.159	0.084	0.195	0.083	0.106	0.431	0.121	0.074	0.004
Calculated Growth Rate	**≥-0.04772**	**0.179782**	**≥-0.0167317**	**N/A**	**0.079676**	**≥-0.012591**	**-0.887989**	**≥-0.062528**	

Appendix 2: Table containing OD600 absorbance values in relation to Biofilm Formation with regards to the *P. aeruginosa* growth established MH broth.

Strain	PAO1	Parent	Meropenem 15	Doripenem 15	Imipenem 15	Ceftazidime 8	Ceftazidime /Avibactam 15	Colistin 30
Timepoint								
0hrs	-0.001	0.009	-0.011	0.018	0.007	-0.007	-0.026	0.034
SD 0hrs	0.027	0.026	0.003	0.010	0.023	0.004	0.017	0.024
3hrs	0.009	0.099	0.110	0.139	0.119	0.042	0.007	0.150
SD 3hrs	0.045	0.059	0.022	0.062	0.058	0.018	0.032	0.023
6hrs	0.385	0.867	0.731	1.021	1.296	0.715	0.132	0.903
SD 6hrs	0.038	0.072	0.124	0.085	0.337	0.134	0.067	0.040
12hrs	0.523	1.151	1.390	1.653	1.537	1.534	0.042	1.064
SD 12hrs	0.065	0.350	0.188	0.555	0.159	0.095	0.042	0.202
24hrs	0.380	1.210	1.112	0.638	0.721	0.814	0.171	0.563
SD 24hrs	0.151	0.349	0.285	0.253	0.252	0.092	0.110	0.329
48hrs	0.416	0.557	0.508	0.632	0.871	0.950	0.080	0.433
SD 48hrs	0.082	0.283	0.310	0.214	0.184	0.208	0.037	0.104

Appendix 3: Table containing OD600 absorbance values in relation to growth detected from the *P. aeruginosa*/*S. aureus* co-infection experiments.

Strain	PAO1	Parent	Meropenem 15	Doripenem 15	Imipenem 15	Ceftazidime 8	Ceftazidime /Avibactam 15	Colistin 30	Negative (MH)
Timepoint									
0hrs	0.013	0.014	0.012	0.014	0.012	0.012	0.011	0.016	0.003
SD 0hrs	0.002	0.001	0.002	0.003	0.001	0.001	0.001	0.004	0.001
3hrs	0.092	0.065	0.066	0.084	0.078	0.068	0.064	0.088	0.004
SD 3hrs	0.015	0.004	0.008	0.006	0.007	0.006	0.003	0.010	0.001
6hrs	0.332	0.299	0.333	0.338	0.364	0.321	0.291	0.368	0.000
SD 6hrs	0.012	0.017	0.011	0.014	0.021	0.011	0.023	0.020	0.008
12hrs	1.533	0.699	1.137	0.927	1.319	1.571	0.819	1.516	0.047
SD 12hrs	0.010	0.051	0.079	0.049	0.096	0.151	0.065	0.034	0.072
24hrs	2.490	1.689	1.822	1.109	2.375	2.939	1.129	2.033	0.255
SD 24hrs	0.317	0.444	0.335	0.022	0.244	0.372	0.251	0.244	0.352
48hrs	1.449	1.090	0.863	0.836	0.946	1.135	1.580	1.337	0.026
SD 48hrs	0.316	0.111	0.083	0.044	0.063	0.098	0.128	0.253	0.011

Appendix 4: Table containing OD600 absorbance values in relation to biofilm formation detected from the *P. aeruginosa*/*S. aureus* co-infection experiments.

Strain	PAO1	Parent	Meropenem 15	Doripenem 15	Imipenem 15	Ceftazidime 8	Ceftazidime /Avibactam 15	Colistin 30
Timepoint								
0hrs	0.146	0.125	0.118	0.121	0.125	0.150	0.136	0.112
SD 0hrs	0.018	0.012	0.030	0.023	0.001	0.006	0.008	0.015
3hrs	0.212	0.225	0.244	0.176	0.457	0.267	0.205	0.154
SD 3hrs	0.020	0.051	0.085	0.010	0.084	0.007	0.021	0.005
6hrs	0.244	0.670	0.931	1.168	0.414	0.731	0.351	0.639
SD 6hrs	0.042	0.190	0.327	0.090	0.051	0.500	0.080	0.055
12hrs	1.197	0.626	0.721	1.046	0.599	1.236	1.205	1.415
SD 12hrs	0.089	0.204	0.159	0.126	0.229	0.182	0.083	0.341
24hrs	0.114	0.046	0.029	0.013	0.033	0.123	0.024	0.227
SD 24hrs	0.029	0.032	0.013	0.023	0.021	0.049	0.013	0.031
48hrs	0.173	0.027	0.023	0.055	0.020	0.022	0.049	0.006
SD 48hrs	0.023	0.007	0.005	0.009	0.012	0.007	0.015	0.016

Appendix 5: Table containing OD600 absorbance values in relation to growth detected from *P. aeruginosa* strains within M9 Minimal Media broth with 20% Glucose.

Strain	PAO1	Parent	Meropenem 15	Doripenem 15	Imipenem 15	Ceftazidime 8	Ceftazidime /Avibactam 15	Colistin 30	Negative (MH)
Timepoint									
0hrs	0.030	0.029	0.027	0.026	0.030	0.028	0.020	0.030	0.000
SD 0hrs	0.004	0.004	0.006	0.003	0.015	0.003	0.004	0.003	0.001
3hrs	0.039	0.042	0.034	0.049	0.037	0.058	0.046	0.043	-0.003
SD 3hrs	0.008	0.005	0.005	0.010	0.005	0.023	0.006	0.005	0.006
6hrs	0.062	0.058	0.050	0.086	0.063	0.090	0.065	0.062	0.002
SD 6hrs	0.006	0.008	0.009	0.017	0.005	0.033	0.012	0.008	0.001
12hrs	0.099	0.145	0.122	0.101	0.115	0.128	0.078	0.088	-0.001
SD 12hrs	0.015	0.026	0.024	0.019	0.015	0.013	0.012	0.010	0.001
24hrs	2.486	1.777	1.909	1.125	2.289	3.017	0.966	2.025	0.255
SD 24hrs	0.387	0.482	0.336	0.027	0.156	0.429	0.108	0.220	0.418
48hrs	0.149	0.218	0.196	0.166	0.216	0.227	0.113	0.131	0.003
SD 48hrs	0.026	0.013	0.021	0.019	0.048	0.022	0.018	0.042	0.002

Appendix 6: Table containing OD600 absorbance values in relation to growth detected from *P. aeruginosa* strains within M9 Minimal Media broth with 20% Alanine supplement.

Strain	PAO1	Parent	Meropenem 15	Doripenem 15	Imipenem 15	Ceftazidime 8	Ceftazidime /Avibactam 15	Colistin 30	Negative (MH)
Timepoint									
0hrs	0.031	0.031	0.029	0.051	0.023	0.036	0.033	0.048	0.002
SD 0hrs	0.002	0.004	0.004	0.016	0.005	0.010	0.021	0.027	0.002
3hrs	0.035	0.034	0.026	0.038	0.029	0.040	0.038	0.046	-0.003
SD 3hrs	0.004	0.004	0.003	0.005	0.003	0.003	0.004	0.003	0.007
6hrs	0.047	0.050	0.044	0.068	0.043	0.057	0.075	0.059	0.001
SD 6hrs	0.004	0.005	0.005	0.008	0.003	0.009	0.011	0.003	0.002
12hrs	0.063	0.090	0.074	0.077	0.078	0.081	0.066	0.070	-0.001
SD 12hrs	0.003	0.018	0.009	0.011	0.004	0.009	0.003	0.007	0.001
24hrs	2.490	1.689	1.822	1.109	2.375	2.939	1.129	2.033	0.255
SD 24hrs	0.317	0.444	0.335	0.022	0.244	0.372	0.251	0.244	0.352
48hrs	0.122	0.168	0.188	0.138	0.174	0.175	0.092	0.130	0.001
SD 48hrs	0.010	0.006	0.009	0.016	0.022	0.010	0.006	0.032	0.002

Appendix 7: Table containing OD600 absorbance values in relation to biofilm formation detected from the *P. aeruginosa* growth detected within M9 Minimal Media with 20% Glucose supplement.

Strain	PAO1	Parent	Meropenem 15	Doripenem 15	Imipenem 15	Ceftazidime 8	Ceftazidime /Avibactam 15	Colistin 30
Timepoint								
0hrs	0.033	0.051	0.039	0.047	0.030	0.044	0.016	0.028
SD 0hrs	0.031	0.039	0.048	0.023	0.013	0.004	0.016	0.017
3hrs	0.019	0.122	0.184	0.114	0.100	0.118	0.034	0.073
SD 3hrs	0.036	0.100	0.029	0.040	0.065	0.046	0.026	0.023
6hrs	0.045	0.200	0.149	0.140	0.264	0.244	0.050	0.107
SD 6hrs	0.035	0.142	0.057	0.027	0.073	0.057	0.035	0.063
12hrs	0.094	0.239	0.229	0.218	0.225	0.211	0.047	0.140
SD 12hrs	0.060	0.113	0.040	0.046	0.058	0.053	0.015	0.030
24hrs	N/A	N/A	N/A	N/A	N/A	N/A	N/A	N/A
SD 24hrs	N/A	N/A	N/A	N/A	N/A	N/A	N/A	N/A
48hrs	0.068	-0.074	-0.038	0.032	-0.073	-0.062	-0.093	0.053
SD 48hrs	0.055	0.019	0.078	0.021	0.025	0.020	0.019	0.177

Appendix 8: Table containing OD600 absorbance values in relation to biofilm formation detected from the *P. aeruginosa* growth detected within M9 Minimal Media with 20% Alanine supplement.

Strain	PAO1	Parent	Meropenem 15	Doripenem 15	Imipenem 15	Ceftazidime 8	Ceftazidime /Avibactam 15	Colistin 30
Timepoint								
0hrs	0.024	0.045	0.044	0.012	0.023	0.047	0.021	0.032
SD 0hrs	0.011	0.033	0.034	0.017	0.020	0.008	0.010	0.019
3hrs	0.050	0.476	0.583	0.495	0.190	0.184	0.115	0.257
SD 3hrs	0.051	0.098	0.036	0.045	0.023	0.026	0.028	0.061
6hrs	0.349	1.013	0.906	0.890	1.227	1.208	0.091	0.585
SD 6hrs	0.515	0.254	0.096	0.048	0.153	0.293	0.059	0.317
12hrs	0.092	0.447	0.538	0.457	0.327	0.258	0.025	0.274
SD 12hrs	0.082	0.290	0.085	0.086	0.048	0.088	0.023	0.050
24hrs	N/A	N/A	N/A	N/A	N/A	N/A	N/A	N/A
SD 24hrs	N/A	N/A	N/A	N/A	N/A	N/A	N/A	N/A
48hrs	-0.009	-0.014	0.091	0.298	-0.032	-0.027	-0.028	0.252
SD 48hrs	0.019	0.012	0.157	0.028	0.001	0.005	0.007	0.007